MACQUARIE University
SYDNEY·AUSTRALIA

UNIVERSITÄT BERN

Graduate School for Cellular and Biomedical Sciences
University of Bern

Faculty of Medicine and Health Sciences
Macquarie University, Sydney

Parasite-host interactions during the blood and liver stage of rodent malaria parasites

PhD Thesis submitted by

Cilly Bernardette Schnider from **Germany**

for the joint degree of

PhD of Science in Cell Biology from the University of Bern

and

Doctor of Philosophy from the Macquarie University, Sydney

Supervisors

Prof. Dr. Volker Heussler, Institute of Cell Biology, Faculty of Science of the University of Bern
Prof. Dr. Roger Chung, Faculty of Medicine and Health Sciences, Macquarie University

Accepted by the Faculty of Medicine, the Faculty of Science and the Vetsuisse Faculty of the University of Bern at the request of the Graduate School for Cellular and Biomedical Sciences

Bern, Dean of the Faculty of Medicine

Bern, Dean of the Faculty of Science

Bern, Dean of the Vetsuisse Faculty Bern

Declaration of Originality/Copyright Statement, Statement of Authority of Access and Statement of Ethical Conduct

Last name, first name: Schnider, Cilly Bernardette

University of Bern matriculation number: 08-737-561

Macquarie University matriculation number: 43343341

This work has not previously been submitted for a degree or diploma in any university. To the best of my knowledge and belief, the thesis contains no material previously published or written by another person except where due reference is made in the thesis itself. All data, tables, figures and text citations, which have been reproduced from any other source, including the internet, have been explicitly acknowledged as such.

I hereby declare that this thesis represents my original work and that I have used no other sources except as noted by citations.

I am aware that in case of non-compliance, the Senate is entitled to withdraw the doctorate degree awarded to me on the basis of the present thesis, in accordance with the "Statut der Universität Bern (Universitätsstatut; UniSt)", Art. 69, of 7 June 2011.

This thesis may be made available for loan and limited copying in accordance with the Copyright Act 1968.

The research associated with this thesis abides by the International and Australian codes on human and animal experimentation, the guidelines by the Australian Government's Office of the Gene Technology Regulator and the rulings of the Safety, Ethics and Institutional Biosafety Committees of the University (permit number AEC reference number 2012/019-7).

All experiments performed were conducted in strict accordance with the guidelines of the Swiss Tierschutzgesetz (TSchG; Animal Rights Laws) and approved by the ethical committee of the University of Bern (permit number BE109/13).

Cilly Bernardette Schnider

Zurich, 27.06.2018

To my daughters, Milla and Annabelle

and my grandmother, Eva Hildebrandt.

"I think science is beautiful. I mean, what is more beautiful than discovering something that has never been known before? That is just sort of awe inspiring."

Ben A. Barres, Neurobiologist

Table of Contents

Summary **8**

Preface **10**

1. Introduction **11**

1.1. Malaria distribution, vector and current treatment **11**
1.1.1. Vector, distribution and surroundings 11
1.1.2. *Plasmodium* species 12
1.1.3. Study of *Plasmodium* and its interaction with the host 13
1.1.4. Current control measures against malaria 14
1.1.5. Vaccines 15
1.1.6. Vector control 16
1.1.7. Conclusion 16
1.2 Life cycle **17**
1.2.1. Mosquito stage 17
1.2.2. Liver stage 18
1.2.3. Blood stage 19
1.3. PVM Biology **20**
1.3.1. Invasion and PVM formation 20
1.3.2. Molecular mechanism of egress from the PVM and host cell 21
1.3.3. Egress from hepatocytes (Figure 4A) 22
1.3.4. Blood stage egress (Figure 4B) 23
1.3.5. Gametocyte egress (Figure 4C) 26
1.3.6. Nutrient acquisition 27
1.3.7. Export across the PVM 27
1.3.8. PVM remodeling and molecular make-up of the PVM 30
1.3.9. Outlook – Identification of novel PVM proteins 32
1.3.10. Conclusion 33
1.4. Host-pathogen interactions – the heme pathway **33**
1.4.1. RBCs and Reticulocytes 33
1.4.2. Heme pathway 34
1.4.3. Hemoglobin is a nutrition source during the blood stage 37
1.4.4. Conclusion 42
1.5. Project Aims **43**

2. Publication and manuscripts **44**

2.1. BioID reveals novel proteins of the *Plasmodium* parasitophorous vacuole membrane **45**
2.2. *Plasmodium* requires host porphobilinogen deaminase for intraerythrocytic growth **65**
2.3. Coproporphyrinogen oxidase confers resistance to the blood stage infection of *Plasmodium* species **84**

3. Discussion **100**

3.1 BioID identifies novel PVM, PV and PPM proteins **100**
3.2 Five consecutive genes in the final BioID list. *Is there more to it?* **105**
3.3 Are host heme pathway enzymes PBGD and CPOX required for *Plasmodium* growth? **110**
3.4 During the blood stage, *Plasmodium* has a requirement for Pbgd **112**
3.5 Identification of a putative *UROS* encoding gene in the *P. falciparum* and *P. berghei* genome using Hidden Markov Models **114**

3.6 Mice display increased survival upon CPOX host-deficiency 115
3.7 Conclusion and outlook 117

References 119

Acknowledgements 134

Appendices 136

Curriculum Vitae 148

List of Publications 150

Summary

Malaria is a parasitic disease which puts almost half of the world's population at risk of infection. It is caused by *Plasmodium*, a parasite transmitted by *Anopheles* mosquitoes. During its life cycle in the vertebrate host, the malaria parasite invades and multiplies in hepatocytes and in red blood cells. During invasion of sporozoites and merozoites, the host cell membrane invaginates around the parasite to form the parasitophorous vacuole membrane (PVM). The membrane is extensively remodeled by the parasite: host cell membrane proteins are removed and parasite proteins are incorporated. The PVM shields the parasite from a direct attack by cytosolic host cell immune responses and provides the host-parasite interface. Important roles of the PVM are nutrient acquisition, excretion of waste products and export of host-targeted proteins which add to parasite fitness and virulence. Finally, egress is critical for parasite release from its host cell and the first step is PVM disintegration. PVM biology and remodeling is of great interest, but despite all of these important tasks fulfilled by proteins in the PVM, the composition is not yet clear. Here, a proximity labeling technique (BioID) was used to identify PVM or PVM-interacting proteins in *P. berghei* blood stage parasites. Using this technique, many of the already known PVM proteins were found. Apart from known resident PVM proteins, I detected several proteins that were that were hitherto unknown as PVM proteins. Uncharacterized protein candidates were endogenously GFP-tagged and analyzed using live- and fixed-cell microscopy during the liver and the blood stage. Using this approach, I was able to identify several novel PVM proteins, and proteins that come in close proximity to the PVM.

During the intraerythrocytic symptomatic blood stage, *Plasmodium* digests up to 70% of host hemoglobin. Heme is an essential component of a number of proteins including hemoglobin and is essential for life. It is synthesized by a pathway involving at least eight enzymatic steps, and deficiency of any of these result in porphyria. Despite the abundance of hemoglobin and heme during the blood stage, the parasite expresses all enzymes of its canonical heme pathway, which can facilitate the *de novo* heme synthesis. Previous research has indicated that the parasite heme pathway is non-essential during the blood stage, and that the deficiency of host heme enzymes can influence parasite growth. That *Plasmodium* can be greatly influenced by the host background is well established. Here we hypothesized that host porphobilinogen deaminase (PBGD) and coproporphyrinogen oxidase (CPOX), two additional heme pathway enzymes, play a role during the blood stage. To facilitate this goal, in-depth studies by using rodent malaria species were utilized to infect mice deficient in PBGD and CPOX. Blood from porphyric patients was infected with *P. falciparum* and parasite growth was significantly

inhibited. Host PBGD was localized to the parasite periphery which could indicate that the parasite imports this enzyme during the blood stage. PBGD deficient mice are more resistant to malaria infection which suggests that *Plasmodium* relies on host PBGD to sustain its growth in erythrocytes and cause blood-stage infection. CPOX deficient mice displayed an increased survival, probably due to iron deficiency anemia, but the exact underlying mechanism remains to be elucidated. A novel role for PBGD and CPOX was described in this thesis adding to the understanding of host-pathogen interactions during the blood stage. Together this thesis has identified a number of novel PVM proteins during the blood and liver stage which will help to gain a deeper understanding of PVM biology. Deficiency of host enzymes can influence *Plasmodium* and here two novel host proteins, PBGD and CPOX are added to them. This thesis increased the understanding of host-parasite interactions during the blood and liver stage of *Plasmodium*.

Preface

Malaria is a devastating infectious disease, which concentrates in the poorest countries of the world, and accounts for over 200 million cases each year. Children under five are particularly vulnerable, and more than 70% of all malaria deaths are placed into this age group. In malaria endemic countries, recurring infections cause a significant economic loss. Countries with poor health care infrastructure provide limited access to rapid diagnostic tests and life-saving antimalarials, which directly intensifies the cycle of poverty. Antimalarials are losing their effectiveness due to emerging resistance by the parasite. Urgently, effective vaccines or novel therapeutics are required, for which a better understanding of parasite biology is needed.

This Cotutelle thesis will begin with an introduction of the background of malaria infection, and the causative agent of the disease. An overview of parasite biology will be given to then introduce a host-derived membrane, which surrounds the parasite during its intracellular stage. Parasite-host interactions are the second focus of this thesis, and are exemplified by using the host and parasite heme pathway. Three research paper will be presented, one on the identification of novel parasite membrane-proteins, and two on host heme proteins and how they impact the parasite during the intraerythrocytic stage. It will conclude with a final discussion on what this thesis has contributed to the research field towards a clearer understanding of *Plasmodium* and its biology.

1. Introduction

1.1. Malaria distribution, vector and current treatment

Despite advances in our understanding of the disease and its causes, malaria still represents one of the biggest health burdens worldwide. Malaria is caused by parasites of the genus *Plasmodium* and accounted for an estimated 216 million cases in 2016 alone. It is a widespread disease putting 3.4 billion people at risk each year [1]. The World Health Organization (WHO) reported that the worldwide distribution, number of malaria cases and deaths have decreased over the past 15 years due to extensive use of artemisinin combination therapy (ACT), bed nets and insecticide spraying indoors (Figure 1). Currently, an effective vaccine is missing and ACT is challenged by emerging resistance towards artemisinin in South-East Asia, and recently in Africa [2]. While there has been a 50% decrease in malaria deaths since 2000, it still accounted for the deaths of an estimated 445,000 people in 2016, most of whom were children under the age of five [1].

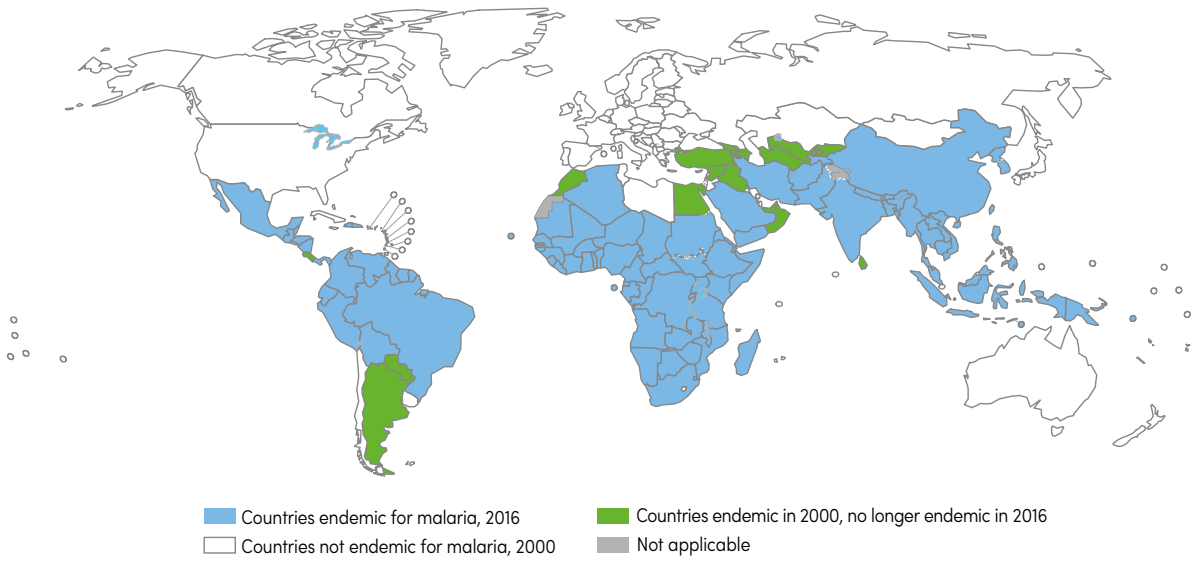

Figure 1: Comparison of malaria endemic countries in 2000 and 2016. Countries in which no case of indigenous malaria is reported over three consecutive years are considered to be malaria free. From: World malaria report 2016 [3]

1.1.1. Vector, distribution and surroundings

Plasmodium parasites are transmitted to humans by the bite of an infected female *Anopheles* mosquito. Worldwide there are 460 species of *Anopheles* mosquitoes, and among the 150 species that can transmit malaria, 30 to 40 are common transmitters [4, 5]. They are predominantly found in areas with high humidity, and rely on water bodies for larvae development, which takes between several days and a couple of weeks, mainly depending on

water temperature [6]. Ninety percent of all malaria cases are localized to tropical and sub-tropical Africa, where conditions for *Anopheles* mosquito development are ideal [3]. The remainder of cases occur in the Southeast Asian (7%) and Mediterranean (2%) region. Seasonal changes of temperatures, humidity, rainfall and surface water are important, as peaks of malaria cases and wet seasons are directly correlated with each other. The insect host influences the spread of malaria. The genetic background of the vertebrate host and of the parasite itself are important, as well as access to and quality of medical care [7]. In Africa, only one-third of febrile children are taken for a medical check [1].

Conflicts and unstable governments have directly lead to a rise in malaria cases and deaths from 2015 to 2106, due to reduction of adequate health facilities and care in parts of Nigeria, controlled by terrorists, and Venezuela [1, 3]. During the West African Ebola outbreak in 2014/15, patients were often coinfected with *Plasmodium*, leading to a higher mortality rate [8]. Increased mortality was not only due to comorbidities, but also because the health-care systems in affected countries could not cope with both Ebola and malaria infections [9]. In an era of anthropogenic climate change, the distribution of the vector will likely be impacted, and is currently estimated to increase its global distribution. While global warming is now a fact, regional impacts can differ, and there are many variables to be considered in determining *Anopheles* distribution and malaria transmission [10-13].

1.1.2. *Plasmodium* species

After transmission, *Plasmodium* parasites reproduce in the vertebrate host twice, once in the liver and then in erythrocytes. Parasites are taken up by another mosquito and the life cycle continues. There are more than 250 species of *Plasmodium,* but only five are known to infect humans: *Plasmodium falciparum, P. vivax, P. ovale, P. malariae,* and *P. knowlesi [14]*. Among these, *P. falciparum* is by far the deadliest, and accounted for 99% of all fatal malaria cases in 2015. It is predominantly found in Africa and causes placental and cerebral malaria (CM), which are often lethal. Clinical symptoms of CM range from impaired consciousness to coma, caused by sequestration of infected red blood cells (iRBCs) in the microvasculature adhering to endothelia, and/or cytokine reactions [15]. Placental malaria is manifested by a variety of symptoms: maternal anemia, low birth weight, placental insufficiency and premature delivery all lead to higher maternal and perinatal mortality [16].

Globally *P. vivax* accounts for only 4% of cases, but for 36% cases outside of Africa, and is the predominant species in the Americas [1]. *P. vivax* accounts for lower mortality, due to a general lower blood parasite load. Like *P. ovale* it can persist in a dormant stage in the liver, as a so-

called hypnozoite, and can initiate a malaria relapse even after several years of remaining silent [17-19]. Within the genus *Plasmodium,* a selection of species are established for laboratory malaria research in rodents; *P. chabaudi*, *P. yoelii*, *P. berghei*, and *P. vinckei* which naturally infect thicket rats.

1.1.3. Study of *Plasmodium* and its interaction with the host

Different models exist to study malaria. *P. falciparum* can be cultured *in vitro* using red blood cells (RBCs), but for *in vivo* models rodents are preferred, which can be infected with a variety of rodent malaria parasites. An advantage of using rodent malaria parasites is the possibility of analyzing the complete life cycle *in vivo*, which is very complicated in *P. falciparum* and involves non-human primates. Today it is possible to manipulate the genome of a number of *Plasmodium* species in order to learn more about parasite-host interactions, parasite biology, and virulence. In the past, different techniques were implied and new approaches are constantly added [20, 21]. As part of this, large-scale genetic screens were implemented to detect certain phenotypes, and to identify critical genes essential for *Plasmodium* virulence [22-24].

Malaria parasites have exerted selective pressure on the human genome over thousands of years, which has resulted in natural resistance within some populations [25]. Using mathematical modelling to date the frequency of mutations in the human genome, and comparing malaria resistance-exerting genes and other mutations, a strong selection towards resistance genes has been confirmed [26]. There are many examples of genetic polymorphisms, leading to resistance or susceptibility to malaria [27, 28]. One is sickle cell disease (SCD), characterized by abnormal hemoglobin, due to a mutation affecting the β-globin, resulting in an abnormal RBC shape. Heterozygous individuals are more resistant to *P. falciparum* malaria compared to individuals who do not carry the mutation [29]. While heterozygous individuals are mostly healthy, homozygous individuals, if not treated, have a high infantile mortality of 50-90% in endemic areas [30]. Although this cost is extremely high, SCD continues to be under positive selective pressure by *P. falciparum* in endemic regions, highlighting the parasite pressure on the human genome [31]. Therefore, malaria has a direct influence on this devastating disease, which is highly prevalent in Africa (85%), where medical treatment is often complicated by poor infrastructure, high cost and poor access to medical care.

Another example of global importance is the Duffy antigen receptor for chemokines (DARC), which is expressed on the RBC surface [32, 33]. DARC-negative individuals are protected from *P. vivax* and *P. knowlesi* malaria, when carrying the homozygous mutation. Causative for the protection is *P. vivax* utilization of the Duffy receptor for RBC invasion. As a consequence, in

Africa where DARC negativity is common, *P. vivax* is rare or absent compared to *P. falciparum* [33]. The examples of SCD and DARC negativity highlight the importance of a better understanding of host-pathogen interaction, and the power of the host genetic background.

To study the influence of the host background in an experimental setting, a vast variety of inbred mouse strains with variable susceptibility to malaria infection are available. Mice used in this thesis were of the SJL/J, C57BL/6 and BALB/c strains, and were infected with *P. chabaudi* and *P. berghei*. SJL/J mice are susceptible to infection with *P. chabaudi*, but do not develop experimental CM when infected with *P. berghei* [34]. C57BL/6 on the contrary are resistant to infection with *P. chabaudi*, and develop experimental CM when infected with *P. berghei* [35, 36]. BALB/c mice are resistant to infection with *P. berghei*, and partially susceptible to infections with *P. chabaudi* [34, 37]. As in humans, different mouse strains are resistant or susceptible to infection with *Plasmodium*, which makes them an important part of research by reflecting host polymorphisms that are present around the globe. In the past this has led to the identification of several novel genetic loci by crossing mice with variable susceptibility to malaria infection [38, 39].

1.1.4. Current control measures against malaria

Most antimalarials available target the *Plasmodium* blood stage. Control of malaria has a long history, which began with the recognition of the disease, dating back to a Chinese document from 2700 BC [40]. The earliest mention of the well-known antimalarial derived from *Artemisia annua* dates back to 168 BC [41]. Artemisinin, the active ingredient of *A. annua*, and its derivatives inhibit phosphatidylinositol-3-kinase (PI3K), which plays a role in protein export from the endoplasmic reticulum [42]. Its extensive use from the mid-2000s onwards resulted in resistant parasites, and one of the resistance genes was pinpointed, resulting in an increase of PI3K levels [43-47]. Today, artemisinin and artemisinin derivatives remain the base of ACT, widely used to treat *P. falciparum* malaria, with cure rates exceeding 90% [48].

Quinine, still used today, was first mentioned in the European literature over 400 years ago by Fragoso and Monardes, and Jesuit missionaries from South America were responsible for bringing Quinine to Europe [49]. The natural component, derived from the bark of the cinchona tree, was heavily used as a malaria treatment until the beginning of the last century, when synthetic antimalarials were invented. Quinine belongs to the group of quinoline derivatives of which chloroquine was extensively used from the 1940s. Chloroquine acts on the *Plasmodium* blood stage, during which the parasite digests vast amounts of hemoglobin. Free heme is produced as a by-product which is toxic and is converted into hemozoin crystals. Chloroquine

accumulates in the parasites' food vacuole (FV) and interferes with the detoxification of free heme [50].

The extensive use of chloroquine led to the emergence of chloroquine-resistant *P. falciparum* parasites in Southeast Asia and South America from the 1950s onwards [51]. Chloroquine-resistant parasites display a lower internal concentration of the drug [52]. Two importer proteins were found to be responsible [53, 54]: *P. falciparum* chloroquine resistance transporter (PfCRT) and *P. falciparum* multidrug resistance transporter 1 (PfMDR1), where pfCRT excretes chloroquine across the PV [50, 55], and PfMDR1 interferes with the import of chloroquine into the FV [56-58]. PfMDR1 alterations have also been associated with resistance to other drugs, such as quinine derivatives and artemisinin [59]. Still, a chloroquine/primaquine combination is widely used for *P. vivax* treatment in areas known to be sensitive to chloroquine. Chloroquine resistant *P. vivax* was first reported in 1989 and since then, resistant parasites have been treated by using ACT [17]. Primaquine is the only treatment available for hypnozoites [48].

Antibiotics such as tetracyclines are used to treat malaria by acting on the protein biosynthesis in the mitochondria. Their mode of action is slow, because they exert their antimalarial effect during the second cycle of replication, hence they are combined with other fast-acting antimalarials [60, 61]. Antifolates are antimalarials which interfere with the essential *Plasmodium* folate metabolism. They are often used in combination with other drugs as the their sole use can induce resistance rapidly - resistant parasites are now found worldwide [62]. The parasite becomes resistant to different drugs by different mechanisms. For instance, the drug-binding site of the target molecule is altered, the drug is actively removed from the parasite by using ATP-dependent transport molecules, or the protein-protein interaction network is affected [63-65].

1.1.5. Vaccines

Chloroquine/primaquine and ACT target the parasite during the blood stage. Preceding the blood stage is the asymptomatic liver stage, and vaccine efforts to date have been targeted at parasites of the pre-erythrocytic stage to prevent symptomatic malaria during the blood stage. Several vaccines have been developed, but so far they have shown only limited effects [66]. RTS,S/AS01, the first licensed malaria vaccine, is addressing the pre-erythrocytic stage by targeting the circumsporozoite protein, present on the surface of sporozoites and liver stage parasites [67]. It was recently trailed in a phase III clinical trial which included two age groups, infants aged between 6 and 12 weeks, and children between 5 and 17 months. Vaccinations

were given three times as monthly doses. Partial protection of the older children was higher compared to infants, but overall protection declined after 12 months noted over a period of up to 7 years [68, 69]. Some children were also given a booster injection at 18 months after the third injection which showed no difference in severe malaria cases in both age groups. The booster injection, however, increased the efficacy and number of prevented cases. The number of prevented cases was moderate, at 36.3 %in children and only 25.9% in infants [70]. RTS,S/AS01 is now approved by the European Medicines Agency but not recommended by the WHO as part of their Expanded Programme of Immunizations for infants, due to its low effectiveness [71].

Other vaccines have targeted parasites at various stages: blood stage parasites such as those that block the transmission of the parasite from the blood stage to the mosquito vector, pre-erythrocytic stages and sexual stages. For blood stage vaccines, herd immunity would then be needed in order to make these vaccines effective. All vaccines apart from RTS,S/AS01 are still in phase I and II clinical trials (for an up-to date overview please see "Tables of Malaria Vaccine Projects Globally" by the WHO) [72-76]. The development of a vaccine has been hindered by the antigenic variation of the *P. falciparum* erythrocyte membrane protein 1 (PfEMP1) displayed on the erythrocyte surface by the parasite [77-79]. *Plasmodium* parasites are genetically diverse and have a high complexity, shuffling between the inside and outside of cells of their vertebrate hosts. Different immune reactions are necessary from the host to successfully eliminate the parasite [17].

1.1.6. Vector control

In 1898, Ross and Grassi revealed the role of mosquitoes in the transmission of malaria as a vector. Following this discovery, breeding grounds of mosquitoes were eliminated where possible and later, during the 1940s onwards, dichlorodiphenyltrichloroethane (DDT) insecticide spraying indoors began to be used [80]. Later on, bed nets were distributed, which are now treated with insecticides. One unforeseen impact of the extensive use of insecticides has been the emergence of pesticide-resistant mosquitoes [81].

1.1.7. Conclusion

A cure, resistant-proof drug or effective vaccine for malaria is still missing [82]. In contrast to recent developments, mortality from severe malaria remains high. It has been reported that there will be a shift in deaths from the mostly under-fives to the older population due to acquired immunity playing an important role in malaria protection in individuals over five years of age

[83]. Lower infection rates lead to a lower protection into adulthood by acquired immunity, leading to increased susceptibility later in life, that is responsible for this shift in disease burden [84-86]. Meanwhile, bacteremia is more common in children infected with *P. falciparum*, as an infection with the parasite predisposes children to bacteremia. A reduction of *P. falciparum* infections would therefore positively influence one of the major causes of deaths and childhood illness in sub-Saharan Africa [87]. Available funds for malaria eradication programs have been shrinking, contributing to spikes in malaria cases and deaths [88, 89]. Malaria is not only a major health burden but also slows down economic progress and development: it is estimated that malaria is responsible for a 1.3% reduction in economic growth in countries in which malaria is endemic [90, 91]. The long-term goal to eradicate malaria can only be achieved by addressing many factors simultaneously, including vector control, blocking transmission, rapid and precise diagnostics, access to treatment, development of novel, resistance-proof drugs or vaccines, and reliable access to high-quality medical care. Many of these obstacles of malaria eradication are directly dependent on basic research, and a better understanding of the parasite and its interaction with the host biology is urgently needed to reach this goal [92, 93]. Current understanding of the parasite-host interaction is presented in this chapter, with particular focus upon the parasite membrane, and the role of the heme pathway in parasite-host biology.

1.2 Life cycle

The causative agent of malaria is the apicomplexan parasite *Plasmodium*, which is transmitted to humans by the bite of infected female *Anopheles* mosquitoes (Figure 2). The parasite develops in the vertebrate host and produces sexual stages until a mosquito takes up infected blood and the life cycle continues. Throughout the life cycle, the parasite undergoes many changes and adaptations, especially in different host environments such as host skin or liver, and the mosquito midgut.

1.2.1. Mosquito stage

The mosquito stage is where *Plasmodium* sexual reproduction takes place. During the blood meal of a mosquito, parasitized blood is taken up into the midgut. Triggered by temperature change and xanthurenic acid, gametocytes - sexual *Plasmodium* stages - are activated and released from the RBC once in the midgut (Figure 2E). Male gametocytes fertilize female gametocytes to form a zygote that develops into a motile ookinete, which migrates out of the midgut epithelium and develops into a mature oocyst between the epithelium and basal layer

[94]. Sporogony yields thousands of sporozoites that travel with the mosquito hemolymph into the salivary glands, where they are injected into the host skin during a blood meal [95].

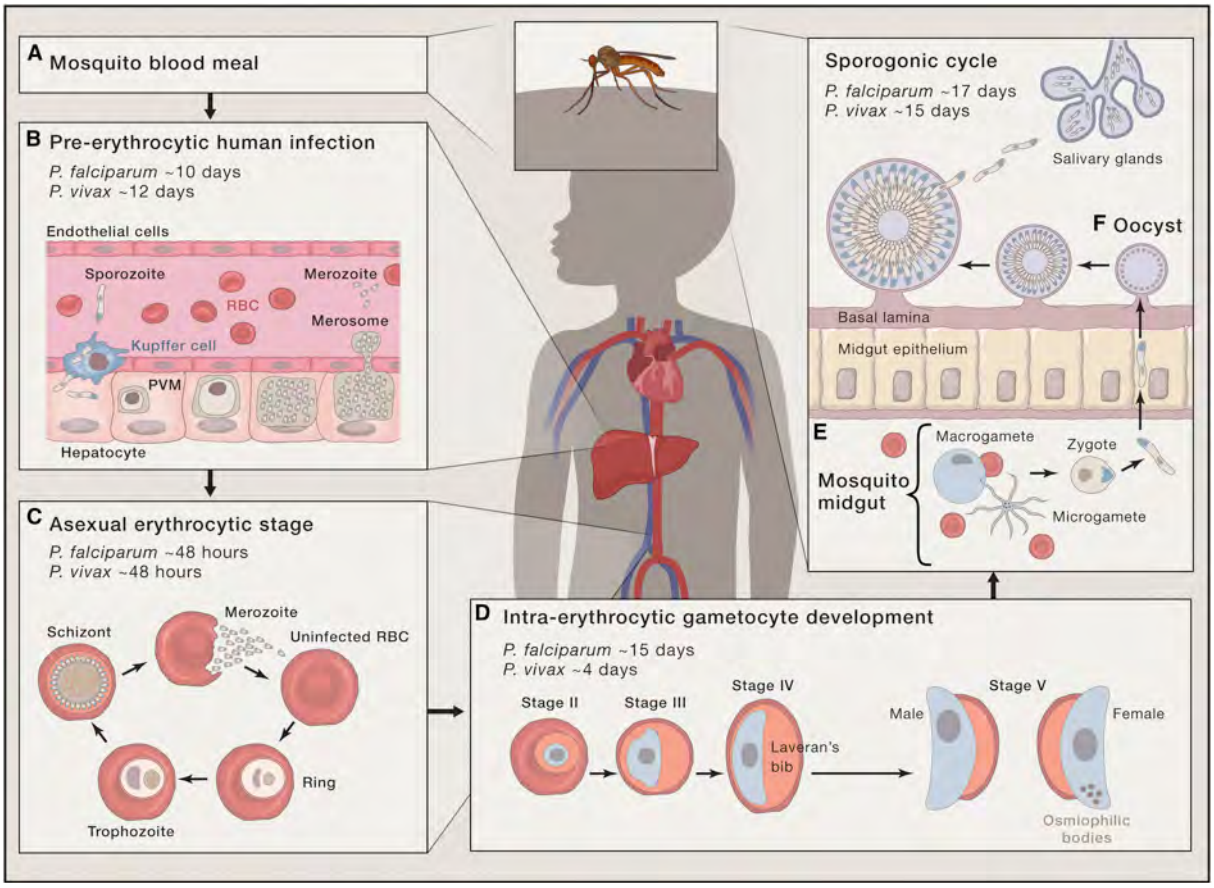

Figure 2: The *P. falciparum* life cycle. The parasite undergoes a complex life cycle between the mosquito (vector) and mammalian host. It can be divided into sexual reproduction within its mosquito host and asexual multiplication within the mammalian host. (A) and (B) Sporozoites are transmitted via the bite of an infected female *Anopheles* mosquito and travel with the bloodstream to the liver. During the liver stage, sporozoites undergo schizogony forming up to 30.000 daughter merozoites. Merosomes bud off and burst to release infective merozoites. (C) Merozoites then infect RBCs and develop from ring to trophozoite to the schizont stage, leading to the formation of infective merozoites. (D) They infect other RBCs, and as part of this repetitive cycle some parasites differentiate into gametocytes that fuse in the mosquito midgut to undergo sexual reproduction (E) once taken up during another blood meal. Fused gametocytes develop from zygote to an ookinete into an oocyst (F), which produces thousands of sporozoites, ready to infect the next mammalian host. From: [95]

1.2.2. Liver stage

A female mosquito requires blood to produce eggs. During the blood meal, the mosquito first injects saliva into the host skin to prevent coagulation. If infected with *Plasmodium* parasites, sporozoites residing in the salivary glands will be injected into the host skin (Figure 2A). Sporozoites move by gliding motility. Around half of them will be able cross the epithelia to enter the bloodstream or lymphatic vessels [96]. Parasites that remain in the skin can form infective merozoites in case of the rodent parasite *P. berghei*, but parasites destined for lymph nodes will be eliminated [97, 98]. Parasites which successfully enter blood vessels travel via the bloodstream to liver sinusoids, where they bind to highly sulfated heparan-sulfate

proteoglycans, which activates them to switch from migration to invasion mode [99]. To gain access to hepatocytes, most sporozoites pass through Kupffer cells and the space of Disse (Figure 2B) [100]. They then transmigrate several hepatocytes until they finally settle in one, where they grow inside a parasitophorous vacuole (PV), surrounded by a parasitophorous vacuole membrane (PVM), originated from host cell membrane (HCM) during the invasion process. Sporozoites multiply by undergoing nuclear division (schizogony), each single parasite forming up to 30.000 merozoites. This is a massive expansion but as only a very small number of hepatocytes are infected, the liver stage is clinically silent. The liver is a lymphatic organ, continuously exposed to a variety of antigens, making it a highly tolerogenic organ, ideal for this first multiplication step in the mammalian host [101, 102]. After forming infectious merozoites, the PVM is ruptured and merozoites are released into the hepatocyte cytoplasm. Hundreds of merozoites, surrounded by host cell membrane, bud off and enter the bloodstream, where they burst when reaching lung capillaries [103, 104]. Free merozoites are now ready to invade RBCs.

1.2.3. Blood stage

Invasion of RBCs takes less than one minute, and is an highly orchestrated event [105]. Free merozoites invade RBCs, a process during which the HCM invaginates around the parasite forming a vacuole. The parasite develops through different developmental stages including, ring, trophozoite, schizont, forming up to 36 new daughter merozoites (Figure 2C). During the ring stage, the parasite establishes itself within its new host. The host cell is extensively remodeled by exporting proteins across the PVM into the RBC cytoplasm and to the HCM [106]. Throughout the trophozoite stage, the parasite grows in size, followed by the schizont stage, where it undergoes schizogony. In late schizonts, the parasite plasma membrane (PPM) is wrapped around individual nuclei, and single merozoites are formed.

The PVM and HCM are ruptured, and free merozoites are able to invade new RBCs. The cycle is repeated multiple times, until there is a substantial number of RBCs infected, which then leads to clinical symptoms, such as fever, chills and headache, caused by cytokine release of macrophages, that were initially attracted by waste products released by ruptured iRBCs [107, 108]. Depending on the immune status of the infected individual, treatment options, and parasite species, this might lead to death caused by multi-organ failure [109]. As part of the blood stage, some parasites commit to sexual development, forming female and male gametocytes (Figure 2D). Sexual stages are activated once taken up by an *Anopheles* mosquito.

1.3.PVM Biology

In the mammalian host, *Plasmodium* differentiates, grows and replicates intracellularly in hepatocytes and RBCs inside a vacuole surrounded by the PVM. Being originated from the HCM, the PVM shields the parasite from a direct attack by host cell immune responses [110]. Other important roles are nutrient acquisition, excretion of waste products, and export of host-targeted proteins, which add to parasite fitness and virulence. Finally, egress is critical for parasite release from its host cell, and the first step is PVM disintegration. Invasion and egress alike are driven by different sets of proteases [111, 112]. Recently, the role of plasmepsin IX and X have been characterized, which are essential for invasion and egress [113, 114].

1.3.1. Invasion and PVM formation

Invasion of host cells is highly orchestrated, during which the PVM is formed. For blood stage parasites, PVM formation is well studied, displayed in Figure 3. As mentioned earlier, RBC invasion takes less than a minute in *P. falciparum*, including PVM formation [115]. Merozoites attach to the RBC via surface coat proteins, and reorient themselves by pointing their apical end towards the RBC membrane [116]. Host proteins of the erythrocyte binding-like proteins (EBLs) and *P. falciparum* reticulocyte-binding protein homologs (PfRhs) families, are responsible for irreversible attachment to the erythrocyte followed by the invasion process [117]. Following this, the PfRh5 complex binds to basigin, a host cell receptor, a step essential for invasion [118]. The parasite complex rhoptry neck (RON) is integrated into the host cell membrane, also the first remodeling of the HCM, that later forms the PVM. A tight junction, also termed moving junction (MJ), is formed between RON2, part of the RON complex deposited into the RBC membrane, and parasite protein apical membrane antigen 1 [119]. The merozoite actively moves itself into the RBC by using the MJ, and during this movement the HCM that will become the PVM is remodeled and host cell proteins are removed. Apicomplexan parasites contain a special set of secretory organelles: micronemes, rhoptries, and dense granules, all of which secrete their contents during invasion [120]. Contents of the rhoptry bulb are released via the MJ into the RBC cytoplasm. Rhoptries contain a variety of proteins, that need to be processed to be active. Plasmepsin IX is responsible for the activation of some of these proteins [113]. Once the merozoite is emerged into the RBC the HCM is sealed, forming the PVM, retaining the parasite in a vacuole [121].

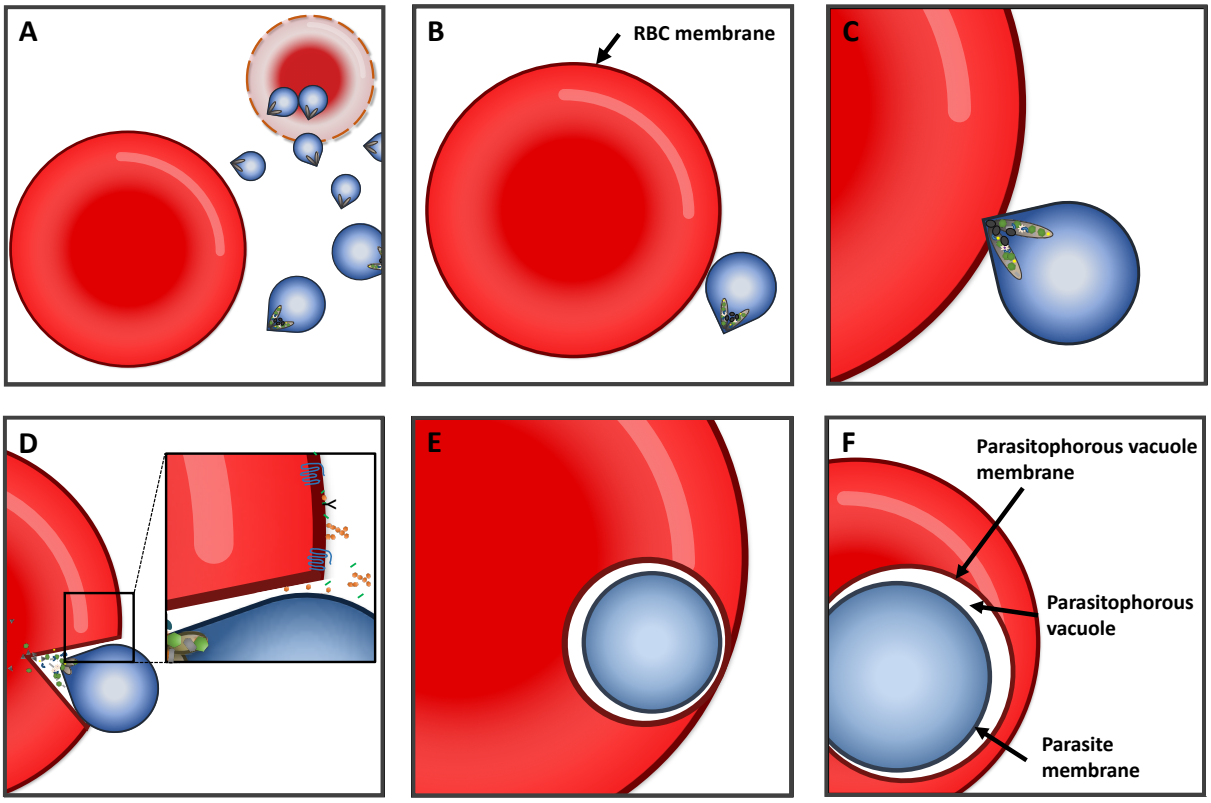

Figure 3: PVM formation during erythrocyte invasion. (A) After an infected RBC is ruptured, merozoites are set free to invade a fresh RBC. (B) Invasion of the merozoite is initiated with attachment to the RBC membrane followed by (C) reorientation of the apical side towards the host membrane. (D) A tight junction is formed and the merozoite propels itself into the RBC, thereby the HCM invaginates to form a vacuole. During this process and the tight junction, HCM proteins are removed. (E) The HCM, now PVM, is finally sealed and the parasite can develop inside the RBC. (F) After its establishment, the PVM is heavily remodeled by the parasite.

1.3.2. Molecular mechanism of egress from the PVM and host cell

After development and multiplication, egress of *Plasmodium* from its host cells is critical for transmission. To egress, parasites must degrade two membranes; the PVM is lysed first, followed by HCM lysis [122, 123]. This is a two-step process, and HCM and PVM are sensitive to different sets of proteases, indicating that these are two separate events facilitated by different mediators [111]. In erythrocytes PVM and HCM rupture occurs within seconds [122], but PVM rupture in hepatocytes precedes HCM rupture by several hours [122, 124]. In RBCs, the HCM is ruptured, releasing free merozoites, but in hepatocytes, several thousands of merozoites are packaged within HCM and enter the blood vessels as merosomes [104]. Similarly to asexual stages, once activated in the mosquito midgut, the sexual stages of *Plasmodium* degrade the PVM first followed by HCM degradation [125]. Recently, an aspartic protease inhibitor, 49c, was recognized to block PVM degradation in *P. falciparum* during the blood stage [113]. In *P. berghei* infected hepatocytes 49c also impaired and delayed egress from hepatocytes, which was also observed *in vivo* in rodents.

Compared to invasion, where many processes have been identified, egress of *Plasmodium* is not studied very well. The whole process is highly regulated and orchestrated, some proteins responsible for egress have been identified and studied in detail, but many open questions remain. Differences in the PVM composition exist between liver and blood stage, as well as in gametocytes, which are pointed out as part of the following chapters.

1.3.3. Egress from hepatocytes (Figure 4A)

To egress from their host hepatocytes, parasites degrade two membranes, via an inside-out mode. The liver stage PVM comprises small pores allowing the free diffusion of molecules [126]. During merozoite development this permeability of the PVM then changes, allowing bigger molecules to enter, before it finally ruptures [123]. Sturm et al. found that PV egress is inhibited by the cysteine protease inhibitor E64, indicating a role of cysteine proteases [104]. Both *P. falciparum* and *P. berghei* express serine repeat antigens (SERA) paralogs belonging to the family of cysteine proteases [127, 128]. In *P. falciparum,* the family consists of nine members, all of which are expressed during blood and liver stage. In *P. berghei* the SERA family consists of five proteins, four of which are also expressed during the liver stage [129, 130]. SERA proteins are abundant and reside in the PV. There have been many studies on SERA proteins showing that they play an essential role during egress; this was supported by the fact that they are upregulated shortly before PVM rupture [131-135]. While some SERAs were found to be non-essential, other SERA family members were subsequently upregulated, indicating compensatory mechanisms by the parasite to maintain appropriate levels of SERAs [130]. SERAs need to be activated via proteolytic cleavage by the subtilisin-like protease 1 (SUB1), with a SUB1 cleavage site that is well preserved within the SERA family. SUB1 was initially identified as a blood stage protein, but is also expressed during the liver stage. SUB1 knockout parasites failed to rupture their PVM during the liver stage [136-138]. One of these knockout studies confirmed that in SUB1 deficient parasites SERA3 processing during the liver stage was absent [135, 136]. In the same knockout study, SUB1 deficient parasites failed to process merozoite surface protein 1 (MSP1), and those parasites were not able to establish a blood stage infection [136].

SUB1 itself needs to be activated proteolytically and the dipeptidyl aminopeptidase 3 (DPAP3) protease was found to be responsible for producing mature SUB1 [131, 139]. DPAP3 is a member of the family of DPAP proteins; *P. falciparum* and *P. berghei* each express three members of these exopeptidases. DPAP3, mostly expressed in merozoites, is also known to be involved in hemoglobin digestion and is a key regulator of proteolysis; some 200 host and

parasite proteins are processed during egress, more than half of them depend on DPAP3 [140, 141]. SUB1 is not a PV or PVM protein. It is known to reside in exonemes, structures within the parasite cytoplasm, but shortly prior to egress, the contents of these exonemes are discharged into the PV space after induction of an unidentified egress signal [142]. Other PVM resident proteins play a role in PVM rupture such as Liver-Specific Protein 1 (LISP1). LISP1 deficient parasites are unable to rupture their PVM [143]. Similarly, *P. berghei* phospholipase, another resident PVM protein was identified to be important. Upon knockout of this protein, parasites showed a defect in PVM rupture [124]. *Plasmodium* cGMP-dependent protein kinase (PKG) was found to be essential for merosome formation in *P. berghei*, indicating a role in liver stage egress of this kinase [139].

Directly after PVM rupture, the host cell death is induced and merozoites reside freely in the hepatocyte cytoplasm until the formation of merosomes, bags packed with free merozoites, which are released into the bloodstream by squeezing between two epithelial cells. The membrane of merosomes is derived from the HCM. Merosome formation facilitates different immune evasion strategies. First, they prevent phosphatidylserine presentation on the HCM to avoid being eaten by phagocytes, such as Kupffer cells, by keeping Ca^{2+} levels low [104]. In the bloodstream, parasites travel incognito as they are enclosed in host-derived membrane. Last, merosomes rupture in the lung microvasculature, as blood flow is slower compared to in bigger vessels, creating ideal conditions for the initial contact with a RBC, where invasion is probably easier [144].

1.3.4. Blood stage egress (Figure 4B)

Just like in hepatocytes, blood stage parasites reside in erythrocytes within an PV, surrounded by the PVM. Several minutes prior to egress, the vacuole swells due to H_2O influx [145]. Following egress signals, proteins are released from micronemes and exonemes to facilitate PVM rupture [146]. Comparable to the liver stage, egress of blood stage parasites is sequential, although HCM rupture after PVM disintegration occurs faster [147]. Recently it has been shown that the PVM is permeabilized 10 to 30 minutes prior to its actual breakdown [122]. Different protease inhibitors were added to iRBCs; E64 treatment prevents PVM rupture, but leupeptin and antipain prevent HCM rupture [148]. EGTA-AM, which irreversibly chelates calcium (Ca^{2+}) ions required for calpain activation, was shown to support PVM rupture but prevents rupture of HCM [149]. This highlights that the two membranes are disintegrated by different types of proteases. Host proteases, such as calpain-1, are hijacked by the parasite to facilitate egress from RBCs. Calpains remain inactive in the cytoplasm, but upon Ca^{2+} binding

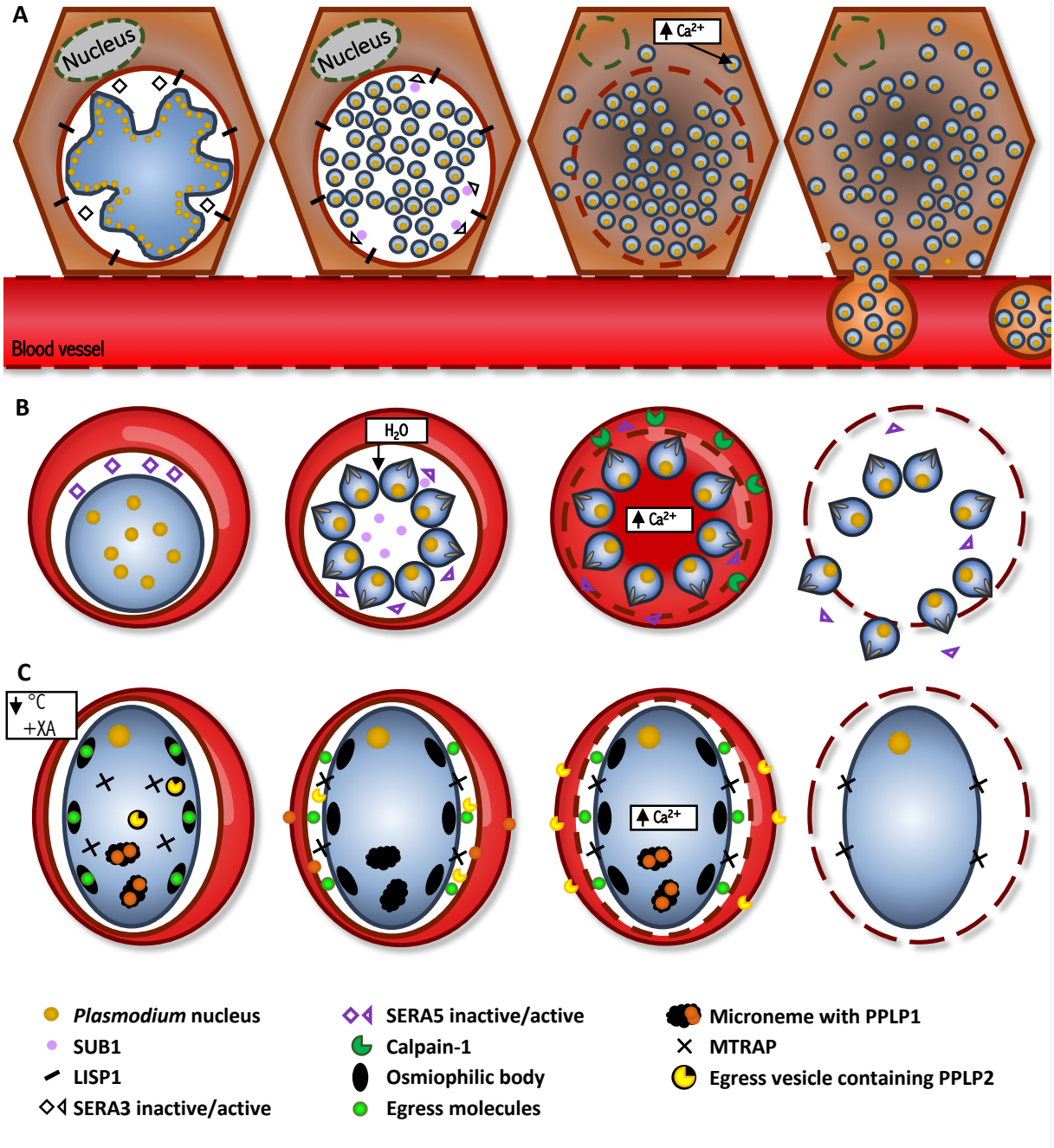

Figure 4: Egress of intracellular *Plasmodium* parasites: In the mammalian host *Plasmodium* resides within a vacuole surrounded by the PVM. (A) During the liver stage LISP1 is an integral PVM protein, essential for PVM rupture. In the PV, SERA proteases are abundant, such as SERA3, which could contribute to host cell death or egress. During PVM rupture, Ca^{2+} is released from the PV into the host cytoplasm, which undergoes cell death immediately. To prevent the Ca^{2+} induced signaling cascade that will display phosphatidylserine on the HCM and will act as a phagocytic signal, merozoites actively take up Ca^{2+} from the host cytosol. Parasites leave hepatocytes in merosomes, HCM-derived vesicles packed with merozoites, and squeeze through the endothelium to enter the bloodstream. The HCM finally ruptures in the lung capillaries, releasing individual merozoites. (B) The PV of blood stage parasites contains SERA proteins such as SERA5. Prior to PVM rupture during the asexual blood stage, H_2O influx from the RBC causes PV swelling and may contribute to egress. SUB1 is resident in exonemes, whose contents are released into the PV upon egress stimuli. SUB1 proteolytically activates SERA5, facilitating egress, then PVM rupture releases Ca^{2+} into the RBC cytoplasm. Host-calpain-1, which is activated by Ca^{2+}, is hijacked to degrade cytoskeletal proteins. Infective merozoites are now able to invade fresh RBCs. (C) Gametocytes contain osmiophilic bodies (OB), vesicles filled with egress molecules. Upon external stimuli, when taken up by a mosquito during a blood meal, xanthurenic acid (XA) or a temperature drop in the mosquito midgut activates gametocytes. They then release Ca^{2+} from internal stores, and OB contents for PVM rupture. Cysteine/serine proteases then facilitate egress from RBCs, enabling fusion of male and female gametocytes. Modified from: [153].

become proteolytically active and associate with membranes. Ca^{2+} is stored in the parasites' FV, but is detected in the PV prior PVM rupture [150, 151]. Chelation of intracellular Ca^{2+} in schizonts inhibits egress and HCM permeabilization [152].

Kinases have also been found to be critical for RBC egress. Ca^{2+} dependent protein kinase (CDPK) 5 knockout parasites failed to rupture both PVM and HCM in *P. falciparum* parasites [154]. PKG, the upstream kinase of CDPK5, regulates egress, demonstrated in knockout parasites or wild-type parasites treated with a PKG inhibitor [155]. Similar to the liver stage, SERAs play an important role during blood stage egress, highlighted by knockout studies and failure to egress from erythrocytes [132, 133]. It has recently been shown that SUB1 is activated by plasmepsin X during the blood stage, and that this is essential for RBC egress [114]. Comparable to the liver stage, during blood stage egress SERAs are proteolytically activated. This was absent in parasites with downregulated plasmepsin X. SERA5 is cleaved by SUB1 and DPAP3, and this processing is essential for RBC egress [131]. The *P. falciparum* SERA6, which is the orthologue of SERA3 in *P. berghei*, is cleaved by SUB1, mirroring findings during the liver stage [134, 136].

The exact mechanism by which SERAs contribute to egress remains to be elucidated, whereas for SERA5 it has been shown that it can bind peptides, and its role in egress is non-enzymatic [156]. SERA5 is an abundant protein and facilitates downstream processing of cellular substrates [157]. It has been described as a central player of proteases involved in egress as it exhibits 28 protein associations [158]. SERA5 knockout attempts have been unsuccessful so far, indicating the essential nature of this protein [128]. In agreement with its essential role, antibody titers against SERA5 were shown to correlate with parasite growth inhibition in *in vitro* cultures; high titers lead to stronger growth inhibition [157]. During the blood stage, SUB1 cleaves a number of PV and merozoite proteins. As in the liver stage MSP1 is a SUB1 target, which is essential during blood and liver stage [159, 160].

After PVM rupture, the HCM needs to be disintegrated to release merozoites. MSP1, a large precursor protein, is SUB1-processed prior to egress and this processing is essential for parasite survival [161]. Mature MSP1 is able to bind to spectrin, one of the host cytoskeletal proteins cleaved during RBC egress after PVM rupture. Merozoites that were inefficiently processed and lacked surface-bound MSP1 showed severe egress defects, making SUB1 and MSP1 two of the major players in host cell egress [162]. Falcipain-2, an enzyme with a dual function, was shown to be involved RBC egress. Usually involved in hemoglobin digestion, it is also capable of cleaving ankyrin and protein 4.1, two additional cytoskeletal proteins [163]. Falcipain-2 inhibition using a peptide resulted in declined egress [164]. Plasmepsin-2, which is similarly

involved in hemoglobin digestion, was also found to be able to digest spectrin, protein 4.1, and actin. However, knockouts verified that it is non-essential during the blood stage, and both proteins failed to exhibit an egress phenotype [111].

1.3.5. Gametocyte egress (Figure 4C)

For successful PVM rupture of sexual stages the parasite requires a temperature drop and contact with xanthurenic acid, but changes in host potassium levels are also sufficient to induce PVM rupture. According to Sologub et al, PVM rupture occurs within two minutes post-activation, after six minutes the PVM has disappeared, and HCM rupture follows 15 minutes later. As in the earlier mechanisms described, gametocyte PVM and HCM rupture is sensitive to different sets of protease inhibitors, which indicates that the two disruptions are distinct [125]. It has been postulated that this might be another immune evasion strategy of the parasite, as the alternative pathway of the human complement system is active for roughly one hour in the mosquito midgut post-feed [153].

The gametocyte PVM ruptures at multiple sites [125], indicating that perforation might be the mode of PVM degradation. Perforin-like proteins have been identified and studied in both rodent and human parasites, but have only recently been linked to PVM rupture. In *P. falciparum*, perforin-like protein 1 (PPLP1) has been shown to locate to the PVM and HCM after microneme discharge. Treatment of RBCs with recombinant PPLP1 confirmed RBC lysis in a dose dependent manner. PPLP1 discharge from micronemes was found to be inhibited by Ca^{2+} chelation, and binding to its target membranes was Ca^{2+} dependent [152]. Pore formation is a highly orchestrated process, initiated by Ca^{2+} release.

Osmiophilic bodies (OB) play a crucial role in gametocyte egress, and they are clearly associated to regions where PVM rupture was initiated [125]. In activated gametocytes, they migrate to the PPM and release their contents into the PV, part of which are gametocyte specific proteins such as PPLP2, Pfg377, *Plasmodium* male development gene-1/protein of early gametocyte 3 (MDV-1/Peg3) and gamete egress and sporozoite traversal (GEST) [165]. PPLP2 is important for gametocyte egress, but PPLP2 knockout parasites ruptured their PVM conventionally [165]. Pfg377 is important for the formation of OB, while MDV-1/Peg3 and GEST have been shown to be important for PVM disruption [166-168]. Recently, a screen based on OB proximity labeling followed by mass spectrometry identification, revealed a novel protein important for gametocyte egress, merozoite thrombospondin-related anonymous protein (MTRAP) [169]. MTRAP *P. berghei* and *P. falciparum* knockout parasites displayed a gametocyte egress defect, that was pinpointed to failed PVM rupture [169, 170].

Identical to asexual stages, for RBC gametocyte egress Ca^{2+} levels are also important, being released post-activation after PVM rupture from internal stores within the parasite [171]. Besides Ca^{2+} levels, protease activity is essential for release from the RBC as demonstrated in several studies using protease inhibitors [172, 173]. While there are still open questions about gametocyte egress, some effector proteins identified in asexual parasites, such as falcipain-1, plasmepsin VI, SERA-6, SERA-7, and PfSUB3, are also expressed in gametocytes and could potentially contribute to gametocyte egress [174].

1.3.6. Nutrient acquisition

Essential nutrients have to be imported via the PVM, and waste products need to be excreted. However, mature erythrocytes are devoid of organelles that would produce substrates that would benefit the parasite, such as a nucleus, endoplasmic reticulum, Golgi apparatus and mitochondria. Hence, *de novo* synthesis of proteins is impossible, RBCs are metabolically mostly inactive, and do not synthesize phospholipids [175]. However, RBCs are filled with hemoglobin, one of the main nutritional sources of blood stage parasites. Nutrient acquisition is facilitated by pores in the PVM (allowing passage of molecules up to 1400 Da during the blood stage [176]) and the tubovesicular network, an PVM extension that reaches into the RBC cytosol [177]. Waste disposal across the HCM and nutrient acquisition from blood plasma is then facilitated via new permeation pathways (NPP) at the HCM [178]. NPPs are induced by the parasite during the trophozoite stage to increase HCM permeability [179]. During the liver stage, the cut-off for molecules that are able to passage the PVM freely is lower, at 855 Da [126]. During the liver stage, *P. berghei* scavenges lipoic acid from the hepatocyte to use it as a cofactor, important for parasite development [180]. Although the parasite is able to synthesize its own lipoic acid, it has a certain requirement for host lipoic acid [181].

Interestingly, during the liver stage, the PVM of *P. berghei* parasites was associated with acidic vesicles from the hepatocyte [182]. Disruption of these acidic vesicles resulted in schizonts of smaller size, which could be due to disruption in the availability of a nutritional source for the parasite. Following on from this study, it seems that the PVM can fuse with host late endocytic vesicles, probably for parasite nutrient supply [183, 184].

1.3.7. Export across the PVM

All proteins and other substrates destined to be exported need to cross two membranes; first the PPM followed by the PVM. After crossing the PPM proteins are unfolded in the PV space, before they are exported across the PVM [185]. Metabolites and everything below the 1400 Da

cut-off during the blood stage [176], and 855 Da during the liver stage [126], can cross the PVM freely. An exception to this has been reported in the case of Ca^{2+}. The RBC cytosol exhibits a naturally low Ca^{2+} environment, but the parasite depends on an internal Ca^{2+} signaling system [186, 187]. It would therefore be detrimental for the parasite to lose its Ca^{2+} via the PVM, and indeed the PVM was found to be impermeable for Ca^{2+} towards the host cytosol. In fact, under experimental conditions Ca^{2+} concentrations in the PV can be 100-1000-fold higher compared to the RBC cytosol. Furthermore, it was demonstrated that during PV formation, the parasite is able to trap extracellular Ca^{2+}, and upon induced calcium release from internal stores, Ca^{2+} is actively pumped into the PV space [188]. Under conditions of low extracellular Ca^{2+} and a permeabilized PVM, the parasite reacts by releasing Ca^{2+} from its internal stores into the PV space, indicating that a high concentration of Ca^{2+} in the PV is crucial for the parasite. This was later confirmed, when parasites were stressed with a transient drop of Ca^{2+} levels, which resulted in decreased invasion of these parasites. According to Gazarini and colleagues, the erythrocyte HCM Ca^{2+} ATPase is transferred to the PVM upon PVM formation, and then actively pumps Ca^{2+} into the PV [188]. In agreement with this, the presence of Ca^{2+} activated channels at the liver stage PVM, which allow import of host molecules, was confirmed by using a Ca^{2+} channel blocker [123]. Availability, storage, and release of Ca^{2+} is critical for successful egress of the parasite [189].

Roughly 10% of all *P. falciparum* proteins are exported into the RBC cytoplasm, but they exceed the size cut-off of molecules that are able to transmigrate the PVM freely. A proportion of exported proteins contain a short *Plasmodium* export element (PEXEL) or host-targeting (HT) motif, but there are also PEXEL/HT-negative exported proteins (PNEPs). Both classes of proteins are transported through a PVM pore, the translocon for exported proteins (PTEX) [190]. The PTEX translocon is made up of five different proteins: heat shock protein 101 (HSP101), exported protein 2 (EXP2), PTEX150, thioredoxin 2 (TRX2) and PTEX88 (Figure 5). The first three proteins form the translocon core, and are essential during the blood stage. Two additional proteins have been found to be non-essential. Although being dispensable, TRX2-KO parasites exhibited reduced growth rates and severe disease in a malaria mouse model, indicating that the component is of importance [191]. In PTEX88 knockout parasites, blood stage development was affected, another hint towards the importance of the component [192]. Experimental evidence has identified EXP2 as being associated with the PVM's membrane spanning form, followed by attachment of PTEX and then HSP101 [193]. PTEX150 is tightly bound to HSP101 and EXP2 via its C-terminus, and a truncated version of the protein

showed decreased affinity to HSP101 and EXP2 [194]. HSP101 is probably the molecular motor of the translocon [195].

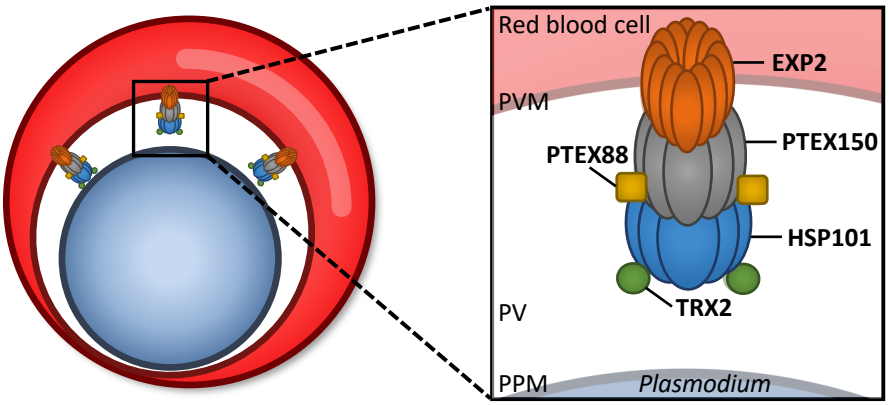

Figure 5: The PTEX translocon. Proteins destined for export into the host cell cytoplasm including PEXEL, HT and PNEP proteins cross the PVM through the PTEX translocon. This is a protein complex located at the PVM. It is made upon five different units: heat shock protein 101 (HSP101), exported protein 2 (EXP2), and PTEX150, PTEX88 and thioredoxin 2 (TRX2).

It is still not yet clear how export is facilitated during the liver stage. In fact, only a few proteins such as LISP2 and *Plasmodium* circumsporozoite protein have been so far identified as being exported into the hepatocyte cytoplasm [196, 197]. Components of the PTEX translocon, that facilitates export during the blood stage, are differently expressed during the liver stage. EXP2 is expressed in liver stages and localizes to the PVM [198]. PTEX150 colocalizes with EXP2 at the liver stage [199]. HSP101 is not present during early liver stages, but is present during late liver stages [191, 198]. The staining pattern of EXP2, HSP101 and PTEX150 was found to be punctuated in individual merozoites, which could be a preparation for the blood stage, to facilitate rapid establishment of the PTEX translocon at the blood stage PVM [191].

A PEXEL-containing GFP was not transported to the cytosol in liver stages but it was stuck in the PVM [198]. It is still unclear whether the PTEX translocon plays a role during liver stages, but one theory is that the individual components might carry out other functions, rather than being part of the multiprotein complex [200]. This hypothesis was proposed because localization studies of four out of the five translocon components indicated that EXP2 and PTEX88 were found at the periphery, TRX2 was additionally found in foci inside the parasite cytoplasm and HSP101 was absent during the first 48 hours of liver development [200].

Export of proteins into the host cell cytoplasm is important for remodeling of the host cell, and for transport to the HCM, and is present in all intracellular *Plasmodium* stages [201]. A large-scale knockout study estimated that 25% of all proteins exported across the PVM are essential for parasite survival [202]. By remodeling the host cell and establishing a membranous structure called the Maurer's clefts (MC), the parasite ensures protein transport and assembly of protein complexes across the cytosol to the HCM. [203, 204]. At the host cell surface the parasite receives environmental information or is able to induce sequestering, crucial for parasite evasion from the circulation and destruction by the spleen, a major virulence factor [205, 206]. To summarize, exported proteins can be delivered to three locations: soluble in the RBC cytoplasm, in MC, or to the HCM either bound to the skeleton or the membrane surface [195].

1.3.8. PVM remodeling and molecular make-up of the PVM

PVM and HCM rupture are sensitive to different sets of protease inhibitors, indicating that their breakdown is either differentially regulated or due to a different composition of the two membranes [103, 104, 111]. Although derived from the HCM, surface proteins of the HCM are removed by the parasite upon invasion and PVM formation [207]. This is probably done proteolytically, similar to removal of PPM proteins during invasion [112, 208]. This removal was also confirmed by the absence of host membrane proteins during the blood and liver stage. In *T. gondii*, the MJ formation was shown to remove host cell membrane proteins during invasion, which could also be the case for the *Plasmodium* PVM [209]. After removal of host proteins, parasite proteins are incorporated into the PVM. Throughout parasite growth and development, the PVM protein composition is altered according to the parasites requirements. The liver and RBC PVM also contain different proteins, while some localize to the PVM during both stages.

It has been hypothesized that rhoptries contain membrane material and indeed, rhoptry secretion occurs during invasion and subsequent PVM formation. A number of rhoptry proteins have been identified in the PVM after rhoptry secretion in *Toxoplasma gondii* [210].

In line with this, the rhoptry-associated protein (RAP) complex has been recently shown to be important for PVM morphology in *P. berghei* parasites [211]. Similar results were shown for high molecular weight rhoptry protein 2 (RhopH2) and stomatin in *P. falciparum* [212]. As the parasite matures, RhopH2 localizes to the RBC cytoplasm in *P. falciparum* [213]. RhopH2 is believed to peripherally associate with the PVM, rather than being an internal membrane protein. Using pull-down assays, it has also been shown to interact with an array of proteins, amongst them other RhopH complex proteins, during the ring and trophozoite stage.

Conditional knockouts of RhopH2 further showed an impact on growth, proliferation, and cycle two of merozoite invasion [213]. The PVM location was also confirmed for the other two RhopH complex proteins (RhopH1 and RhopH3) during the *P. falciparum* blood stage [214].

Other proteins are present at the PVM during different parasite stages, reflected for instance by early transcribed membrane proteins (ETRAMPs). The ETRAMP family consists of 14 proteins in *P. falciparum*, and the members are stage-specifically expressed and best characterized in blood stages [215, 216] (reviewed in [177]). The composition of the PVM can differ between blood and liver stage parasites. One of the ETRAMPs exclusively localizes to the *P. berghei* liver PVM, upregulated in infective sporozoites 3 (UIS3) [217]. UIS3 is one of the few proteins that interacts directly with host proteins. It has been shown to bind to liver-fatty acid binding protein (L-FABP), and downregulation of L-FABP resulted in impaired parasite growth [218]. UIS4 is PVM-localized during the blood stage of *P. falciparum*, and the liver stage of *P. berghei* [219]. UIS3 and UIS4 are essential during the liver stage development in rodents [216, 220]. Other proteins, like the first identified PVM protein exported protein 1 (EXP1) are present at the PVM during both stages of *P. falciparum* and *P. berghei* [221, 222]. Like UIS3, EXP1 recruits host-derived Apolipoprotein H, via its cytosol facing C-terminal, which is important for normal liver stage development [223].

Intra-erythrocytic *P. berghei*-induced structures (IBIS) is a *P. berghei* liver stage PVM protein that has only been recently identified [224]. During the blood stage, it is not PVM-localized but found in MC, indicating that there might be distinct functions of this protein depending on parasite stage. During the blood stage, knockout of the protein resulted in slower growth, but no liver stage phenotype was detected [224]. Interestingly, IBIS generally colocalizes with UIS4 at the PVM, but also localizes to structures distinct to UIS4, and this is observed throughout the entire liver stage [224].

Remodeling of the PVM still poses many open questions, but one such factor important for remodeling has been identified. Sporozoite and liver stage asparagine-rich protein (SLARP) has been found to be important during the early stages of PVM remodeling in hepatocytes. SLARP knockout parasites were able to infect hepatocytes. However key PVM components were not detected in the PVM, due to down-regulation of the respective genes, resulting in developmental arrest [225].

Five years ago Tobias Spielmann reviewed all known PVM proteins, but additional proteins have been identified since then [177]. A few PVM proteins have been already discussed in the above chapters but a complete list is presented in Supplementary Table 1. To date, 41 proteins are found at the PVM during the liver and blood stage; a few are transient residents only, or

have multiple localizations throughout the parasite or host cell. Orthologues between *P. berghei* and *P. falciparum* are given where applicable, as well as the species where localization was initially noted (in *P. berghei, P. falciparum* or in some cases *P. yoelii*).

After their synthesis, PVM proteins are transported and inserted into the membrane. How this is facilitated is still largely unknown. For EXP1, insertion into the PVM has been shown to be independent of PTEX150 and HSP101, the responsible chaperones of the PTEX translocon. It was therefore suggested that another route must be taken by this integral PVM protein [226]. These could either be accomplished via an unidentified translocon or via vesicular trafficking from the PPM to the PVM. How the parasite distinguishes between proteins destined to the PPM or PVM is currently unknown, and no such signal sequence has been identified so far [226]. These examples demonstrate that there are still many open questions around PVM biology, especially around how proteins are targeted and incorporated into this membrane.

1.3.9. Outlook – Identification of novel PVM proteins

The mechanism of PVM degradation to enable egress has been only partly resolved. It is likely that there are unidentified PVM-resident proteins that contribute to this. There have been some attempts at identifying PVM proteins, but its close proximity to the PPM have made this difficult. One approach has been to selectively lyse the different membranes. For instance, the erythrocyte HCM can be lysed by streptolysin O (SLO), leaving the PVM and PPM intact. The remaining parasite can be lysed and the pellet fraction will contain PVM and PPM proteins while all other soluble, non-membrane bound proteins will be present in the supernatant. Saponin selectively lyses the RBC membrane and PVM, giving access to proteins of the PPM in the pellet after lysis [227]. Saponin and SLO both induce pores into the membranes. Because of this it is difficult to separate porated membranes from the membrane of interest [228]. Other factors that have contributed to the limited knowledge about PVM proteins is the lack of functional domains, such as a signal peptide that directs proteins to the PVM, or the lack of homologues of PVM proteins from other Apicomplexa.

Understanding the molecular processes involved in PVM rupture is essential for targeting egress at that step, but remain unknown. Identification of novel PVM proteins is hindered by the fact that a PVM targeting motif is unknown, and many proteins are unique to the genus *Plasmodium*, therefore comparison to other PVM-forming apicomplexan parasites such as *Toxoplasma* is not possible [177]. Biochemical analysis is hindered by the close physical proximity of the PPM and PVM, which creates difficulties in separating the two for individual analyses [229].

1.3.10. Conclusion

Identification and understanding of the molecular players could lead to a novel drug target, preventing PVM disruption, thereby inhibiting egress. Infected erythrocytes and hepatocytes both provoke reactions from the innate and adaptive immune system. Inside hepatocytes, parasites are directly labeled with host autophagy markers, but these are removed by PVM shedding, while other *Plasmodium* proteins are expressed at the RBC surface with great variety, such as PfEMP1, to prevent being targeted for destruction by immune cells [230-234]. On the other hand, the parasite has developed its own strategies to circumnavigate the host immune system [235]. To target *Plasmodium* egress during the liver and blood stage, a deeper understanding of PVM components and biology is needed. The first aim of this thesis is to identify novel PVM proteins during the blood and liver stage of *Plasmodium*.

1.4. Host-pathogen interactions – the heme pathway

Throughout the blood stage, *Plasmodium* parasites reside within mature RBCs or reticulocytes. Erythropoiesis, the process through which mature RBCs are produced, is highly orchestrated. During erythropoiesis, massive amounts of heme are produced. Heme is the constituent of several proteins including hemoglobin, which fulfills the task of oxygen and carbon dioxide distribution throughout the body. RBCs lack most organelles such as the Golgi apparatus, nucleus, and mitochondria, and are often described as “bags full of hemoglobin”. During their blood stage development, *Plasmodium* utilizes hemoglobin as its main nutritional source and incorporates host heme into its mitochondrial cytochromes. *Plasmodium* comprises its own heme pathway for *de novo* heme production throughout the life cycle, and this has been studied in detail. Interestingly, host heme enzymes seem important for parasite development during the blood stage as well, but this process is still enigmatic. As part of this thesis, porphobilinogen deaminase and coproporphyrinogen oxidase, two host heme enzymes, are studied in detail for their role during blood stage malaria infection.

1.4.1. RBCs and Reticulocytes

Erythropoiesis is tightly regulated, and takes place mainly in the bone marrow and in the spleen, until cells differentiate to reticulocytes, at which point they migrate into blood vessels. Different *Plasmodium* species exhibit preferences for either RBCs or reticulocytes. While *P. falciparum* invades mature RBCs, *P. vivax* only invades reticulocytes. It has recently been demonstrated that young reticulocytes, which still express the transferrin surface receptor CD71, are the preferred cell-type of *P. vivax* during invasion [236], and that it expresses a specific receptor,

which binds to transferrin receptor 1 on the host reticulocyte for invasion [237]. The membrane of reticulocytes contains enzymes that synthesize phospholipids, therefore phospholipid synthesis is still active in these cells compared to RBCs, which could also be a beneficial source of phospholipids for the parasite. Compared to reticulocytes and other RBC precursors, mature RBCs are metabolically mostly inactive, and do not synthesize phospholipids [175, 238]. They are highly specialized cells, devoid of organelles, and are responsible for oxygen transport throughout the body. To do so, they make use of hemoglobin, which contains an iron atom at its center, which in its ferrous stage can reversibly bind to oxygen [239]. Carbonic anhydrases and the anion exchange activity of the RBC membrane Band 3 protein mediate the recognition of metabolically active tissues, thereby replacing carbon dioxide with oxygen where needed [240]. Hemoglobin, the main component of RBCs, is produced during erythropoiesis and discussed below.

1.4.2. Heme pathway

Heme is an essential component of hemoglobin, cytochromes, catalases and other molecules [241]. The mammalian heme canonical pathway consists of eight enzymes catalyzing the production of heme from succinyl coenzyme A and L-glycine, derived from the citric acid cycle (Figure 6). The first step is catalyzed by the mitochondrial enzyme aminolaevulinate synthase (ALAS), followed by the next four cytosolic steps: aminolaevulinate dehydrase (ALAD), porphobilinogen deaminase (PBGD), uroporphyrinogen III synthase (UROS) and uroporphyrinogen decarboxylase (UROD). The final steps are catalyzed in the mitochondria by coproporphyrinogen oxidase (CPOX), protoporphyrinogen oxidase (PPOX) and ferrochelatase (FC) which catalyzes the insertion of ferrous iron to finally form protoheme [242]. Globin protein production is induced after heme production, and hemoglobin is assembled as a tetramer of two α- and two β-globin chains with heme as a prosthetic group. Deficiency in any of the heme pathway enzymes leads to a group of diseases called porphyria (Figure 6), caused by lower heme formation and accumulation of pathway products, especially porphyrinogens in their oxidized porphyrin state [243, 244]. The porphyrias can be divided into acute or cutaneous types, and attacks of acute porphyrias can be fatal in rare cases [245]. Symptoms of acute porphyria, which mainly affects the nervous system, are gastrointestinal and neuropathic symptoms. Cutaneous porphyria symptoms, include photosensitivity and skin conditions such as redness, edema, and blisters. The attacks can be triggered by drugs which influence heme requirement, interfere with heme regulation or interfere with the heme pathway enzymes [246]. Fasting can be another trigger which activates ALAS, and leads to a higher production of heme

intermediates [247]. Heme requirement can rise due to increased oxidative processes performed by cytochromes (which contain heme) [248].

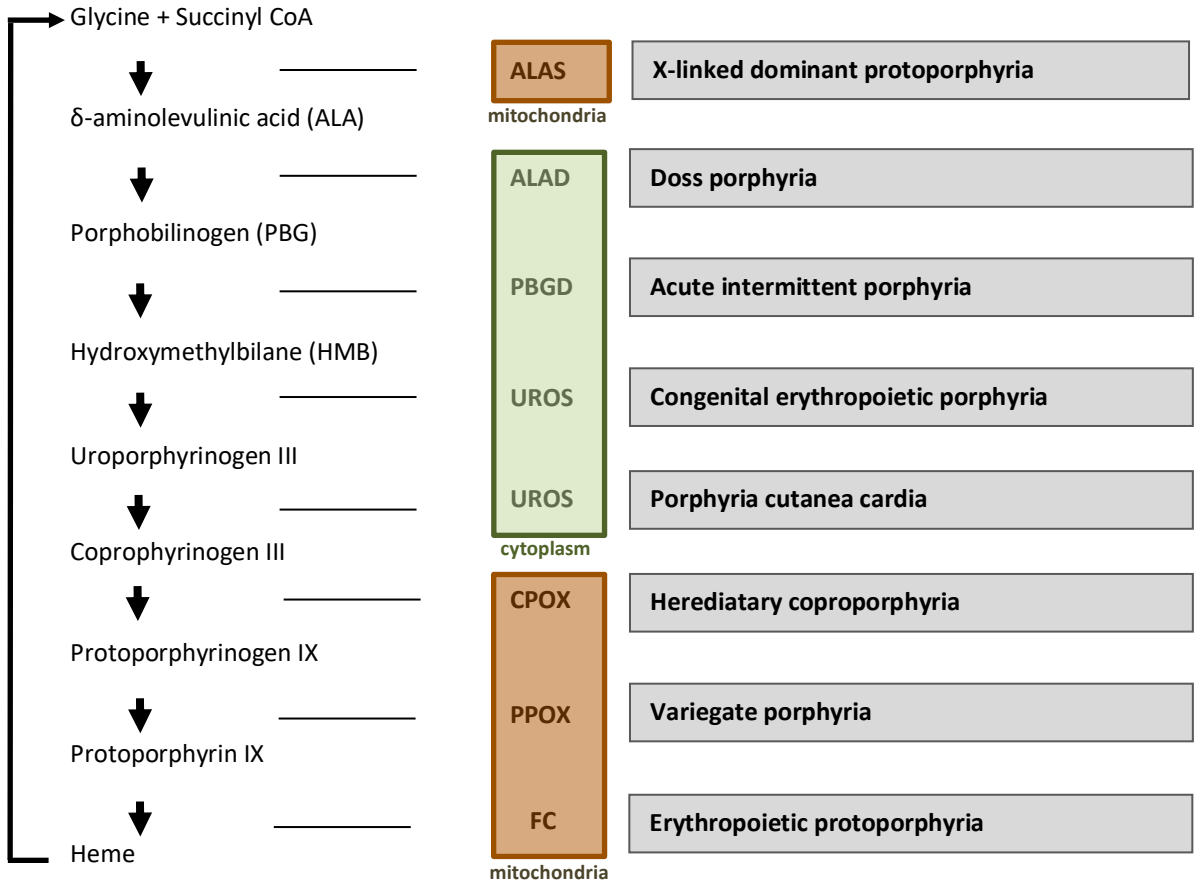

Figure 6: The heme pathway and types of porphyrias which are induced by heme enzyme deficiencies. Deficiency of each enzyme of the heme pathway results in a different type of porphyria. Heme exerts a negative feedback control on ALAS and this is rate-limiting. ALAS, aminolevulinic acid synthase; ALAD, aminolevulinic acid dehydratase; PBGD, porphobilinogen deaminase; UROS, uroporphyrinogen III synthase; UROD, uroporphyrinogen decarboxylase; CPOX, coproporphyrinogen oxidase; PPOX, protoporphyrinogen oxidase; FC, ferrochelatase.

As part of this thesis, two mouse strains with mutations in the PBGD or CPOX gene were analyzed. Therefore, more details about these heme enzymes are provided here. More details on the heme pathway including substrates, intermediates and the final heme molecule are given in Supplementary Figure 1 [249].

ALAS is the first enzyme of the heme pathway, and catalyzes the condensation of succinyl coenzyme A and L-glycine, derived from the citric acid cycle, to yield δ-aminolevulinic acid. It is the rate-limiting enzyme of heme production and regulates the pathway on transcriptional and post-transcriptional level. ALAS itself is regulated by heme [250]. A gain of function mutation in the erythroid ALAS gene causes an upregulation of substrate production (glycine and succinyl CoA) and leads to X-linked dominant protoporphyria [251].

ALAD catalyzes two molecules of δ-aminolevulinic acid to form porphobilinogen (PBG)

PBGD requires two molecules of (PBG) as a cofactor to perform the third step of the heme pathway, enabling head to tail condensation of four molecules of PBG, to yield the linear tetrapyrrole hydroxymethylbilane (HMB) [252]. Deficiency in PBGD can result in acute intermittent porphyria (AIP), that has a prevalence of around 1 in 75,000 in Europe. AIP is characterized by irregular, acute episodes of gastrointestinal and neuropathic symptoms, due to a build-up of porphyrin intermediates. Between those episodes, the patient is healthy [253]. Around 200 causative mutations have been described for AIP, whose manifestations of disease symptoms are dependent on factors such as residual enzyme activity, but also various other stimuli, such as fasting and drug use, especially barbiturates and sulfonamide antibiotics [254, 255]. Inhibitors of PBGD have been identified that are very similar to PBG, however they are not commercially available, and the synthesis requires many intermediate steps preventing a large-scale synthesis [256].

UROS cyclizes HMB (which is unstable) to form uroporphyrinogen III, and this also involves a rotation of the molecule. HMB can also be non-enzymatically cyclized, but results in the formation of uroporphyrinogen I, which is physiologically unusable [257].

UROD catalyzes the decarboxylation of four acetate groups of uroporphyrinogen III to yield coproporphyrinogen III.

CPOX executes the sixth heme pathway step, by performing oxidative decarboxylation of two out of coproporphyrinogen's four rings to produce protoporphyrinogen IX [258]. It comprises an N-terminal mitochondrial target sequence, leading it to the mitochondrial intermembrane space (IMS), acting as a homodimer with no cofactor needed for activity [243, 259]. Using cell culture assays, increased or reduced activity levels of CPOX were linked to increased or decreased amounts of heme, indicating a regulatory role of CPOX in the heme pathway [260]. Deficiency in CPOX enzyme activity can result in hereditary coproporphyria (HCP) which has 0.2 newly diagnosed cases per million each year [244, 253, 261]. Harderoporphyria, a variant form of HCP, is characterized by mutations affecting a specific part of the enzyme [262]. Around 20 causative mutations have been described in the literature. They are rare in the human population, but could be underdiagnosed, as manifestations of HCP symptoms are often absent in individuals even in the same family with the same CPOX mutation [263]. It is estimated that half of the affected individuals remain asymptomatic carriers [248]. HCP belongs to the group of acute hepatic porphyrias. Acute attacks are triggered by substances acting on the liver, such as hormones, fasting and porphyrinogenic drugs, such as progesterone contraceptives, and barbiturates [248]. It is characterized by gastrointestinal symptoms, seizures, and hypertension,

as well as an increased amount of substrates excreted in feces and urine [253, 259]. There is no specific CPOX inhibitor available but previous research has identified, heme, bilirubin, cadmium, and mercury to have inhibitory effects on the protein [264]. Inhibition by heme could be due to a feedback loop, important for CPOX regulation.

PPOX oxidizes protoporphyrinogen IX to form protoporphyrin IX.

FC performs the last step of the heme pathway, and catalyzes the insertion of ferrous iron into protoporphyrin IX, yielding protoheme IX. It is localized but not synthesized in the mitochondria and is, after ALAS, the second rate-limiting enzyme of the pathway. Similarly to all heme enzymes, it is highly conserved in prokaryotes and eukaryotes [265]. Deficiencies in FC caused by a mutation result in erythropoietic protoporphyria [266].

1.4.3. Hemoglobin is a nutrition source during the blood stage

Plasmodium endocytoses hemoglobin and digest it in their FV to gain access to amino acids [267]. During erythrocytic growth, up to 70% of hemoglobin within a RBC is digested by the parasite, therefore providing it with one of its main nutrition sources [268]. By demonstrating that *P. falciparum* is able to grow within cell culture medium supplemented only with a single amino acid, isoleucine (the only amino acid lacking in hemoglobin), Liu et al, proved that hemoglobin is indeed one of the most important nutrient sources of blood stage parasites. This was further emphasized when the hemoglobin degradation machinery was impaired, impeding the growth of the parasite, even though the medium was complemented with isoleucine [269]. The parasite relies on heme as a cofactor for cytochromes in its mitochondria [270]. As part of hemoglobin breakdown, vast amounts of free heme are produced, which is highly toxic to the parasite by inducing membrane changes or inhibiting enzymes [271]. Therefore free heme is polymerized and stored as hemozoin to prevent damage by reactive free heme [272] and to keep free heme levels low [273]. Preventing hemozoin formation, for instance by chloroquine, increases free heme concentration and is fatal for the parasite [268, 273].

Hemoglobin is the main component of RBCs, but how is it synthesized by a metabolically mostly inactive cell missing cellular organelles? While some heme pathway enzymes are present in RBCs, heme biosynthesis is minimal in RBCs, and occurs in progenitor cells in which heme pathway enzymes are highly expressed, and all cellular organelles are present [274-276]. In addition to heme synthesis in blood progenitors, heme synthesis in non-erythroid cells, called housekeeping heme synthesis, is also important [277]. Erythroid production of heme is estimated to account for 75% of produced heme, and the remaining 25% are believed to be produced in the liver [278, 279]. In the liver, 50% of all heme is incorporated into cytochrome

P450, which is of importance, as cytochrome P450 metabolizes endogenous and foreign molecules [280].

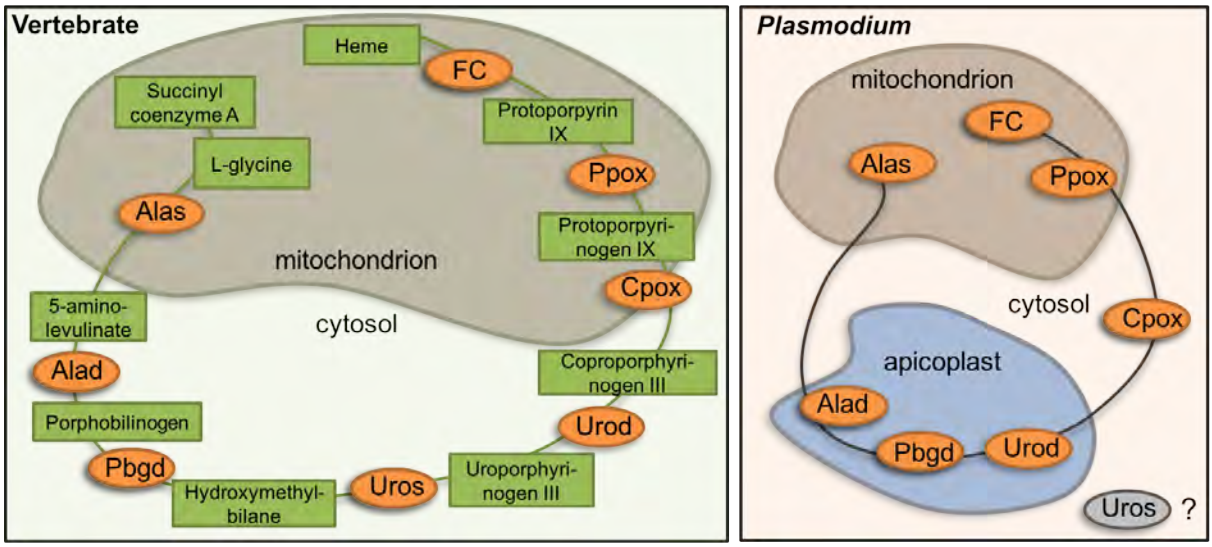

Figure 7: Enzymes and intermediate products of the heme biosynthetic pathway. The canonical heme pathway in the vertebrate host and *Plasmodium* is a hybrid pathway for both. It uses succinyl coenzyme A and L-glycine to produce heme. Oval shapes contain the enzymes and rectangular boxes the substrates and products.

In non-erythrocytic stages, especially while residing in the mosquito, the parasite has limited access to hemoglobin as a nutritional source. During hemoglobin breakdown, heme is made available and can be utilized in other parasite proteins. *Plasmodium* parasites have their own *de novo* heme pathway (Figure 7) that is able to cover for the absence of hemoglobin, spanning the apicoplast (ALAD; PBGD; UROD), cytosol (CPOX) and mitochondria (ALAS; PPOX; FC), with all heme enzymes represented apart from UROS [281]. To date, *Plasmodium* UROS remains to be identified and it is unclear how the parasite compensates for the absence of this enzyme. UROS is necessary to cyclize and rotate unstable HMB, and non-enzymatically cyclized HMB is physiologically unusable [257]. PfPBGD, the preceding heme enzyme, can exhibit low UROS activity. Compared to host enzyme activity, PfPBGD activity is low [282]. Despite the abundance of hemoglobin during the blood stage, *P. falciparum* and *P. berghei* synthesize heme *de novo* [283]. The *Plasmodium* heme pathway is not essential during the blood stage, but is important for oocyst formation, essential for sporozoite development, and was lately also confirmed to be essential during the liver stage [284, 285]. Almost two decades ago, *Plasmodium* heme metabolism has been described as a major antimalarial drug target [267]. Much research effort has gone into answering questions concerning the heme pathway, heme metabolism, and the role of host heme. Several *Plasmodium* heme enzymes were

subjected to knockout or knockdown studies to shed light on this, and the findings are presented here.

One such study knocked out the first and the last enzyme of the *P. berghei* heme pathway, and analyzed parasites during the life cycle [285]. In the blood stage, no significant difference in parasite growth was observed, compared to wild-type parasites. However, during the mosquito stage, oocyst numbers were reduced, and no sporozoites could be detected in the salivary glands. In liver stages, ALAS knockout sporozoites failed to induce a blood infection in mice, but infectivity was restored when mice were given drinking water supplemented with aminolevulinic acid (ALA), which is usually synthesized by ALAS from succinyl coenzyme A and L-glycine [285]. Similar results were observed for *P. falciparum* when ALAS and FC knockout or double knockout parasites grew normally during the blood stage [270]. In FC knockout parasites, *de novo* heme synthesis was not detected, they displayed a reduction in male gamete formation, and did not develop any oocysts, making FC essential during the mosquito stage [270]. A third research group has confirmed that *P. berghei* FC is essential during the mosquito and liver stage [284].

P. falciparum CPOX and PBGD knockout parasites were used to infect RBCs supplemented with ALA. The absence of these two enzymes did not influence the parasitized cells' ability to incorporate ALA into heme, indicating that host heme enzymes are able to cover for the absence of PfCPOX and PfPBGD [286]. Importantly, this effect was not observed when the surrounding RBC was removed; no coproporphyrinogen III (CPP), protoporphyrin IX (PPIX) or heme with incorporated ALA was detected, indicating that host heme enzymes are responsible for the ALA incorporation into heme in these knockout parasites. This study also suggested that there is no activity of parasite heme enzymes during the blood stage [286]. To conclude, *de novo* synthesis of heme by the parasite is stimulated by exogenous ALA (which enters the RBC via NPP induced by the parasite), and PPIX is produced by normally inactive host enzymes. PPIX is then used by PfFC to produce heme.

ALAS, PBGD and UROD were knocked out in *P. berghei* and all showed regular oocyst formation. Oocyst size however was smaller in all knockouts and no salivary gland sporozoites were observed. All three knockout parasites failed to establish an infection in mice, but for ALAS this was rescued by addition of ALA during sporogony [287]. Rescued ALAS knockout parasites were able to develop a (reduced) liver infection *in vivo* and subsequent (delayed) blood stage infection. As part of these studies they also confirmed that liver stage parasites are able to scavenge ALA *in vivo* [287].

Three enzymes (ALAD; PBGD; UROD) of the canonical *Plasmodium* heme pathway are localized to the apicoplast. This is their second essential endosymbiont, next to their mitochondria [288]. It is thought to be of cyanobacterial origin, therefore it was hypothesized that the parasite must have originally comprised a second heme pathway, acquired via cyanobacteria [288, 289]. Strikingly, both endosymbionts are usually found in close proximity during the blood stage. Could substrate exchange be the reason [238, 290-292]? That is unlikely: during most of the liver stage, the apicoplast and mitochondria are often found apart from each other [293]. It seems that the parasite lost functional genes from both pathways, because only three out of eight enzymes are apicoplast-localized. Additional studies implicated that enzymes of both heme pathways (acquired via uptake of the apicoplast and mitochondria) might still be active. Parasites, when given access to isopentenyl pyrophosphate, can survive apicoplast absence [294]. Apicoplast-devoid infected RBCs were able to maintain a functional heme pathway, albeit absence of three *Plasmodium* heme enzymes. The origin of these enzymes (whether host or parasite derived) was not identified [286].

While the three enzymes are apicoplast-targeted, the genes encoding for ALAD, PBGD and UROD have been transferred from the apicoplast genome to the *Plasmodium* nuclear genome, as most apicoplast genes have, and contain an apicoplast target sequence. They therefore need to be transported from the nucleus to the apicoplast [295]. Here the Golgi is responsible for sorting apicoplast-targeted proteins; it is therefore unlikely that these proteins diffuse freely and remain soluble and available in the cytoplasm after translation [296]. It is also possible that there are unidentified additional mitochondrial or cytosolic heme pathway enzymes, that are able to compensate for absence of apicoplast localized enzyme. The retained ability of parasites to synthesize heme, even in the absence of an apicoplast, could hint at the existence of an unidentified non-canonical heme pathway [286], also postulated by Goldberg and colleagues [297]. Such a pathway was recently described for gram-positive bacteria using coproporphyrin as a substrate instead of protoporhyrin to produce coproheme, which is then later decarboxylated to yield protoheme [298]. While these are all valid points, it is likely that absence of the apicoplast enzymes was covered by cytosolic host heme enzymes (ALAD; PBGD; UROD) [286].

Other studies have focused on the role of host enzymes synthesizing heme during the *Plasmodium* blood stage. Functional studies of uninfected RBC extracts failed to detect synthesis of the final product heme, but CPP and PPIX, the preceding products, were detected [286]. The formation of PPIX is only possible through CPOX, indicating that uninfected RBCs

contain CPOX. Although it is believed to localize to the IMS, similar results have been observed for cytochrome c, also localized to the IMS, but was discovered in the cytosol [299].

Host cell ALAD and FC have been localized inside the parasite, indicating that the parasite imports host enzymes [300, 301]. Using a combination of different assays, PfALAD activity accounted for 10%, the remaining activity was postulated to be covered by the host ALAD enzyme during the *P. falciparum* blood stage [302]. This phenomenon has been described for different proteins, but the underlying import mechanism remains to be identified as the PVM allows free passage of molecules only up to 1400Da [303, 304]. Following on from their initial findings, Bonday and colleagues then propose a mechanism of how host ALAD is scavenged from the RBC [305].

In principle, host FC (hFC) could be scavenged from the RBC to fulfil the final step of heme synthesis. Whether hFC is present in mature RBCs is an ongoing debate, because it localizes to the mitochondria and mature RBCs lack mitochondria. FC catalyzes the production of heme, and the parasite uses heme in its respiratory cytochromes, also present in the mitochondria [289]. While mass spectrometry detected hFC in mature RBCs [274, 306] other studies have failed to do so due to the high hemoglobin content of RBCs and low abundance of these enzymes [307, 308]. In a recent study, FC was indeed found, but the authors indicated a 0.1% contamination with reticulocytes in their sample, which could explain the presence of hFC [306]. As part of this study, all cytoplasmic heme enzymes (ALAD, PBGD, UROS, UROD) were identified as well as CPOX and FC, which are mitochondria-localized [306].

It is possible that during mitochondrial destruction hFC remains in the cytoplasm, or that after hFC synthesis residual hFC is still present in the cytoplasm, waiting to be transported to the mitochondria, shortly prior to RBC maturation. Functional studies, similarly to mass spectrometry studies, have found contradictory evidence on the presence of hFC in RBCs. During infection, hFC was present in the *P. falciparum* cytoplasm, detected by immunofluorescence [301]. Both enzyme activities have been measured, and surprisingly, hFC accounted for 80% of the enzyme activity compared to 20% of PfFC. *In vitro* studies showed hFC activity to be three times higher than PfFC [301]. Studies on rodent and human *Plasmodium* species have identified hFC as being required for parasite growth, albeit having its own FC. *P. berghei* FC knockout parasites displayed no growth difference during the blood stage [309]. Interestingly, these findings were connected to hFC but not to elevated substrate [309]. Finally, scavenged host enzymes could also be used to supplement the parasites' own *de novo* heme synthesis [310]. Together these data support the hypothesis that the mature RBC retains a vestigial and partial heme biosynthesis pathway but does not contain all heme enzymes

[286]. So far, no role of host PBGD and CPOX during malaria infection has been described, which is why this thesis sets out to do so.

Previously it was shown that PfPBGD and PfCPOX knockout parasites can incorporate ALA into heme, indicating that host enzymes are able to cover for the absence of the parasite enzymes [286]. Importantly, RBC removal showed no ALA incorporation into heme, indicating that the parasite has a requirement for these enzymes to synthesize heme *de novo* in the absence of its own heme enzymes and that there is no activity of parasite heme enzymes while in RBCs [286]. PbPBGD knockout parasites showed no oocyst formation defect. Oocyst size, however, was smaller, no salivary glands sporozoites were observed and the parasites also failed to establish an infection in mice [287]. CPOX has not yet been subjected to knockout studies in *P. berghei*, therefore information on its role during the mosquito or liver stage is missing. It was postulated that PfCPOX might not be active in the blood stage [286]. It is however interesting to note that PfCPOX was bacterially expressed and confirmed to be active which might be important during other parasite stages apart from the blood stage [311]. By reducing available host enzymes by using an enzyme deficient host this hypothesis could be answered and settle the debate whether host heme enzymes are important during the *Plasmodium* blood stage. The presence of hFC in mature RBCs is still not clear, but PBDG is cytosolic and CPOX was confirmed to be present in the RBC cytosol. Studies on these proteins, therefore are useful to see whether these are used by the parasite to form a hybrid pathway between the host and parasite enzymes to perform *de novo* production of heme. To answer this, in-depth studies on rodent and human malaria parasites were performed *in vivo* in the rodent and *in vitro* in the human host.

1.4.4. Conclusion

Current strategies to control malaria comprise of anti-malarials that target the parasite at the clinical blood stage, and insecticides or mosquito-nets that prevent its transmission. Recently, state-of-the art anti-malarials have been reported to lose their effectiveness because *Plasmodium* species develop resistance, due to their high mutation rate and huge variation in the host response to the disease [312, 313]. Immunization approaches by using attenuated sporozoites or the vaccine RTS,S/01 have shown some promising results, but have also disappointed in regard of effectiveness [67, 314]. All of the above-mentioned measures against malaria have been successful in some respects – some countries suffering from malaria in the past are now declared malaria-free. Extensive drug use and vector control have halved the estimated deaths between 2000 and 2015. This was mainly due to a massive increase in funding from only US$200 million annually to US$2 billion annually, which was mainly spent on access

to ACT and distribution of insecticide treated bed nets [315, 316]. However, the recent WHO malaria report informed about a slight increase in malaria deaths comparing the years 2015 and 2016 [1, 3]. This suggests that these preventative strategies have reached a maximal point of effectiveness, and therefore novel treatment and prevention strategies are urgently needed to reverse this trend, and lead to the ultimate goal of completely preventing future malaria infections.

1.5. Project Aims

Host-parasite interactions are highly complex and increase in complexity for parasitic diseases when different hosts and vectors are involved. A deeper understanding of parasite biology and the role of the host will improve the knowledge and therefore ease the path to malaria eradication. This thesis seeks to improve the understanding of both parasite and host contributions to malaria infection. When the parasite has invaded mammalian blood cells, it forms a PVM that acts as a membrane between the parasite and the host RBC membrane. However, the protein components of the PVM remain largely unknown, and therefore this project has utilized a proximity-based detection technique (BioID) to identify new protein components of the PVM. To evaluate host-mediated pathways of malarial infection, the mouse genome was randomly mutated (ENU), and a mutant was identified that confers a modest degree of protection against malarial infection. The project of this thesis was to identify the mutation responsible for this phenotype and its involvement in *Plasmodium* infection. This was mapped to a gene of the host heme pathway, and therefore this project has explored the role of host enzymes which synthesize heme on *Plasmodium*. This was extended to a second mutagenized host heme enzyme by using a mouse strain that was established by collaborators from the Monash University. Its contribution during *Plasmodium* infection was described.

Specifically, the aims of this thesis were:

Aim 1 – to identify novel PVM proteins during the blood and liver stage by establishing BioID.
Aim 2 – to characterize the role of host PBGD and CPOX during the blood stage of malaria infection.

2. Publication and manuscripts

2.1. BioID reveals novel proteins of the *Plasmodium* parasitophorous vacuole membrane

Candidate's contribution to this chapter: 95% (majority of experimental work, data analysis, paper writing and figure preparation).

Remaining 5% of experimental work was contributed by Damaris-Bausch Fluck who analyzed the mass spectrometry data, and Paul Burda and Francis Brühlmann who provided basic laboratory assistance with some experiments.

AMERICAN SOCIETY FOR MICROBIOLOGY | mSphere™ AN OPEN ACCESS JOURNAL PUBLISHED BY THE AMERICAN SOCIETY FOR MICROBIOLOGY
Accepted Manuscript
RESEARCH ARTICLE
Host-Microbe Biology

BioID reveals novel proteins of the *Plasmodium* parasitophorous vacuole membrane

Cilly Bernardette Schnider[a,b,c], Damaris Bausch-Fluck[d,e], Francis Brühlmann[a], Volker T. Heussler[a], Paul-Christian Burda[a]#*

[a]Institute of Cell Biology, University of Bern, Bern, Switzerland.
[b]Graduate School for Cellular and Biomedical Sciences, University of Bern, Bern, Switzerland.
[c]Department of Biomedical Sciences, Faculty of Medicine and Health Sciences, Macquarie University Sydney, NSW, Australia.
[d]Institute of Molecular Systems Biology, ETH Zurich, Zurich, Switzerland.
[e]Department of Health Sciences and Technology, BMPP, ETH Zurich, Zurich, Switzerland
#Address correspondence to Paul-Christian Burda, burda@bnitm.de.
*Present address: Bernhard Nocht Institute for Tropical Medicine, Hamburg, Germany

ABSTRACT

During their development within the vertebrate host, *Plasmodium* parasites infect hepatocytes and red blood cells. Within these cells, parasites are surrounded by a parasitophorous vacuole membrane (PVM). The PVM plays an essential role for the interaction of parasites with their host cells, however only a limited number of proteins of this membrane have been identified so far. This is partially because a systematic proteomic analysis of the PVM's protein content has been difficult in the past, due to difficulties to separate the PVM from other membranes such as the parasite plasma membrane. In this study, we adapted the BioID technique to *in vitro* cultivated *Plasmodium berghei* blood stage parasites and utilized the promiscuous biotin ligase BirA* fused to the PVM-resident exported protein 1 to biotinylate proteins of the PVM. These we further processed by affinity purification, liquid chromatography based mass spectrometry (LC-MS/MS) and label-free quantitation leading to a list of 61 known and candidate PVM proteins. Seven proteins were analyzed further during blood and liver stage development. This resulted in the identification of three novel PVM proteins, which were the serine/threonine protein phosphatase UIS2 and two conserved *Plasmodium* proteins with unknown functions (PBANKA_0519300 and PBANKA_0509000). In conclusion, our study expands the number of known PVM proteins and experimentally validates BioID as a powerful method to screen for novel constituents of specific cellular compartments in *P. berghei*.

IMPORTANCE

Intracellular pathogens are often surrounded by a host-cell derived membrane. This membrane is modified by the pathogens to their own needs and is crucial for their intracellular lifestyle. In *Plasmodium* parasites, this membrane is referred to as the PVM and only a limited number of its proteins are known so far. Here, we applied in rodent *P. berghei* parasites a method called BioID, which is based on biotinylation of proximal and interacting proteins by the promiscuous biotin ligase BirA*, and demonstrated its usefulness in identification of novel PVM proteins.

INTRODUCTION

Malaria is a widespread disease putting half of the world's population at risk of infection and leading to nearly half a million deaths per year (1). The causative agent of the disease is *Plasmodium,* a parasite transmitted by infected *Anopheles* mosquitoes during a blood meal. After injection into the skin of a vertebrate host, *Plasmodium* sporozoites actively enter blood vessels and reach the liver where they infect hepatocytes. Here they undergo a first round of multiplication. After release from the liver, parasites repeatedly invade and multiply within red blood cells (RBCs), leading to the symptoms of malaria. Within hepatocytes and RBCs, *Plasmodium* parasites reside within a specialized compartment referred to as the parasitophorous vacuole (PV) and are surrounded by the PV membrane (PVM), which is initially formed by invagination of the host cell membrane (HCM) during the process of invasion (reviewed in (2)). The PVM is extensively remodeled by the parasite, and as the interface between the parasite and its host cell it plays fundamental roles in nutrient acquisition, host cell remodeling, waste disposal, environmental sensing and protection from innate defense mechanisms of the host cell (reviewed in (3)). At the end of parasite development in hepatocytes and RBCs, parasites induce disruption of

the PVM and the HCM, which is essential for their release from host cells and for propagating the infection. Only a limited number of PVM proteins have been identified so far and the functions of most of these remain elusive (reviewed in (3, 4)). These include the earliest known PVM protein exported protein 1 (EXP1), which contains a classical N-terminal signal peptide and is inserted into the PVM of blood and liver stage parasites with its transmembrane domain, whereby the C-terminus faces the host cell cytoplasm (5–8).

EXP1 was shown to be refractory to gene deletion, indicating an essential role for asexual blood stage development as gene targeting is performed in this stage (9). In line with its predicted glutathione S-transferase activity, EXP1 has the ability to conjugate glutathione onto hematin *in vitro* (10). Furthermore, evidence was provided that the C-terminal portion of EXP1 specifically interacts with host Apolipoprotein H and that this interaction is crucial for development of the parasite within the liver (11). Other prominent PVM proteins are the components of the *Plasmodium* translocon of exported proteins (PTEX), mediating the export of proteins into the host cell (12), and proteins belonging to the family of the early transcribed membrane proteins (ETRAMPs) (13).

In general, many more PVM proteins have been identified in blood stage parasites in comparison to liver stages, where only a handful of PVM proteins are known so far (reviewed in (3, 4)). Apart from EXP1, these liver stage PVM proteins include the two members of the ETRAMP family UIS3 and UIS4, the knockout of which leads to parasites arrested in early liver stage development (14, 15), or the phospholipase PbPL whose deletion results in parasites that are impaired in rupturing the liver stage PVM during egress from host hepatocytes (16).

A systematic proteomic analysis of the PVM's protein composition has been difficult in the past, due to difficulties to separate the PVM from other membranes like the parasite plasma membrane (PPM). In this study, we applied the BioID technique to identify novel proteins of the *Plasmodium* PVM. This biochemical approach is based on the promiscuous biotin ligase BirA*, which can be fused to a protein of interest and upon addition of biotin leads to the biotinylation of proximal and potentially interacting proteins that can be affinity purified and identified by mass-spectrometry (17). Using EXP1 as a bait, we identified 61 known and candidate PVM proteins. We further analyzed a subset of these candidates by endogenous GFP-tagging during blood and liver stage development, leading to the discovery of three novel PVM proteins.

RESULTS

Tagging of the PVM-resident protein EXP1 with the biotin ligase BirA*

To identify novel proteins of the *Plasmodium* PVM, we adapted the BioID approach and fused the biotin ligase BirA* to EXP1, which is a known protein of the PVM in blood and liver stage parasites (Fig. 1A). For this aim, we generated the plasmid pL0017-^{C}EXP1-BirA*-V5, encoding an EXP1-BirA* fusion protein with a C-terminal V5-tag under the control of the constitutive *P. berghei eef1α* promoter (Fig. 1B). This vector integrates by single crossover homologous recombination into either the *c-* or *d-ssu-*rRNA locus of *P. berghei* and conveys resistance to pyrimethamine. We transfected it into blood stage schizonts of marker-free parasites expressing mCherry under the constitutive *P. berghei hsp70* promoter (16). The parental strain expressing mCherry was used as a control and is further referred to as wild-type (WT). We obtained transgenic EXP1-BirA*-V5 parasites after drug selection and confirmed successful integration into the genome by PCR (Fig. S1).

To investigate whether this construct is expressed in blood stages and leads to the biotinylation of PVM proteins, we isolated the blood of mice infected with transgenic EXP1-BirA*-V5 parasites by cardiac puncture and cultivated it in an *in vitro* schizont culture for 18 hours in the presence of 150 µM biotin. Biotinylated proteins were visualized by immunofluorescence analysis (IFA) using fluorescently labeled streptavidin. As expected, we observed a strong streptavidin signal, which was peripherally located around parasites and co-localized with the V5-tagged EXP1-BirA* fusion protein (Fig. 1C). We further confirmed this finding by performing Western blots of EXP1-BirA*-V5 parasites grown in the presence or absence of biotin and parental WT parasites cultivated in the presence of biotin. We observed a substantial increase in biotinylated proteins in lysates of EXP1-BirA*-V5 parasites grown in the presence of biotin in comparison to WT and no-biotin controls (Fig. 1D), where only very few biotinylated proteins were visible. In conclusion, these data demonstrate that EXP1-BirA*-V5 is active and biotinylates a range of target proteins at the parasite periphery.

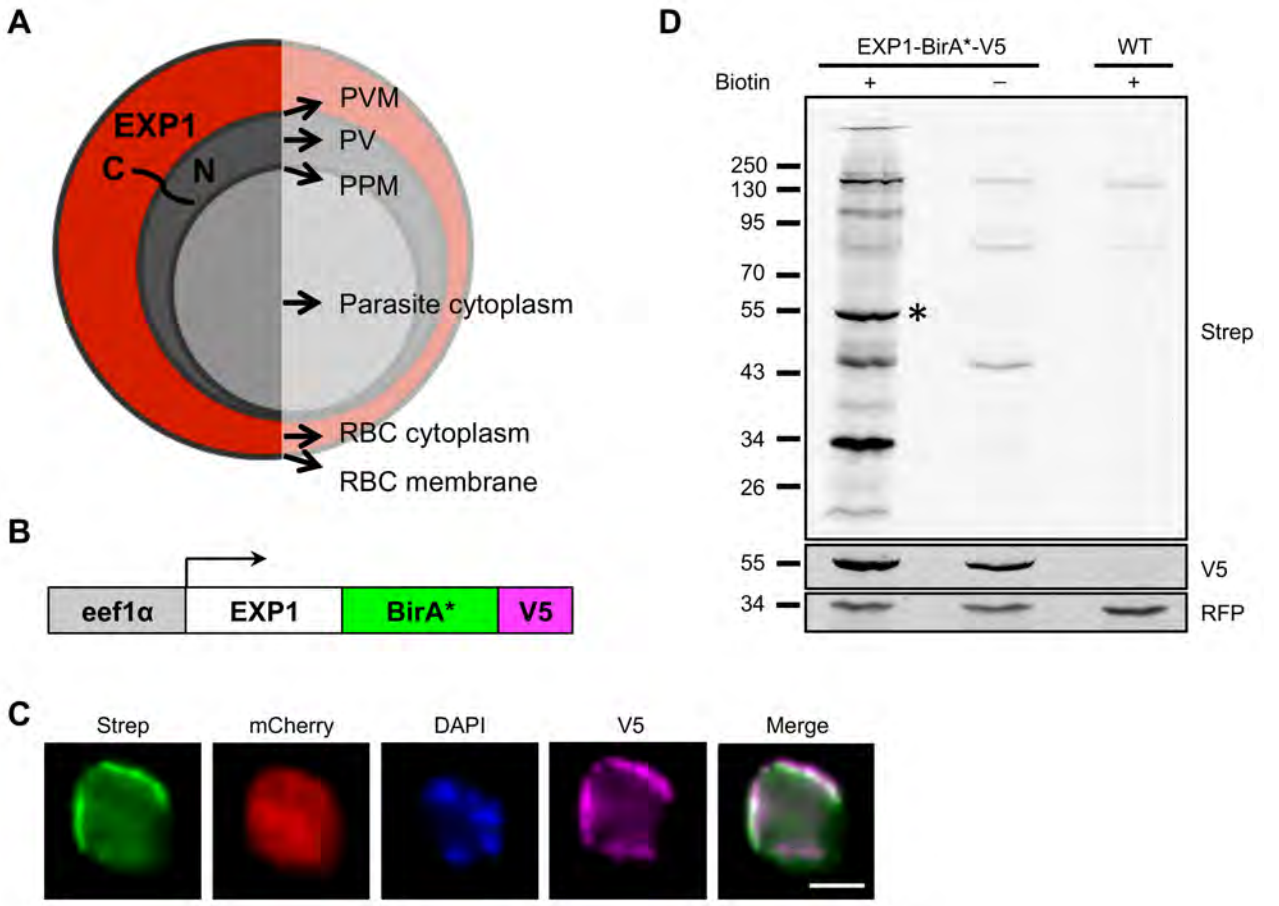

Figure 1. Expression of EXP1-BirA*-V5 leads to biotinylation of proteins at the parasite periphery. A) Localization of EXP1 within *Plasmodium* infected erythrocytes. B) Schematic representation of the expression cassette encoding EXP1 fused to BirA* with a C-terminal V5-tag driven by the constitutive eef1alpha promoter. C) IFA of EXP1-BirA*-V5 blood stage parasites grown for 18 hours in the presence of biotin. Biotinylated proteins were detected by AlexaFluor488-labeled streptavidin (Strep, green). The cytosolic mCherry is shown in red and the V5 signal in purple. Parasite nuclei were stained with DAPI and are displayed in blue. Scale bar 2 µm. D) Western blot of lysates from EXP1-BirA*-V5 parasites grown for 18 hours with or without biotin and WT parasites grown in the presence of biotin. Lysates were probed with fluorescently labeled Streptavidin to detect biotinylated proteins. The EXP1-BirA*-V5 fusion protein is predicted to be 55 kD (asterisk). Cytosolic mCherry detected with an anti-RFP antibody served as loading control.

Identification of novel PVM candidate proteins by mass spectrometry

To identify the targets labeled by EXP1-BirA*-V5, we performed two independent experiments, in which we affinity purified biotinylated proteins using streptavidin-conjugated magnetic beads and analyzed them by label-free quantitative mass spectrometry. We compared EXP1-BirA*-V5 parasites to parental WT parasites, which were both grown in the presence of biotin. Altogether, we identified 1157 proteins, quantitative information could be extracted for 631 proteins and 357 were reliably quantified with at least two independent peptide measurements across all samples. We considered those proteins as significantly enriched in EXP1-BirA*-V5 parasites, which were at least three times more abundant in EXP1-BirA*-V5 in comparison to WT parasites in both independent experiments with an adjusted p-value below 0.05 as calculated based on ANOVA models (Fig. 2, Fig. S2, Table S1). Out of these 82 proteins we further excluded all proteins, which did not contain a signal peptide and/or at least one transmembrane domain, resulting in a final list of 61 candidate proteins, including several already identified PVM-resident proteins, such as all components of the PTEX complex (PTEX150, Hsp101, PTEX88, TRX2, EXP2) and two members of the ETRAMP family (Fig. 3, Table S2).

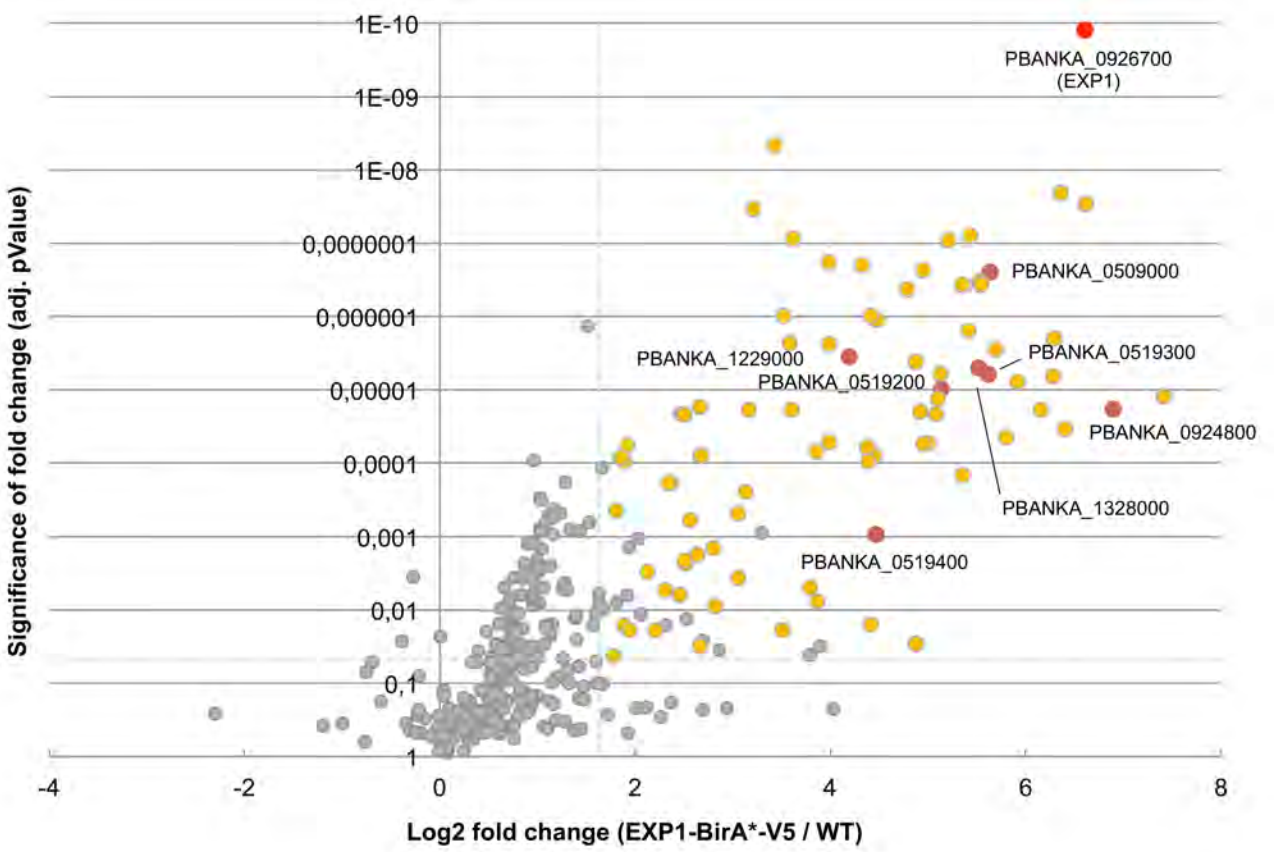

Figure 2. Identification of PVM candidates by quantitative mass-spectrometry. Volcano plot depicting quantified proteins. The x-axis shows the average fold change (log2) in protein abundance in EXP1-BirA*-V5 samples in comparison to WT controls and the y-axis shows the average adjusted p-value, both based on two independent experiments. Proteins meeting the selection criteria (for details see main text) and considered significantly enriched in EXP1-BirA*-V5 parasites are displayed in yellow. The bait protein (EXP1, PBANKA_0926700) and candidates selected for further localization studies are highlighted in red. For a complete list of all identified proteins see Table S1 and for a Venn diagram showing the overlap between the two independent experiments see Figure S2. Proteins significantly enriched in EXP1-BirA*-V5 parasites and containing a signal peptide and/or at least one transmembrane domain are displayed and further described in Figure 3 and Table S2.

Localization of selected candidates by endogenous GFP-tagging

Out of the proteins identified by mass spectrometry, we selected seven proteins and determined their localization by C-terminal GFP-tagging. We concentrated on candidates not localized yet in *P. berghei* and *P. falciparum* at the time of analysis, most of which were annotated as proteins with unknown function. Each corresponding gene was targeted using the pOB277 vector (18) that integrates by single crossover homologous recombination into the endogenous locus, leading to expression of a GFP-tagged version of the protein under its endogenous promoter (Fig. S3A). Successful integration into the desired locus was confirmed by PCR (Fig. S3B) and transgenic blood stage parasites were analyzed live by fluorescence microscopy. We hereby focused our analysis on schizonts and free merozoites, as these stages allow discrimination between a putative PVM, PV and PPM localization. We did not perform further co-localization experiments in the blood stage, as a discrimination of PVM, PV and PPM proteins in this stage by IFA is very difficult to achieve, due to the close proximity of the PVM and the PPM (3). Instead, we decided to include liver stage parasites in our analysis, where such a discrimination by IFA is possible. The cytomere stage is particularly suited for localization studies, since parasites are very large at this time point and the PPM has already started to invaginate (19), allowing a clear differentiation between a potential PVM and PV/PPM localization.

P. berghei ID	Product	SP	TM	*P. falciparum* ID
PBANKA_0311700	rhoptry neck protein 6, putative	Yes	0	PF3D7_0214900
PBANKA_0411700	co-chaperone p23, putative	Yes	0	PF3D7_0314000
PBANKA_0623100	tryptophan-rich protein	No	1	none
PBANKA_0304800	serine repeat antigen 4	Yes	0	PF3D7_0207400*
PBANKA_1008500	translocon component PTEX150	Yes	0	PF3D7_1436300
PBANKA_0830200	high molecular weight rhoptry protein 2	Yes	0	PF3D7_0929400
PBANKA_0305100	serine repeat antigen 1	Yes	0	PF3D7_0207700*
PBANKA_0931300	dipeptidyl aminopeptidase 1, putative	Yes	0	PF3D7_1116700
PBANKA_1212500	conserved Plasmodium protein, unknown function	Yes	0	PF3D7_1014100
PBANKA_0509000	**conserved Plasmodium protein, unknown function**	**Yes**	**1**	**PF3D7_1024800**
PBANKA_1002600	6-cysteine protein	Yes	0	PF3D7_0404900
PBANKA_0919100	parasitophorous vacuolar protein 1, putative	Yes	0	PF3D7_1129100
PBANKA_1035200	LCCL domain-containing protein	Yes	0	PF3D7_1407000
PBANKA_0305000	serine repeat antigen 2	Yes	0	PF3D7_0207600*
PBANKA_1443300	merozoite surface protein 9, putative	Yes	0	PF3D7_1228600
PBANKA_0931200	heat shock protein 101	Yes	0	PF3D7_1116800
PBANKA_0618600	conserved Plasmodium protein, unknown function	Yes	0	PF3D7_0721100
PBANKA_1349000	MSP7-like protein	Yes	0	PF3D7_1335000
PBANKA_1365500	exported protein IBIS1	No	1	none
PBANKA_0100500	PIR protein	No	1	none
PBANKA_0941300	translocon component PTEX88	Yes	0	PF3D7_1105600
PBANKA_1229000	**Plasmodium exported protein (PHIST), unknown function**	**No**	**1**	**none**
PBANKA_0517000	early transcribed membrane protein	Yes	1	PF3D7_1033200*
PBANKA_1328000	**serine/threonine protein phosphatase UIS2**	**Yes**	**0**	**PF3D7_1464600**
PBANKA_0519300	**conserved Plasmodium protein, unknown function**	**Yes**	**0**	**none**
PBANKA_0311800	acyl-CoA synthetase, putative	Yes	0	PF3D7_0215300
PBANKA_1349200	MSP7-like protein	Yes	0	PF3D7_1334400
PBANKA_0519200	**conserved Plasmodium protein, unknown function**	**Yes**	**0**	**none**
PBANKA_0519000	S-antigen, putative	Yes	0	PF3D7_1035200*
PBANKA_1441700	conserved Plasmodium protein, unknown function	Yes	0	PF3D7_1226900
PBANKA_0924800	**conserved Plasmodium protein, unknown function**	**Yes**	**1**	**PF3D7_1123500**
PBANKA_1030600	p1/s1 nuclease, putative	Yes	0	PF3D7_1411900, PF3D7_1412000
PBANKA_0519100	conserved Plasmodium protein, unknown function	Yes	0	none
PBANKA_1300700	LCCL domain-containing protein	Yes	0	PF3D7_1475500
PBANKA_0416000	high molecular weight rhoptry protein 3, putative	Yes	0	PF3D7_0905400
PBANKA_1418300	golgi protein 1, putative	Yes	0	PF3D7_1320000
PBANKA_0204500	LCCL domain-containing protein	Yes	0	PF3D7_0109100
PBANKA_1032100	rhoptry-associated protein 1	Yes	0	PF3D7_1410400
PBANKA_0209200	parasite-infected erythrocyte surface protein	Yes	1	PF3D7_0103900
PBANKA_0304900	serine repeat antigen 3	Yes	0	PF3D7_0207500*
PBANKA_1037300	conserved Plasmodium protein, unknown function	Yes	0	PF3D7_1404900
PBANKA_1316300	conserved Plasmodium protein, unknown function	No	2	PF3D7_1452600
PBANKA_0201600	early transcribed membrane protein	Yes	1	none
PBANKA_0623300	tryptophan-rich protein	Yes	0	none
PBANKA_0216761	reticulocyte binding protein, putative	Yes	1	none
PBANKA_1334300	exported protein 2	Yes	0	PF3D7_1471100
PBANKA_1200600	Plasmodium exported protein, unknown function	Yes	0	none
PBANKA_1358000	thioredoxin 2	Yes	0	PF3D7_1345100
PBANKA_0702800	protein disulfide isomerase	Yes	0	PF3D7_0827900
PBANKA_1400600	cytoadherence linked asexual protein, putative	Yes	1	none
PBANKA_1107100	subtilisin-like protease 1	Yes	0	PF3D7_0507500
PBANKA_1437300	endoplasmin, putative	Yes	0	PF3D7_1222300
PBANKA_0519400	**conserved Plasmodium protein, unknown function**	**Yes**	**0**	**none**
PBANKA_1101400	rhoptry-associated protein 2/3	Yes	0	none
PBANKA_1315700	rhoptry neck protein 2	Yes	1	PF3D7_1452000
PBANKA_0942500	thioredoxin, putative	Yes	0	PF3D7_1104400
PBANKA_0300600	Plasmodium exported protein, unknown function	No	2	none
PBANKA_0701100	conserved Plasmodium protein, unknown function	Yes	0	none
PBANKA_0820000	DnaJ protein, putative	No	6	PF3D7_0919100
PBANKA_0100700	Plasmodium exported protein, unknown function	Yes	0	none
PBANKA_1425900	conserved Plasmodium protein, unknown function	Yes	0	PF3D7_0811600

Figure 3. PVM candidates with a signal peptide and/or at least one transmembrane domain. PVM or PV localization of candidate proteins in *P. berghei* and *P. falciparum* based on this work and published studies that used electron and/or fluorescence microscopy techniques for protein localization are indicated. Proteins that show at least a partial PVM localization during blood and/or liver stage development in *P. berghei* or *P. falciparum* are indicated in green, while proteins with at least a partial PV localization and no further PVM localization are shown in blue. Candidate proteins analyzed in this study are highlighted in bold. *P. falciparum* orthologs were identified in plasmodb.org and in some cases synteny was used as a further indicator to support orthology (indicated by asterisks). Candidates are ordered by an increasing average p-value. For details regarding localizations (including references) see Table S2. SP, signal peptide. TM, number of transmembrane domains.

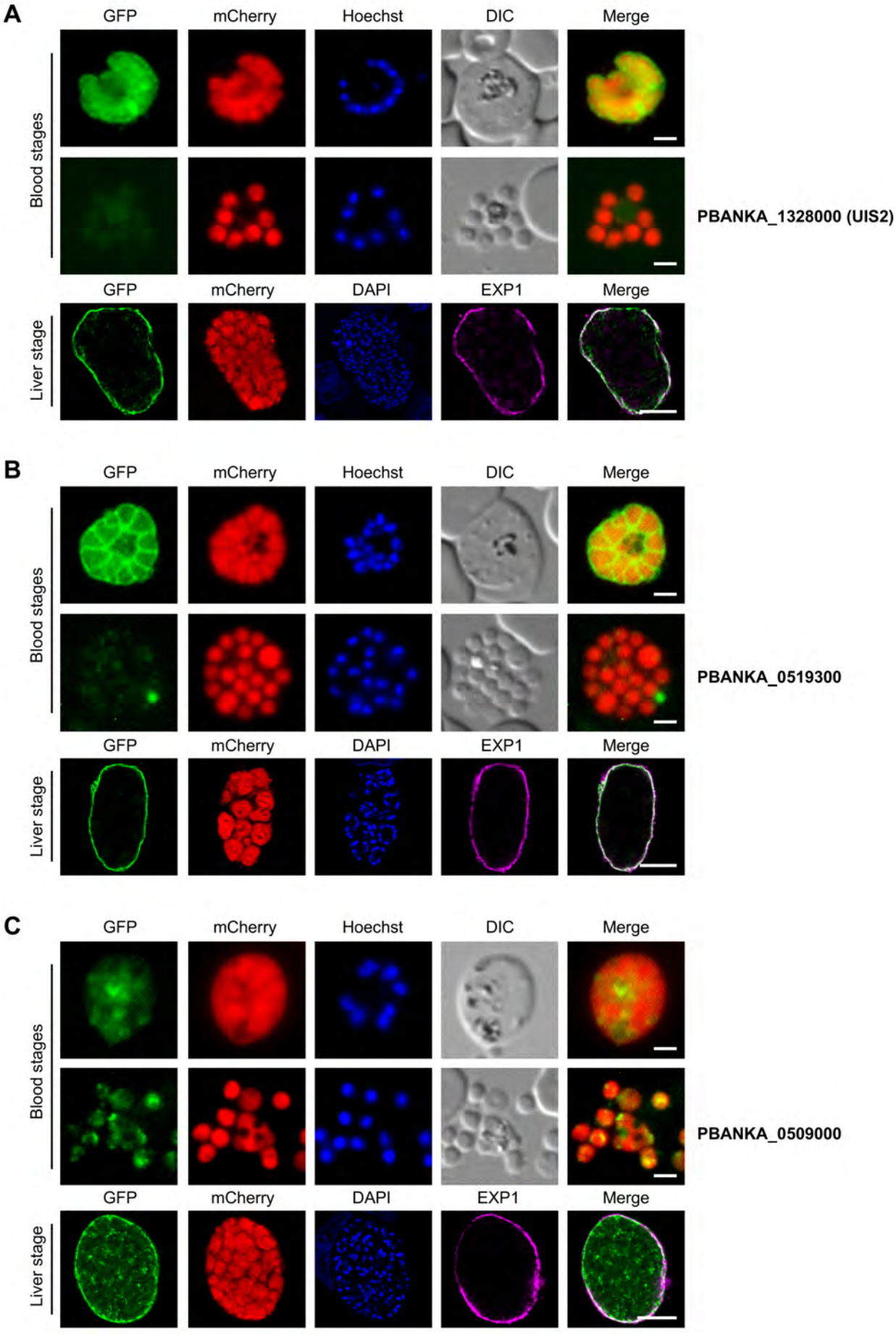
A
GFP
mCherry
Hoechst
DIC
Merge
Blood stages
PBANKA_1328000 (UIS2)
GFP
mCherry
DAPI
EXP1
Merge
Liver stage
B
GFP
mCherry
Hoechst
DIC
Merge
Blood stages
PBANKA_0519300
GFP
mCherry
DAPI
EXP1
Merge
Liver stage
C
GFP
mCherry
Hoechst
DIC
Merge
Blood stages
PBANKA_0509000
GFP
mCherry
DAPI
EXP1
Merge
Liver stage

Figure 4. Candidates with a PVM localization. Live cell microscopy images of developing blood stage merozoites (upper panels) or free blood stage merozoites (middle panels) as well as an IFA of fixed liver stage cytomeres stained with an antiserum against EXP1 (lower panels) are shown for parasites expressing endogenously GFP-tagged PBANKA_1328000 (A), PBANKA_0519300 (B) or PBANKA_0509000 (C), respectively. The endogenously GFP-tagged proteins are shown in green, the cytosolic mCherry in red and the EXP1 signal in the IFA of fixed liver stage parasites is displayed in purple. DNA of Hoechst or DAPI stained nuclei is shown in blue. DIC, differential interference contrast. Scale bars for all blood stages 2 µm and for the liver stage 10 µm.

We therefore concentrated on fully developed cytomere liver stage parasites, which were fixed and stained with an antiserum against EXP1 to perform co-localization analysis by confocal microscopy.

Candidate proteins with PVM localization

Out of the seven GFP-tagged proteins, three proteins were located clearly to the PVM during liver stage development (Fig. 4).

These were the serine/threonine phosphatase UIS2 (PBANKA_1328000) and two conserved *Plasmodium* proteins with unknown function (PBANKA_0519300 and PBANKA_0509000). During blood stage development, UIS2-GFP mainly surrounded developing merozoites as a whole, while free merozoites were not enclosed by a UIS2 signal, suggesting that the peripheral staining in developing schizonts is derived from a PVM localization of the protein during blood stage development. In line with this, in liver stage parasites UIS2 was found to co-localize with EXP1, indicating a PVM localization also during this stage of development (Fig. 4A). The GFP signal of PBANKA_0519300 in infected RBCs was found at the parasite periphery and between forming merozoites, pointing to a localization of this protein in the PV or PPM and maybe additionally to the PVM. Free merozoites of this parasite line were not surrounded by a GFP signal, excluding a PPM localization and suggesting that PBANKA_0519300 is localized to the PV and possibly additionally to the PVM during blood stage development. In liver stage parasites, PBANKA_0519300 localized to the PVM, confirmed by co-localization with EXP1 (Fig. 4B). PBANKA_0509000 showed a weak, hazy staining within the parasite cytoplasm in blood stage parasites, however partially co-localized with EXP1 in liver stage cytomeres (Fig. 4C), demonstrating that also this protein can be transported to the PVM during parasite development.

Candidate proteins with PV/PPM or other localizations

Two other conserved *Plasmodium* proteins with unknown functions (PBANKA_0519400 and PBANKA_0519200) were found mainly in the PV or PPM during blood and liver stage development (Fig. 5).

PBANKA_0519400 surrounded developing blood stage merozoites individually, while no GFP signal was found around free merozoites, pointing to a PV localization of this protein during blood stage development. Similarly, in liver stage cytomeres, the protein did not co-localize with EXP1 and instead showed a typical PV/PPM localization (Fig. 5A). To investigate this further, we performed co-localization analysis with the PPM marker protein merozoite surface protein 1 (MSP1). PBANKA_0519400 only partially co-localized with MSP1 and concentrated at the parasite periphery of late liver stage parasites, which is consistent with a PV localization also during liver stage development (Fig. S4). The other protein, PBANKA_0519200, also surrounded developing merozoites individually, however free merozoites of this parasite line were clearly surrounded by a GFP signal, indicating a PPM localization of this protein in blood stage parasites. During liver stage development, PBANKA_0519200 did not co-localize with EXP1 and showed a typical PV/PPM localization (Fig. 5B). Co-staining with the PPM marker MSP1 showed a partial co-localization with this protein especially in liver stage merozoites. PBANKA_0519200 also concentrated at the parasite periphery during liver stage development, indicating that this protein localizes additionally to the PV during this stage of development (Fig. S5).

Another conserved *Plasmodium* protein with unknown function (PBANKA_0924800) showed one single focus per parasite in developing and free blood stage merozoites, suggesting a secretory pathway or invasion organelle location. During liver stage development, the protein also appeared as discrete foci in cytomere stage parasites, indicating a similar localization as observed in blood stage parasites (Fig. 6A). Finally, a *Plasmodium* exported protein (PHIST) with unknown function (PBANKA_1229000) was exported to the host cell cytosol in developing merozoites, while no signal was observed in free merozoites. In liver stage cytomere stage this protein was also secreted by the parasite but mainly localized to the PV (Fig. 6B).

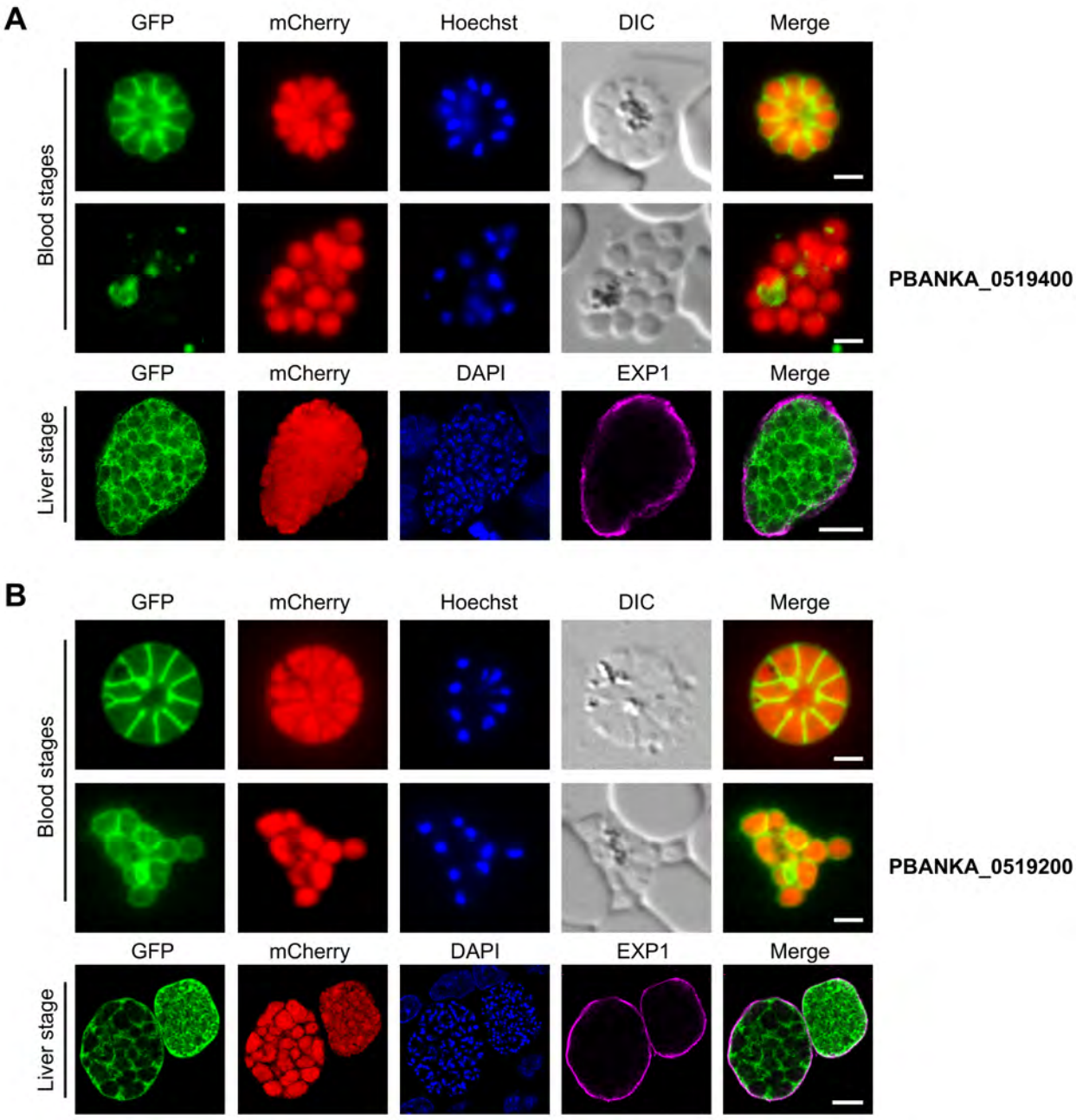

Figure 5. Candidates that are localized to the PV and/or PPM. Live cell microscopy images of developing blood stage merozoites (upper panels) or free blood stage merozoites (middle panels) as well as an IFA of fixed liver stage cytomeres stained with an antiserum against EXP1 (lower panels) are shown for parasites expressing endogenously GFP-tagged PBANKA_0519400 (A) and PBANKA_0519200 (B), respectively. The endogenously GFP-tagged proteins are shown in green, the cytosolic mCherry in red and the EXP1 signal in the IFA of fixed liver stage parasites is displayed in purple. DNA of Hoechst or DAPI stained nuclei is shown in blue. DIC, differential interference contrast. Scale bars for all blood stages 2 µm and for the liver stage 10 µm.

DISCUSSION

During their development within RBCs and hepatocytes, *Plasmodium* parasites are surrounded by a PVM. This membrane represents the interphase between parasite and host and plays a fundamental role for its interaction with the host cell. In this study we used BioID in combination with endogenous GFP-tagging to identify novel PVM proteins in *P. berghei*.

Based on our two BioID experiments we obtained a list of 61 candidate proteins, potentially located to the blood stage PVM. Many of these were already known to be localized to this compartment, such as all components of

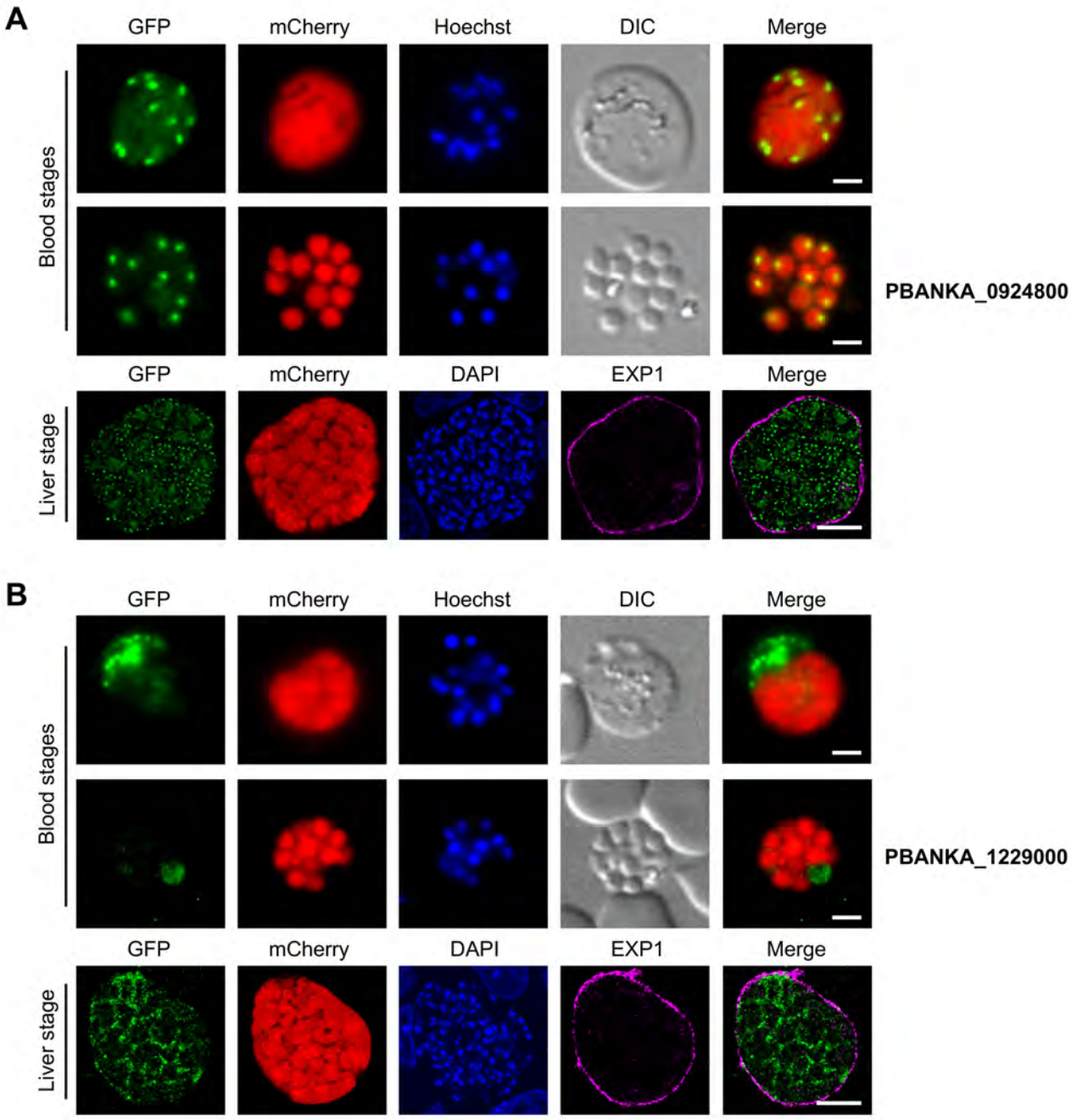

Figure 6. Localization of PBANKA_1229000 and PBANKA_0924800 during blood and liver stage development. Live cell microscopy images of developing blood stage merozoites (upper panels) or free blood stage merozoites (middle panels) as well as an IFA of fixed liver stage cytomeres stained with an antiserum against EXP1 (lower panels) are shown for parasites expressing endogenously GFP-tagged PBANKA_1229000 (A) and PBANKA_0924800 (B), respectively. The endogenously GFP-tagged proteins are shown in green, the cytosolic mCherry in red and the EXP1 signal in IFAs of fixed liver stage parasites is displayed in purple. DNA of Hoechst or DAPI stained nuclei is shown in blue. DIC, differential interference contrast. Scale bars for all blood stages 2 µm and for the liver stage 10 µm.

the PTEX complex. In general, this confirms a good coverage of our approach. However, a considerable number of the 61 candidate proteins are known not to locate to the PVM, which was evident in the endogenous GFP-tagging approach of this study as well, where four of the seven analyzed proteins were found in other non-PVM compartments such as the PV or the PPM. This occurrence of quite a high number of off-target hits might be derived from the fact that the EXP1-BirA*-V5 fusion protein is already active during its transport through the secretory pathway. Hereby the PPM and the PV have to be crossed and proteins of these compartments as well as other proteins of the secretory pathway might become biotinylated. Furthermore, we currently cannot

completely exclude the possibility that the constitutive expression of EXP1 driven by the strong *P. berghei eef1α* promotor or its fusion to the BirA*-V5 protein might interfere with the proper targeting of EXP1 to the PVM. Possibly, this could lead to a partial PV-localization of the EXP1-BirA* fusion protein, which could biotinylate not only proteins of the PVM but also of the PV and PPM there.

Rather than an in-depth analysis of single candidate proteins, we performed a GFP-tagging approach for seven candidate genes during blood and liver stage development as a proof of concept for our BioID approach. This analysis resulted in the identification of three previously unknown proteins of the liver stage PVM, which were the serine/threonine protein phosphatase UIS2 and two conserved *Plasmodium* proteins with unknown functions (PBANKA_0519300 and PBANKA_0509000).

UIS2 was initially discovered in a screen for genes that display an upregulated expression in salivary gland sporozoites (20) and has been shown to be essential for blood stage development in *P. berghei* and *P. falciparum* (21, 22). Similar to our results obtained in this study, UIS2 also localizes to the PVM of *P. falciparum* blood stage parasites (22). It is interesting to note that the localization of UIS2 in *P. berghei* blood stages is slightly more diffuse as compared to its localization in *P. falciparum*, which might be due to strain-specific differences in expression. By utilization of a conditional knockout approach, Zhang and colleagues provided evidence that UIS2 plays a role in transformation of *P. berghei* sporozoites to liver stages through a function in dephosphorylating eIF2α-P in the parasite cytoplasm (21). In this regard, our observation that UIS2 localizes to the PVM during blood and liver stage development is very interesting, as it indicates that UIS2 might have another non-cytoplasmic and yet to be identified function in PVM biology.

The other two novel proteins of the liver stage PVM, PBANKA_0519300 and PBANKA_0509000, were both shown to be not essential for blood stage development in *P. berghei* (23, 24), but the function of these two proteins during liver stage development has not been analyzed so far. The *P. falciparum* ortholog of PBANKA_0509000, which was recently named EXP3, was localized to the blood stage PVM as well (22, 24). Remarkably, although likely not essential for *P. falciparum* blood stage development, EXP3 was shown to be part of a newly described exported protein-interacting complex (EPIC), which has been proposed to be involved in the trafficking of virulence determinants to the surface of the infected erythrocyte (24). Thus, the fact that we did localize the *P. berghei* ortholog of EXP3 also to the liver stage PVM is intriguing, as this suggests that an EPIC-like complex could also be involved in trafficking of parasite proteins to the infected hepatocyte, a hypothesis which clearly needs further investigation.

In this study, we used the promiscuous biotin ligase BirA* to identify novel proteins of the *Plasmodium* PVM. A very promising approach for the future might be the application of the engineered ascorbate peroxidase (APEX). This enzyme can also be fused to a protein of interest and, similarly to BirA*, can lead to biotinylation of nearby proteins, with the big difference of having a much shorter labeling time of one minute in comparison to the many hours of labeling time, which are needed to achieve satisfactory biotinylation levels in a BioID experiment (25). Thereby the temporal specificity of the biotinylation reaction could be increased and it might become possible to look at the stage specific proteome of the PVM and to specifically identify proteins involved in PVM remodeling early in infection or to identify PVM-localized proteins involved in membrane disruption processes of late stage parasites during egress from host cells.

The BioID technique has become a powerful and widely used tool in cell biology and was already applied in several parasite species, including *Trypanosoma brucei* (26), *Toxoplasma gondii* (27–29) and *P. falciparum* (22). In *P. berghei* it has been used in an *in vivo* setting, where the biotinylation reaction was carried out in parasite-infected mice (30). Here, we show for the first time the successful application of BioID in *in vitro* cultivated *P. berghei* blood stage parasites and demonstrate its usefulness in identification of novel proteins of the *Plasmodium* PVM, altogether contributing to our understanding of the molecular make-up of this fascinating interface between parasite and its host cell.

EXPERIMENTAL PROCEDURES

Ethics statement

All experiments performed were conducted in strict accordance with the guidelines of the Swiss Tierschutzgesetz (TSchG; Animal Rights Laws) and approved by the ethical committee of the University of Bern (Permit Number: BE109/13).

Experimental animals

Balb/c Mice used in the experiments were between 6 and 10 weeks of age and from Harlan Laboratories, Charles River or bred in the central animal facility at the University of Bern. Mosquito feeds were performed on anaesthetized mice (Ketavet/Domitor) and all efforts were made to minimize suffering.

Mosquito infection
Infection with *P. berghei* parasites was initiated by intraperitoneal injection of blood stabilates. After reaching a parasitemia of 4%, 40 µl of infected blood mixed with 160 µl of PBS, were injected intravenously into mice, pretreated with an intraperitoneal injection of 200 µl phenylhydrazine (6 mg/ml in PBS) two to four days prior to infection. At three to four days after infection, mice with a parasitemia of at least 7% were anaesthetized for one hour to allow feeding of 150 female *Anopheles stephensi* mosquitoes. Mosquitoes were kept at 20.5°C with 80% humidity and for infection experiments, sporozoites were isolated from infected salivary glands 16–27 days post-blood meal.

Culture and infection of HepG2 cells with *P. berghei*
HepG2 cells (obtained from the European cell culture collection) were cultured as described previously (31). For infection, 5 x 10^4 cells were seeded in 24-well plates with coverslips. The next day, *P. berghei* sporozoites were isolated from salivary glands of infected *A. stephensi* mosquitoes and added to HepG2 cells in culture medium additionally containing 2.5 µg/ml amphotericin B (PAA Laboratories). After an incubation period of two hours, the sporozoite-containing medium was removed and fresh infection medium was added. Subsequently, medium was changed once per day.

Cloning of DNA constructs
All PCR reactions were performed using Phusion DNA polymerase (NEB). PCR products were routinely cloned into pJET1.2 (Fermentas) and confirmed by sequencing (Microsynth). The plasmid pL0017-^{C}EXP1-BirA*-V5 was generated by first amplifying the BirA* coding sequence from pcDNA3.1-mycBioID (17) using primers BirA-V5-fw and BirA-V5-rev, whereby a V5-tag was added to the C-terminal end of BirA*. The PCR product was then cloned into pL0017 (32) using *BamHI* and *NotI* restriction sites. Subsequently, the EXP1 coding sequence was amplified from blood stage cDNA using primers EXP1-fw and EXP1-rev and cloned in frame with BirA*-V5 into the pL0017 vector using *BamHI* and *NotI* restriction sites. To generate the plasmids for C-terminal endogenous GFP-tagging of PVM candidates, the C-terminal homology regions of the candidate genes were amplified by PCR and cloned in frame with GFP into pOB277 (18) using *ApaI* and *KpnI* restriction sites. All primer sequences are listed in Table S3.

Transfection of *P. berghei* parasites and confirmation of correct integration
The plasmid pL0017-^{C}EXP1-BirA*-V5 and the pOB277-based GFP-tagging vectors were linearized using restriction enzymes shown in Table S4. Linearized plasmids were transfected into blood stage schizonts of *P. berghei* ANKA mCherry$_{Hsp70}$ parasites (16) using standard methods of transfection (33). Transfected parasites were selected by supplementing the drinking water of infected mice with pyrimethamine (Sigma). Parasite genomic DNA was isolated from 0.05% saponin-treated infected red blood cells using the Nucleospin Blood QuickPure kit (Macherey-Nagel) and successful integration of the plasmid into the genome was confirmed by diagnostic PCR using GoTaq Flexi DNA polymerase (Promega). All primer sequences are listed in Table S3.

Live-cell imaging and Immunofluorescence assay
Blood stage parasites from schizont cultures or from a drop of tail blood were imaged live and for visualization of DNA, 1 µg/ml Hoechst 33342 (Sigma) was added. Blood-stage IFA was performed as described previously (19). Primary antibodies were rat anti-RFP (Chromotek) and mouse anti-V5 (Invitrogen). As secondary antibodies donkey anti-rat AlexaFluor594 (Invitrogen) and goat anti-mouse Cy5 (Dianova) were used. Streptavidin-AlexaFluor488 (Invitrogen) and 1 µg/ml DAPI (Sigma) were applied together with the secondary antibodies and coverslips were mounted using Dako Fluorescent Mounting Medium (Dako). All blood stage images were taken on a Leica DM5500 B epifluorescence microscope using a HCX Plan-Apochromat 100x/1.4 oil objective and image processing was performed using ImageJ.
For liver stage IFA, 5 x 10^4 HepG2 cells were seeded onto coverslips in 24-well plates and infected the following day with *P. berghei* sporozoites. At different time points post-infection, cells were fixed with 4% PFA in PBS for 20 minutes at room temperature, followed by permeabilization with ice-cold methanol for at least 30 minutes. Unspecific binding sites were blocked by incubation in 10% FCS in PBS, followed by incubation with primary antibodies (rabbit anti-GFP (Invitrogen), chicken anti-EXP1 and rat anti-MSP1 (both generated at the Bernhard Nocht Institute, Hamburg, Germany)) and subsequently with fluorescently labeled secondary antibodies (goat anti-rabbit AlexaFluor488 (Invitrogen), goat anti-rat AlexaFluor647 (Invitrogen) and donkey anti-chicken Cy5 (Dianova)) diluted in 10% FCS in PBS. DNA was stained with 1 µg/ml DAPI. Labeled cells were mounted on microscope slides with Dako Fluorescent Mounting Medium and analyzed by using a Leica TCS SP8 confocal microscope with a HC PL 100x/1.40 oil objective. Image processing was performed using ImageJ.

Western Blot
Western blotting was performed as described previously (34) using rat anti-RFP (Chromotek) and mouse anti-V5 (Invitrogen) as primary antibodies. Goat anti-rat IgG 680LT IRDye and goat anti-mouse IgG 680LT IRDye (both LI-COR) were used as secondary antibodies. Biotinylated proteins were detected using IRDye 800CW labeled streptavidin (LI-COR).

BioID of PVM proteins
Infection with EXP1-BirA*-V5 and WT mCherry$_{Hsp70}$ parasites was initiated by intraperitoneal injection of blood stabilates into two mice per parasite line. After reaching a parasitemia of 3-4%, mice were sacrificed and blood was removed by cardiac puncture and incubated in an overnight schizont culture as previously described (33). Incubation was done for 18 hours in the presence or absence of 150 µM biotin (Sigma). Schizonts were enriched on a nycodenz gradient and a small sample was taken for western blot as described above. Detergent-based extraction and affinity capture of biotinylated proteins was basically done as described before (27), however incubation on Streptavidin Mag Sepharose beads (GE Healthcare) was done at 4° C over night with continuous agitation.

Mass spectrometric analysis
Mass spectrometric analysis was performed by the proteomics and mass spectrometry core facility at

the Department of BioMedical Research of the University of Bern. Proteins were reduced, alkylated and digested with Trypsin for six hours at 37° C on beads. Digests were loaded onto a pre-column (PepMap C18, 5µm, 300A, 300µm x 15mm length) at a flow rate of 20 µL/min with solvent A (0.1% Formic Acid in water/acetonitrile 98:2). After loading, peptides were eluted in back flush mode onto the analytical Nano-column (C18, 5 µm, 300A, 0.075 mm i.d. x 150 mm length) using an acetonitrile gradient of 5% to 40% solvent B (0.1% Formic Acid in water/acetonitrile 4,9:95) in 40 min at a flow rate of 400 nL/min. The column effluent was directly coupled to a Fusion LUMOS mass spectrometer (Thermo Fischer) via a Nano spay ESI source. Data acquisition was made in data dependent mode with precursor ion scans recorded in the Fourier transform detector (FT) with resolution 120'000 (at m/z=400) parallel to top speed fragment spectra of the most intense precursor ions in the Linear trap for a cycle time of 3 seconds maximum.

Protein identification and label free quantitation

Raw files were converted to mzXML format with ProteoWizard v3.0.6002 (http://proteowizard.sourceforge.net/) and searched with Comet (v2015.01, (35)) against a combined *P. berghei* sequence database from www.uniprot.org and plasmodb.org (PlasmoDB-28) with the following parameters: fully tryptic, 2 missed cleavages allowed, 20 ppm precursor mass tolerance, fixed carbidomethylated cysteines, variable modification on methionines and further processed with the transproteomic pipeline (TPP, v4.7, (36)) to obtain identified peptide and protein list at the false discovery rate of 1%. LC-MS/MS runs were aligned and precursor intensities were calculated in ProgenesisQI (Nonlinear Dynamics, v2). Protein abundances and significant testing results of EXP1-BirA*-V5 versus WT parasites were calculated with MSstats (v3.2.2, (37)) based on ANOVA models for each replicate separately. P-value was adjusted according to Benjamini and Hochberg. Only proteins with at least two independent peptide measurements were taken into account. Proteins with a fold change of at least three versus wild-type and an adjusted p-value below 0.05 in both biological replicates were regarded as significantly enriched in EXP1-BirA*-V5 parasites.

Data availability

All data generated or analyzed during this study are included in this published article (and its Supplemental Information files). The mass spectrometry proteomics data have been deposited to the ProteomeXchange Consortium via the PRIDE partner repository (38) with the data set identifier PXD007857.

ACKNOWLEDGEMENTS

We thank Tobias Spielmann and Claire Doble for critical reading of the manuscript and Anthony Zakher for his assistance in cloning some of the GFP-tagging constructs. This work was supported by an international Macquarie Research Excellence Scholarship (iMQRES) to CBS and by grants from the EVIMalaR EU Consortium and the Swiss National Foundation to VTH (310030_159519). Images were acquired on equipment supported by the Microscopy Imaging Center (MIC) of the University of Bern. CBS, FB and PCB performed the experiments and DBF analyzed the mass spectrometry data. The project was conceived by PCB and experiments were designed by CBS, PCB and VTH. The paper was written and the figures were prepared by PCB and CBS. All authors commented on the manuscript.

REFERENCES

1. World Health Organization. 2016. World Malaria Report 2016.

2. De Niz M, Burda P-C, Kaiser G, Del Portillo HA, Spielmann T, Frischknecht F, Heussler VT. 2017. Progress in imaging methods: insights gained into *Plasmodium* biology. Nat Rev Microbiol 15:37–54.

3. Spielmann T, Montagna GN, Hecht L, Matuschewski K. 2012. Molecular make-up of the *Plasmodium* parasitophorous vacuolar membrane. Int J Med Microbiol 302:179–186.

4. Nyboer B, Heiss K, Mueller A-K, Ingmundson A. 2017. The *Plasmodium* liver-stage parasitophorous vacuole: A front-line of communication between parasite and host. Int J Med Microbiol 0–1.

5. Simmons D, Woollett G, Bergin-Cartwright M, Kay D, Scaife J. 1987. A malaria protein exported into a new compartment within the host erythrocyte. EMBO J 6:485–91.

6. Ansorge I, Paprotka K, Bhakdi S, Lingelbach K. 1997. Permeabilization of the erythrocyte membrane with streptolysin O allows access to the vacuolar membrane of *Plasmodium falciparum* and a molecular analysis of membrane topology. Mol Biochem Parasitol 84:259–61.

7. Sanchez GI, Rogers WO, Mellouk S, Hoffman SL. 1994. *Plasmodium falciparum*: exported protein-1, a blood stage antigen, is expressed in liver stage parasites. Exp Parasitol 79:59–62.

8. Charoenvit Y, Mellouk S, Sedegah M, Toyoshima T, Leef MF, de V la, Beaudoin RL, Aikawa M, Fallarme V, Hoffman SL. 1995. *Plasmodium yoelii*: 17-kDa hepatic and erythrocytic stage protein is the target of an inhibitory monoclonal antibody. Exp Parasitol 80:419–429.

9. Maier AG, Rug M, O'Neill MT, Brown M, Chakravorty S, Szestak T, Chesson J, Wu Y, Hughes K, Coppel RL, Newbold C, Beeson JG, Craig A, Crabb BS, Cowman AF. 2008. Exported Proteins Required for Virulence and Rigidity of *Plasmodium falciparum*-Infected Human Erythrocytes. Cell 134:48–61.

10. Lisewski AM, Quiros JP, Ng CL, Adikesavan AK, Miura K, Putluri N, Eastman RT, Scanfeld D, Regenbogen SJ, Altenhofen L, Llinás M, Sreekumar A, Long C, Fidock DA, Lichtarge O. 2014. Supergenomic network compression and the discovery of EXP1 as a glutathione transferase inhibited by artesunate. Cell 158:916–928.

11. Sá E Cunha C, Nyboer B, Heiss K, Sanches-Vaz M, Fontinha D, Wiedtke E, Grimm D, Przyborski JM, Mota MM, Prudêncio M, Mueller A-K. 2017. *Plasmodium berghei* EXP-1 interacts with host Apolipoprotein H during *Plasmodium* liver-stage development. Proc Natl Acad Sci U S A 114:E1138–E1147.

12. de Koning-Ward TF, Gilson PR, Boddey JA, Rug M,

Smith BJ, Papenfuss AT, Sanders PR, Lundie RJ, Maier AG, Cowman AF, Crabb BS. 2009. A newly discovered protein export machine in malaria parasites. Nature 459:945–9.

13. Spielmann T, Fergusen DJP, Beck H-P. 2003. etramps, a new *Plasmodium falciparum* gene family coding for developmentally regulated and highly charged membrane proteins located at the parasite-host cell interface. Mol Biol Cell 14:1529–44.

14. Mueller A-K, Labaied M, Kappe SHI, Matuschewski K. 2005. Genetically modified *Plasmodium* parasites as a protective experimental malaria vaccine. Nature 433:164–7.

15. Mueller A-K, Camargo N, Kaiser K, Andorfer C, Frevert U, Matuschewski K, Kappe SHI. 2005. *Plasmodium* liver stage developmental arrest by depletion of a protein at the parasite-host interface. Proc Natl Acad Sci U S A 102:3022–7.

16. Burda PC, Roelli MA, Schaffner M, Khan SM, Janse CJ, Heussler VT. 2015. A *Plasmodium* phospholipase is involved in disruption of the liver stage parasitophorous vacuole membrane. PLoS Pathog 11:e1004760.

17. Roux KJ, Kim DI, Raida M, Burke B. 2012. A promiscuous biotin ligase fusion protein identifies proximal and interacting proteins in mammalian cells. J Cell Biol 196:801–810.

18. Patzewitz E-M, Guttery DS, Poulin B, Ramakrishnan C, Ferguson DJP, Wall RJ, Brady D, Holder AA, Szöőr B, Tewari R. 2013. An ancient protein phosphatase, SHLP1, is critical to microneme development in *Plasmodium* ookinetes and parasite transmission. Cell Rep 3:622–9.

19. Burda P-C, Schaffner M, Kaiser G, Roques M, Zuber B, Heussler VT. 2017. A *Plasmodium* plasma membrane reporter reveals membrane dynamics by live-cell microscopy. Sci Rep 7:9740.

20. Matuschewski K, Ross J, Brown SM, Kaiser K, Nussenzweig V, Kappe SHI. 2002. Infectivity-associated Changes in the Transcriptional Repertoire of the Malaria Parasite Sporozoite Stage. J Biol Chem 277:41948–41953.

21. Zhang M, Mishra S, Sakthivel R, Fontoura BMA, Nussenzweig V. 2016. UIS2: A Unique Phosphatase Required for the Development of *Plasmodium* Liver Stages. PLOS Pathog 12:e1005370.

22. Khosh-Naucke M, Becker J, Mesén-Ramírez P, Kiani P, Birnbaum J, Fröhlke U, Jonscher E, Schlüter H, Spielmann T. 2017. Identification of novel parasitophorous vacuole proteins in *P. falciparum* parasites using BioID. Int J Med Microbiol.

23. Fonager J, Pasini EM, Braks JAM, Klop O, Ramesar J, Remarque EJ, Vroegrijk IOCM, van Duinen SG, Thomas AW, Khan SM, Mann M, Kocken CHM, Janse CJ, Franke-Fayard BMD. 2012. Reduced CD36-dependent tissue sequestration of *Plasmodium*-infected erythrocytes is detrimental to malaria parasite growth *in vivo*. J Exp Med 209:93–107.

24. Batinovic S, McHugh E, Chisholm SA, Matthews K, Liu B, Dumont L, Charnaud SC, Schneider MP, Gilson PR, de Koning-Ward TF, Dixon MWA, Tilley L. 2017. An exported protein-interacting complex involved in the trafficking of virulence determinants in *Plasmodium*-infected erythrocytes. Nat Commun 8:16044.

25. Rhee H-W, Zou P, Udeshi ND, Martell JD, Mootha VK, Carr SA, Ting AY. 2013. Proteomic Mapping of Mitochondria in Living Cells via Spatially Restricted Enzymatic Tagging. Science (80-) 339:1328–1331.

26. Morriswood B, Havlicek K, Demmel L, Yavuz S, Sealey-Cardona M, Vidilaseris K, Anrather D, Kostan J, Djinovic-Carugo K, Roux KJ, Warren G. 2013. Novel bilobe components in *Trypanosoma brucei* identified using proximity-dependent biotinylation. Eukaryot Cell 12:356–67.

27. Chen AL, Kim EW, Toh JY, Vashisht AA, Rashoff AQ, Van C, Huang AS, Moon AS, Bell HN, Bentolila LA, Wohlschlegel JA, Bradley PJ. 2015. Novel components of the *Toxoplasma* inner membrane complex revealed by BioID. MBio 6:e02357-14.

28. Gaji RY, Johnson DE, Treeck M, Wang M, Hudmon A, Arrizabalaga G. 2015. Phosphorylation of a Myosin Motor by TgCDPK3 Facilitates Rapid Initiation of Motility during *Toxoplasma gondii* egress. PLOS Pathog 11:e1005268.

29. Nadipuram SM, Kim EW, Vashisht AA, Lin AH, Bell HN, Coppens I, Wohlschlegel JA, Bradley PJ. 2016. *In Vivo* Biotinylation of the *Toxoplasma* Parasitophorous Vacuole Reveals Novel Dense Granule Proteins Important for Parasite Growth and Pathogenesis. MBio 7:e00808-16.

30. Kehrer J, Frischknecht F, Mair GR. 2016. Proteomic Analysis of the *Plasmodium berghei* Gametocyte Egressome and Vesicular bioID of Osmiophilic Body Proteins Identifies Merozoite TRAP-like Protein (MTRAP) as an Essential Factor for Parasite Transmission. Mol Cell Proteomics 15:2852–2862.

31. Graewe S, Rankin KE, Lehmann C, Deschermeier C, Hecht L, Froehlke U, Stanway RR, Heussler V. 2011. Hostile takeover by *Plasmodium*: Reorganization of parasite and host cell membranes during liver stage egress. PLoS Pathog 7:e1002224.

32. Franke-Fayard B, Trueman H, Ramesar J, Mendoza J, Van Der Keur M, Van Der Linden R, Sinden RE, Waters AP, Janse CJ. 2004. A *Plasmodium berghei* reference line that constitutively expresses GFP at a high level throughout the complete life cycle. Mol Biochem Parasitol 137:23–33.

33. Janse CJ, J R, Waters A. 2006. High Efficiency Transfection and Drug Selection of Genetically Transformed Blood Stages of the Rodent Malaria Parasite *Plasmodium berghei*. Nat Protoc 1:346–356.

34. Wacker R, Eickel N, Schmuckli-Maurer J, Annoura T, Niklaus L, Khan SM, Guan J-L, Heussler VT. 2017. LC3-association with the parasitophorous vacuole membrane of *Plasmodium berghei* liver stages follows a noncanonical autophagy pathway. Cell Microbiol 19:e12754.

35. Eng JK, Jahan TA, Hoopmann MR. 2013. Comet: an open-source MS/MS sequence database search tool. Proteomics 13:22–4.

36. Deutsch EW, Mendoza L, Shteynberg D, Farrah T, Lam H, Tasman N, Sun Z, Nilsson E, Pratt B, Prazen B, Eng JK, Martin DB, Nesvizhskii AI, Aebersold R. 2010. A guided tour of the Trans-Proteomic Pipeline. Proteomics 10:1150–9.

37. Choi M, Chang C-Y, Clough T, Broudy D, Killeen T, MacLean B, Vitek O. 2014. MSstats: an R package for statistical analysis of quantitative mass spectrometry-based proteomic experiments. Bioinformatics 30:2524–6.

38. Vizcaíno JA, Csordas A, del-Toro N, Dianes JA, Griss J, Lavidas I, Mayer G, Perez-Riverol Y, Reisinger F, Ternent T, Xu Q-W, Wang R, Hermjakob H. 2016. 2016 update of the PRIDE database and its related tools. Nucleic Acids Res 44:D447-56.

SUPPLEMENTAL INFORMATION

Supplemental Figures

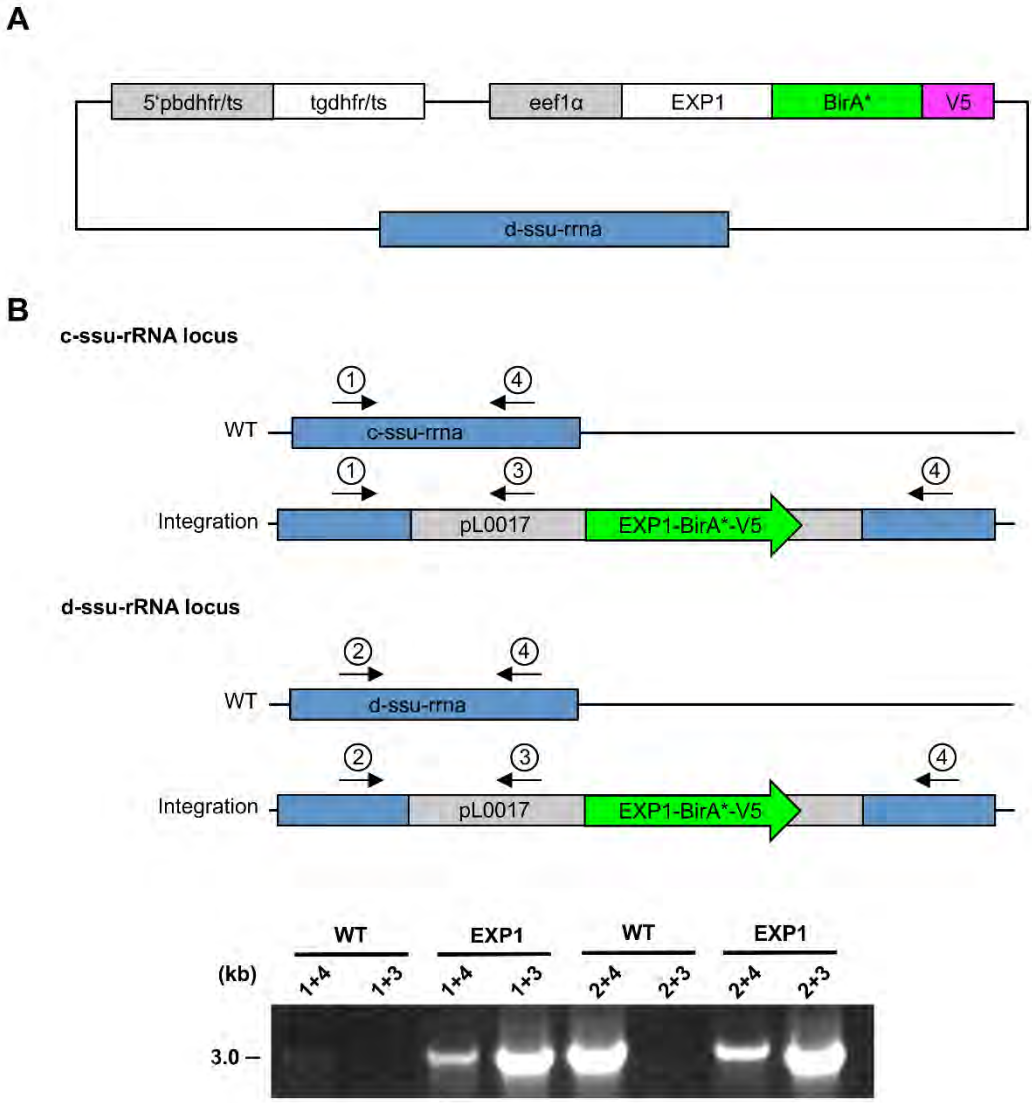

Figure S1. Integration PCR of EXP1-BirA*-V5 parasites (related to Figure 1). A) Schematic representation of the pL0017 based plasmids used to generate EXP1-BirA*-V5 parasites. This vector integrates into the c- or the d-ssu-rRNA locus via single crossover recombination and conveys resistance to pyrimethamine. B) Diagnostic PCR of EXP1-BirA*-V5 parasites. Successful integration of the transfected plasmid into either of two possible loci in the *P. berghei* genome was tested by PCR. Locations of primers used for PCR analysis are shown. For each locus, one primer pair (1 and 4, 2 and 4, respectively) yields a PCR product of 3 kb if no integration has taken place. In the case of successful integration, the primers are too far apart (>14 kb) to result in a complete PCR product under the chosen conditions. To further confirm integration, additional primer pairs (1 and 3, 2 and 3) were used, which only generate a PCR product of 3 kb if the plasmid has integrated. All primer sequences are listed in Table S3.

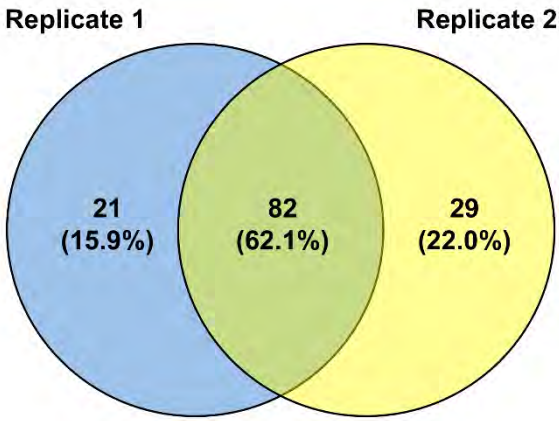

Figure S2. Overlap between the two independent experiments (related to Figure 2). Venn diagram showing the overlap between the two replicates and containing all proteins, which were at least three times enriched in EXP1-BirA*-V5 in comparison to WT control parasites with a p-value < 0.05.

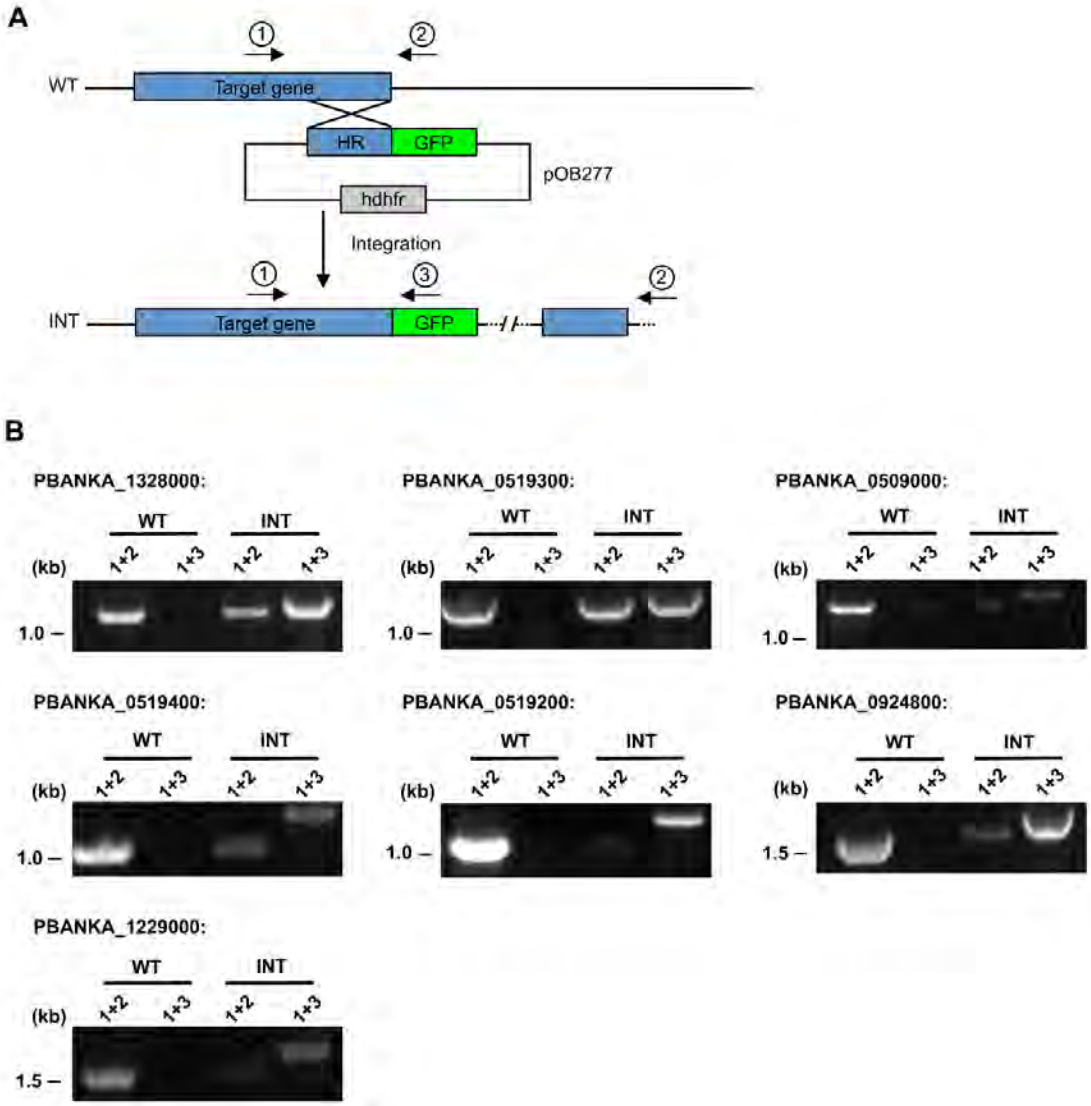

Figure S3. Integration PCR of parasites expressing endogenously GFP-tagged candidate proteins (related to Figures 4, 5 and 6). A) Schematic representation of the target locus in WT parasites and in parasites after successful integration (INT) by single-crossover recombination of the pOB277-based vector for endogenous GFP-tagging of target genes. Locations of primers used for PCR analysis are shown. For each locus, one primer pair (1 and 2) yields a PCR product if no integration has taken place. In the case of successful integration, the primers are too far apart to result in a complete PCR product under the chosen conditions. Another primer pair (1 and 3) only generates a PCR product if the plasmid has integrated. B) Agarose gels with PCR products from genomic DNA of WT controls and the parasite lines indicated above each gel. All primer sequences are listed in Table S3.

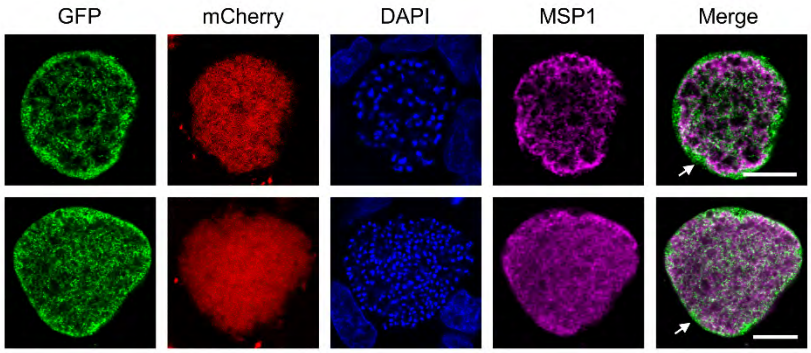

Figure S4. IFA of fixed liver stages of PBANKA_0519400 parasites stained with an antiserum against the PPM marker MSP1 (related to Fig. 5). The endogenously GFP-tagged protein is shown in green, the cytosolic mCherry in red and the MSP1 signal in purple. DNA of DAPI stained nuclei is displayed in blue. Arrows indicate areas, where the GFP-signal is surrounding the PPM marker MSP1, indicating a PV localization during liver stage development. Scale bars 10 µm.

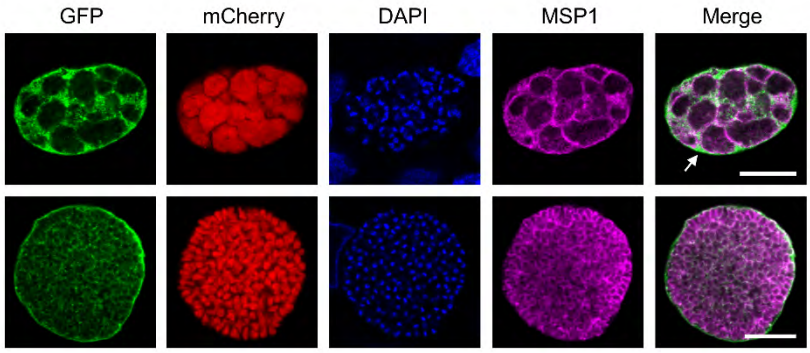

Figure S5. IFA of fixed liver stages of PBANKA_0519200 parasites stained with an antiserum against the PPM marker MSP1 (related to Fig. 5). The endogenously GFP-tagged protein is shown in green, the cytosolic mCherry in red and the MSP1 signal in purple. DNA of DAPI stained nuclei is displayed in blue. Arrows indicate areas, where the GFP-signal is surrounding the PPM marker MSP1, indicating a PV localization during liver stage development. Scale bars 10 µm.

Table S1 List of all proteins identified by quantitative mass-spectrometry in the two independent experiments with a 1% false discovery rate (related to Fig. 2 and Fig. 3). Protein probabilities, sequence coverage, number of unique peptides are indicated for each sample (replicate 1-WT, replicate 1-EXP1-BirA*-V5, replicate 2-WT, replicate 2-EXP1-BirA*-V5). In addition, the calculated log2 fold changes (EXP1-BirA*-V5/WT) and the corresponding adjusted p-value for the two replicates are indicated out of which the average log2 fold change and the average adjusted p-value was obtained. The last column indicates significantly enriched proteins in the EXP1-BirA*-V5 sample according to the criteria described in the main text.

Table S2: Localization of PVM candidate proteins in *P. berghei* and *P. falciparum* based on this work and published studies that used electron and/or fluorescence microscopy techniques for protein localization (related to Fig. 3). Given localizations were obtained in asexual blood stage parasites, if not stated otherwise. Proteins that show at least a partial PVM localization during blood and/or liver stage development are indicated in green, while proteins with at least a partial PV localization during blood and/or liver stage development and no further PVM localization are shown in blue. Candidate proteins further analyzed in this study are highlighted in bold. *P. falciparum* orthologs were identified in plasmodb.org and in in some cases synteny was used as a further indicator to support orthology (indicated by asterisks). Candidates are ordered by an increasing average p-value. BS, blood stages. LS, liver stages. GM, gametocytes.

Table S3: Primers used in this study.

Generation of EXP1-BirA*-V5 parasites:		
Name	**Lab-No.**	**Sequence (5'-3')**
BirA-V5-fw	999	AAGGATCCAGCGGCCGCGACAAGGACAACACCGTGC
BirA-V5-rev	1000	AATCTAGATTACGTAGAATCGAGACCGAGGAGAGGG TTAGGGATAGGCTTACCCTTCTCTGCGCTTCTCAGGG
EXP1-fw	1003	AAGGATCCATGAAAATCAATATAGCTTCAATTC
EXP1-rev	1004	AAGCGGCCGCTTTGTTGAAGATTTGGCATGTTAAG
Integration PCR of EXP1-BirA*-V5 parasites:		
Name	**Lab-No.**	**Sequence (5'-3')**
c-ssu-fw	728	GTGTAGTAACATCAGTTATTGTGTG
d-ssu-fw	729	ATACTGTATAACAGGTAAGCTGTTATTGTG
pL0017-rev	730	TTTCCCAGTCACGACGTTG
cd-ssu-rev	731	CTTAGTGTTTTGTATTAATGTCGATTTG
Generation of endogenously GFP-tagged candidate parasite lines:		
Name	**Lab-No.**	**Sequence (5'-3')**
1328000-ET-fw	1134	AAGGTACCACTGGGTAGAGGGTATTTTGG
1328000-ET-rev	1135	AAGGGCCCAAATATAGCAATTTTATCAATGGAATTTTTC
0519300-ET-fw	1152	AAGGTACCAAATCAAATGCAAACGGTAAGC
0519300-ET-rev	1153	AAGGGCCCTATGTTATATATAAAGTTACTTACATTTTCTG
0509000-ET-fw	1154	AAGGTACCTGAATTTGTTAAAAGTCAAAATTATAGC
0509000-ET-rev	1155	AAGGGCCCAGCATTTAACCAAGGTGCAGATAATC
0519400-ET-fw	1156	AAGGTACCGATAATCCACCGAAGAACGAAG
0519400-ET-rev	1157	AAGGGCCCACTCAAAACAAATTGAAGCATATCC
0519200-ET-fw	1166	AAGGTACCATACATGGGGAATCTGAGGATG
0519200-ET-rev	1167	AAGGGCCCAATATCTTCTTCCATCAAGACATATTC
0924800-ET-fw	1136	AAGGTACCTATAAATGATGGATGGGACAGC
0924800-ET-rev	1137	AAGGGCCCTAGGTGTAATTTTCTCTTTTTAAAAAAATAAC
1229000-ET-fw	1164	AAGGTACCAATCCCAATGTTCGTGGTAATG
1229000-ET-rev	1165	AAGGGCCCATAATTGTCTTGAGAACTGTATTTATTAATTTTG
Integration-PCR of endogenously GFP-tagged candidate parasite lines:		
Name	**Lab-No.**	**Sequence (5'-3')**
1328000-IPCR-fw	1245	GGCCTCTTAATTTATTTGTTAATGG
1328000-IPCR-rev	1246	AAAAATGCACAATAAAATGAATCC
0519300-IPCR-fw	1259	CACTGATCAAAAAGAGAAACAACC
0519300-IPCR-rev	1260	GAGAACTTTGTAAATCTTCATTTTATTCC
0509000-IPCR-fw	1261	GATTTGATGCTACTATTGTTTCTGC
0509000-IPCR-rev	1262	TTGTAATAAACTGGTAATGAAGTTCC
0519400-IPCR-fw	1263	AAAGACGAAAAAGGAATTGATGG
0519400-IPCR-rev	1264	AAATTTCTGAGTTTGCACTTTTCC
0519200-IPCR-fw	1267	GAAGATTTAAATAACACTTCATATAATGG
0519200-IPCR-rev	1268	AACCTTAAAATTCTTCATTTATCG
0924800-IPCR-fw	1247	GAAAAATATGCCTAAAATGACAACC
0924800-IPCR-rev	1248	ATATGCTTCTCTTATTTCCCAAGC
1229000-IPCR-fw	1265	ACAAGTGGTAATTCAAAAGGTTCC
1229000-IPCR-rev	1266	AAAGCGAAGTATATTAAGCAGTGG
GFP-rev	1242	TCGATGCCCTTCAGCTCG

Table S4: Restriction enzymes used for linearization of targeting constructs for parasite transfection.

Plasmid for generation of parasite line	Restriction enzyme(s)
EXP1-BirA*-V5	ApaI/SacII
PBANKA_1328000-GFP	HindIII
PBANKA_0519300-GFP	EcoRV
PBANKA_0509000-GFP	ClaI
PBANKA_0519400-GFP	HindIII
PBANKA_0519200-GFP	BstXI
PBANKA_0924800-GFP	PacI
PBANKA_1229000-GFP	FspAI

2.2. *Plasmodium* requires host porphobilinogen deaminase for intraerythrocytic growth

Contribution: 85% (majority of experimental work and data analysis, paper writing and figure preparation).

Gaetan Burgio and Simon Foote performed the ENU injections. Denis C Bauer performed the bioinformatics analysis on the raw data from exome sequencing. Hao Yang, Lora Starrs, Anna Ehmann, Farid Rahimi and Brendan J McMorran performed the *P. falciparum* studies. Elena Di Pierro and Giovanna Graziadei provided the AIP blood samples and biochemical analysis of the AIP patients.

Host porphobilinogen deaminase deficiency confers malaria resistance during intraerythrocytic growth

Cilly Bernardette Schnider[1,2,a#], Hao Yang[1#], Lora Starrs[1], Anna Ehmann[1], Farid Rahimi[3], Elena Di Pierro[4], Giovanna Graziadei[4], Denis C. Bauer[5], Simon J. Foote[1], Gaetan Burgio[1] and Brendan J. McMorran[*1]

[1]Department of Immunology and Infectious Disease, John Curtin School of Medical Research, Australian National University, Canberra, ACT 2601, Australia.
[2]Department of Biomedical Sciences Faculty of Medicine and Health Sciences, Macquarie University, NSW 2109 Australia.
[3]Research School of Biology, Australian National University, Canberra, ACT 2601, Australia.
[4]Rare Diseases Center, Internal Medicine Unit, Department of Medicine and Medical Specialties, Fondazione IRCCS Ca' Granda - Ospedale Maggiore Policlinico, Via Francesco Sforza, 35, 20122 Milan, Italy.
[5]Digital Productivity, CSIRO, Macquarie Park, NSW 2113, Australia.
[a]Current address: Institute of Cell Biology, University of Bern, Bern, Switzerland.
[#]These authors contributed equally to the work.
*Corresponding author: Brendan J. McMorran, PhD; brendan.mcmorran@anu.edu.au. Department of Immunology and Infectious Disease, John Curtin School of Medical Research, Australian National University, Canberra, ACT, 2601, Australia. Phone: +61 2 6125 7182, Fax: +61 2 6247 4823.

ABSTRACT

The selective pressure imparted by malaria has led to many mutations in erythrocytic genes that confer host resistance. Identification and characterization of mutations affecting host resistance to malarial infection enables a deeper understanding of host–pathogen interactions and potentially new ways in which to prevent infection. Using ENU-induced mutagenesis, and screening for erythrocyte abnormalities and resistance to malaria, we identified a novel nonsense mutation in the gene encoding porphobilinogen deaminase (PBGD) in mice. Heterozygotes exhibited microcytosis and 25% reduction in cellular PBGD activity, but were healthy otherwise. When challenged with blood-stage *Plasmodium chabaudi*, the heterozygotes were significantly protected against infection, showed reduced parasite growth, and had a survival advantage. The mutation did not affect erythrocyte susceptibility to parasite invasion or the host immune response. Instead, the mechanism of resistance to infection involved intraerythrocytic parasite death and reduced propagation of viable parasites. A similar effect was observed when *P. falciparum* was cultured in erythrocytes from patients with acute intermittent porphyria (AIP), who have low PBGD levels. We observed reduced propagation of viable parasites and increased intraerythrocytic parasite death in AIP erythrocytes compared to normal erythrocytes; parasite invasion and establishment inside AIP erythrocytes were unaffected. Furthermore, the growth capacity of PBGD-null parasites, which grew at the same rate as their wild-type counterparts in normal erythrocytes, was reduced further in the AIP erythrocytes. These results suggest that PBGD deficiency confers resistance to infection with *Plasmodium* during the blood-stage.

INTRODUCTION

Symptomatic and lethal stages of malaria occur when *Plasmodium* parasites invade and replicate within erythrocytes. The ongoing relationship between parasite and host, spanning primordial vertebrates and human evolutionary history, has exerted significant selective pressures on human populations. This has manifested as polymorphisms and mutations that produce altered erythrocytic proteins, many of which are associated with host resistance to infection. These include hemoglobinopathies and deficiencies in cytoskeletal proteins and enzymes that are highly expressed in erythrocytes; they act either directly by impeding parasite invasion or growth, or indirectly on host immune responses and parasite clearance [1-4]. By virtue of its parasitic lifestyle during the blood stage of the disease, *Plasmodium* scavenges erythrocyte enzymes, including protein kinases, cellular redox regulators, and those involved in heme biosynthesis [5-9]. Depriving parasites of such host enzymes may also contribute to resistance to malarial infection and facilitate identifying novel antimalarial therapeutics as reported in model systems [10, 11].

Heme is an essential cofactor in many proteins and enzymes, for example, in hemoglobin as a carrier of oxygen and carbon dioxide. The canonical heme biosynthetic pathway uses eight enzymes, which catalyze conversion of glycine and succinyl-CoA into protoporphyrin, and subsequent Fe^{2+} incorporation. Heme biosynthesis is essential in humans and deficiency of any of the synthetic enzymes is lethal. However, mutations that depress enzyme production or activity are known and cause porphyria. Characteristic symptoms of porphyria may include mild to severe skin photosensitivity, liver malfunction and neurological problems, and are caused by build-up of toxic porphyrin precursors and their derivatives. Specific symptoms and disease severity depend on the composition and levels of these molecules, which in turn are determined by enzyme activity and responsible mutations.

Plasmodium has a canonical heme biosynthesis pathway [12]. Interestingly, essentiality of the pathway differs according to the parasite life cycle stage. *P. berghei* made genetically deficient in either the first (δ-aminolevulinic acid synthase; ALAS) or last (ferrochelatase; FC) enzyme of the pathway are not viable in the mosquito stages, but propagate in the mouse bloodstream and cause symptoms that are indistinguishable from those by wild-type parasites [13, 14]. Similarly, the growth of *P. falciparum* cultured in human erythrocytes is not affected by deletion of FC, or two other pathway enzymes, porphobilinogen deaminase (PBGD) and coproporphyrinogen oxidase [13, 15]. These enzyme-deficient parasite lines may acquire heme directly from the degradation of host hemoglobin, based on the observation that no heme is synthesized in FC-deficient *P. falciparum* [13]. Additional parasite heme-acquisition pathways involving co-opting of the host heme-biosynthetic enzymes that participate in *de novo* synthesis have also been reported [5, 9, 16]. Even though heme biosynthesis is restricted to erythroid progenitors, mature erythrocytes contain detectable amounts of active enzymes, [17-19], including PBGD, which is biosynthetically active in mature erythrocytes [15].

Previously, we showed that the growth of both *P. chabaudi* and *P. falciparum* was significantly perturbed in mouse and human erythrocytes with reduced levels of FC (erythropoietic protoporphyric erythrocytes). In contrast, *P. falciparum* parasites grew normally in X-linked dominant protoporphyric erythrocytes, which have normal levels of FC, but elevated porphyrin precursors. Collectively, this indicated that, rather than any non-specific effects caused by FC-insufficiency impacting on the parasite, *Plasmodium* has a specific requirement for host FC to sustain its growth in erythrocytes [20]. Here, we provide evidence that *Plasmodium* might have a similar reliance on erythrocytic PBGD. We found that PBGD-insufficiency, both in mice carrying a novel mutation in the gene encoding PBGD, and in human erythrocytes from acute intermittent porphyria (AIP) patients, results in impaired parasite growth.

RESULTS

To investigate if the *Pbgd*^{MRI58155} mutation affects the host-response to malarial infection, cohorts of heterozygous and wild-type mice were inoculated with *P. chabaudi adami* DS, which is typically lethal to this parental mouse strain (SJL/J). We observed a significantly altered course of infection in heterozygotes compared to wild-type mice. Parasitemias were lower than wild-type mice between days seven and ten in female mice (Figure 1A), and days nine and ten in male mice (Figure 1B). A modest but significant survival advantage was observed for female heterozygotes ($p = 0.00016$); 90% of these animals survived for at least one day longer than their wild-type littermates, although 11 out of 12 heterozygous mice eventually succumbed (Figure 1C). Two of 21 heterozygous male mice survived the infection, although this was not statistically significant (Figure 1D).

In order to investigate the *Pbgd*^{MRI58155} further, we analyzed the blood in detail. *Pbgd*^{MRI58155} mice displayed microcytosis, accompanied by moderately elevated reticulocyte counts, and reduced hematocrit and total hemoglobin, but with normal mean erythrocytic hemoglobin levels. We confirmed that the phenotype was heritable after crossing the G1 animal with SJL/J mice and observing that the G1 microcytosis phenotype was passed on to approximately half the offspring. Intercrossing two affected G2 mice produced the wild-type phenotype in approximately one third of the progeny and the G1 founder phenotype in the other two thirds (Supplementary Table 1). Collectively this indicated a fully penetrant dominant inheritance of the microcytotic phenotype (i.e., heterozygous for the MRI58155 allele) but embryonic lethality in homozygotes.

Whole-exome sequencing of two heterozygous G3 mice and subsequent segregation analysis of mutations in candidate genes identified a single base substitution (A to G) in chromosome 9 (Chr9 44341074, mm10), which is located in the murine *Pbgd* gene (NM_013551). This mutation, designated *Pbgd*^{MRI58155}, is predicted to disrupt splicing of exon 6 and results in a truncated protein comprising 90 amino acids; this protein lacks all conserved residues and domains required for catalytic function of PBGD (Figure 2A).

The mutation completely segregated with the microcytic phenotype over more than ten generations of breeding. Compared to wild-type mice, reduced amounts of PBGD were observed in immunoblots of proteins extracted from spleen, liver, bone marrow, and erythrocytes from heterozygous mice; furthermore the truncated protein encoded by *Pbgd*^{MRI58155} was not detectable (Figure 2B and Supplementary Figure 1). PBGD activity was significantly lower in heterozygous than in wild-type erythrocytes (30.5 ± 2.2 versus 39.5 ± 3.5 nkat/L; $p = 0.048$, (Figure 2C). Urine from heterozygous mice appeared lightly pink in color. The heterozygous mice also exhibited modest splenomegaly, but normal liver size, and normal iron content in both organs; serum cytokine levels were also similar to wild-type mice (Supplementary Tables 2 and 3). Assaying erythrocyte life span (Supplementary Figure 2A) and osmotic fragility (Supplementary Figure 2B) indicated no effects of the mutation. In addition, production of erythroid progenitors was also unaffected (Supplementary Figure 2C).

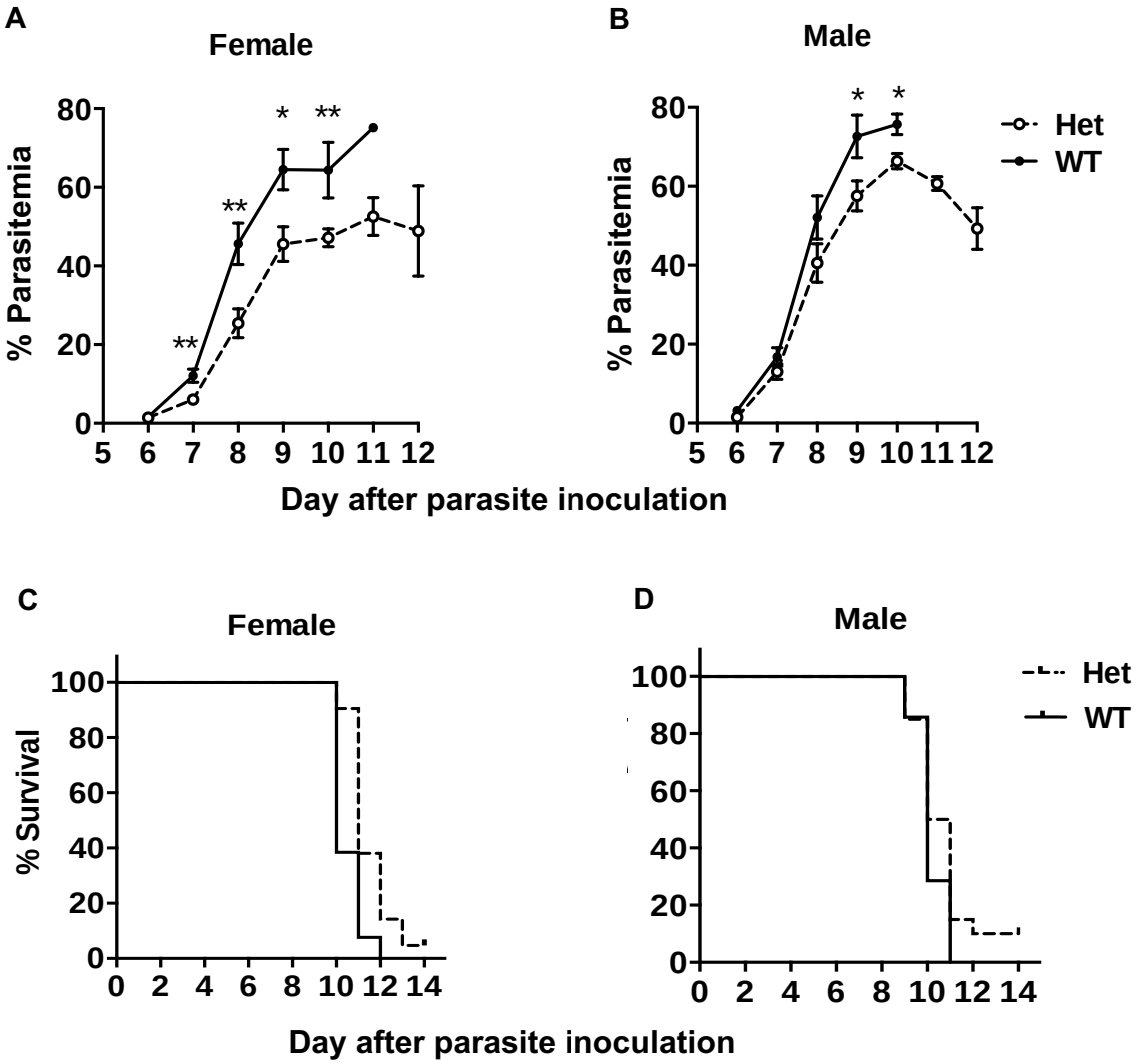

Figure 1: Mice with the *Pbgd*^{MRI58155} mutation display an increased resistance to infection with *P. chabaudi*. **A** Female *Pbgd*^{MRI58155} heterozygotes (Het) and wild-type littermates (WT) were infected with *P. chabaudi* (1 × 10^4 parasites; 13–21 mice per group) and analyzed for percentage of parasitemia. Graph represents the average parasitemia of three individual biological replicates. **B** Male *Pbgd*^{MRI58155} heterozygotes (Het) and wild-type littermates (WT) were infected with *P. chabaudi* (1 × 10^4 parasites; 13–21 mice per group) and analyzed for percentage of parasitemia. Graph represents the average parasitemia of two individual biological replicates. **C** Female *Pbgd*^{MRI58155} heterozygotes (Het) and wild-type littermates (WT) were infected with *P. chabaudi* (1 × 10^4 parasites; 13–21 mice per group) and analyzed for survival. **D** Male *Pbgd*^{MRI58155} heterozygotes (Het) and wild-type littermates (WT) were infected with *P. chabaudi* (1 × 10^4 parasites; 13–21 mice per group) and analyzed for survival. Log-rank (Mantel–Cox test) for differences in survival yielded p-values of 0.0016 (female) and 0.16 (male).

We investigated whether the reduced parasitemia observed in the heterozygous mice was due to compromised merozoite capacity to invade erythrocytes. We used an *in vivo* cell-invasion assay [21], in which mixtures of differently labeled heterozygous and wild-type erythrocytes were transfused into recipient wild-type mice infected with *P. chabaudi*, and the percentages of transferred erythrocytes that became infected determined. Following injection of the labeled erythrocytes into the recipient at the point of parasite schizogony, the proportion of newly infected erythrocytes measured during the next 30 min to 20 h were similar between the two donor types. After 39 h, the percentage of infected cells had increased, reflecting a second schizogony and infection cycle, but were still similar comparing wild-type and heterozygous cells (Figure 2D). Overall, no significant differences between heterozygous and wild-type cells were observed at any of the time points tested. These results indicate that the heterozygous erythrocytes' susceptibility to merozoite invasion is equal to their wild-type counterparts. We then investigated if the ability of the *P. chabaudi* parasites to grow within erythrocytes was affected by PBGD insufficiency. Thus, we determined the numbers of dead or dying intraerythrocytic *P. chabaudi* parasites in infected heterozygous or wild-type mice using TUNEL [22]. The mean percentages (± SEM) of TUNEL-

labeled parasites measured in samples collected eight and nine days after infection were 9.0 ± 1.0 and 12.6 ± 1.2 in wild-type mice and 10.4 ± 1.4 and 15.8 ± 1.7 in heterozygous mice; the heterozygous values were significantly greater than those of the wild-type at both time points ($p < 0.05$; Figure 2E). This finding suggests that in heterozygous erythrocytes, a greater proportion of parasites are dying, in turn reducing production of new, viable parasites and explaining the observed reduced parasitemia and relatively better survival.

PBGD deficiency in humans can manifest as AIP (MIM 176000). The disease is characterized by occasional, acute episodes of gastrointestinal and neuropathic symptoms; between episodes, the patient is healthy. Acute attacks result from high urinary excretion of the heme precursors, especially δ-aminolevulinic acid and porphobilinogen [23]. We obtained blood samples from seven AIP patients, all with confirmed *PBGD* gene mutations and reduced PBGD activity; four patients reported a typical history of episodes of acute symptoms with elevated urinary δ-aminolevulinic acid and porphobilinogen levels but were not symptomatic at the time of blood collection (Table 1 and Supplementary Table 4).

Table 1. AIP patient samples assayed for *P. falciparum* growth assays.

AIP type	PBGD mutation (*PBGD* ID, or novel)	PBGD protein defect (predicted % normal cellular PBGD activity)	Number of patient samples
AIP A	c.[498+93_1086+211del3137];[=] (novel)	p.(Arg167_Ter362del) (50%)	1
AIP B	c.[913-1 G>C];[=] (novel)	p.(His305_Ter362del) (50%)	4
AIP C	c.[580C>T];[=] (H971935)	p.(Gln194Ter) (50%)	1
AIP D	c.[760_763delCTGAinsTCG];[=] (novel)	p.(Leu254Serfster11) (50%)	1

The AIP C mutation (H971935) has been previously described [24].

Erythrocytes isolated from these AIP samples and from healthy individuals, all shipped from Italy (HC Italy, n = 2), and from the Australian Red Cross Blood Service (HC Australia, n = 1), were infected with growth-stage-synchronized *P. falciparum* parasites (pigmented trophozoites and schizonts). Cultures were incubated for up to 72 h and sampled at different time points to count the number of parasitized cells, determine parasite development stages, and compare parasite propagation and their intraerythrocytic development, over time. Following the first 24 h of culturing, while parasites egress from donor erythrocytes and invade the surrounding test cells, we observed no differences in parasitemia fold-change (Figure 3A) and similar proportions of ring-stage and early-trophozoite parasites in both the AIP and HC erythrocytes (Supplementary Figure 3). After 72 h, while parasites had replicated in test erythrocytes and undergone a further cycle of schizogony and cell invasion, the number of parasitized erythrocytes in the HC samples was more than double the number present at 24 h, which was statistically significant ($p < 0.001$). In contrast, numbers of parasitized AIP cells after 72 h had increased only negligibly, or not at all. In three AIP samples (mutation types A, C, and D), the 72-h parasitemia fold-change was also significantly lower than in HC erythrocytes ($p < 0.05$) (Figure 3A). Examination of parasite development stages indicated reduced numbers of late-stage pigmented trophozoites and schizonts at 48 h, and fewer ring-stage parasites at 72 h (Supplementary Figure 3). We also conducted TUNEL assays on samples after 48 h culturing. This revealed that the number of dead or dying intraerythrocytic parasites in the AIP samples was more than three times the number observed in HC cells ($p < 0.05$) (Figure 3B). Collectively, these results indicate that the *P. falciparum* could normally infect the AIP erythrocytes and establish within them, but that their intraerythrocytic growth was perturbed such that they either died inside the erythrocyte and/or produced fewer viable merozoites. A *P. falciparum* clone carrying a genetic disruption of the parasite *Pbgd* homolog (PF3D7_1209600) was shown previously to grow as well as its wild-type parent strain (3D7) in normal human erythrocytes [15]. We obtained these lines (designated here as Pf*Pbgd*-KO and 3D7) and compared their growth characteristics using the same parasite-culturing approach described above. Two normal erythrocyte samples (HC Australia and HC Italy) and six AIP erythrocyte samples (from AIP patients with mutation types B, C, and D) were tested. Both parasite lines cultured in the HC erythrocytes established similar parasitemia levels and increased more than six-fold after 72 h. In contrast, when the two lines were cultured in AIP erythrocytes, the growth of Pf*Pbgd*-KO parasites was noticeably reduced compared to that of the 3D7 (Figure 3C and Supplementary Figure 4). These differences were significant in the four AIP samples with mutation type B at 24 h and in the AIP sample with mutation type C at 72 h ($p < 0.001$).

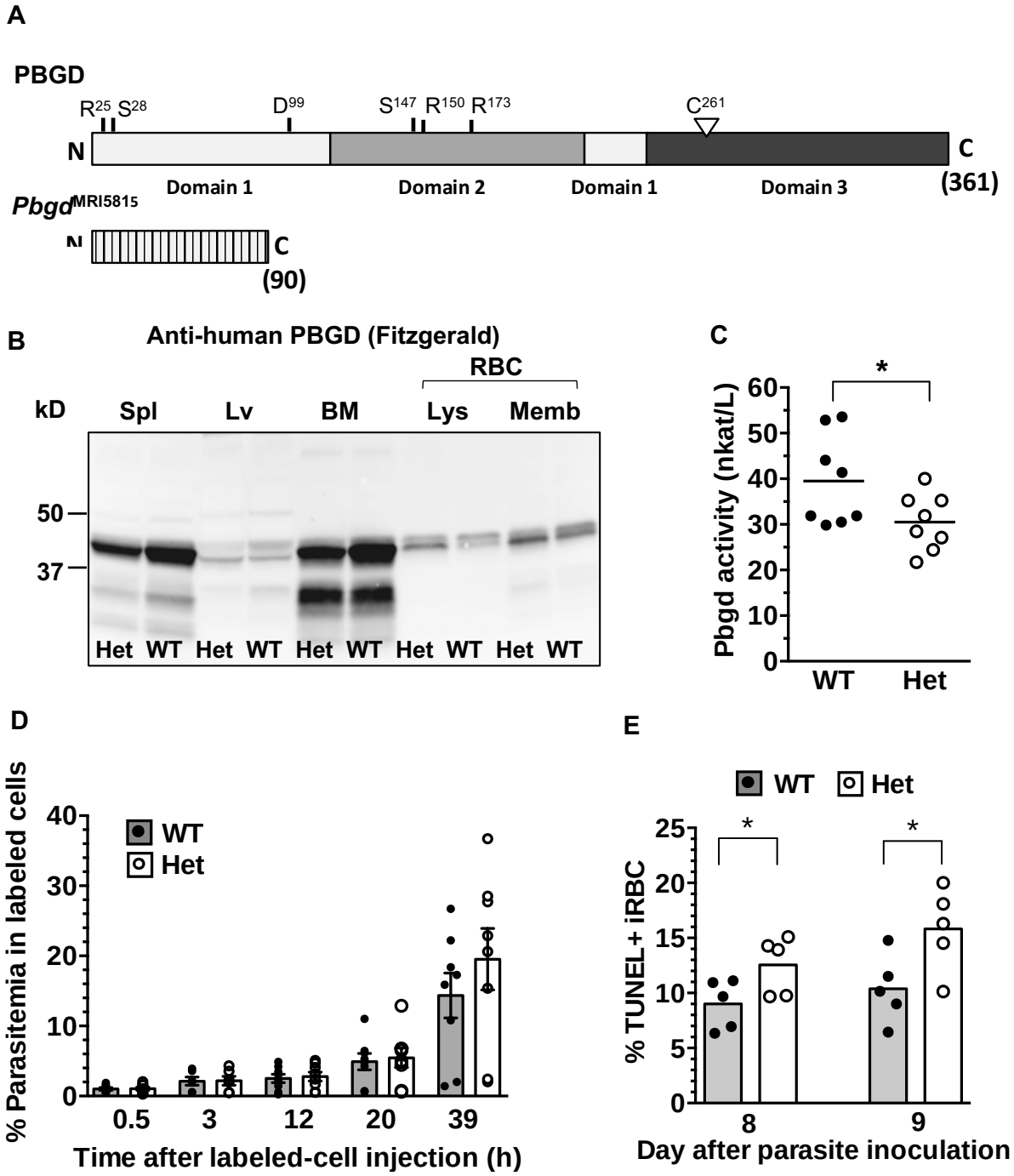

Figure 2: Analysis of mice with the *Pbgd*^{MRI58155} mutation. A Schematic of the full-length, 361-residue murine PBGD protein, including locations of the three domains and active-site residues, R25 and S28 (sulfate-binding), D99 (catalytic), S147, R150, and R173 (pyrrole-cofactor interacting) and C261 (pyrrole-cofactor binding), based on the human PBGD crystal structure [25]. The predicted 90-residue protein expressed by the PbgdMRI58155 allele is shown below. It lacks the sequences containing the catalytic domain and cofactor-binding sites. **B** Immunoblotting of PBGD in various tissues from wild-type (WT) and *Pbgd*$^{MRI58155/+}$ heterozygous (Het) mice. The full-length PBGD protein is detected at ~39 kDa. Tissues analyzed were spleen (Spl), liver (Lv), bone marrow (BM), and erythrocytes (RBC) fractionated into hemoglobin-depleted lysates (Lys) and membrane (Memb). **C** *Pbgd*^{MRI58155} heterozygotes (Het) and wild-type littermates (WT) were infected with *P. chabaudi* (1×10^4 parasites; 13–21 mice per group) and analyzed for percentage of parasitemia. **D** Proportions of labeled cells infected with parasites. Eight WT mice infected with *P. chabaudi* were injected intravenously with differently labeled WT and Het blood cells (at day 8 post-inoculation) and % parasitemia determined in each labeled cell type at indicated time points. **E** Proportions of TUNEL-positive parasite-infected erythrocytes in WT and Het mice (five per group) infected with *P. chabaudi* for eight and nine days. In all figures, error bars represent SEM. * $p < 0.05$, ** $p < 0.01$, calculated using the two-tailed Student's *t*-test assuming equal variance.

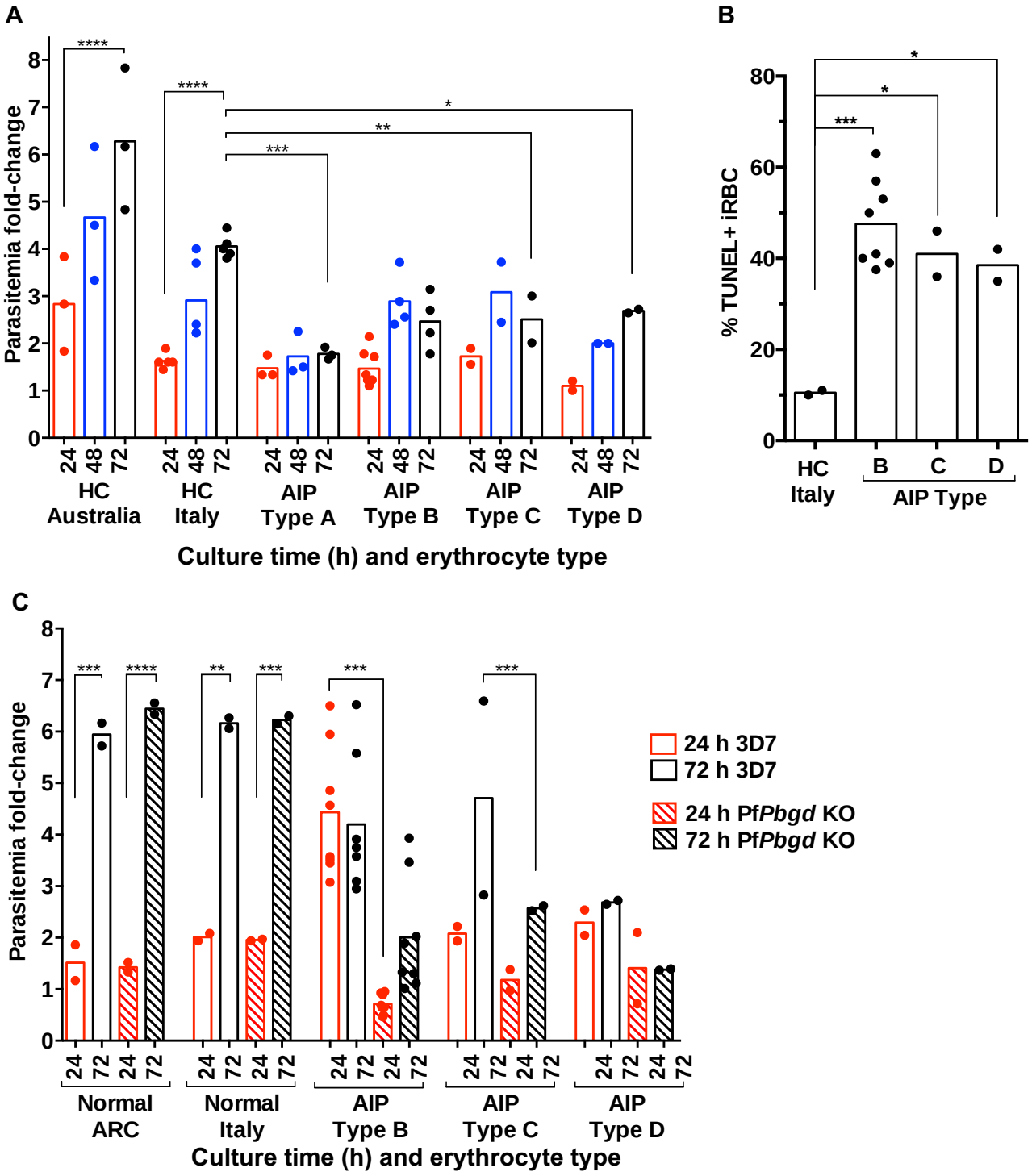

Figure 3. *P. falciparum* growth in erythrocytes from patients with AIP. **A** Comparison of *P. falciparum* growth in AIP and healthy control (HC) erythrocytes. **B** Proportions of TUNEL-positive parasite-infected erythrocytes (iRBC) after culture for 48 h. **C** Comparison of growth of wild-type (3D7) and Pf*Pbgd* knockout *P. falciparum* (Pf*Pbgd* KO) in AIP and HC erythrocytes. The four different AIP B samples were assayed in duplicate at 24 h, and once at 48 h, and 72 h. All other samples were assayed in duplicate or triplicate. * $p < 0.05$, ** $p < 0.01$, *** $p < 0.001$, **** $p < 0.0001$, calculated using the two-tailed Student's *t*-test assuming equal variance.

There were no significant increases in parasite numbers observed for the wild-type line between 24 and 72 h, which was consistent with results in the above experiments that used a different 3D7 strain. Therefore, while deletion of parasite *Pbgd* gene did not affect its ability to grow in normal erythrocytes, which confirms a previous study [15], its growth

was perturbed in host erythrocytes with insufficient PBGD. Together this might indicate a certain requirement of host PBGD of *Plasmodium*. However other explanations of the herein reported results could also indicate that the resistance to malaria infection in PBGD deplete mice and human erythrocytes could be due to an off-target effect.

DISCUSSION

Here, we describe the identification and characterization of an ENU-induced mutation in the murine *Pbgd* gene (*Pbgd*^{MRI58155}). Mice heterozygous for this mutation display a relatively normal phenotype, distinguished by microcytosis and a modest, but significant decrease in erythrocytic PBGD activity, although they exhibited no overt symptoms characteristic of AIP. Previous studies showed that a more profound deficiency of PBGD is necessary in mice to mimic the human condition [26]. The protein expressed by the *Pbgd*^{MRI58155} allele is predicted to be truncated and completely inactive, and consistent with this prediction, we never obtained homozygous pups. However, rather than the predicted 50% reduction in enzyme activity, heterozygotes retained ~75% of normal enzyme activity in their blood. It is possible that a partially functional protein is expressed by the mutant allele, or expression by the wild-type allele is compensatory increased. The most prominent consequence of the *Pbgd*^{MRI58155} mutation, and indeed the phenotypic basis of its identity, was a modest microcytic anemia, although erythrocyte number and erythrocytic hemoglobin concentrations were normal. Reduced biosynthesis of heme in erythroid progenitors can often lead to generation of microcytic anemia, although this is not characteristic of human AIP, and is not a reported effect for the *Pbgd*-null and hypomorphic mutations [26]. However, microcytic erythrocytes have been observed in cats with *Pbgd* mutations that display AIP symptoms [27]. Overall, the *Pbgd*^{MRI58155} allele results in a phenotype consistent with a mild, asymptomatic form of AIP.

We used the *Pbgd*^{MRI58155} mouse line, as well as erythrocytes from AIP patients with PBGD deficiency to investigate potential dependence of *Plasmodium* on the host enzyme for its growth and survival. These studies were motivated by previous observations that other host heme biosynthetic enzymes are co-opted by the parasite and that they may be potential antimalarial therapeutic targets [5, 9, 11, 16, 20]. We found that parasite growth was significantly perturbed in both mice and human erythrocytes with reduced PBGD levels. This was evidenced by reduced parasite propagation, increased intraerythrocytic parasite death, and modest but significant protection against *P. chabaudi* infection in the *Pbgd*^{MRI58155} mutant mice. Our experiments using mice and analysis of parasite development in the AIP erythrocytes demonstrated that invasion of mutant erythrocytes by merozoites was not inhibited. We also excluded other possible indirect effects of the enzyme deficiency in the mouse, including their immune function and cellular hemoglobin levels, relevant indices of which were relatively normal. We therefore propose that the reason parasite growth was impaired in mutant mice and AIP erythrocytes is that *Plasmodium* has a certain requirement for host PBGD. This hypothesis is supported by our observation that parasites lacking their own version of *Pbgd* grew less well compared to wild-type counterparts in AIP erythrocytes. This is despite the apparent dispensability of the parasite enzyme if the host erythrocyte is PBGD-replete. It is possible the parasite requires a certain threshold level of enzyme to grow, a proportion of which is contributed from the erythrocyte; the parasite growth defect is only manifested in host cells with reduced PBGD levels. It is also possible that the parasite 5requires precursors of the heme biosynthetic pathway, which may be produced by infected host cells [15].

In conclusion, our data indicate that *Plasmodium* has a certain requirement erythrocytic PBGD for its growth and propagation in erythrocytes, but that the parasite PBGD homolog is dispensable, unless host PBGD is depleted. In addition our data cannot fully exclude the possibility that the resistance of PBGD deplete mice and human erythrocytes is due to an off-target effect. An interesting investigation would be to test specific small-molecule inhibitors for PBGD, which have been developed [28] but would require the synthesis of these as they are unavailable to test. This would then elucidate the role of host PBGD during malaria infection and whether our hypothesis of a certain requirement of the enzyme by the parasite can be confirmed.

EXPERIMENTAL PROCEDURES

Ethics statement

Blood sampling and experimental procedures involving patients were performed in accordance with the 1983 revision of the Declaration of Helsinki. The study was approved by the Ethical Committee of Fondazione IRCCS Ca' Granda, Ospedale Maggiore Policlinico, Milan, Italy (Project Number 246_2015) and The Australian National University Human Research Ethics Committee (2014/765).

All procedures involving animals conformed to the *Australian code of practice for the care and use of animals for scientific purposes* by the Australian National Health and Medical Research Council (NHMRC) and were approved by the Macquarie University Animal Ethics Committee (Project Numbers: ARA 2012/017 and 2012/019) and the Australian National University Animal Experimentation Ethics Committee (2014/53).

Animals
Mice were bred and housed under specific pathogen-free conditions. Mice were housed under controlled temperature (21°C) with a 12:12 h light-dark cycle and fed a diet of Rat and Mouse Premium Breeder chow (Gordons Specialty Feeds, Glen Forest, WA, Australia). Seven-week-old SJL/J male mice were injected IP with 150 mg/kg of *N*-ethyl-*N*-nitrosourea (ENU) at 1-week intervals. Mutagenized G0 mice were crossed with background SJL/J mice. G1s were bled after seven weeks for blood analysis. The G1 58155 founder displayed a mean corpuscular volume that was two standard deviations smaller than average; it was crossed with SJL/J and resulting G2s were used in further experiments. For each experimental procedure, heterozygous *Pbgd*^{MRI58155} mice were compared to their wild-type littermates and housed together of up to 5 animals per cage (Green Line IVC, Tecniplast, PA). Sample sizes were chosen based on statistical power calculations to limit the number of animals used.

Immunoblotting
For the mouse studies, proteins were extracted by homogenization of collected tissues and cells in denaturing SDS sample buffer (ThermoFisher Scientific, Australia) and clarified by centrifugation. Human erythrocyte membranes were prepared by lysis of uninfected cells in ice-cold 2.5 mM sodium phosphate buffer (pH 7.4) containing cOmplete™ Protease Inhibitors (Roche, Australia), followed by centrifugation (12,000×*g*, 10 min) and washing in the same buffer. Purified parasite samples were prepared from *P. falciparum* cultured in normal erythrocytes and enriched by Percoll density-gradient centrifugation [29]. Parasitized cells were washed in PBS, treated with 0.15% saponin (10× parasite pellet volume) for 10 min, and the released parasites then washed twice in cold PBS containing protease inhibitors and lysed in RIPA lysis buffer (Sigma Aldrich, Australia). Soluble and insoluble fractions of the parasite lysate were recovered after centrifugation (12,000×*g*, 10 min) and analyzed separately. The later fraction consisted mostly of insoluble hemozoin. All samples were mixed with denaturing SDS sample buffer and subjected to SDS-PAGE using 8% gradient gels [30]. Gels were blotted onto membranes, and membranes were incubated with antibodies described in Supplementary Methods.

***P. chabaudi* infections**
Experiments used the rodent parasite *P. chabaudi adami* DS (408XZ). Parasite stocks were prepared by passage through resistant C57BL/6 mice as described previously [21]. Experimental mice were infected IP with a dose of 1×10^4 parasitized erythrocytes. Blood-stage parasitemia was determined by microscopically examining thin blood smears obtained by tail bleeding (1 µL per day from days 7 to 14 after infection) and staining in 10% Giemsa solution. Percentages of infected erythrocytes were calculated.

PBGD assay
Whole-blood samples were collected by cardiac puncture, erythrocytes purified and duplicate samples from five wild-type and five heterozygous mice were analyzed for PBGD activity as described in Supplemental Methods.

TUNEL staining and immunofluorescence
Deoxyuridine triphosphate nick-end labeling by the terminal deoxynucleotidyl transferase (TUNEL) labels degraded or sheared DNA, revealing parasite apoptosis or necrosis. TUNEL and staining cells for immunofluorescence microscopy was performed on blood smears from *P. chabaudi* infected mice or *P. falciparum* cultures as described [22], but with some modifications described in Supplementary Methods. Slides were examined at room temperature using an Axio Observer inverted fluorescence microscope or a LSM 800 confocal microscope with Airyscan, both using 630× magnification and coupled to a Axiocam 503 monochrome cameras (Zeiss, Australia). All images were acquired and processed using Zen microscope and imaging software (Zeiss, Australia).

Study subjects
We studied erythrocytes obtained from seven Italian Caucasian AIP patients recruited at the Department of General Medicine, Fondazione IRCC Ca' Granda, Ospedale Maggiore Policlinico, Milan, Italy. All patients had a confirmed biochemical and genetic diagnosis: three patients were asymptomatic carriers and four of them experienced typical acute attacks. (Supplementary Table 1).

Collection and preparation of purified erythrocytes
Blood from patients with AIP and Italian healthy controls was collected by venepuncture into 5-mL tubes containing EDTA. Blood was shipped at 4 °C within 7 days of collection from the Ospedale Maggiore Policlinico, Milan, Italy to the Australian National University, Canberra, Australia. To purify erythrocytes, samples were centrifuged (170×*g*, 13 min), and plasma and white-cell fractions removed. The remaining erythrocytes were washed twice in RPMI. Erythrocytes were stored at 4 °C for up to one further week before being infected with parasites. Matched normal control samples were shipped, purified, and stored similarly to experimental samples.

***P. falciparum* growth-inhibition assays**
P. falciparum parasites were cultured as described in Supplementary Methods. For growth assays, parasites were propagated in normal erythrocytes (from Australian Red Cross Blood Service), purified using Percoll density-gradient centrifugation [29], and then added to test erythrocytes at a final parasitemia of ~1%. Parasitemias and parasite development stages were determined after culturing for up to 72 h using Giemsa-stained thin blood smears. Growth assays were conducted in duplicate or triplicate for each patient sample unless indicated otherwise. At least 1000 cells were counted on each slide. In some experiments, parasite growth was quantified by flow cytometry after staining culture samples (fixed in Cytofix solution) with 5 µg/mL Hoechst 33342 for 5 min. Fluorescence signals were measured using a LSR Fortessa cell analyzer (BD Biosciences). At least 100,000 events were recorded per sample. BD FACS software was used to process and analyze the data.

Statistical analysis
For malaria survival, statistical significance was determined using the Mantel–Cox test. For other results, two-tailed Students *t*-test was used.
Other experimental details are described in Supplementary Methods.

Author Contributions
CBS, HY, LS, AE, FR, and BJM performed experiments and DCB analyzed the exome sequencing data. The project was conceived by BJM, GB and SJF and experiments were designed by CBS, HY, BJM and GB. The blood samples, and the genetic and biochemical analysis of the AIP patients were provided and performed by EDP and GG. The paper was written and the figures were prepared by CBS, EDP, GG, GB and BJM. All authors read and approved the final manuscript.

Disclosure of Conflicts of Interest.
The authors declare that they have no conflicts of interest to disclose.

ACKNOWLEDGEMENTS
We thank Ceri Flowers for administrative support, Diana Spinelli for recruitment of the AIP patients, Shelley Lampkin for technical assistance, Elinor Hortle for assisting with the cytokine assays, Gavin Symonds and Zeiss Australia for confocal imaging analysis, Tania de Koning-Ward for advice and assistance in the project, and the Australian Red Cross Blood Service for red cells and human serum. Authors were supported by an International Macquarie University Research Excellence Scholarship (CBS), the NHMRC (490037, 605524, APP1047090 and APP1066502) and the Australian Research Council (DP120100061). Funders had no role in the design of the study and collection, analysis, and interpretation of data or in writing the manuscript.

REFERENCES
Ahmed, R. and Leeper, F.J. (2003). A new synthesis of porphobilinogen analogues, inhibitors of hydroxymethylbilane synthase. Organic & biomolecular chemistry 1, 21-23.

Allison, A.C. (2009). Genetic control of resistance to human malaria. Curr Opin Immunol 21, 499-505.

Bonday, Z.Q., Dhanasekaran, S., Rangarajan, P.N. and Padmanaban, G. (2000). Import of host δ-aminolevulinate dehydratase into the malarial parasite: identification of a new drug target. Nature medicine 6, 898-903.

Bonday, Z.Q., Taketani, S., Gupta, P.D. and Padmanaban, G. (1997). Heme biosynthesis by the malarial parasite. Import of δ-aminolevulinate dehydrase from the host red cell. J Biol Chem 272, 21839-21846.

Brizuela, M., Huang, H.M., Smith, C., Burgio, G., Foote, S.J. and McMorran, B.J. (2014). Treatment of erythrocytes with the 2-cys peroxiredoxin inhibitor, Conoidin A, prevents the growth of *Plasmodium falciparum* and enhances parasite sensitivity to chloroquine. PloS one 9, e92411.

Clavero, S., Bishop, D.F., Haskins, M.E., Giger, U., Kauppinen, R. and Desnick, R.J. (2010). Feline acute intermittent porphyria: a phenocopy masquerading as an erythropoietic porphyria due to dominant and recessive hydroxymethylbilane synthase mutations. Human molecular genetics 19, 584-596.

Dhanasekaran, S., Chandra, N.R., Chandrasekhar Sagar, B.K., Rangarajan, P.N. and Padmanaban, G. (2004). δ-Aminolevulinic acid dehydratase from *Plasmodium falciparum*: indigenous versus imported. J Biol Chem 279, 6934-6942.

Gill, R., Kolstoe, S.E., Mohammed, F., Al D-Bass, A., Mosely, J.E., Sarwar, M., et al. (2009). Structure of human porphobilinogen deaminase at 2.8 Å: the molecular basis of acute intermittent porphyria. The Biochemical journal 420, 17-25.

Hill, A.V. (1999). The immunogenetics of resistance to malaria. Proc Assoc Am Physicians 111, 272-277.

Ke, H., Sigala, P.A., Miura, K., Morrisey, J.M., Mather, M.W., Crowley, J.R., et al. (2014). The heme biosynthesis pathway is essential for *Plasmodium falciparum* development in mosquito stage but not in blood stages. J Biol Chem 289, 34827-34837.

Koncarevic, S., Rohrbach, P., Deponte, M., Krohne, G., Prieto, J.H., Yates, J., 3rd, et al. (2009). The malarial parasite *Plasmodium falciparum* imports the human protein peroxiredoxin 2 for peroxide detoxification. Proceedings of the National Academy of Sciences of the United States of America 106, 13323-13328.

Laemmli, U.K. (1970). Cleavage of structural proteins during the assembly of the head of bacteriophage T4. Nature 227, 680-685.

Lelliott, P.M., Lampkin, S., McMorran, B.J., Foote, S.J. and Burgio, G. (2014). A flow cytometric assay to quantify invasion of red blood cells by rodent *Plasmodium* parasites in vivo. Malaria journal 13, 100.

Lindberg, R.L., Porcher, C., Grandchamp, B., Ledermann, B., Burki, K., Brandner, S., et al. (1996). Porphobilinogen deaminase deficiency in mice causes a neuropathy resembling that of human hepatic porphyria. Nature genetics 12, 195-199.

Martinez di Montemuros, F., Di Pierro, E., Biolcati, G., Rocchi, E., Bissolotti, E., Tavazzi, D., et al. (2001). Acute intermittent porphyria: heterogeneity of mutations in the hydroxymethylbilane synthase gene in Italy. Blood Cells Mol Dis 27, 961-970.

McMorran, B.J., Marshall, V.M., de Graaf, C., Drysdale, K.E., Shabbar, M., Smyth, G.K., et al. (2009). Platelets kill intraerythrocytic malarial parasites and mediate survival to infection. Science 323, 797-800.

Min-Oo, G. and Gros, P. (2005). Erythrocyte variants and the nature of their malaria protective effect. Cellular microbiology 7, 753-763.

Nagaraj, V.A., Sundaram, B., Varadarajan, N.M., Subramani, P.A., Kalappa, D.M., Ghosh, S.K. and Padmanaban, G. (2013). Malaria parasite-synthesized heme is essential in the mosquito and liver stages and complements host heme in the blood stages of infection. PLoS pathogens 9, e1003522.

Nagel, R.L. and Roth, E.F., Jr. (1989). Malaria and red cell genetic defects. Blood 74, 1213-1221.

Nyalwidhe, J. and Lingelbach, K. (2006). Proteases and chaperones are the most abundant proteins in the parasitophorous vacuole of *Plasmodium falciparum*-infected erythrocytes. Proteomics 6, 1563-1573.
Pasini, E.M., Kirkegaard, M., Mortensen, P., Lutz, H.U., Thomas, A.W. and Mann, M. (2006). In-depth analysis of the membrane and cytosolic proteome of red blood cells. Blood 108, 791-801.

Pasini, E.M., Kirkegaard, M., Mortensen, P., Mann, M. and Thomas, A.W. (2010). Deep-coverage rhesus red blood cell proteome: a first comparison with the human and mouse red blood cell. Blood transfusion = Trasfusione del sangue 8 Suppl 3, s126-139.

Pasini, E.M., Kirkegaard, M., Salerno, D., Mortensen, P., Mann, M. and Thomas, A.W. (2008). Deep coverage mouse red blood cell proteome: a first comparison with the human red blood cell. Molecular & cellular proteomics : MCP 7, 1317-1330.

Puy, H., Gouya, L. and Deybach, J.C. (2010). Porphyrias. Lancet 375, 924-937.

Rivadeneira, E.M., Wasserman, M. and Espinal, C.T. (1983). Separation and concentration of schizonts of *Plasmodium falciparum* by Percoll gradients. The Journal of protozoology 30, 367-370.

Sicard, A., Semblat, J.P., Doerig, C., Hamelin, R., Moniatte, M., Dorin-Semblat, D., et al. (2011). Activation of a PAK-MEK signalling pathway in malaria parasite-infected erythrocytes. Cellular microbiology 13, 836-845.

Sigala, P.A., Crowley, J.R., Henderson, J.P. and Goldberg, D.E. (2015). Deconvoluting heme biosynthesis to target blood-stage malaria parasites. eLife 4.

Sigala, P.A. and Goldberg, D.E. (2014). The peculiarities and paradoxes of *Plasmodium* heme metabolism. Annu Rev Microbiol 68, 259-278.

Smith, C.M., Jerkovic, A., Puy, H., Winship, I., Deybach, J.C., Gouya, L., et al. (2015). Red cells from ferrochelatase-deficient erythropoietic protoporphyria patients are resistant to growth of malarial parasites. Blood 125, 534-541.

Smith, C.M., Jerkovic, A., Truong, T.T., Foote, S.J., McCarthy, J.S. and McMorran, B.J. (2017). Griseofulvin impairs intraerythrocytic growth of *Plasmodium falciparum* through ferrochelatase inhibition but lacks activity in an experimental human infection study. Sci Rep 7, 41975.

Varadharajan, S., Sagar, B.K., Rangarajan, P.N. and Padmanaban, G. (2004). Localization of ferrochelatase in *Plasmodium falciparum*. The Biochemical journal 384, 429-436.

SUPPLEMENTAL INFORMATION

Supplemental Figures

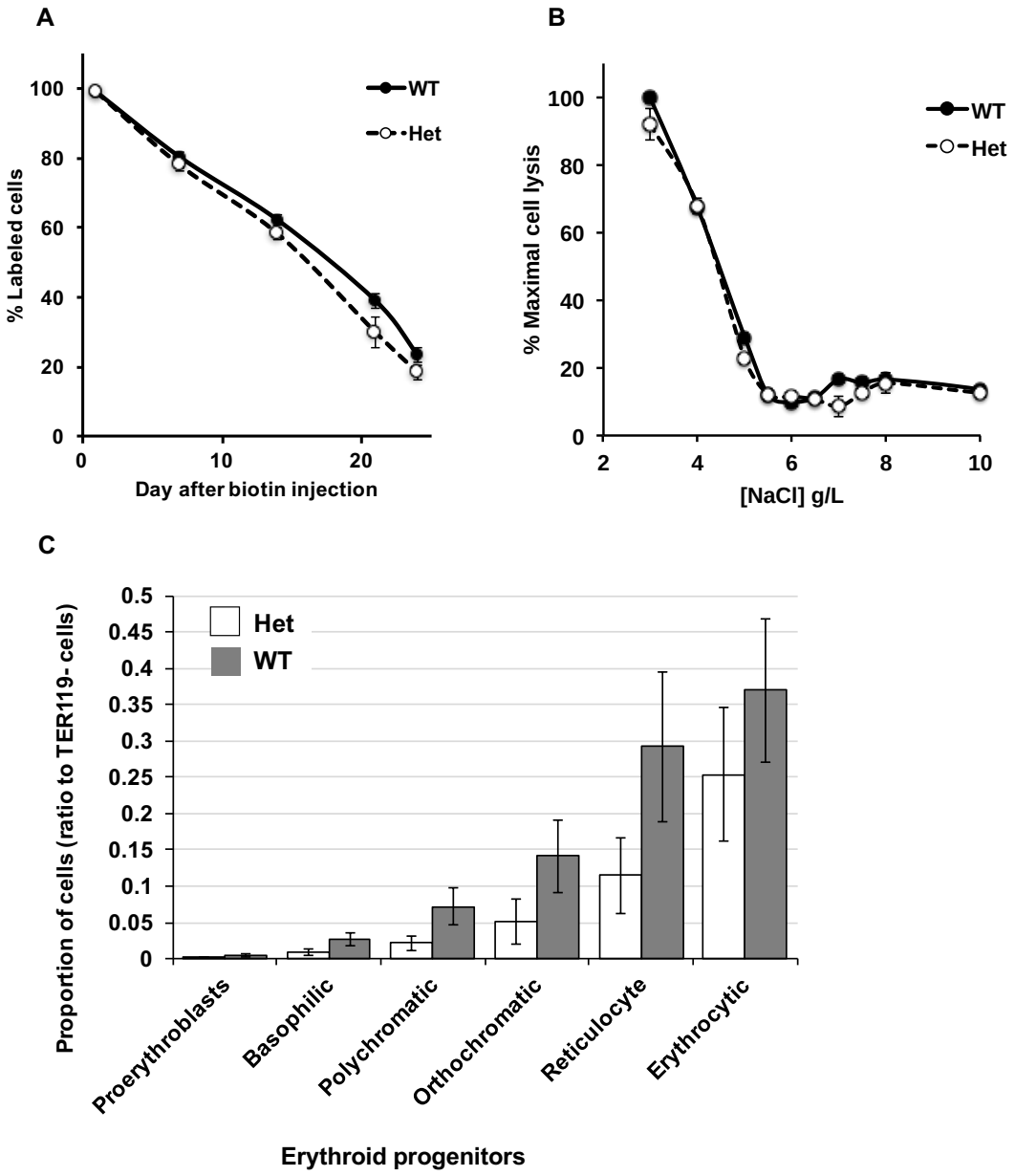

Supplementary Figure 1. Hematological analysis of the *Pbgd*^{MRI58155} mouse line.

A Comparison of erythrocyte life span, **B** osmotic strength, and **C** bone-marrow erythroid progenitor cells in *Pbgd*^{MRI58155} heterozygotes (Het, n=6–9 mice) and wild-type littermates (WT, n=6–7 mice). Error bars represent SEM. No significant differences between groups, using the two-tailed Student's *t*-test assuming equal variance.

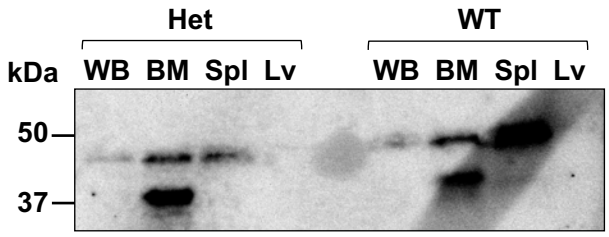

Supplementary Figure 2. PBGD expression in mouse tissues.

Immunoblotting of PBGD in various tissues from one wild-type (WT) and one *Pbgd*$^{MRI58155/+}$ heterozygous (Het) mouse using a rabbit anti-human PBGD antibody (Sigma Aldrich). The full-length PBGD protein is detected at ~39 kDa. Tissues analyzed were whole blood (WB), bone marrow (BM), spleen (Sp) and liver (Lv).

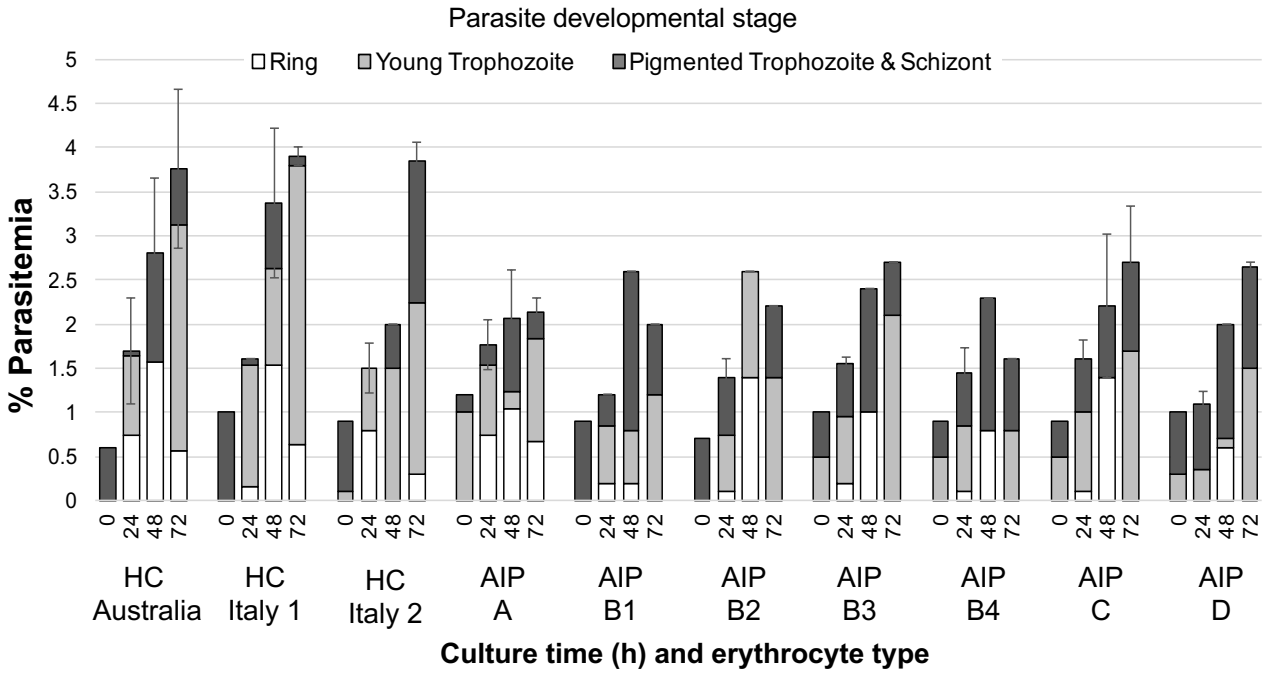

Supplementary Figure 3. *P. falciparum* growth and developmental stages in erythrocytes from AIP patients.

The AIP patient samples assayed for *P. falciparum* growth, including *PBGD* mutation and predicted catalytic activity are the same as those shown in Table 1. Percentage parasitemia and parasite developmental stage for wild-type parasites cultured in each of the AIP and healthy control (HC) erythrocyte samples. Data were collected by counting of Giemsa-stained blood smears. The four different AIP B samples were assayed in duplicate at 24 h, and once at 48 h, and 72 h. All other samples were assayed in duplicate or triplicate. Error bars represent SD. These data were used to calculate parasitemia fold-changes shown in Fig 2A.

Supplemental Tables

Supplementary Table 1. Hematological parameters of wild-type and *Pbgd*^{MRI58155} heterozygous mice

	RBC	WBC	MCV(fL)	HCT	% Retics	HGB (g/L)	MCHC (g/L)
Heterozygous	10.11 ± 0.17	11.09 ± 0.38	49.95 ± 0.22***	0.50 ± 0.008***	5.84 ± 0.26***	141.8 ± 2.5***	215.5 ± 7.4
Wild type	10.25 ± 0.05	11.44 ± 0.45	52.40 ± 0.23	0.54 ± 0.003	3.24 ± 0.21	153.4 ± 0.8	210.7 ± 6.5

Automated full blood analysis on wild type (n = 24) and heterozygous (n = 63) mice. RBC = erythrocyte; WBC = white blood cell; MCV = mean corpuscular volume; HCT = hematocrit; % Retics = proportion of reticulocytes; HGB = hemoglobin concentration; MCHC = mean corpuscular hemoglobin concentration. Values are mean ± SEM. ** $p < 0.01$; *** $p < 0.001$.

Supplementary Table 2. Spleen and liver indices, and non-heme iron content in wild-type and *Pbgd*^{MRI58155} heterozygous mice (n = 3 per group)

	Spleen index	Liver index	Spleen iron (mg/g)	Liver iron (mg/g)
Heterozygous	0.477 ± 0.017*	5.80 ± 0.33	15.2 ± 1.2	3.59 ± 0.65
Wild type	0.408 ± 0.009	5.96 ± 0.16	11.4 ± 0.2	4.58 ± 0.62

Values are mean ± SD. * $p < 0.05$.

Supplementary Table 3. Serum cytokine concentrations in wild-type (n = 5) and *Pbgd*^{MRI58155} heterozygous (n = 8) mice

	IL-2	IL-4	IL-6	IFNγ	TNFα	IL10	IL17A
Heterozygous	119 ± 55	122 ± 56	84 ± 54	68 ± 42	140 ± 85	93 ± 42*	110 ± 51*
Wild type	192 ± 51	157 ± 56	156 ± 87	111 ± 53	186 ± 92	146 ± 34	187 ± 53

All cytokine concentrations are pg/mL plasma. Values are mean ± SD. * $p < 0.05$

Supplementary Table 4. AIP patient blood biochemistry.

AIP patient ID	ALA/Creatinine ratio	PBG/Creatinine ratio	Total urinary porphyrins (μg/L)	% Urine porphyrin types (URO, EPTA, ESA, PENTA, COPRO I, COPRO III)	PBGD activity (pmol/h/mg Hb)
A	7.3	6.6	142	19, 2, 2, 22, 7, 47	42.0
B1	2.3	0.4	73	4, 1, <1, 10, 37, 48	61.1
B2*	18.6	11.1	179	43, 3, 3, 22, 17, 12	74.8
B3*	24.4	3.4	575	24, 2, 3, 23, 8, 41	56.9
B4	1.5	0.3	88	8, 4, 1, 8, 58, 21	57.5
C*	9.19	34.0	450	No data	70.9
D*	7.4	3.1	416	21, 2, <1, 27, 9, 41	34.8

* Patients were symptomatic for AIP at the time of blood collection.

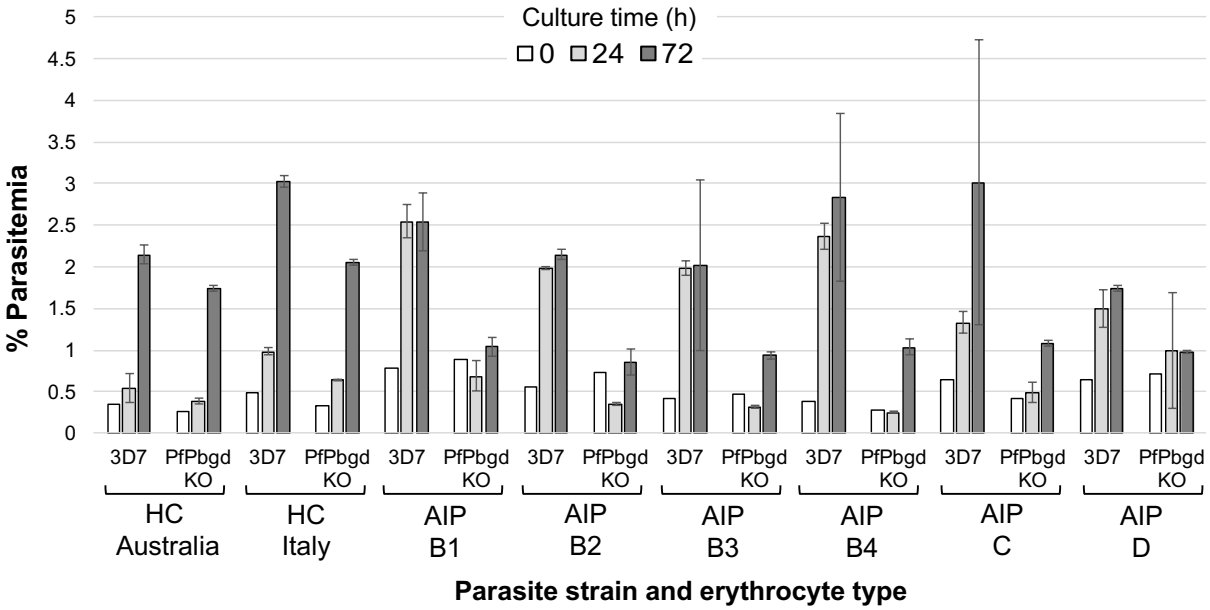

Supplementary Figure 4. *P. falciparum* 3D7 and PfPbgd-KO growth and developmental stages in erythrocytes from AIP patients.

The AIP patient samples assayed for *P. falciparum* growth, including *PBGD* mutation and predicted catalytic activity are the same as those shown in Table 1. Percentage parasitemia for *Pbgd* knockout *P. falciparum* (PfPbgd KO) and parental wild-type (3D7) cultured in AIP and normal eyrthrocytes. Data were collected by flow cytometry. All samples were assayed in duplicate. Error bars represent SD.

Supplemental Methods

Mouse phenotype analysis

Complete blood cell counts were obtained using an ADVIA® 2120 hematology system. Erythroid progenitors were examined by staining the bone-marrow-derived cells from mutant and wild-type mice with anti-TER119 and anti-CD44 (eBioscience). Cells were analyzed on a BD FACSARIA™-II flow cytometer, recording 10,000 events per sample. Populations were gated as described [31]. Cytokine Flexset assays (BD Bioscience) were used to measure plasma cytokine concentrations, according to the manufacturer's instructions.

Erythrocyte life span was determined by intravenous administration of 1 mg of NHS-biotin-ester dissolved in 0.9% (w/v) saline, and blood was sampled by tail-snipping each day for 7 days, and stained with anti-TER119 and anti-CD71 (eBioscience). Cells were resuspended in PBS/1% BSA solution containing 108 counting beads/μL, and the number of $TER119^+ CD71^-$ cells calculated per bead.

Hepatic and splenic iron levels were measured in tissues dried at 45 °C for 48 h and then digested in a 10% hydrochloric acid/10% trichloroacetic acid (TCA) solution for 48 h at 65 °C. Samples were centrifuged (10000×*g* for 5 min); 200 μL of supernatant was added to 1 mL of 1,10-phenanthroline monohydrate solution and incubated for 15 min at ~23 °C. After incubation, absorbance was measured at $\lambda = 508$ nm.

Erythrocytic osmotic fragility was determined by incubating blood samples diluted 1:100 in NaCl solutions ranging from 0 to 160 mM. After 30 min at 37 °C, samples were centrifuged and absorbance of the supernatant measured at $\lambda = 545$ nm. Percentage lysis was calculated by comparison to 100% lysis in water.

Whole-exome sequencing

DNA from two phenodeviant MRI58155 mice was isolated using a Qiagen DNeasy Blood and Tissue Kit (Hilden, Germany). DNA (≥10 μg) was prepared for paired-end genomic library sequencing using a kit from Illumina (San Diego, CA). Exomes were enriched using the Agilent SureSelect kit. Samples were sequenced using a Hiseq 2000 platform. Variants were identified and filtered as described [32]. Briefly, we mapped the short sequence tags (reads) on the mouse genome (mm10/NCBI38) using BWA V0.61 [33] and BOWTIE2 [34]. Nucleotide variants were identified using SAMTOOLS V0.1.19 [35] and GATK [36]. Through our variant-filtration process, we retained those variants that are "common" and "private" to the two mutants, and not shared by other SJL/J mice or previously sequenced ENU-mutant mice. Remaining variants were annotated using ANNOVAR [37].

PBGD assay

Whole blood samples were centrifuged at 1500×*g* for 10 min. The plasma and buffy coat were removed. To obtain hemolysates, erythrocytes were washed thrice in phosphate-buffered saline (PBS; 10 mM sodium phosphate, 2.7 mM KCl, 140 mM NaCl, pH 7.4) then diluted 50-fold in the assay buffer (50 mM Tris containing 0.2% Triton X-100, 20 mM citric acid, pH 8.2), incubated at 56 °C for 15 min, and finally cooled on ice. Aliquots (125 μL) of the hemolysates were mixed with 245 μL assay buffer containing 175 μM porphobilinogen (Sigma Aldrich, Castle Hill, Australia) and incubated at 37 °C for 60 min. The reaction was terminated by adding 375 μL 12.5% TCA, and oxidation of URO III to URO I was allowed to occur for 30 min at ~23 °C. After centrifugation (1000×*g*, 5 min), 200 μL of clarified supernatant was transferred to brown glass vials, stored at 4 °C, and subjected to ultrahigh-performance liquid chromatography (UHPLC) within 72 h. Samples from each mouse were assayed and analyzed twice in separate reactions. The UHPLC system consisted of a Dionex UltiMate™ 3000 in line with a fluorescence FLD-3400 detector. A Hypersil Gold C18 column (1.9 μm particle size, 50 × 2.1 mm internal diameter; Thermo Fisher Scientific, Australia) was used for elution. The mobile phase consisted of 9% (v/v) acetonitrile in 1 M ammonium acetate–acetic acid buffer, pH 5.16 (solvent A), and 10% acetonitrile (v/v) in methanol (solvent B) [38-40]. The elution program was 0% B (100% A) for initial 2 min, 0% B (100% A) to 10% B (90% A) for 2–6 min, 10% B (90% A) to 90% B (10% A) for 1 min, and isocratic 90% B for further 2 min. The flow rate was set at 0.8 mL/min and column temperature at 35 °C. Eluents were detected at $\lambda ex = 404$ nm and $\lambda em = 618$ nm. To quantify standards, a solution containing 50 nmol/L URO I in 12.5% TCA was prepared using a 1 mM stock solution dissolved in 1 M HCl (Sigma Aldrich). The concentration of the standard was calculated using absorbance and $\lambda = 405$ nm and $\varepsilon = 505 \times 10^3$ L cm^{-1} mol^{-1} [40]. Standard curves were generated by varying the injection volume and integrating the corresponding areas under the peaks.

Immunoblotting

The antibodies used in the immunoblotting experiments were rabbit anti-human PBGD IgG from Sigma Aldrich (HPA006114) or Fitzgerald Industries International (70R-3343) for the murine tissue sample studies, and mouse anti-human PBGD IgG_1 monoclonal antibody from Santa Cruz Biotechnology (sc-271585) and an *N*-terminal Ank-1 ''p89'' antibody (kindly provided by Connie Birkenmeier, Jackson Laboratory, USA) for human and *P. falciparum* cell studies. Following blotting with HRP-conjugated secondary antibodies (Sigma Aldrich), protein bands were visualized by chemiluminescent detection (SuperSignal West Pico Substrate, ThermoFisher Scientific).

***P. falciparum* culture**

P. falciparum was cultured in 2.5% hematocrit O+ human RBCs according to described method [41]. The cell culture medium (CCM) comprised of RPMI 1640 supplemented with 8.8 mM D-glucose, 22 mM HEPES, 208 nM hypoxanthine (Sigma-Aldrich, Missouri, US), 46.1 nM gentamicin, 2.1 g/L AlbuMAX® I, 2.8 mM L-glutamine (Life Technologies, Australia), and 4.2% (v/v) O+ human serum. Cultures were maintained in flasks filled with $1\%O_2/3\%CO_2/96\%N_2$ gas mix, and kept in an orbital shaking incubator at 50 rpm at 37°C. Culture parasitemias were maintained at between 0.5% and 10%, and checked every 1-2 days using Giemsa-stained thin blood smear microscopy. Culture medium was changed every 1-2 days by pelleting infected cells at 500 *g* for 5 minutes and resuspending in fresh CCM. The human RBCs and sera were provided by Australian Red Cross Blood Service. Blood was washed three times using CCM that lacks hypoxanthine, AlbuMAX® I, and human serum, and centrifuged at 2800 RPM for 5 minutes for each wash. The *P. falciparum* strain 3D7 was donated by R. Anders (La

Trobe University, Melbourne, Australia). The Pf*Pbgd*-KO and 3D7 wild-type parental lines were gifts from Professor Daniel E. Goldberg, Washington University School of Medicine, St. Louis, MO.

TUNEL staining and immunofluorescence

Culture samples and mouse blood samples were fixed for at least 24 h in Cytofix solution (BD Biosciences) diluted four-fold in PBS. Slides coated with polyethylenimine (0.1% v/v) were smeared with fixed blood and stained overnight in the reaction mix from the Apo BrdU TUNEL Assay Kit (Molecular Probes, Eugene, OR). TUNEL-labeled DNA was detected using a biotinylated anti-BrdU antibody and streptavidin-Alexa Fluor 594 conjugate (ThermoFisher Scientific, Australia). At least 100 infected cells were counted on each slide, and each AIP or normal erythrocyte sample was assayed twice. For immunofluorescence microscopy, cells were prepared on slides as described above and incubated with 2 μg/mL rabbit polyclonal IgG anti-human PBGD (14797-1-AP from Proteintech) or rabbit IgG isotype control (Novus Biologicals) and anti-rabbit Alexa594-conjugated secondary antibody, prepared in PBS containing 1% (w/v) BSA. After staining, slides were mounted in SlowFade™ Gold Antifade Mountant with DAPI (ThermoFisher Scientific, Australia) and glass coverslips (#1 from Menzel-Gläser). Slides were examined at room temperature using an Axio Observer inverted fluorescence microscope or a LSM 800 confocal microscope with Airyscan, both using 630× magnification and coupled to a Axiocam 503 monochrome cameras (Zeiss, Australia). All images were acquired and processed using Zen microscope and imaging software (Zeiss, Australia).

Supplemental Material References

1. Allison, A.C., Genetic control of resistance to human malaria. Curr Opin Immunol, 2009. **21**(5): p. 499-505.
2. Hill, A.V., The immunogenetics of resistance to malaria. Proc Assoc Am Physicians, 1999. **111**(4): p. 272-7.
3. Min-Oo, G. and P. Gros, Erythrocyte variants and the nature of their malaria protective effect. Cell Microbiol, 2005. **7**(6): p. 753-63.
4. Nagel, R.L. and E.F. Roth, Jr., Malaria and red cell genetic defects. Blood, 1989. **74**(4): p. 1213-21.
5. Bonday, Z.Q., et al., Import of host δ-aminolevulinate dehydratase into the malarial parasite: identification of a new drug target. Nat Med, 2000. **6**(8): p. 898-903.
6. Dhanasekaran, S., et al., δ-Aminolevulinic acid dehydratase from *Plasmodium falciparum*: indigenous versus imported. J Biol Chem, 2004. **279**(8): p. 6934-42.
7. Koncarevic, S., et al., The malarial parasite *Plasmodium falciparum* imports the human protein peroxiredoxin 2 for peroxide detoxification. Proc Natl Acad Sci U S A, 2009. **106**(32): p. 13323-8.
8. Sicard, A., et al., Activation of a PAK-MEK signalling pathway in malaria parasite-infected erythrocytes. Cell Microbiol, 2011. **13**(6): p. 836-45.
9. Varadharajan, S., et al., Localization of ferrochelatase in *Plasmodium falciparum*. Biochem J, 2004. **384**(Pt 2): p. 429-36.
10. Brizuela, M., et al., Treatment of erythrocytes with the 2-cys peroxiredoxin inhibitor, Conoidin A, prevents the growth of *Plasmodium falciparum* and enhances parasite sensitivity to chloroquine. PLoS One, 2014. **9**(4): p. e92411.
11. Smith, C.M., et al., Griseofulvin impairs intraerythrocytic growth of *Plasmodium falciparum* through ferrochelatase inhibition but lacks activity in an experimental human infection study. Sci Rep, 2017. **7**: p. 41975.
12. Sigala, P.A. and D.E. Goldberg, The peculiarities and paradoxes of *Plasmodium* heme metabolism. Annu Rev Microbiol, 2014. **68**: p. 259-78.
13. Ke, H., et al., The heme biosynthesis pathway is essential for *Plasmodium falciparum* development in mosquito stage but not in blood stages. J Biol Chem, 2014. **289**(50): p. 34827-37.
14. Nagaraj, V.A., et al., Malaria parasite-synthesized heme is essential in the mosquito and liver stages and complements host heme in the blood stages of infection. PLoS Pathog, 2013. **9**(8): p. e1003522.
15. Sigala, P.A., et al., Deconvoluting heme biosynthesis to target blood-stage malaria parasites. Elife, 2015. **4**.
16. Bonday, Z.Q., et al., Heme biosynthesis by the malarial parasite. Import of δ-aminolevulinate dehydrase from the host red cell. J Biol Chem, 1997. **272**(35): p. 21839-46.
17. Pasini, E.M., et al., In-depth analysis of the membrane and cytosolic proteome of red blood cells. Blood, 2006. **108**(3): p. 791-801.
18. Pasini, E.M., et al., Deep-coverage rhesus red blood cell proteome: a first comparison with the human and mouse red blood cell. Blood Transfus, 2010. **8 Suppl 3**: p. s126-39.
19. Pasini, E.M., et al., Deep coverage mouse red blood cell proteome: a first comparison with the human red blood cell. Mol Cell Proteomics, 2008. **7**(7): p. 1317-30.
20. Smith, C.M., et al., Red cells from ferrochelatase-deficient erythropoietic protoporphyria patients are resistant to growth of malarial parasites. Blood, 2015. **125**(3): p. 534-41.

21. Lelliott, P.M., et al., A flow cytometric assay to quantify invasion of red blood cells by rodent Plasmodium parasites in vivo. Malar J, 2014. **13**: p. 100.
22. McMorran, B.J., et al., Platelets kill intraerythrocytic malarial parasites and mediate survival to infection. Science, 2009. **323**(5915): p. 797-800.
23. Puy, H., L. Gouya, and J.C. Deybach, Porphyrias. Lancet, 2010. **375**(9718): p. 924-37.
24. Martinez di Montemuros, F., et al., Acute intermittent porphyria: heterogeneity of mutations in the hydroxymethylbilane synthase gene in Italy. Blood Cells Mol Dis, 2001. **27**(6): p. 961-70.
25. Gill, R., et al., Structure of human porphobilinogen deaminase at 2.8 Å: the molecular basis of acute intermittent porphyria. Biochem J, 2009. **420**: p. 17-25.
26. Lindberg, R.L., et al., Porphobilinogen deaminase deficiency in mice causes a neuropathy resembling that of human hepatic porphyria. Nat Genet, 1996. **12**(2): p. 195-9.
27. Clavero, S., et al., Feline acute intermittent porphyria: a phenocopy masquerading as an erythropoietic porphyria due to dominant and recessive hydroxymethylbilane synthase mutations. Hum Mol Genet, 2010. **19**(4): p. 584-96.
28. Ahmed, R. and F.J. Leeper, A new synthesis of porphobilinogen analogues, inhibitors of hydroxymethylbilane synthase. Org Biomol Chem, 2003. **1**(1): p. 21-3.
29. Rivadeneira, E.M., M. Wasserman, and C.T. Espinal, Separation and concentration of schizonts of *Plasmodium falciparum* by Percoll gradients. J Protozool, 1983. **30**(2): p. 367-70.
30. Laemmli, U.K., Cleavage of structural proteins during the assembly of the head of bacteriophage T4. Nature, 1970. **227**(5259): p. 680-5.
31. Chen, K., et al., Resolving the distinct stages in erythroid differentiation based on dynamic changes in membrane protein expression during erythropoiesis. Proc Natl Acad Sci USA, 2009. **106**(41): p. 17413-8.
32. Bauer, D.C., et al., Genome-wide analysis of chemically induced mutations in mouse in phenotype-driven screens. BMC Genomics, 2015. **16**(1): p. 866.
33. Li, H. and R. Durbin, Fast and accurate short read alignment with Burrows-Wheeler transform. Bioinformatics, 2009. **25**(14): p. 1754-60.
34. Langmead, B. and S.L. Salzberg, Fast gapped-read alignment with Bowtie 2. Nat Methods, 2012. **9**(4): p. 357-9.
35. Li, H., et al., The Sequence Alignment/Map format and SAMtools. Bioinformatics, 2009. **25**(16): p. 2078-9.
36. McKenna, A., et al., The Genome Analysis Toolkit: a MapReduce framework for analyzing next-generation DNA sequencing data. Genome Res, 2010. **20**(9): p. 1297-303.
37. Wang, K., M. Li, and H. Hakonarson, ANNOVAR: functional annotation of genetic variants from high-throughput sequencing data. Nucleic Acids Res, 2010. **38**(16): p. e164.
38. Benton, C.M., et al., Ultra high-performance liquid chromatography of porphyrins in clinical materials: column and mobile phase selection and optimisation. Biomed Chromatogr, 2012. **26**(6): p. 714-9.
39. Benton, C.M., et al., Ultra high-performance liquid chromatography of porphyrins. Biomed Chromatogr, 2012. **26**(3): p. 331-7.
40. Erlandsen, E.J., et al., Determination of porphobilinogen deaminase activity in human erythrocytes: pertinent factors in obtaining optimal conditions for measurements. Scand J Clin Lab Invest, 2000. **60**(7): p. 627-34.
41. Trager, W. and J.B. Jensen, Human malaria parasites in continuous culture. Science, 1976. **193**(4254): p. 673-5.

2.3. Coproporphyrinogen oxidase confers resistance to the blood stage infection of *Plasmodium* species

Contribution: 80% (experimental work, majority of data analysis and majority of paper writing and figure preparation).

Lora Jensen, Hao Yang and Gaetan Burgio performed the IVET, splenic retention and *P. falciparum* studies. Elena Di Pierro and Giovanna Graziadei provided the HCP blood sample and biochemical analysis of the HCP patients. Ashlee J. Conway, Fiona C. Brown, Stephen M. Jane and David J. Curtis provided the *Cpox*$^{+/W373X}$ mouse strain.

Coproporphyrinogen oxidase confers resistance to the blood stage infection of *Plasmodium* species

Cilly Bernardette Schnider[1,2,a], Lora Jensen[1], Hao Yang[1], Ashlee J. Conway[3], Fiona C. Brown[3], Elena Di Pierro[4], Giovanna Graziadei[4], Stephen M. Jane[5], David J. Curtis[3], Simon J. Foote[1], Brendan J. McMorran[1] and Gaetan Burgio[1].

[1]Department of Immunology and Infectious Disease, John Curtin School of Medical Research, Australian National University, Canberra, ACT 2601, Australia.
[2]Department of Biomedical Sciences Faculty of Medicine and Health Sciences, Macquarie University, NSW 2109 Australia.
[3]Australian Centre for Blood Diseases, Monash University and Clinical Haematology, Alfred Health, Melbourne 3004, Australia.
[4]Rare Diseases Center, Internal Medicine Unit, Department of Medicine and Medical Specialties, Fondazione IRCCS Ca' Granda - Ospedale Maggiore Policlinico, Via Francesco Sforza, 35, 20122 Milan, Italy.
[5]Central Clinical School, Monash University, Melbourne 3004, Australia.
[a]Current address: Institute of Cell Biology, University of Bern, Bern, Switzerland
*Corresponding author: Gaetan Burgio, MD, PhD; gaetan.burgio@anu.edu.au. Department of Immunology and Infectious Disease, John Curtin School of Medical Research, Australian National University, Canberra, ACT, 2601, Australia. Phone: +61 2 6125 9428. Fax: +61 2 6247 4823.

ABSTRACT

During the symptomatic stage of malaria, *Plasmodium* parasites reside within red blood cells. Depending on the host genetic background, malaria infection can be less severe or even averted, and there has been a strong selective pressure in malaria endemic regions over thousands of years. Identification of novel host factors that confound malaria infection could increase our understanding of the biology of the interaction between the parasite and its host. Hemoglobin is produced by the canonical heme pathway, enzymes of which have been linked to malaria resistance. Here we report for the first time that host coproporphyrinogen oxidase (CPOX), a heme pathway enzyme, plays a role during malaria infection. Using mice heterozygous for a mutation leading to a premature stop codon in the *Cpox* gene, we were able to demonstrate an increase in survival following infection with the rodent parasite *P. berghei,* we however failed to detect a lower parasitemia which was unusual. We detected an iron deficiency anemia blood phenotype characterized by microcytic, osmotically less fragile erythrocytes and mild reticulocytosis and leukocytosis. During infection with *P. berghei*, *Cpox* mutant mice were more likely to be invaded and intraerythrocytic growth was promoted. Patients with hereditary coproporphyria suffer from symptoms caused by low levels of CPOX due to a mutation in the gene encoding for *CPOX*. We infected the blood of one patient *in vitro* using *P. falciparum* and found that parasites display a defect in maturation. Together these findings indicated that mutated host *CPOX* confers malaria resistance *in vivo* and *in vitro* in rodent and human malaria parasites. We postulate that the survival advantage is due to a bystander effect of the *Cpox* mutation in mice.

Introduction

Today, malaria still represents one of the biggest health burdens worldwide. It is caused by parasites of the genus *Plasmodium* and accounted for an estimated 216 million cases in 2016 [1]. An effective vaccine is missing, mosquitoes have developed resistance against insecticides and artemisinin combination therapy is challenged by the emergence of multidrug resistant parasites in South-East Asia and in Africa [2]. During the symptomatic intraerythrocytic stage of the parasite lifecycle, up to 70% of the total hemoglobin of a red blood cell (RBC) is digested, forming one of the main sources of parasite nutrition [3]. In other life cycle stages, the parasite has limited access to hemoglobin as a source of nutrition. Heme - a core component of hemoglobin - is synthesized by the eight enzymes of the canonical heme pathway, and is absolutely essential for all forms of life. It is produced during erythropoiesis in the mitochondria and cytosol but some of the eight heme pathway enzymes remain present in mature RBCs, which are devoid of mitochondria [4, 5].

Plasmodium has its own heme pathway that is equally expressed throughout the life cycle [6]. The role of *Plasmodium* heme enzymes during the blood stage is intriguing as there is a vast abundance of available host heme, which is also utilized by the parasite [7]. Previous work has indicated that a number of *Plasmodium* heme enzymes can be disrupted during the blood stage without affecting parasite survival or maturation. Most importantly, the two rate-limiting parasite enzymes aminolaevulinate synthase (ALAS)

and ferrochelatase (FC) have been successfully disrupted in *P. berghei* and *P. falciparum* [7-10]. It is therefore possible that the *de novo* heme pathway of the parasite is able to cover for insufficient amounts of heme during the blood stage but is not essential for survival [11]. Previously, host aminolaevulinate dehydrase (ALAD), porphobilinogen deaminase (PBGD) and FC were shown to be present inside the parasite, demonstrating that the parasite might import host enzymes to complement its own heme enzymes [12, 13 and Cilly Schnider unpublished results]. In comparison to the parasite enzyme, host PBGD and FC were shown to be much more active possibly making the import of host enzymes biologically attractive [13, 14].

Deficiency in humans of any of the host heme enzymes leads to porphyria, a group of diseases caused by substance build-up and/ or insufficient amounts of heme produced. It has been shown that *P. falciparum* growth is affected when grown in blood from porphyric patients, with deficiency in FC [10]. Accordingly, studies using a FC deficient mouse model infected with *P. chabaudi* confirmed these results *in vivo* [10].

Coproporphyrinogen oxidase (CPOX) executes the sixth heme pathway step, by performing oxidative decarboxylation of coproporphyrinogen III to yield protoporphyrinogen IX. Deficiency in CPOX enzyme activity can result in hereditary coproporphyria (HCP) which has approximately 0.2 newly diagnosed cases per million each year [15, 16]. These mutations are hence rare in the human population, but could be underdiagnosed, as manifestations of HCP symptoms are often absent in individuals of the same family with the same *CPOX* mutation [17]. CPOX deficient mice (*Cpox*$^{+/W373X}$), initially derived as part of an N-ethyl-N-nitrosurea (ENU) dominant mutagenesis screen, carry a mutation at amino acid 373, replacing a tryptophan with a premature stop codon. Similarly to HCP patients in humans, *Cpox*$^{+/W373X}$ females present many biochemical similarities to human HCP patients including diminished mRNA expression, protein levels and build-up of porphyrin intermediates [18]. Previous research has confirmed that PfCPOX is not essential during the blood stage for heme formation indicating that the host background is able to be used by the parasite to compensate for the absence of CPOX [19]. Here we report that deficiency in host CPOX confers malaria resistance in mice by increasing survival upon infection with *P. berghei*. We tested one human blood sample of a patient with the rare HCP disease and *P. falciparum* intra-erythrocytic growth was impaired.

RESULTS

Cpox$^{+/W373X}$ mice display a survival advantage when infected with *P. berghei* but not with *P. chabaudi*

Cpox$^{+/W373X}$ mice display a fully penetrant microcytic and regenerative anemia phenotype from the complete blood count. This is characterized by a lower mean corpuscular volume, normal hemoglobin and hematocrit levels (Table 1). Leukocytosis, anisocytosis and a slight reticulocytosis and an increase of 10% in RBC number was noted (Figure 1A and Table 1). Target cells and microcytic, hypochromic erythrocytes were noted on Giemsa stained peripheral blood smears [18].

Table 1: Blood examination of *Cpox*$^{+/W373X}$ mice.

	Cpox$^{+/W373X}$	*Cpox*$^{+/+}$		*Cpox*$^{+/W373X}$	*Cpox*$^{+/+}$
WBC (10^3 cells/µl)	10.97 ± 0.42	8.44 ± 0.31 ***	**MCHC (g/l)**	285 ± 3.3	277 ± 18.2
RBC (10^6 cells/µl)	11.91 ± 0.11	10.7 ± 0.09 ***	**RDW (%)**	18.5 ± 0.19	13.8 ± 0.22 ***
HGB (g/)	147 ± 2	146 ± 10	**HDW (g/l)**	23.4 ± 0.26	19.3 ± 0.24 ***
HCT ([No Units])	0.52 ± 0.005	0.53 ± 0.004	**Platelets (10^3 cells/µl)**	1096 ± 35	999 ± 38
MCV (fl)	43.24 ± 0.18	49.45 ± 0.2 ***	**#Retic (x10^9 cells/l)**	4.03 ± 0.3	3.31 ± 0.24 **
MCH (pg)	12.33 ± 0.14	13.67 ± 0.9	**Reticulocytes (%)**	472.5 ± 32	352 ± 26 ***

7 weeks old *Cpox*$^{+/W373X}$ mice and their *Cpox*$^{+/+}$ littermates were subjected to a full blood analysis on an ADVIA 120 Automated Hematological Analyzer. WBC = white blood cell count, RBC = red blood cell count, HGB = hemoglobin, HCT = hematocrit, MCV = mean corpuscular volume, MCH = mean corpuscular hemoglobin, MCHC = mean corpuscular hemoglobin concentration, RDW = Red cell distribution width, HDW = hemoglobin concentration distribution width, %Retics = percentage of reticulocytes 18-22 mice were analyzed per group. **p<0.01 *** p<0.001 ± indicate SEM.

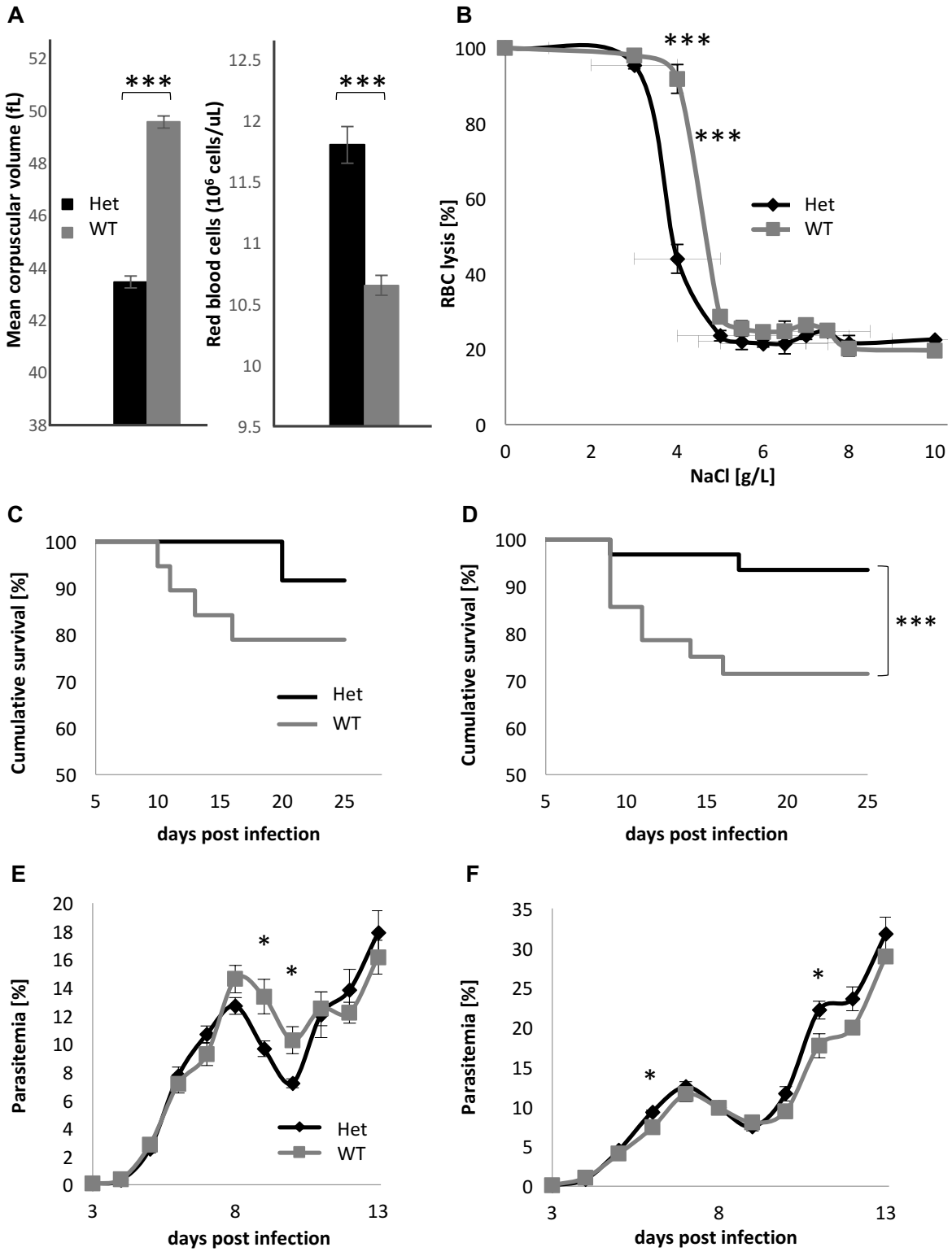

Figure 1: Blood phenotype and *P. berghei* infection profile in *Cpox*$^{+/W373X}$ and *Cpox*$^{+/+}$ mice. Blood parameters were measured using an Advia Hematology Analyzer. (A) Mean corpuscular volume and RBC number of *Cpox*$^{+/W373X}$ and *Cpox*$^{+/+}$ RBCs. (B) *Cpox*$^{+/W373X}$ and *Cpox*$^{+/+}$ RBCs were subjected to lysis in different concentrations of NaCl. (C) Mice were infected with 1×10^4 *P. berghei* and parasitemia was monitored by flow cytometry. Cumulative survival of male mice (n = 12-19 mice per group). (D) Cumulative survival of female mice (n = 28-31 mice per group). (E) Total parasitemia of male mice (n = 7-15 mice per group). (F) Total parasitemia of female mice (n = 8-13 mice per group). * $p<0.05$ *** $p<0.001$. Error bars indicate SEM.

Female *Cpox*$^{+/W373X}$ mice show similar biochemical features to those observed in human HCP patients which are characterized by a build-up of some porphyrins and an increased ratio of coproporphyrin III to I isomers in the feces [18]. While characterizing the blood from *Cpox*$^{+/W373X}$ and comparing it with their *Cpox*$^{+/+}$ littermates, we also noted a difference in osmotic fragility in that *Cpox*$^{+/W373X}$ RBCs are less osmotically fragile compared to *Cpox*$^{+/+}$ littermates (Figure 1B).

Previous reports have demonstrated that the host heme metabolism is required for the parasite to survive blood stage malaria infection [7, 8, 19]. Human porphyric patients and mice deficient in heme enzymes were reported to be resistant to malaria infection [10]. We therefore postulated that *Cpox*$^{+/W373X}$ mice would be resistant to the rodent malaria parasites *P. chabaudi* and/or *P. berghei.* It was previously reported that the BALB/c background is resistant to *P. berghei* infection but partially susceptible to *P. chabaudi* [28, 29]. To assess the level of susceptibility of *Cpox*$^{+/W373X}$ mice to rodent malaria, *Cpox*$^{+/W373X}$ mice and *Cpox*$^{+/+}$ were inoculated intraperitoneally with $1x10^4$ parasitized *P. berghei* RBCs. Circulating parasitemia and survival were monitored from day 3 to 25 post inoculation. The Kaplan-Meier curve for males (Figure 1C) did not reveal a significant survival advantage. Females (Figure 1D) displayed a slight (10% survival increase, $p < 0.001$), yet significant survival advantage for the *Cpox*$^{+/W373X}$ mice. All mice were resistant to experimental cerebral malaria as these mice are on a BALB/c mouse background [30]. The course of parasitemia monitored over eleven days was similar between the *Cpox*$^{+/W373X}$ and *Cpox*$^{+/+}$ male mice with wild-type mice displaying a significant higher parasitemia at day nine and ten (Figure 1E). Female *Cpox*$^{+/W373X}$ mice showed a modest increase in parasitemia at day six and eleven post infection (Figure 1F). The number of reticulocytes was significantly higher during early and late infection in male and female mice (Supplementary Figure 1A and B), but the number of infected reticulocytes was almost identical (Supplementary Figure 1C and D). Using counting beads, we also measured anemia which was similar for both sexes (Supplementary Figure 1E and F). We also infected *Cpox*$^{+/W373X}$ and *Cpox*$^{+/+}$ mice with *P. chabaudi*; no male mice survived infection past day 14 (Supplementary Figure 2A) and no female mice survived past day 19 post-inoculation (Supplementary Figure 2B). No survival advantage was noted. The parasitemia of *Cpox*$^{+/W373X}$ and *Cpox*$^{+/+}$ mice was almost identical during the entire course of infection (Supplementary Figure 2 C and D). Together this suggests that *Cpox*$^{+/W373X}$ mice are resistant to *P. berghei* infection only. *P. berghei* parasite invades and grows preferentially in reticulocytes whereas *P. chabaudi* parasites have a specific tropism for mature RBCs [31]. We therefore hypothesized that resistance to *P. berghei* would be caused by a defect in invasion or maturation in the reticulocytes and/or mature RBCs or an increased clearance in the spleen.

Cpox$^{+/W373X}$ mice don't display invasion defect with *P. berghei*

To assess this postulate, we performed an IVET assay as described previously [21]. We monitored the relative parasitemia for *Cpox*$^{+/W373X}$ and *Cpox*$^{+/+}$ bloods for over two full erythrocyte cycles (60 hours) in RBCs and reticulocytes. We found *Cpox*$^{+/W373X}$ RBCs were significantly 2-folds more likely to be infected 24 and 48 hours post inoculation by *P. berghei* than *Cpox*$^{+/+}$ therefore promoting intra-erythrocytic growth (Figure 2A). This also lead to a 10% increase in parasitemia of *Cpox*$^{+/W373X}$ mice from 12 to 60 hours post inoculation (Supplementary Figure 3A). This was not observed in reticulocytes (Supplementary Figure 3B). Interestingly we found no differences in reticulocyte invasion and growth rates between *Cpox*$^{+/W373X}$ and *Cpox*$^{+/+}$ (Figure 2B, Supplementary Figure 3B).

We postulated that the increased survival to *P. berghei* infection was due to a defect in parasite survival within the RBC. To confirm this hypothesis, we stained infected *Cpox*$^{+/W373X}$ and *Cpox*$^{+/+}$ RBCs using TUNEL at 48 hours post inoculation to detect and count fragmented nuclear DNA within RBCs, indicative of premature parasite death within the RBCs. No difference was noted between *Cpox*$^{+/W373X}$ and *Cpox*$^{+/+}$ (Figure 2C). The number of parasites per RBC was also similar between *Cpox*$^{+/W373X}$ and *Cpox*$^{+/+}$(Figure 2D). Together these results suggest that invasion or early parasite maturation is unlikely to be impaired in *P. berghei* infected *Cpox*$^{+/W373X}$ mice, and is unlikely to be causative for the resistance phenotype in *Cpox*$^{+/W373X}$ mice.

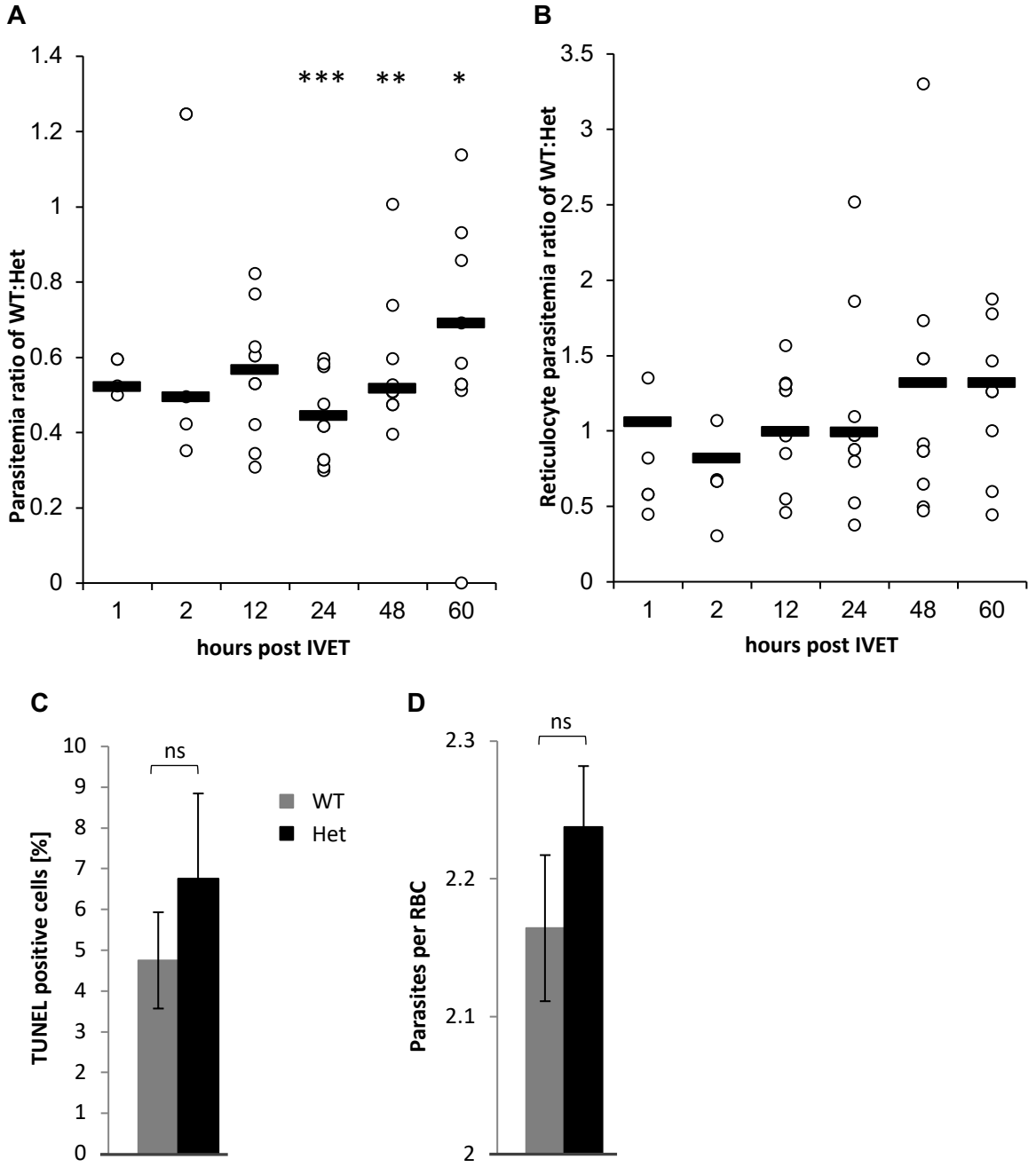

Figure 2: *In vivo* erythrocyte tracking assay monitors invasion and growth during *P. berghei* infection. Blood was labeled with Atto 633 or biotin to distinguish between *Cpox*$^{+/+}$ and *Cpox*$^{+/W373X}$ erythrocytes of female mice. Equal amounts of labeled RBCs for each genotype were injected into infected *Cpox*$^{+/+}$ female mice and labeled RBCs were monitored during infection by flow cytometry. (A) Intraerythrocytic growth as assessed by IVET whereby the relative invasion efficiency into *Cpox*$^{+/W373X}$ and *Cpox*$^{+/+}$ erythrocytes was monitored. Parasitemia ratio was calculated as a ratio of parasite load of *Cpox*$^{+/+}$ to *Cpox*$^{+/W373X}$. (B) Reticulocyte parasitemia displayed is a ratio of *Cpox*$^{+/+}$ to *Cpox*$^{+/W373X}$ infected reticulocytes during the IVET assay. (C) Mice were infected with a high dose of *P. berghei* parasites and 48 h post infection a TUNEL assay was performed. Fragmented DNA indicating parasite death was detected by TUNEL staining of peripheral blood smears. (D) Number of RBCs was determined in peripheral blood smears and counting the number of parasites in infected RBCs. All experiments were done in n = 5-10 mice per group and two replicates. For TUNEL, 100 parasites were counted. * $p<0.05$ ** $p<0.01$ *** $p<0.001$. Error bars indicate SEM.

$Cpox^{+/W373X}$ mice display a clearance defect during *P. berghei* infection

We then hypothesized that the survival advantage against *P. berghei* might be resulting from increased destruction or retention of infected RBCs in $Cpox^{+/W373X}$ mice. We compared the clearance rate in $Cpox^{+/W373X}$ and $Cpox^{+/+}$ mice by measuring the number of RBCs left 12 to 60 hrs post inoculation and by measuring the retention rate in an artificial spleen model. After injection of fluorescently labeled blood into infected mice, the amount of remaining labeled RBCs between $Cpox^{+/W373X}$ and $Cpox^{+/+}$ mice was similar. We did observe a slight decrease of $Cpox^{+/W373X}$ labeled RBCs at 48 hrs post inoculation indicating that $Cpox^{+/W373X}$ RBCs are cleared more efficiently compared to their $Cpox^{+/+}$ littermates. However we failed to detect this trend at the later time point at 60 hrs (Figure 3A). RBC destruction is facilitated by splenic clearance, where RBCs that have decreased deformability cannot travel through the slits and are engulfed by resident macrophages. We therefore postulated an increase retention leading to clearance of the parasitized cells. We measured the splenic retention in an artificial spleen model according to Deplaine, Safeukui [23] using blood from uninfected $Cpox^{+/W373X}$ and $Cpox^{+/+}$ mice. Blood was collected from uninfected $Cpox^{+/W373X}$ and $Cpox^{+/+}$ and labeled with either Atto or biotin dyes and mixed with counting beads. Dyes were also interchanged to control for impact of the staining. Three biological replicates were analyzed and although not statistically significant ($p = 0.2$) there was a tendency of $Cpox^{+/+}$ blood to be retained in this artificial spleen model, suggesting that the $Cpox^{+/W373X}$ blood is less likely to be retained in the spleen. During clearance of RBCs, macrophages play an important role. We have performed these assays in an in vitro model therefore we cannot exclude the possibility that macrophages are responsible for the lower number of remaining RBCs in $Cpox^{+/W373X}$ mice at 48 hrs post infection.

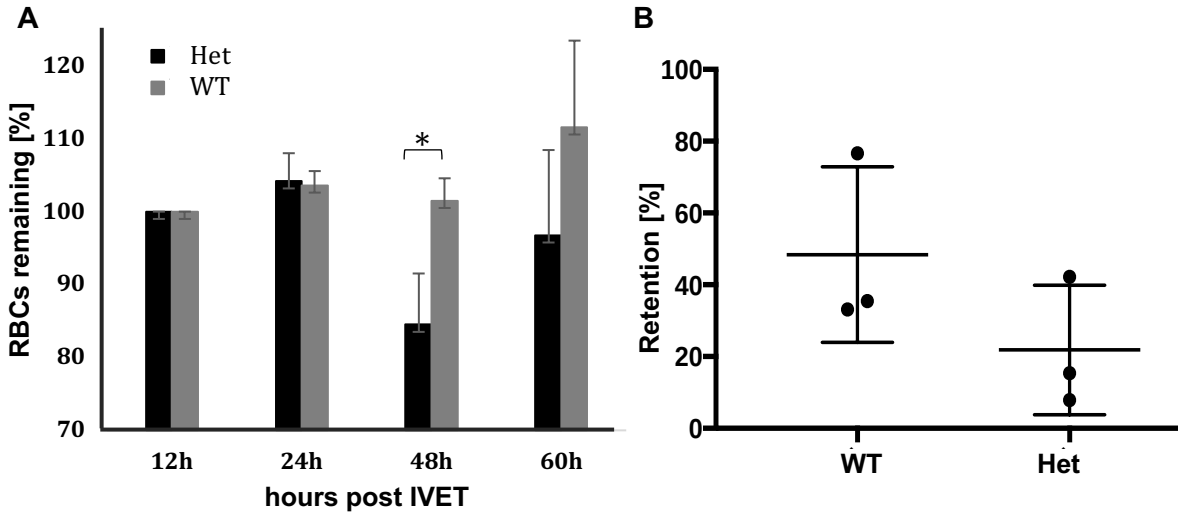

Figure 3: Parasite clearance and splenic retention. During the IVET, remaining RBCs were monitored over time. (A) Remaining RBCs during IVET comparing the two genotypes. Experiments were done in n = 5-10 mice per group and with two replicates. (B) Blood from uninfected and infected $Cpox^{+/W373X}$ and $Cpox^{+/+}$ mice was labeled according to genotype and subjected to passage through an artificial spleen model. Hoechst 33342 was added to detect parasitized RBC during the *in vitro* spleen retention assay, with 3-4 biological replicates and 2 mice per group. * $p<0.05$ ** $p<0.01$ *** $p<0.001$. Error bars indicate SEM.

Blood from a Hereditary coproporphyria (HCP) patient is resistant to *P. falciparum* infection

We obtained blood from an Italian patient with severe HCP, with CPOX deficiency due to an A to G transition at nucleotide 1348, resulting in a change of arginine to glycine at amino acid 450 (pA450G). To date this mutation has not been described in the literature, but mutations are described for amino acids in the vicinity [32].

We hypothesized that the blood from this patient might prevent *P. falciparum* intra-erythrocytic growth or invasion. We infected the HCP blood and two wild-type controls - one blood sample from Italy (Italy RBCs) collected and shipped on the same day and one

from Australia (Australia RBCs) - with 3D7 *P. falciparum* parasites synchronized at the trophozoite stage. We monitored the parasitemia over one full erythrocytic cycle. A slight defect in invasion was noticed (24 hrs time point) compared to the Australian control sample ($p = 0.03$), however there was a similar fold change in parasitemia compared to the Italian control sample (Figure 4). At 48 hrs, the difference between HCP and control erythrocytes was not significant. However, we noted a significant difference in parasitemia after 72 hrs post inoculation. Compared to the control blood sample from Italy ($p = 0.03$) and Australia ($p = 0.03$) the HCP erythrocytes displayed a much lower fold change indicating an impairment of parasite intra-erythrocytic growth. Although parasite growth was slower compared to the control erythrocytes, HCP parasite numbers doubled from 24 hrs to 72 hrs indicating that parasites are able to replicate in and invade HCP erythrocytes ($p = 0.04$).

Table 2: Blood, urine and feces examination of HCP patient.

Porphyria	HCP
Genotype	c.[1348A>G;[=]
Protein effect	p.Arg450Gly
ALA (mg/g creat)	3.9
PBG (mg/g creat)	<0.5
Urine porphyrin (µg/l) and % types (URO; EPTA; ESA; PENTA; COPRO I; COPRO III)	201 (6; 1; <1; 2; 8; 82)
Feces porphyrin (nmol/g dry feces) and % types (URO; EPTA; ESA; PENTA; COPRO I; COPRO III)	69 (2; <1; 3; <1; 9; 83)

Biochemistry data of one patient with severe HCP.

DISCUSSION

During the blood stage *Plasmodium* develops in host RBCs, which are rich in hemoglobin. Parasites express their own *de novo* heme pathway but key enzymes of the pathway have been shown to be non-essential during the blood stage, probably due to vast amounts of available host heme. Previously it was reported that deficiency in host heme enzymes confers resistance to malaria in mice. For instance, *in vitro* parasite growth was decreased in blood from porphyric patients, triggered by defective heme enzymes [10]. Here we reported on the role of the host CPOX heme enzyme during malaria infection. This study investigated a mouse model of HCP infected with *P. berghei* and *P. chabaudi* as well as RBCs obtained from one severe HCP patient infected with *P. falciparum*.

For the first time we demonstrate that $Cpox^{+/W373X}$ mice display an increased survival, although this was accompanied with a lower parasitemia upon *P. berghei* infection. We noted no difference during *P. chabaudi* infection. *P. falciparum* infected RBCs from one HCP patient displayed a lower parasitemia indicating a growth or invasion defect in CPOX deficient erythrocytes *in vitro*. One of the most notable observations in the mouse was the fact that although they showed increased survival to *P. berghei*, no reduced parasite load was observed. Normally increased survival is associated with a lower parasitemia, and indeed this has been a common trend for all other host heme enzymes when they were knocked down. For example, when mice deficient in FC were infected with *P. chabaudi*, they showed an increased survival along with a 50% decrease in parasitemia [10]. Mice deficient in host Pbgd displayed a 20% lower parasitemia and a mild increase in survival upon infection with *P. chabaudi* but not *P. berghei* (Cilly Schnider, unpublished results). In contrast, the parasitemia of female $Cpox^{+/W373X}$ mice was even higher compared to $Cpox^{+/+}$ mice. Together these indicate that the mode of resistance observed here is different from what has been observed in other heme enzyme deficient mice. Conway and colleagues established the HCP phenotype in female mice only. Our studies however have noted similar results amongst male and female mice indicating that the resistance phenotype is probably not due to the HCP phenotype. Therefore, the underlying cause of the increased survival is unlikely to be due to heme deficiency but may be a bystander effect of the *Cpox* mutation.

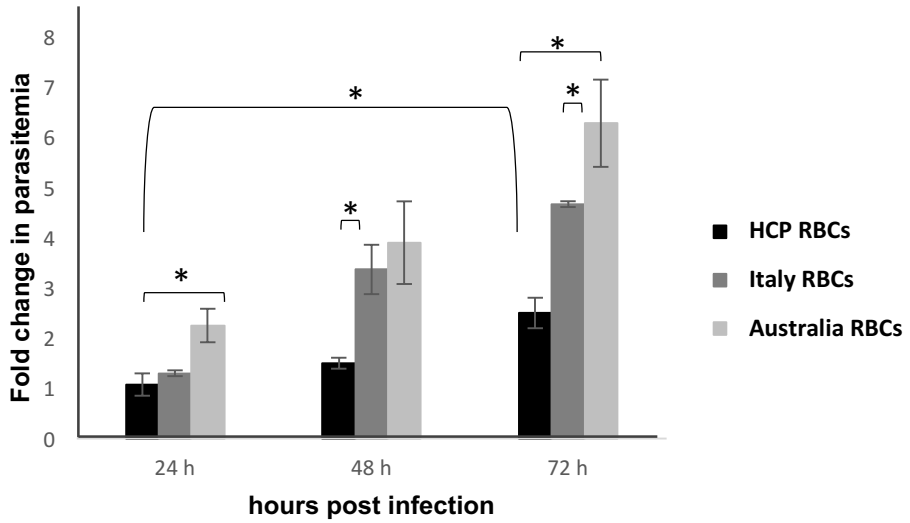

Figure 4: *P. falciparum* growth assay in erythrocytes from a patient with HCP. One blood sample from an HCP patient from Italy was infected with *P. falciparum*. As controls two normal blood samples, one from a healthy volunteer shipped at the same time and a blood sample from one Australian healthy volunteer were used. *p<0.05. Error bars indicate SEM of technical replicates.

By performing an IVET assay, we demonstrated that reduced invasion is not the underlying cause of resistance. In contrast, a two-fold increase in invasion and a higher parasite load was noted for *Cpox*$^{+/W373X}$ mice compared to their wild-type littermates. We also noted a lower number of RBCs in *Cpox*$^{+/W373X}$ mice after two invasion cycles indicating a clearance phenotype. However we failed to detect a difference at later time points. Using an *in vitro* splenic retention assay we demonstrated that the RBCs from *Cpox*$^{+/W373X}$ mice were less likely to be retained than *Cpox*$^{+/+}$ indicating that increased sequestration is unlikely to be the mechanism of resistance. RBC from *Cpox*$^{+/W373X}$ mice are microcytic. It is therefore more likely for them to pass the splenic slits, which is in concordance with the results from our *in vitro* splenic clearance assay. It is possible that the increased clearance is due to activation of macrophages rather than the RBC being retained in the slits of the spleen. Infection of splenectomized and normal *Cpox*$^{+/W373X}$ and *Cpox*$^{+/+}$ mice could establish the role of spleen-resident macrophages. It could also be assessed if there is a difference in spontaneous RBC lysis between genotypes which could explain a possible spleen and macrophage-independent RBC destruction [33].

The full blood count of *Cpox*$^{+/W373X}$ mice revealed a fully penetrant microcytic and hypochromic regenerative anemia phenotype characterized by leukocytosis, anisocytosis and a light reticulocytosis and erythrocytosis. In addition to a mild increase in reticulocyte numbers, *Cpox*$^{+/W373X}$ mice also presented an increase in erythrocyte precursors and larger spleens with increased red pulp [18]. In contrast, RBC half-life was not augmented indicating a normal turnover of RBCs [18] therefore erythroblast expansion in the spleen could be the underlying cause of the increase in red pulp [34]. During *P. berghei* infection a striking difference in reticulocytosis has been noted in *Cpox*$^{+/W373X}$ mice and this could be due to an already upregulated erythropoiesis, which is normally tightly regulated and repressed [35]. This might be a compensation mechanism against the microcytic anemia of *Cpox*$^{+/W373X}$ mice. Microcytosis and hypochromia are a hallmark of red cell polymorphisms which are associated with increased malaria protection, such as in the case of the thalassemias [36]. However microcytosis not always confers malaria resistance and in concordance with this, we did not see a growth or invasion defect, we in fact noted the converse in that *Cpox*$^{+/W373X}$ RBCs were two folds more likely to be invaded by parasites. Together this indicates a red cell autonomous survival advantage of *Cpox*$^{+/W373X}$ mice.

During infection we noted that anemia measured by remaining RBCs was similar between the two genotypes. The IVET assay only tracked labeled RBCs but did not take into account newly produced RBCs, therefore we cannot confirm whether *Cpox*$^{+/W373X}$ mice

upregulate erythropoiesis during *P. berghei* infection. However in support of this hypothesis, after the characteristic "dip" of number of reticulocytes, which disappear during *P. berghei* infection, *Cpox*$^{+/W373X}$ mice displayed much higher reticulocyte numbers after the recovery from low reticulocyte numbers. In the future these open questions should be addressed. Interestingly, leukocytosis is not usually present in patients with porphyrias, as inflammation is not usually observed during a porphyric attack [37]. The leukocytosis in *Cpox*$^{+/W373X}$ mice could be responsible for the increased survival by clearing infected RBCs from the circulation. Elevated ferritin levels were measured previously in *Cpox*$^{+/W373X}$ mice [18]. Increased ferritin levels are associated with acute or chronic inflammation, pregnancy, malignancy or liver disease [38]. Low ferritin levels are an indicator of iron deficiency anemia and have been linked to malaria protection. The high ferritin levels of *Cpox*$^{+/W373X}$ mice are unlikely to be the cause of increased survival upon *P. berghei* infection reported here. However leukocytosis and elevated ferritin levels could indicate a bystander effect of the *Cpox* mutation leading to inflammation. To test this hypothesis a cytokine assay to measure different types of cytokines could be used to determine whether an underlying inflammation is present in CPOX deficient mice.

HCP is caused in humans by a defective *CPOX* gene leading to insufficient amounts of CPOX enzyme with many different mutations described so far [39]. Although the HCP condition is extremely rare, we were fortunate to complement our findings from the mouse study by obtaining a blood sample from a human HCP patient [40]. The blood was infected with *P. falciparum* and compared to the control a lower parasitemia was noted, which indicated an impairment of the parasite intra-erythrocytic growth. Similar results in a previous study using blood from porphyric patients indicated that host FC has a similar effect on *P. falciparum*, as parasite growth was impaired. However as part of the same study, blood from patients deficient in ALAS did not impair parasite growth. Strikingly, three ALAS-deficient patient samples were tested and two showed a moderately increased parasite growth during *P. falciparum* infection, therefore promoting parasite maturation [10]. Blood from porphyric patients deficient in PBGD or uroporphyrinogen III synthase (UROS) was previously infected and displayed a defect in parasite growth and parasite invasion respectively (Cilly Schnider and Clare Smith, unpublished data). Together these indicate that deficiency in host heme enzymes is often associated with a defect in parasite growth or invasion, similar to what we have observed here. It is important to note that we only accessed one blood sample of this rare porphyria and that *in vitro* studies do not mirror *in vivo* studies as variables such as the immune response or clearance by the spleen and macrophages are absent.

Together we have demonstrated for the first time that host CPOX plays a role during the *Plasmodium* blood stage. *In vitro P. falciparum* studies in HCP erythrocytes confirmed earlier studies, where a growth defect was noted. The phenotype for *Cpox*$^{+/W373X}$ mice was unusual with an increased survival. RBCs of *Cpox*$^{+/W373X}$ mice promoted invasion and hence no decreased but a slightly increased parasitemia was noted. Underlying inflammation or upregulated erythropoiesis might be the underlying mechanism that promotes survival of *Cpox*$^{+/W373X}$ mice as a bystander effect, independent of host CPOX availability.

EXPERIMENTAL PROCEDURES

Mice

Cpox$^{+/W373X}$ were maintained by crossing to BALB/c background. Mice were genotyped using a fluorescent-based PCR assay with primers specific for the mutation (amplifluor assay). All animal experiments were approved by the Animal Ethics committee of the Australian National University (AEEC 2014/054) and Macquarie University (ARA 2012/017). Mice were subjected to full blood counts at seven weeks old using an Advia 2120 Automated Hematological Analyzer (Siemens, Berlin, Germany).

Malarial infection

Mice were infected with the rodent parasites *P. chabaudi adami DS* or *P. berghei ANKA*. Parasite stocks were harvested from passage through donor resistant C57BL/6 for *P. chabaudi* and resistant SJL/J mice for *P. berghei*. 250µl of a frozen parasite vial was injected into the intraperitoneal cavity of the donor mice. When these mice reached 5-10% parasitemia, the blood was collected via cardiac puncture and diluted into 25ml Krebs buffer with 0.2% glucose [20] to reach a final concentration of $1x10^4$ parasitized RBCs.

Blood parasitemia assessment

Blood stage parasitemia was monitored by Giemsa stained peripheral blood smears or by flow cytometry according to Lelliott et al [21]. Thin blood smears were methanol-fixed for 1 minute and then stained in a 10% Giemsa solution (Sigma-Aldrich, St. Louis, MO) at pH 7.4 for 10 minutes. Parasitemia was assessed by counting at least 500 parasitized cells by light microscopy at a magnification of ×1000. For flow

cytometry, briefly 2µl of whole blood samples were stained with 1µg/ml anti-CD45-allophycocyanin (APC)–eFluor 780 (clone 30-F11), 1µg/ml anti-CD71 (TFR1)-PerCP-eFluor 710 (clone R17217) (eBioscience, San Diego, CA), 4µM Hoechst 33342 (Sigma-Aldrich, St Louis, MO) and 12µM JC-1 (Thermo Scientific, Waltham, MA) in MTRC (154mM NaCl, 5.6mM KCl, 1mM $MgCl_2$, 2.2mM $CaCl_2$, 20mM HEPES, 10mM glucose, 4mM EDTA, 0.5% BSA, pH 7.4, filter sterilized). All samples analyzed through flow cytometry were performed on BD LSRFortessa (BD Biosciences, Franklin Lakes, NJ) and analyzed on FACSDiva™ and FlowJo softwares. Parasitemia was determined by gating on Hoechst 33342 and JC-1 positive populations. Anemia was assessed by using 5µl of counting beads (123count eBeads, eBioscience, San Diego, CA) combined with flow cytometry.

***In vivo* erythrocyte tracking (IVET)**

An *in vivo* erythrocyte tracking (IVET) assay to track invasion and growth of the parasite irrespective of the host background was conducted according to Lelliott et al. [21]. Briefly, 1.5 to 2ml of blood from *Cpox*$^{+/W373X}$ and wild-type littermates (*Cpox*$^{+/+}$) uninfected mice was collected by cardiac puncture. The blood was pooled for each genotype, halved and stained with 10µg/ml of Atto 633 or 125µg/ml of EZ-Link™ Sulfo-NHS-LC-biotin (biotin) (Thermo Scientific, Waltham, MA) for 45 minutes at room temperature. Cells were then incubated at room temperature for 30 minutes, and washed twice in 1x mouse tonicity phosphate buffered saline (MTPBS; 150mM NaCl, 4mM Na_2PO_4, 4nM NaH_2PO_4, pH 7.3). The cells were stained and mixed in various combinations (*Cpox*$^{+/W373X}$-biotin + *Cpox*$^{+/+}$-Atto dye and *Cpox*$^{+/+}$-Atto + *Cpox*$^{+/W373X}$-biotin), resuspended in 2ml MTPBS, and 200µl injected intravenously into *Cpox*$^{+/+}$ *P. berghei* infected mice when parasites were undergoing schizogony. At 1hr, 2hrs, 14hrs, 24hrs, 48hrs and 60hrs post injection, 2µl tail blood was collected and stained for flow cytometry as previously described. The ratio of infected *Cpox*$^{+/W373X}$ to *Cpox*$^{+/+}$ was determined as an indication of the relative susceptibility to malaria infections between *Cpox*$^{+/+}$ and *Cpox*$^{+/W373X}$ mice. The proportion of labeled blood was also tracked over time to determine the clearance of RBCs from the circulation.

Terminal deoxynucleotidyl transferase dUTP nick end labeling (TUNEL) staining

TUNEL staining protocol was previously published [22]. 48 hrs post high-dose infection, peripheral blood was taken by tail snip from *P. berghei* infected mice and thin blood smears were prepared and fixed in 100% MeOH. Slides were stained for TUNEL assay staining using an APO-BrdU TUNEL assay kit (Thermo Scientific Waltham MA) according to the manufacturer's instructions with a few modifications. Slides were washed with 1ml of wash buffer solution and were incubated overnight at room temperature with TUNEL labeling solution mix (1mM Cobalt Chloride, 25mM Tris-HCl pH 6.6, 200mM sodium cacodylate, 0.25mg/ml BSA, 60uM BrdUTP, 15U Terminal transferase). The slides were rinsed three times. Stained sections were incubated with 100µl of BrdU-antibody for one hour in the dark at room temperature with washes in 1% Bovine Serum Albumin (BSA) dissolved in 1x MTPBS. Slides were labeled with 100µl of nuclear yellow (Thermo Scientific Waltham MA) (1:5000 in 1% BSA in 1x MTPBS) for one minute in the dark. After three washes with 1ml MTPBS, the cells were adhered to the cover slips with 0.1% polyethyleneimine for 10 minutes. Cells were then dried and soaked in 1:1 ethanol: hexamethyldisilazane solution for 10 minutes, followed by two washes with 100% hexamethyldisilazane. The coverslips were air-dried overnight and examined on an upright epifluorescence microscope (ZEISS) using a 600x magnification.

***In-vitro* spleen retention assay**

The RBC deformability was examined according to Deplaine, Safeukui [23] with modifications previously published [24]. Briefly, RBCs from *Cpox*$^{+/+}$ and *Cpox*$^{+/W373X}$ mice were labeled with 10µg/ml of Atto 633 or biotin (Sigma-Aldrich, St Louis, MO). Following the labeling cells were washed three times with MTRC. The RBCs were then mixed in 0-50 proportion and diluted with unstained *Cpox*$^{+/+}$ RBCs to dilute to 20% of labeled RBCs avoid a rapid saturation of the beads. The pre-filtered and post-filtered samples were analyzed by flow cytometry on a BD LSRFortessa (BD Biosciences, Franklin Lakes, NJ).

Osmotic Fragility Assay

Susceptibility of RBC membranes to osmotic stress by using variable concentrations of NaCl was performed as described elsewhere [25].

***P. falciparum* growth assays**

The parasite growth assays conducted in human RBCs used *P. falciparum* strain 3D7, cultured according to the method of [26]. Parasite stocks were grown at 2.5% hematocrit in normal O+ human RBCs (from Australian Red Cross Blood Service, ARCBS) and cell culture medium comprised of RPMI 1640 supplemented with 8.8mM D-glucose, 22mM HEPES, 208nM hypoxanthine (Sigma Aldrich, Australia), 46.1nM gentamicin, 2.1g/L AlbuMAX® I, 2.8mM L-glutamine (Life Technologies, Australia), and 4.2% (v/v) O+ human serum, maintained in flasks filled with a 1%O_2/3%CO_2/96%N_2 gas mix, and kept in an orbital shaking incubator at 50rpm at 37°C. Culture parasitemias were maintained at between 0.5% and 10%, and checked daily using Giemsa-stained thin blood smear microscopy. Culture medium was changed every 1-2 days.

Blood from one individual with hepatic coproporphyria (HCP; *CPOX* mutation: c.[1348 A>G];[=]) and one normal individual (Normal Italy sample) were collected by venepuncture into 5ml sodium citrate tubes at The Hospital Maggiore Policlinico, Milan, Italy. The samples were maintained at 4°C and shipped immediately after collection to The Australian National University, Canberra, Australia. The blood was then centrifuged at 170g for 13 minutes and plasma and white cell fractions removed. The remaining RBCs were washed two times in RPMI and stored at 4°C for one week prior to the growth assay being conducted. For growth assays, trophozoite stage parasites were purified by Percoll gradient [27] and added to the HCP and Normal Italy RBCs at a final percentage parasitemia of approximately 1%. Growth

assays were conducted (in parallel) with normal RBCs from the ARCBS (normal Australian sample). Parasitemias were counted on Giemsa-stained thin blood smears after incubation for up to 72 hrs. At least 500 cells were counted on each slide.
Peripheral blood samples were collected in agreement with the Declaration of Helsinki for medical research involving human subjects, with its subsequent amendments. Informed consent was signed from the subjects. All the experiments were approved by the Ethics Committee of Fondazione IRCCS "Ca' granda"-Ospedale Maggiore Policlinico, Milan in Italy and the Human Research Ethics Committee of the Australian National University in Australia

Statistical analysis
Where applicable, results are expressed as mean ± standard error of the mean (SEM). For statistical analysis, a two-tailed student t-test was employed, where *p<0.05, or as defined in figure legends. For malaria survival and parasite infection challenges, a Log-Rank test was employed to compare the growth curves. Statistical significance for the ratios of invasion assays was determined using the one sample t-test with hypothetical mean of 1.

ACKNOWLEDGEMENTS
We thank Ceri Flowers for administrative support, Dr Diana Spinelli for recruitment of the HCP patients, Shelley Lampkin and Emmaline Brown for technical assistance and the Australian Red Cross Blood Service for RBC and human serum. The authors would like to thank Dr Elinor Hortle for critical reading of this manuscript, valuable input and discussions. Authors were supported by an International Macquarie University Research Excellence Scholarship (CBS), the NHMRC (490037, 605524, APP1047090 and APP1066502) and the Australian Research Council (DP120100061). Funders had no role in the design of the study and collection, analysis, and interpretation of data or in writing the manuscript.

AUTHOR CONTRIBUTIONS
CBS, LH, HY, GB and BJM performed experiments and AJC, FB, SMJ and DJC provided the *Cpox*$^{+/W373X}$ mouse strain. The project was conceived by GB, BJM and SJF and experiments were designed by CBS, LH, BJM and GB. The blood samples, and the genetic and biochemical analysis of the AIP patients were provided and performed by EDP and GG. The paper was written and the figures were prepared by CBS, LH and GB. All authors read and approved the final manuscript.

REFERENCES

1. 2017, W.H.O., World Malaria Report 2017. ISBN: 978-92-4-156552-3.

2. Lu, F., et al., Emergence of Indigenous Artemisinin-Resistant *Plasmodium falciparum* in Africa. N Engl J Med, 2017. 376(10): p. 991-3.

3. van Dooren, G.G., A.T. Kennedy, and G.I. McFadden, The use and abuse of heme in apicomplexan parasites. Antioxid Redox Signal, 2012. 17(4): p. 634-56.

4. Pasini, E.M., et al., In-depth analysis of the membrane and cytosolic proteome of red blood cells. Blood, 2006. 108(3): p. 791-801.

5. Pasini, E.M., et al., Deep coverage mouse red blood cell proteome: a first comparison with the human red blood cell. Mol Cell Proteomics, 2008. 7(7): p. 1317-30.

6. Rizopoulos, Z., K. Matuschewski, and J.M. Haussig, Distinct Prominent Roles for Enzymes of *Plasmodium berghei* Heme Biosynthesis in Sporozoite and Liver Stage Maturation. Infect Immun, 2016. 84(11): p. 3252-3262.

7. Nagaraj, V.A., et al., Malaria parasite-synthesized heme is essential in the mosquito and liver stages and complements host heme in the blood stages of infection. PLoS Pathog, 2013. 9(8): p. e1003522.

8. Ke, H., et al., The heme biosynthesis pathway is essential for *Plasmodium falciparum* development in mosquito stage but not in blood stages. J Biol Chem, 2014. 289(50): p. 34827-37.

9. Rathnapala, U.L., C.D. Goodman, and G.I. McFadden, A novel genetic technique in *Plasmodium berghei* allows liver stage analysis of genes required for mosquito stage development and demonstrates that de novo heme synthesis is essential for liver stage development in the malaria parasite. PLoS Pathog, 2017. 13(6): p. e1006396.

10. Smith, C.M., et al., Red cells from ferrochelatase-deficient erythropoietic protoporphyria patients are resistant to growth of malarial parasites. Blood, 2015. 125(3): p. 534-41.

11. Seeber, F. and D. Soldati-Favre, Metabolic pathways in the apicoplast of apicomplexa. Int Rev Cell Mol Biol, 2010. 281: p. 161-228.

12. Bonday, Z.Q., et al., Heme biosynthesis by the malarial parasite. Import of delta-aminolevulinate dehydrase from the host red cell. J Biol Chem, 1997. 272(35): p. 21839-46.

13. Varadharajan, S., et al., Localization of ferrochelatase in *Plasmodium falciparum*. Biochem J, 2004. 384(Pt 2): p. 429-36.

14. Nagaraj, V.A., et al., Unique properties of *Plasmodium falciparum* porphobilinogen deaminase. J Biol Chem, 2008. 283(1): p. 437-44.

15. Elder, G., et al., The incidence of inherited porphyrias in Europe. J Inherit Metab Dis, 2013. 36(5): p. 849-57.

16. Puy, H., L. Gouya, and J.C. Deybach, Porphyrias. Lancet, 2010. 375(9718): p. 924-37.

17. Blake, D., et al., Fecal coproporphyrin isomers in hereditary coproporphyria. Clin Chem, 1992. 38(1): p. 96-100.

18. Conway, A.J., et al., A mouse model of hereditary coproporphyria identified in an ENU mutagenesis screen. Dis Model Mech, 2017. 10(8): p. 1005-1013.

19. Sigala, P.A., et al., Deconvoluting heme biosynthesis to target blood-stage malaria parasites. Elife, 2015. 4.

20. Jarra, W. and K.N. Brown, Protective immunity to malaria: studies with cloned lines of *Plasmodium chabaudi* and *P. berghei* in CBA/Ca mice. I. The effectiveness and inter- and intra-species specificity of immunity induced by infection. Parasite Immunol, 1985. 7(6): p. 595-606.

21. Lelliott, P.M., et al., A flow cytometric assay to quantify invasion of red blood cells by rodent *Plasmodium* parasites in vivo. Malar J, 2014. 13: p. 100.

22. McMorran, B.J., et al., Platelets kill intraerythrocytic malarial parasites and mediate survival to infection. Science, 2009. 323(5915): p. 797-800.

23. Deplaine, G., et al., The sensing of poorly deformable red blood cells by the human spleen can be mimicked in vitro. Blood, 2011. 117(8): p. e88-95.

24. Huang, H.M., et al., Ankyrin-1 Gene Exhibits Allelic Heterogeneity in Conferring Protection Against Malaria. G3 (Bethesda), 2017. 7(9): p. 3133-3144.

25. Huang, H.M., et al., A novel ENU-induced ankyrin-1 mutation impairs parasite invasion and increases erythrocyte clearance during malaria infection in mice. Sci Rep, 2016. 6: p. 37197.

26. Trager, W. and J.B. Jensen, Human malaria parasites in continuous culture. Science, 1976. 193(4254): p. 673-5.

27. Rivadeneira, E.M., M. Wasserman, and C.T. Espinal, Separation and concentration of schizonts of *Plasmodium falciparum* by Percoll gradients. J Protozool, 1983. 30(2): p. 367-70.

28. Stevenson, M.M., J.J. Lyanga, and E. Skamene, Murine malaria: genetic control of resistance to *Plasmodium chabaudi*. Infect Immun, 1982. 38(1): p. 80-8.

29. Mackey, L.J., et al., Immunopathological aspects of *Plasmodium berghei* infection in five strains of mice. II. Immunopathology of cerebral and other tissue lesions during the infection. Clin Exp Immunol, 1980. 42(3): p. 412-20.

30. Haque, A., et al., Cerebral malaria in mice: interleukin-2 treatment induces accumulation of gammadelta T cells in the brain and alters resistant mice to susceptible-like phenotype. Am J Pathol, 2001. 158(1): p. 163-72.

31. Taylor-Robinson, A.W. and R.S. Phillips, Predominance of infected reticulocytes in the peripheral blood of CD4+ T-cell-depleted mice chronically infected with *Plasmodium chabaudi chabaudi*. Parasitol Res, 1994. 80(7): p. 614-9.

32. Wiman, A., Y. Floderus, and P. Harper, Two novel mutations and coexistence of the 991C>T and the 1339C>T mutation on a single allele in the coproporphyrinogen oxidase gene in Swedish patients with hereditary coproporphyria. J Hum Genet, 2002. 47(8): p. 407-12.

33. Hortle, E., et al., Adenosine monophosphate deaminase 3 activation shortens erythrocyte half-life and provides malaria resistance in mice. Blood, 2016. 128(9): p. 1290-301.

34. Manwani, D. and J.J. Bieker, The erythroblastic island. Curr Top Dev Biol, 2008. 82: p. 23-53.

35. Hattangadi, S.M., et al., From stem cell to red cell: regulation of erythropoiesis at multiple levels by multiple proteins, RNAs, and chromatin modifications. Blood, 2011. 118(24): p. 6258-68.

36. Nagel, R.L. and E.F. Roth, Jr., Malaria and red cell genetic defects. Blood, 1989. 74(4): p. 1213-21.

37. Balwani, M. and R.J. Desnick, The porphyrias: advances in diagnosis and treatment. Blood, 2012. 120(23): p. 4496-504.

38. Cook, J.D., Diagnosis and management of iron-deficiency anaemia. Best Pract Res Clin Haematol, 2005. 18(2): p. 319-32.

39. Bissell, D.M., B. Wang, and J. Lai, Hereditary Coproporphyria, in GeneReviews(R), R.A. Pagon, et al., Editors. 1993: Seattle (WA).

40. Siegesmund, M., et al., The acute hepatic porphyrias: current status and future challenges. Best Pract Res Clin Gastroenterol, 2010. 24(5): p. 593-605.

41. Dailey, H.A. and P.N. Meissner, Erythroid heme biosynthesis and its disorders. Cold Spring Harb Perspect Med, 2013. 3(4): p. a011676.

SUPPLEMENTAL INFORMATION

Supplemental Figures

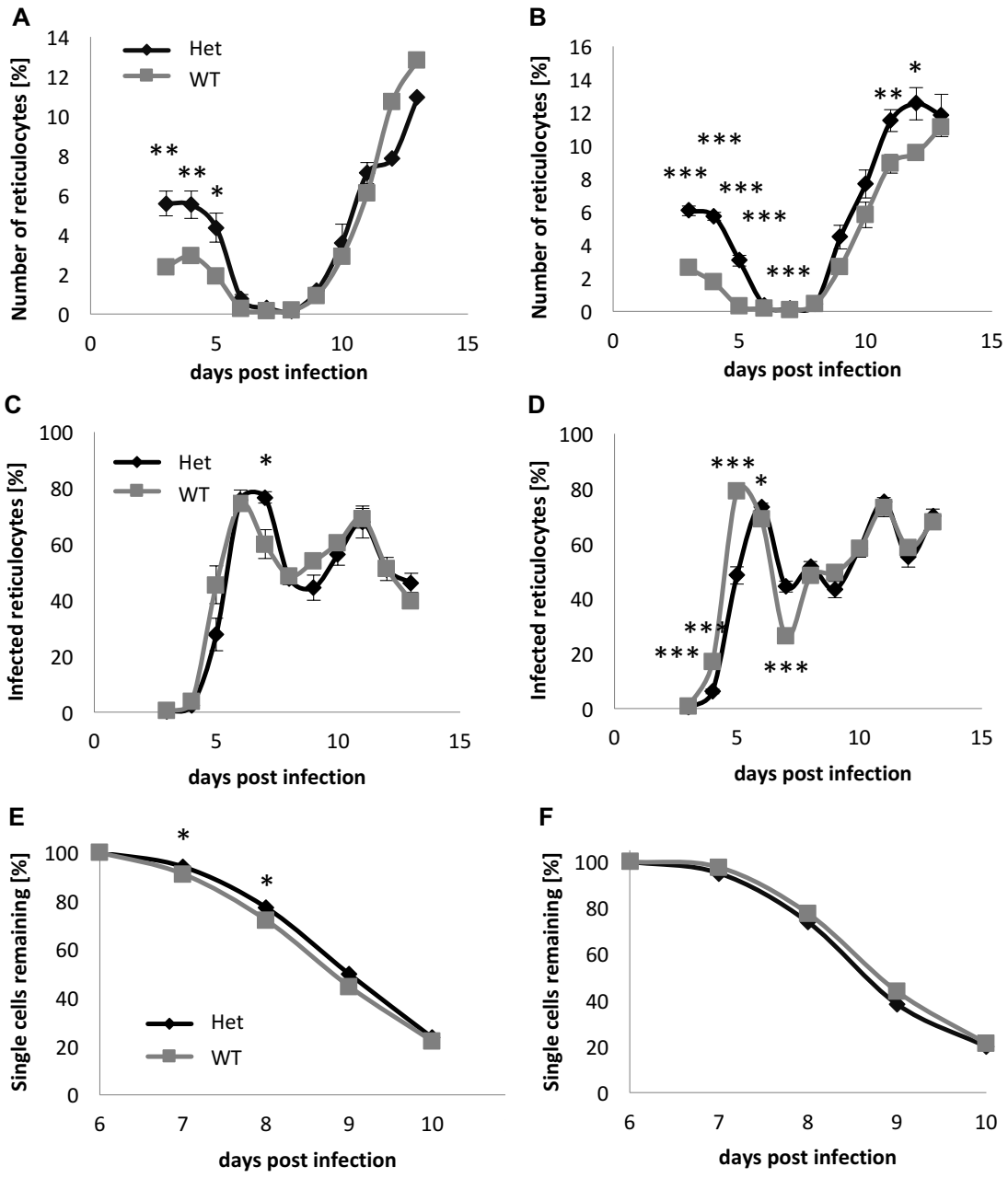

Supplementary Figure 1: Reticulocytosis, infected reticulocytes and anemia during infection of *Cpox*$^{+/W373X}$ with *P. berghei*. Mice were infected with 1×10^4 *P. berghei*. During infection the number of infected and uninfected reticulocytes was monitored daily by flow cytometry (A) of male and (B) female mice. Of these, the parasitized reticulocytes were determined in (C) male and (D) female mice. Anemia was determined by adding counting beads to blood samples and measurement was performed using flow cytometry. Anemia was monitored in (E) male and (F) female mice. All experiments were done in n = 7-15 mice per group. * p<0.05 ** p<0.01 *** p<0.001. Error bars indicate SEM.

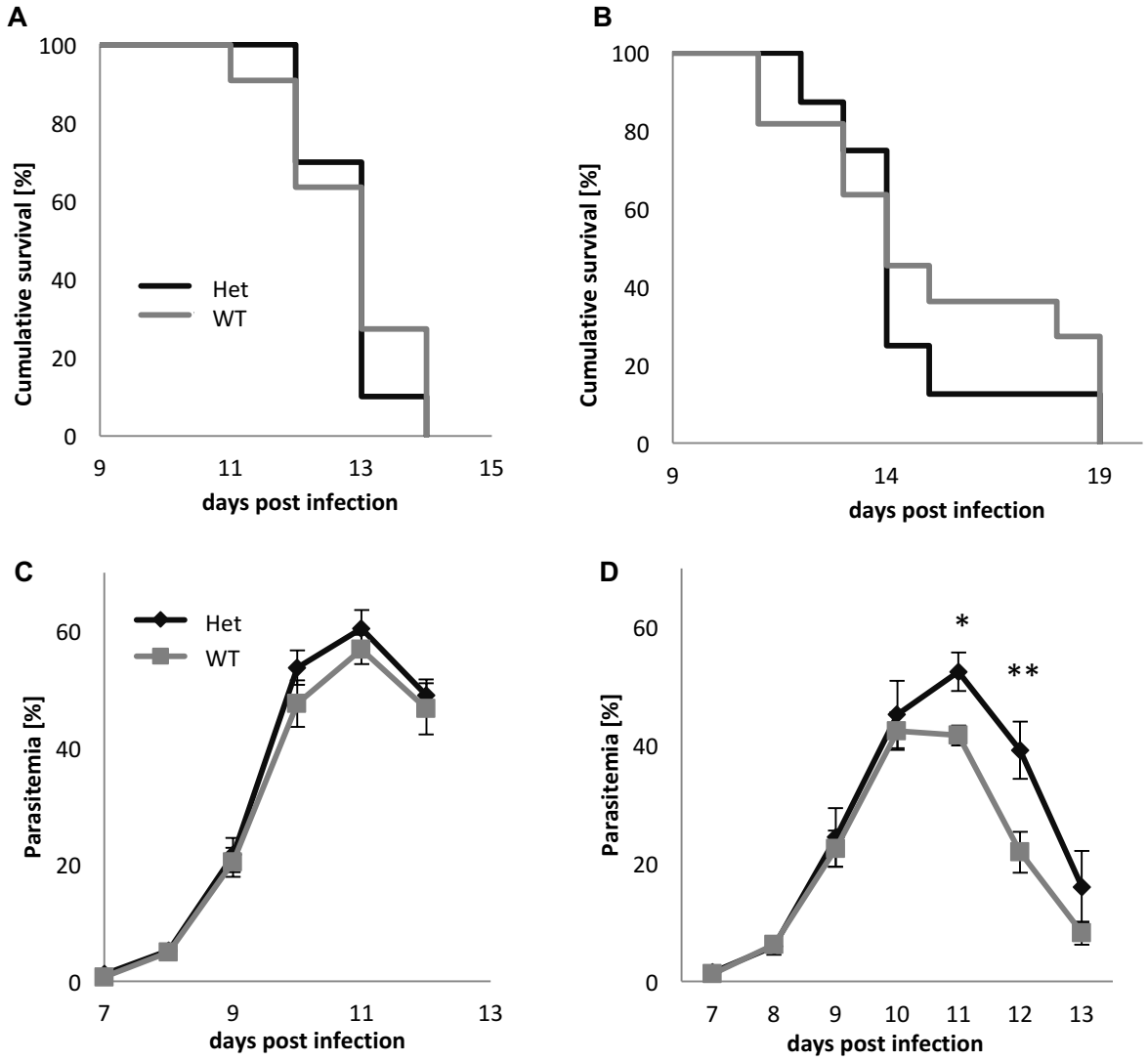

Supplementary Figure 2: *P. chabaudi* infection of *Cpox*$^{+/W373X}$ and *Cpox*$^{+/+}$ mice. Mice were infected with 1×10^4 *P. chabaudi* and parasitemia was monitored daily by light microscopy of Giemsa stained peripheral blood smears. (A) Cumulative survival of male mice. (B) Cumulative survival of female mice. (C) Total parasitemia of male mice. (C) Total parasitemia of female mice. All experiments were done in n = 8-11 mice per group. * $p<0.05$ ** $p<0.01$. Error bars indicate SEM.

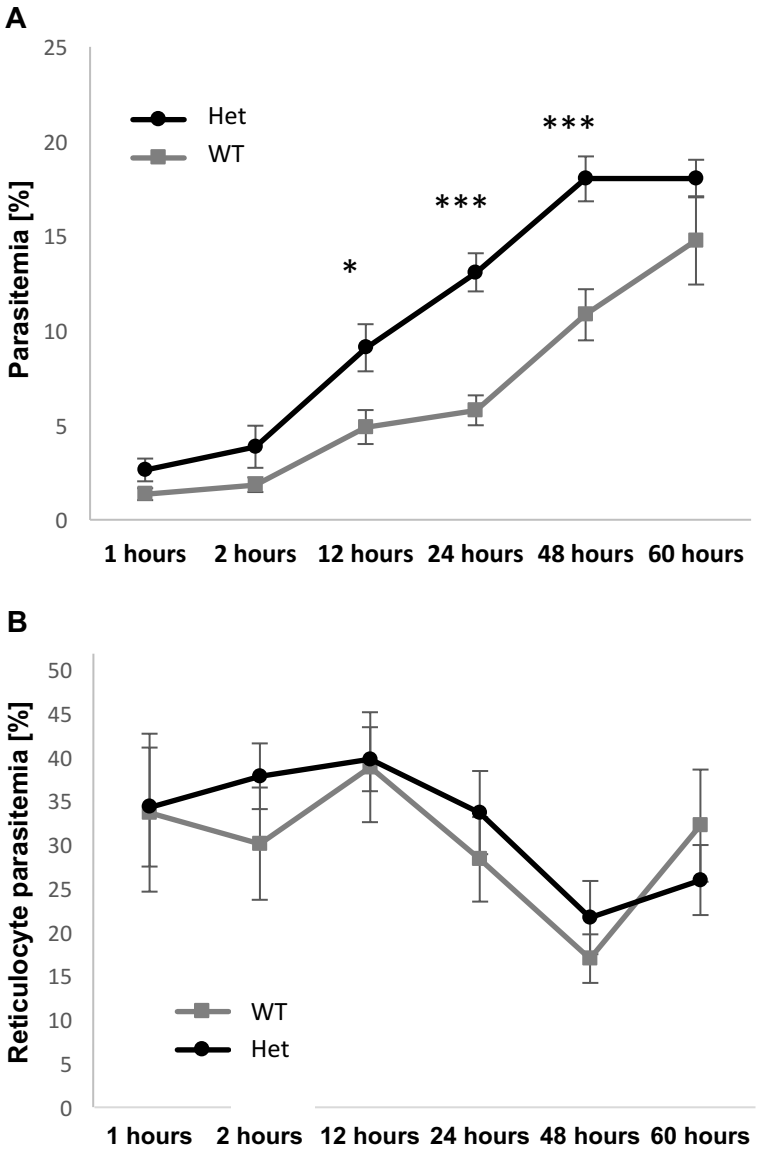

Supplementary Figure 3: *P. berghei* parasitemia during IVET of *Cpox*$^{+/W373X}$ and *Cpox*$^{+/+}$ erythrocytes. Parasitemia was monitored by Giemsa stained peripheral blood smears. (A) Total parasitemia of *Cpox*$^{+/W373X}$ and *Cpox*$^{+/+}$ erythrocytes. (B) Total reticulocyte parasitemia of *Cpox*$^{+/W373X}$ and *Cpox*$^{+/+}$ erythrocytes**.** (C) n = 5-9 mice per group. *p<0.05 *** p<0.001. Error bars indicate SEM.

3. Discussion

This cotutelle thesis was undertaken in collaboration between two research teams with expertise in parasite biology (Heussler, University of Bern), and host-mechanisms that support malarial infection (Burgio, Macquarie University). To gain a deeper understanding of the malaria parasite and its interaction with its host, this project has used rodent *Plasmodium* species to model the blood and liver stages *in vivo* and *in vitro*, from both a parasite and host perspective. A proximity labeling technique was used to identify novel proteins of the PVM, the membrane serving as the border between *Plasmodium* and the host blood cell. The role of nutrient supply from the host to support parasite growth was elaborated by using two novel strains of genetically modified mice which display mild protection from *Plasmodium* infection. This identified a novel mutation in the *Pbgd* gene (encoding the PBGD protein), and subsequent studies demonstrated that this host heme enzyme may be required for parasite survival and growth. A mouse strain which carried a mutation in the *Cpox* gene was received from collaborators at the Monash University, and increased survival upon malaria infection was noted.

3.1 BioID identifies novel PVM, PV and PPM proteins

As part of the *Plasmodium* life cycle in the vertebrate host, the parasite develops and grows intracellularly in a vacuole. The membrane surrounding this vacuole is host-derived, but is extensively altered by the parasite. The PVM connects host and parasite, and plays a fundamental role in host parasite interactions with a range of functions; ensuring nutrient supply, camouflaging from the host cell defense mechanism, disposal of waste products and exporting proteins into the host cell. Because of difficulties in separating the PVM from other parasite membranes, the biochemical composition and variety of proteins at and within the PVM remains largely unknown [317]. However their identity is of interest, as it may yield methods for disrupting the PVM and increasing the susceptibility of the parasite to therapeutic intervention. The research undertaken in this PhD has significantly increased the number of known PVM proteins by applying a proximity-dependent biotinylation assay [318].

At the time when this PVM BioID project was initiated, BioID had previously been applied to other apicomplexan species, to identify novel components of the inner membrane complex in *Toxoplasma* [319]. The same research group extended this approach to the PV [320], and others identified interaction partners of CDPK [321]. Meanwhile, BioID has been adapted to *Plasmodium* parasites by using *in vivo* biotinylation of *P. berghei* infected mice, as well as *in vitro* in *P. falciparum* cultures [169, 322]. In accordance with this, I show that the technique

can be adapted to *in vitro* cultivated *P. berghei* blood stage parasites. In this PhD, BioID was applied to later parasite stages using an *in vitro* biotin labeling system, enriching late *Plasmodium* stages, as reinvasion is very low. The PVM surrounds the parasite in almost all stages, but to study egress, late schizogony is most interesting. The here applied *in vitro P. berghei* BioID is perhaps important for future studies addressing different research questions, as there are still open questions on parasite egress and the responsible effector proteins.

An advantage of BioID is the labeling of not only directly interacting proteins but also proximal proteins and those that only weakly or transiently interact, which has previously been technically challenging [323]. Establishing BioID for a specific research question, however, is not without pitfalls. Tagging a protein of interest with BirA* increases its size by 321 amino acids and can interfere with protein folding and localization [324, 325]. The EXP1-BirA*-V5 construct fortunately localized correctly and was functional. The data confirms that BioID can be used for identification of novel proteins within a subcellular environment, and can be adapted to a variety of experimental setups and *Plasmodium* species. The BioID experimental setup used here was paired with a label-free quantitative MS approach. In the past, it was shown that using peptide intensities rather than the sum of peptide measurements is a more precise way of displaying the data [326]. This approach allowed a reliable quantification of the maximal number of proteins, ensuring to minimize technical and experimental variations, but instead to decipher out real biological differences [323]. The parental parasite line was used as a control which is appropriate [323].

EXP1 was tagged C-terminally since the N-terminus contains the signal peptide [222] and interference with the localization was therefore less likely. The C-terminus extends into the cytosol [226, 327, 328]. During the preparation of proteins for identification by mass spectrometry, host proteins were not separated, and it was postulated that host proteins would be biotinylated. However, only a small number of host proteins were significantly enriched compared to the wild-type control. We did however pick up all endogenously biotinylated mouse proteins with comparable protein intensities and sequence coverage across wild-type and EXP1-BirA*-V5 samples. After the final list of significant proteins was obtained from the mass spectrometry, proteins were included if containing a transmembrane domain or signal peptide, leading to a final list of 61 identified *Plasmodium* proteins. Amongst the 61 proteins, many had already been reported to localize to the PVM or the PV space (validating the BioID approach), such as PTEX components and SERAs. Out of the final list of 61 proteins, further validation was undertaken for 11 high-confidence hits by GFP-fusion tagging. While some of the GFP-tagged proteins displayed low fluorescence and therefore could not be located to a

parasite structure, seven proteins were confirmed within liver- and blood stage parasites which greatly expands the knowledge of peripheral *Plasmodium* proteins present at the PVM, PV and PPM. Notably, a substantial number of the 61 proteins were also found to not be localised to the PVM (and therefore likely false-positive hits). This was confirmed for two of the 11 candidates that were validated by the GFP studies, as they did not locate to the parasite periphery, but rather to secretory organelles. It is noteworthy that in gametocytes PBANKA_0519300 also localized to the parasite periphery in addition to secretory organelles. It was however not established by localization studies whether this was localised to the PV or PVM (the peripheral staining vanished once the gametocyte had left its host RBC).

While the BioID approach was successful in identifying a large subset of parasite components of the PVM, there were a number of false positive hits. This is likely to have been caused by the high sensitivity of the assay (the BirA* enzyme sprays biotin onto close proximity proteins, and may likely label proteins that are in close proximity for short amounts of time), and the fact that the assay requires at least 6-24 hours for labeling [318] (and therefore may label many non-PVM proteins as EXP1 is transported within the parasite). Therefore, in future investigations there are several newer strategies worth considering. First, using the engineered ascorbate peroxidase (APEX), which is fused to a protein of interest, could lead to a lower background because the labeling time is only one minute [329]. This has a further advantage in that it can be used to more tightly within stage dependent windows (i.e.: various stages of parasite life cycle occur over hours/days, and labeling for only one minute would allow precise use at a particular stage) to for example identify proteins that are present during later parasite stages, where encountering egress-specific proteins is more likely.

Trypsin digestion was used in this thesis to cleave proteins off the beads, which removes valuable information because the avidin/biotin binding is not cleaved [330], therefore no biotinylation is detected by mass spectrometry. It is potentially interesting on which part of the protein the BirA* biotinylated target proteins, because this could give information about sterically available and hidden parts of proteins, for instance in protein complexes, or which part of a protein is inserted into a membrane. Localization studies cannot distinguish whether a protein is inserted into a membrane or linked to the membrane by another protein, and information of biotinylated peptides could add valuable information to this. By using BioID or APEX it is possible to get topological and sterical information on the biotinylated proteins as some recent advances have shown: For instance, APEX2 [331] has been used in combination with anti-biotin antibodies. APEX2 is performed followed by whole cell lysate digestion, after which biotinylated peptides are enriched by using anti-biotin antibodies, allowing reliable

identification of biotinylated peptides [332]. This has also been applied to BioID, where lysates were incubated with anti-biotin antibodies, which also allowed the identification of biotinylated peptides by mass spectrometry [330].

Further technical modifications, which facilitate the detection of biotinylated peptides, would be to use Strep-Tactin® or NeutrAvidin™ beads instead of streptavidin beads for the affinity capture of BirA* biotinylated proteins. Strep-Tactin® and NeutrAvidin™ are genetically engineered variants of streptavidin with a lower binding affinity to biotin [333], which enable milder elution conditions from affinity beads (and therefore less likelihood of removal of non-specific interactors), rather than being digested off the beads. Instead of the above biotin-antibody based methods, Strep-Tactin® beads can be used to separate biotinylated peptides from those that were not biotinylated. Another method for elution of proteins from streptavidin beads has been suggested which combines heat and excess biotin [334]. This would combine the use of the advantageous feature of the biotin-avidin binding, which allows stringent washing conditions of beads to remove weak interactors, while finally removing all biotinylated proteins off the beads.

The BirA* protein can also be split into two parts and tagged onto two different proteins that are known interactors [335, 336]. Once they interact, the BirA* protein is active and proximal proteins are biotinylated. This method requires an already identified interaction, and reduces the background, as biotinylation is only induced once this interaction is established. Using this method is potentially interesting for studying complexes present at the PVM, such as the PTEX translocon. Another possibility would be to use TurboId or miniTurbo, engineered BirA* ligases, which label proteins faster while being less toxic compared to APEX, which uses toxic peroxidases as a substrate which then damage APEX [337, 338]. Both techniques remain to be established in Apicomplexa.

While BioID is particularly suited for studies that seek to identify proteins within a close proximity to a bait (in this case EXP1 and therefore identifying proteins associated with the PVM), there are some limitations. One is that it does not provide information on the relative abundance of peptides (and therefore proteins) that are detected. Therefore, future studies could use a complementary quantitative approach, such as stable isotope labeling by amino acids in cell culture (SILAC) [339]. SILAC uses essential amino acids which are either “light”, therefore natural, or “heavy” (which contain ^{2}H instead of H, ^{13}C instead of ^{12}C, and ^{15}N instead of ^{14}N) which are added to the cell culture medium, and can then be used quantified using mass spectrometry [340].

Using SILAC, different approaches can be undertaken to identify and characterize protein-protein interactions, cell differentiation, and nuclear dynamics; this is not an exhaustive list of applications. SILAC has been applied to *P. falciparum* cultures using isoleucine, the only externally required amino acid [269, 341-343], and *Toxoplasma gondii* [344]. However, incorporation of heavy amino acids occurs mostly during cell division and 72 hours to reach 95% labeling has been reported for *P. falciparum* [343]. Therefore, application to *P. berghei* cultures will be complicated by its low *in vitro* reinvasion capacity. Possibly, BioID and SILAC could be paired in *P. falciparum* by using EXP1-BirA*-V5, BirA*-V5 and parental cell lines. An approach of combining BioID with SILAC was published a few months ago for the first time [345]. Each parasite preparation would be subjected to growth in media supplemented with different isoleucine preparations and biotin, pooled, subjected to mass spectrometry and could then be quantitatively assessed.

A similar approach to SILAC, HILAC which uses heavy isotope labeling of newly synthesized proteins was reported to have reduced labeling times. In a cell culture based assay, cells were labeled for only one hour [346]. HILAC is potentially useful to knockouts or knockdowns of *Plasmodium* and the resulting protein upregulations which are induced in an altered cell or organism. For other quantification methods, the use of heavy and light isotopically labelled biotin as a substrate for BioID or APEX2 has been described which could further reduce the background by incubating controls and samples in either heavy or light biotin [330]. For future approaches, it might also be of interest to include a control with a BirA* tag located to a neighboring subcellular environment such as the PPM. It would then be possible to exclude proteins identified in the PPM BioID, reducing the background of non-PVM proteins, not only those which locate to the PPM, but also those that are biotinylated during the transport of the protein to the PPM (and PVM). This is then best paired with one of the above-mentioned techniques using anti-biotin antibodies instead of streptavidin beads.

The initial objective of the project was to identify novel PVM proteins. While this study was designed and underway, several publications from other groups reported that some of the candidate proteins are PVM-localized during the blood stage [322, 347, 348], confirming the PVM localization from the endogenous GFP-tagging approach, that was undertaken in this thesis. Importantly, I was able shown that these PVM proteins also localize to the PVM in liver stage parasites. Often the blood stage is the center of research attention, however the liver stage provides a bottle neck during malaria infection and could potentially be extremely effective if targeted, preventing the symptomatic blood stage [293]. Two PVM candidates have been identified as non-essential during the blood stage [347, 349], however, UIS2 is refractory to

knockout attempts [322]. Whether the essential nature of the protein is due to its PVM localization, or its reported function in dephosphorylating eIF2α-P in the parasite cytoplasm [350], remains to be determined. Overall, this study indicated that UIS2 is an important protein and should be investigated further. UIS2 was also identified in a recently published genome-wide in-silico screen to identify drug targets [351]. The authors also bioinformatically assessed the druggability of UIS2, but came to the conclusion that it would make a poor drug target.

As part of the screen, I also found multiple proteins that were not located to the PVM, but to other localizations at the parasite periphery. PBANKA_0519200 and PBANKA_0519400 have both been localized to the PPM in liver stages, but only the former was localized to the PPM during blood stages as well. In contrast PBANKA_0519400 appears to localize to the PV, as no PPM localization was observed in free merozoites. Although EXP1 was tagged C-terminally, facing the RBC cytosol, BirA* would be active during its transport to the PVM after translation, possibly explaining the detection of some non-PVM proteins. The identification of two novel proteins to the PV and PPM is interesting, as proteins localized to the PPM or associated with the PPM, facing the PV, are often found to be important for parasite invasion [352]. Although initially denoted as being background proteins, their location makes them interesting for future work on parasite invasion.

The work of this thesis has substantially increased the number of confirmed PVM, as well as PV and PPM, proteins. The research community is provided with a list of other possibly important proteins relevant for PVM biology. Functional studies are needed to identify the role of these proteins, and whether they are important for PVM egress. Prior studies have noted the importance of the PVM and PV in many different host-parasite interactions [177, 215, 317, 353]. Parasite egress is of special importance as parasites leave their host cells by an inside-out mode, initiated with PVM rupture. While it is clear that many proteases are involved in this and a number of these have already been identified, the targets remain largely unidentified [111, 125, 153].

3.2 Five consecutive genes in the final BioID list. *Is there more to it?*

Interestingly, the final list of 61 candidate proteins includes five with consecutive genes. Only one of them, PBANKA_0519000, is identified to be the S-antigen, a heat stable protein, localized to the PV which is released into the serum upon egress [354, 355]. It has also been described to be an antigen with a large heterogeneity of different *P. falciparum* isolates, adding to the difficulties of developing an effective vaccine [356]. The successive PBANKA_0519100-400 genes encode proteins with an unknown function [148]. By

comparing the genetic structure between *P. berghei* and *P. falciparum*, it was noted that PBANKA_0519000 is orthologous to PF3D7_1035200. Genes that precede both PBANKA_0519000 and PF3D7_1035200 are highly conserved between species, presenting a region of shared synteny (Figure 8A and Supplementary Figure 2) [357]. Subsequent of PBANKA_0519100-400 are conserved genes as well, and orthology between *P. falciparum* and *P. berghei* was noted: PBANKA_0519600 is orthologous to PF3D7_1036600 (both proteins with unknown function), as are the subsequent genes [357]. It can be concluded that PBANKA_0519100-400 are flanked by regions of shared synteny between chromosome 5 of *P. berghei* and chromosome 10 of *P. falciparum* and that preceding and subsequent genes are orthologous.

There is an overall high degree of conserved synteny between *Plasmodium* species [358, 359]. Comparison between three rodent malaria parasite strains (*P. berghei*, *P. yoelii*, *P. chabaudi*) and *P. falciparum* presented 85% conservation on the genomic level [360]. Genes important for parasite host interactions are often restricted to a specific species infecting a specific host. This can simplify the identification of these genes by using comparative genomics between species adapted to different hosts [361]. Species-differences at the genomic level are mostly located at subtelomeric regions but can also be found in non-subtelomeric regions of the chromosome at synteny breakage points, such as for SERA genes [360, 361]. The region in which the genes of interest lie between with *P. berghei* chromosome 5 and *P. falciparum* chromosome 10, was previously annotated by Kooij and co-workers to be a synteny breakage point within otherwise syntenic chromosomes, outlined above [360]. At this synteny breakage point between PBANKA_0519000 and PBANKA_0519600, only five genes are present but there are ten in the region between PF3D7_1035200 and PF3D7_1036600. This is probably the reason why Kooij and colleagues identified this region to be a synteny breakage points, as they usually give rise to indels (Supplementary Figure 3) [360]. However, I believe this is not the case, and will outline my reasoning in the following sections.

Six of the ten *P. falciparum* proteins belong to the MSP3 family of proteins: MSP3, MSP6, merozoite surface proteins duffy binding-like (MSPDBL) 1 and 2, H101 and MSP11 (H103). MSP3, MSP6, H101, and H103 are paralogues (Figure 8B) [362]. The MSP3 family in *P. falciparum* is characterized by high sequence similarity at the C-terminus, and a MSP3 signature motif (NLRNA/G) (Figure 8C) [363]. Using bioinformatics on the original six MSP3 family members, this list was further extended by four proteins: glutamate-rich protein (GLURP), liver stage antigen 1 (LSA1), M712, and M566, finally spanning the whole region of interest at the synteny break on chromosome 10 [364]. These 10 proteins all share a

conserved 40-residues long C-terminal MSP3 stretch, and following this approach, other species have been investigated to contain this conserved C-terminal stretch. Amongst the identified proteins in non-*P. falciparum* species was also one *P. berghei* protein, PBANKA_0519300 [364], one of the candidate proteins in this thesis, which was localized to the PVM. The precise function of this C-terminal stretch remains to be determined, but it has been shown to self-assemble into an alpha-helical structure and in the case of MSP3 the C-terminal stretch has a high binding affinity to the RBC surface [364, 365]. Interestingly, the MSP3 signature motif (NLRNA/G) is present in PBANKA_0519300 and -400.

Is it possible that PBANKA_0519000-400 are transcribed together? The existence of operon-like structures in *Plasmodium* was postulated, and also that MSP3 and MSP6 might be transcribed in an operon-like manner [360, 366]. Some genes are indeed expressed at the same time, such as the *P. falciparum* SERA family of proteins, but an operon-like structure remains to be identified [367]. Most genes of the PfMSP3 cluster are prominently expressed during later blood stages, indicating a role in erythrocyte invasion with the exception of M712, which is more prominently expressed during earlier stages [361]. Upon comparison of *P. berghei* blood stage RNA sequencing expression data available at PlasmoDB for the region of interest, it is noteworthy, that PBANKA_0519000-400 genes are highly expressed during the schizont stage, and almost absent during the trophozoite stage, and minimally expressed in rings and gametocytes [368]. The preceding and subsequent genes exhibit a different expression pattern (Supplementary Figure 4). Ultimately, they might not be transcribed together but the circumstance that they are simultaneously expressed during the schizont stage is intriguing, as this stage is close to PVM and HCM-rupture, followed by invasion.

It is an ongoing debate, whether rodent malaria species are a useful tool in malaria research. There are numerous species-specific genes often related to virulence such as the *P. falciparum* exclusive var or rif/stevor gene family [361]. While sequestration is observed in *P. berghei*, and is to date an often-used model for sequestration mechanisms in *P. falciparum* [369], it was thought that key factors leading to sequestration in the human host, SBP1 and MAHRP1, are not conserved. A jackhmmer search, a bioinformatics reiterative tool that uses hidden Markov Models, a phylogenetic tree, and re-examination of the genomic location and synteny, revealed that there are indeed SBP1 and MAHRP1 orthologues present in *P. berghei* [205]. This was then experimentally confirmed, proving that genes important for sequestration are conserved between rodent and human malaria species. Interestingly, the identity of SBP1 and MAHRP1 was speculated to be formerly disguised, due to its position at a synteny breakage point [205].

The genetic structure at the synteny break of interest indeed carries the possibility that some of the genes spanning PBANKA_0519100-500 are orthologous to genes spanning PF3D7_1035200-6600. Following this approach, a jackhmmer search of PBANKA_0519100 arrived at PfH101 and PfMSP6, and a search of PBANKA_0519400 at PfMSP3. PBANKA_0519200 and -300 however, did not retrieve any human *Plasmodium* species proteins with a significant E-value, and the search converged after only two iterations (Supplementary Figure 5). As part of a jackhmmer search it is possible to also iterate a protein alignment [370]. Aligning PBANKA_0519200 with -300 arrived at PfMSP11 (Supplementary Figure 6A). PfH101, PfMSP3, PfMSP6, and PfMSP11 are four of the six members of the MSP3 family of proteins clustered on chromosome 10 within the synteny breakage point [363]. Aligning all four genes revealed highly significant E-values with MSP3 proteins of different human malaria species (Supplementary Figure 6B). To confirm the relationships, this search was inverted by using an alignment of all 10 MSP3 cluster proteins. The jackhmmer search arrived at PBANKA_0519100-300 with significant E-values further confirming a relation of proteins on the synteny break between chromosome 5 (*P. berghei*) and chromosome 10 (*P. falciparum*) (Supplementary Figure 7).

The PfMSP3 family is linked to the large PvMSP3 family [363, 371]. As part of the jackhmmer search, *P. vivax* MSP3 proteins often appeared as hits as well. *P. falciparum* chromosome 10 and *P vivax* chromosome 6 are syntenic, and both contain MSP3 clusters, with an increase in paralogues for *P. vivax* (Supplementary Table 2) [361, 372]. The increased number of paralogues of the MSP3 family in both *P. falciparum* and *P. vivax* was hypothesized to be due to increased antigenicity of these proteins, that are immunogenic and present on the surface of merozoites [371]. Other genes with antigenic variation, such as var genes, are organized by using multiple exons, but MSP3 family genes in the two human *Plasmodium* species do not display introns. Together these results indicate that the MSP3 clusters on two human species, and *P. berghei* might be orthologues.

Some proteins of the MSP3 cluster were, and still are, vaccine targets with good immunogenic properties [373, 374]. PfMSPDBL1 and 2 antibodies have been shown to inhibit parasite growth *in vitro*, and antibody titers have been linked to protection from clinical episodes [375]. However, immunization with recombinant GLURP/MSP3 displayed no efficacy [75]. High copy numbers of the PfMSPDBL2 gene are associated with drug-resistance to antimalarials [376]. The exact function and localization for many of the MSP3 cluster proteins remains elusive [377, 378]. In general, MSP proteins can be separated into GPI-anchored membrane incorporated proteins (MSP1, -2, -4, -5, -10, Pf12, Pf38 and Pf92), and peripheral proteins

(MSP3, -6 and -7). The peripheral proteins localize to the PV, and are anticipated to interact with the GPI-anchored family members. This is well established for MSP1 that forms different complexes with MSP3, MSP6, MSP7, MSPDBL1 and 2 [379, 380], of which five are identified to date [381]. GPI-anchored proteins are thought to provide a platform for the peripheral proteins so they can carry out their functions, for example binding to the erythrocyte surface by an unknown receptor, established for MSPDBL1 and 2 [382].

As part of this PhD, three out of four proteins at the synteny breakage point have been localized by GFP-tagging and microscopy. The results of the jackhmmer tool indicated that *P. berghei* proteins of interest are orthologous of the PfMSP3 family of proteins located in the PV, but only PBANKA_0519200 and PBANKA_0519400, are located to the PPM or PV (Figure 8D). Proteins of the MSP3 cluster are not inserted into the PPM as they are missing a GPI anchor and a transmembrane domain, but are thought to be located in the PV [383]. PfLSA1, part of the synteny break was also localized to the PV [384]. However not all proteins of the MSP3 cluster have been localized so far, and although they are related, distinct localizations are possible. PBANKA_0519300 localized to the PVM during the liver stage but in the PV during the blood stage. It is possible that PBANKA_0519300 is associated or inserted into the PVM during the liver stage as it comprised one transmembrane domain on its N-terminal. Potentially, the herein used C-terminal GFP-tagging approach could be interfering with a putative important function. The MSP3 C-terminus was found to be highly conserved throughout 36 different *Plasmodium* field isolates, and could prevent appropriate localization of the protein [363]. PBANKA_0519100, the fourth uncharacterized protein, was not localized as part of this thesis. It would be interesting to do so, and using PBANKA_0519500 as a control, which did not retrieve any result in the jackhmmer search, was not part of the final list of 61 proteins, and is differently expressed during the blood stage according to RNAseq data published on PlasmoDB. Together all of the above indicate, that in addition to the orthologous S-antigen (PBANKA_0519000 and PF3D7_1035200), the four *P. berghei* subsequent genes are orthologous to the MSP3 cluster on chromosome 10. While there are twice as many genes found in *P. falciparum,* this is probably due to paralogs, developed over time. Further research should be undertaken to investigate, whether PBANKA_0519100-400 are indeed MSP3-like proteins and confirmation of this could ultimately lead to a better understanding of these in an *in vivo* malaria experimental background using rodent malaria species.

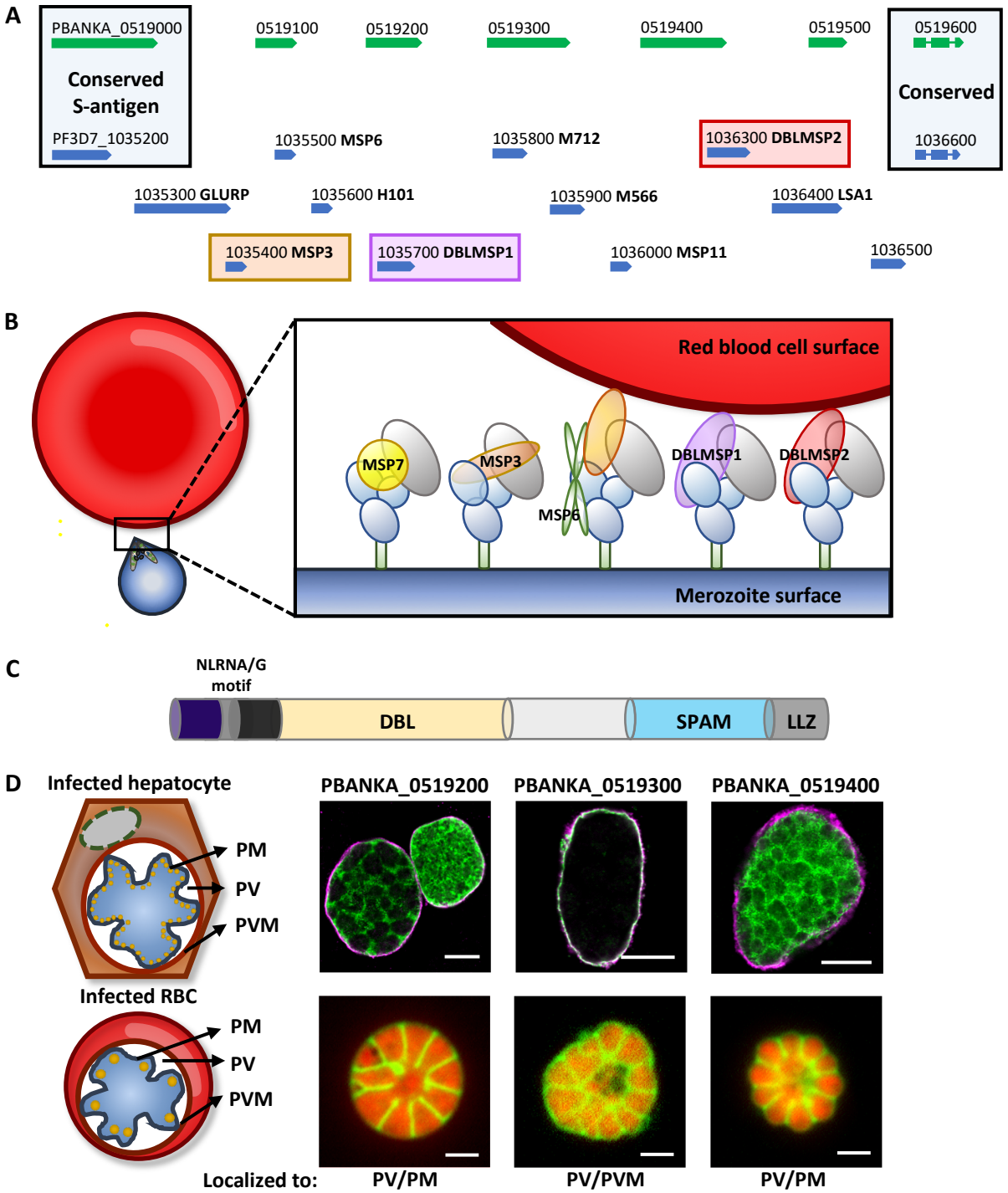

Figure 8: Schematic illustration of the proposed identity of PBANKA_0519100-400. (A) Genes on the *P. berghei* (green) chromosome 5 and of the *P. falciparum* (blue) chromosome 10 are flanked by regions of high synteny highlighted in blue. (B) At the merozoite surface different MSP proteins can be found. Amongst them are the peripherally associated MSP family proteins MSP3, MSPDBL1 and MSPDBL2 [381]. (C) Schematic presentation of the protein structure of MSPDBL1 and MSPDBL2. Adapted from: [380]. (D) The work of this thesis localized PBANKA_0519200-400 during the schizont stage of blood stage and liver stage parasites. During the schizont stage the PVM can be distinguished from the PV and PM.

3.3 Are host heme pathway enzymes PBGD and CPOX required for *Plasmodium* growth?

The work of this thesis has confirmed that alterations of host *Pbgd* and *Cpox* genes lead to variable resistance against the parasite in mice. Host PBDG deficiency was associated with

diminished parasite growth and increased survival in mice upon infection. Host CPOX deficiency was associated with increased survival, but lacking a lower parasitemia, that has been noted for other heme deficient mice. This thesis has led to the investigation of the influence of lower amounts of PBGD and CPOX on *P. falciparum*. In an *in vitro P. falciparum* culture in RBCs from porphyric patients, which have lower amounts of heme enzymes PBGD and CPOX, a growth defect was evident.

The discovery that many erythrocyte polymorphisms led to resistance to malaria-infection started many decades ago and remain an important part of research today, reviewed in [385, 386]. In the past, these studies have also added to the understanding of *Plasmodium*-erythrocyte interaction, for instance by discovering receptors important for parasite invasion [387]. *Plasmodium* has exerted a strong selective pressure on the human genome over many thousands of years. While some polymorphisms have been identified by population-based studies, there are likely more, often affect the RBC and leading to resistance to *Plasmodium* species [28], remaining to be determined [388]. While genome-wide association studies are now obtainable, and whole genome sequencing can be done at a low cost per individual, pinpointing resistance and susceptibility has limitations [389]. The broad spectrum of heterogeneity in the genetic structure in populations in endemic areas (e.g., sub-Saharan African human populations) limits the identification of novel host polymorphisms [25, 390, 391]. A possibility to identify novel host-derived resistance and susceptibility mechanisms is presented in this thesis. By using a N-ethyl-N-nitrosurea (ENU) [392] mutagenesis screen in mice to detect abnormal blood counts in mice, two such novel genes that are responsible for malaria susceptibility and present in human population have been identified. These are the subject of the second part of this thesis.

ENU induces a high number of random nucleotide substitutions in the genome [392-394]. Mice that display a certain phenotype are bred out over several generations to segregate the causative mutation from other ENU induced mutations. A bioinformatics pipeline [395] was used in this thesis to identify possible candidate mutations. But other strategies such as genome mapping can also be applied [396] to pinpoint the responsible mutation [395]. The ENU-derived mutations in the two mouse lines that displayed an abnormal RBC phenotype have been located to genes encoding for *Pbgd* (*Pbgd*^{MRI58155}) and for *Cpox* (*Cpox*$^{+/W373X}$). Previous ENU-induced mutations have identified a number of genes that play a role during malaria infection in rodents, but have also given insights into iron metabolism and erythropoiesis, making it a powerful tool to unlock novel mechanisms [397-403]. Polymorphisms in humans are known for all of these genes, but the influence of these upon malaria infection is unclear, therefore the herein used technique can be useful to unlock novel host polymorphisms. PBGD and CPOX are enzymes

of the canonical heme pathway, of which other enzymes have been previously linked to rodent malaria resistance [309]. The present study was designed to determine the effects of host PBGD and CPOX deficiency during blood stage *Plasmodium* infection. *Pbgd*^{MRI58155} mice infected with *P. chabaudi* showed a mild resistance phenotype, which was characterized in detail. Findings from the mouse studies have been transferred to *in vitro* human studies in Pf*Pbgd*-KO and 3D7 parental strain and to RBC from porphyric patients by using a *P. falciparum in vitro* infection model. Mouse and human studies showed that diminished host PBGD influenced parasite growth.

3.4 During the blood stage, *Plasmodium* has a requirement for Pbgd

PBGD performs the head to tail condensation of four molecules of PBG, crucial for porphyrin production, and deficiencies in PBGD manifest as AIP in humans. AIP attacks are caused by an overload of porphyrin precursors [404]. Reduced heme production leads to an upregulation of ALAS, which stimulates the production of glycine and succinyl CoA, and creates a porphyrin precursor overload of aminolevulinic acid (ALA), porphobilinogen (PBG), and/or other porphyrin precursors or porphyrin metabolic products [405]. In the mouse model used here, a residual enzyme activity of 75% in the *Pbgd*^{MRI58155} mice was measured, and PBGD-deficient mice were healthy, while they were mildly protected from infections with *P. chabaudi*. Often, AIP patients which have natural low levels of PBGD due to a mutation in the *PBGD* gene are asymptomatic carriers especially in non-familial AIP, therefore potential lies in provoking antimalarial effects while leaving the patient free of side-effects [278]. So far there are very few reports of homozygous dominant individuals, which are severely impaired, with the lowest residual PBDG activity reported to be 1% [404, 406]. In mice of the *Pbgd*^{MRI58155} strain, no homozygous pups were viable after embryonic day 9.5, indicating the essential nature of this enzyme.

Metabolic pathways of *Plasmodium* are considered a drug target [407-409]. Some of the already available antimalarials are based on interference with the parasites' metabolism such as chloroquine, which obstructs hemozoin formation. Almost two decades ago, *Plasmodium* heme metabolism was described as a major antimalarial drug target [267]. This was mainly proposed because it was thought that *de novo* production of heme by the parasite was essential for its survival, and was also based on the assumption that host heme was not able to be utilized from the host RBC, and that the parasite had to synthesize its own heme for incorporation into mitochondrial cytochromes [270]. Succinylacetone (SA), an ALAD inhibitor, had been shown to kill parasites and inhibit heme synthesis [283]. However, concentrations of SA used were

high and it is now believed that its antimalarial effect was due to off-target toxicity, because low levels of SA inhibit heme synthesis but do not kill the parasite [270, 297]. The reasoning behind this assumption is that *Plasmodium* heme pathway enzymes are not essential during the blood stage. This has now been confirmed for a number of heme enzymes by different research groups [270, 284-287]. Most importantly, the two rate-limiting parasite enzymes ALAS and FC, which also represent the first and the last enzyme of the pathway, have been successfully genetically disrupted in *P. berghei* and *P. falciparum* [270, 284, 285, 309]. In one of the knockout studies it has also been shown that heme, liberated from host hemoglobin, is utilized by *Plasmodium*, in addition to its *de novo* produced heme [285].

Host cell ALAD and FC have been localized inside the parasite, indicating that the parasite imports host enzymes, as these are too large to be imported through a pore [300, 301]. Following on from their initial findings, Bonday and colleagues demonstrated the underlying mechanism of ALAD being scavenged from the RBC [305]. Host ALAD is thought to be bound to the PPM by an unidentified receptor, and then incorporated into the parasite by an unknown mechanism. This process was able to be inhibited by a truncated ALAD peptide that competed with the full length ALAD to bind to the *P. berghei* membrane. Using this peptide, ALAD enzyme activity was reduced inside the parasite, which lead to its subsequent death. It was also shown that this peptide is only taken up by infected RBCs, leading to the conclusion that it was either actively transported, or taken up by parasite-established NPP. It is important to note that the membrane assay was done on saponin-isolated parasite membranes, which is not physiological as the parasite-host interface would be the PVM. The authors postulated that the PVM regularly engulfs RBC material by the formation of cytosomes [410] and indeed host-derived ALAD was detected in the FV. How host-derived ALAD then leaves the FV is unclear [305]. Another possibility would be that host ALAD would traverse the PVM, enter the PV, and bind to the PPM, and then be transported by either active transport or vesicle formation. Import of other host proteins during the *P. falciparum* blood stage has been described, but the underlying mechanism is unclear, either through MC or through vesicular transport [303]. Results observed from the host ALAD studies could be transferred to the findings obtained from the *P. falciparum* experiments reported here. Host PBGD was localized to the periphery of the parasite, and it could be well possible that binding affinity to the PPM exists, similar to ALAD.

Why would the parasite import host heme enzymes during the blood stage, where plenty of heme is available? Perhaps the availability of host heme enzymes in the cell makes it attractive for the parasite to import these, and use them as part of their heme pathway. For host FC and

PBGD, higher activities have been reported, when comparing them to their parasite counterparts [282, 301]. Apicoplast localized enzymes (ALAD; PBGD; UROD, possibly also UROS) are less efficient in their catalytic abilities compared to their host counterpart, supporting this hypothesis [310]. For PBGD, the catalytic activity has been exceptionally high: compared to PfPBGD, host PBGD showed a 100-fold increase in enzyme activity [282], possibly making it an attractive bait for *Plasmodium*. PfPBGD has another interesting feature because it was established that PfPBGD is able to catalyze the conversion of HMB to uroporphyrinogen III, a task usually performed by UROS. However, the activity was low compared to the host enzyme, which is 100-fold more active. As part of this research study, PfPBGD was mutated, and the enzyme activity was thereby increased five-fold. However increased activity resulted in the UROS activity to be rate-limiting [282], perhaps explaining why the activity of PfPBGD is low, to perform its UROS activity. To date, *Plasmodium* UROS remains to be identified and it is unclear how the parasite compensates for the absence of this enzyme. UROS is necessary to cyclize and rotate unstable HMB, and although it is able to cyclize HMB non-enzymatically, the product is physiologically unusable [257]. In principal, host UROS could be incorporated from the host RBC as it is cytosolic but it cannot explain the absence of UROS from the *Plasmodium* genome, as the parasite relies on heme synthesis during the mosquito stage, where host UROS is not available. The other possibility is that UROS remains to be identified in *Plasmodium*.

3.5 Identification of a putative *UROS* encoding gene in the *P. falciparum* and *P. berghei* genome using Hidden Markov Models

As in the identification of MSP3 cluster orthologues, a jackhmmer search was performed to try to identify UROS in the *Plasmodium* genome. As a starting point, the human UROS protein was used and an iterative jackhmmer search was performed (Supplementary Figure 8A). After five iterative steps a *P. falciparum* protein was identified (with a significant E-value of 0.00057), encoded by the PF3D7_1247600 gene, according to PlasmoDB a conserved *Plasmodium* protein with an unknown function. PF3D7_1247600 is highly conserved across *Plasmodium* species, and has an orthologue in *P. berghei*, PBANKA_1460600 (Supplementary Figure 9). GO terms of these proteins resulted in the following: tetrapyrrole biosynthetic process, membrane and Uros II synthase activity. A *P. berghei* knockout has been established and the gene, PBANKA_1460600, is dispensable during the blood stage [411].

Similar to the MSP3 cluster search, I also performed the opposite jackhmmer search using an alignment of the *P. falciparum* and *P. berghei* proteins as a starting point (Supplementary

Figure 8B). After three iterations, it arrived at the human *UROS* with a significant E-value of 2.5e-10, which was also the only human gene identified. In an interesting paper on *Chromera velia*, which is the closest photosynthetic relative to Apicomplexan parasites, it was shown that *Chromera velia* and Apicomplexa share characteristics of their heme pathway - most striking, they both use succinyl coenzyme A and L-glycine as initial substrates [289]. They identified the same UROS *Plasmodium* homologs by using a BLAST search [289]. UROS could be localized to the apicoplast, as PBGD and UROD are both apicoplast-localized which would enable easy substrate exchange. As most apicoplast genes have transferred to the parasite nucleus, one way to establish their origin is to check whether they contain a bipartite leader sequence, targeting them back to the apicoplast [290]. To test if PF3D7_1247600 and PBANKA_1460600 contain a bipartite leader sequence, the PlasmoAP tool, which uses an algorithm to assesses the presence of this leader sequence, was used [412]. PlasmoAP is available through PlasmoDB, where the proteins' sequence of a protein of interest is used by the program. Indeed, PF3D7_1247600 and PBANKA_1460600 contain an apicoplast leading sequence. Together all of the above indicate that PF3D7_1247600/ PBANKA_1460600 could be *Plasmodium* UROS candidates, which should be investigated further.

3.6 Mice display increased survival upon CPOX host-deficiency

CPOX decarboxylates coproporphyrinogen to produce protoporphyrinogen IX. A BALB/c mouse line deficient in CPOX (*Cpox*$^{+/W373X}$), the sixth heme pathway enzyme, is slightly more resistant to *P. berghei* infection, which manifests in prolonged survival. The mouse line is on a BALB/c background that is naturally resistant to infection with *P. berghei* and resistant to experimental CM, but partially susceptible to infections with *P. chabaudi* [34, 37]. Upon infection with *P. berghei*, *Cpox*$^{+/W373X}$ showed a survival advantage, but no susceptibility or resistance upon infection with *P. chabaudi* was noted. This was not observed during *P. chabaudi* infection, and could be due to the fact that the mice are already susceptible to these parasites, and that depleted host CPOX is not sufficient to counteract this susceptibility. *P. berghei* preferentially invades reticulocytes [238] compared to *P. chabaudi*, which has a tropism for mature RBCs [413]. If CPOX is not required in RBCs, but required in reticulocytes, this could explain the observed difference between *P. berghei* and *P. chabaudi*.

Increased survival was noted for *Cpox*$^{+/W373X}$ mice, however a lower parasitemia was absent, which is somewhat different to what was observed in studies of other host heme enzymes, PBGD and FC [309]. Mice also exhibited leukocytosis, a different blood phenotype when compared to *Pbgd*^{MRI58155} mice, accompanied by elevated ferritin levels. These could be due to

a bystander effect of the *Cpox* mutation, resulting in inflammation. This hypothesis was however not tested. Uninfected *Cpox*$^{+/W373X}$ mice also exhibited a mild anemia phenotype, which could influence the survival of *Cpox*$^{+/W373X}$ mice [414]. In the mouse model, elevated ferritin levels have been noted, leading to the conclusion that iron loading onto heme is impaired. While characterizing the blood from *Cpox*$^{+/W373X}$ and comparing it to their *Cpox*$^{+/+}$ littermates, I noted a difference in osmotic fragility in that *Cpox*$^{+/W373X}$ are less osmotically fragile. During infection with *Plasmodium*, osmotic fragility increases in RBC due to host cell remodeling undertaken by the parasite [415, 416]. In principle, it is possible that due to the decreased osmotic fragility, splenic clearance was decreased. iRBCs often increase in size, which decreases the surface-to-volume ratio, making them more prone to splenic clearance, but *Cpox*$^{+/W373X}$ mice have microcytic red blood cells which should result in reduced clearance [417]. This was confirmed using an artificial spleen model; blood from *Cpox*$^{+/+}$ mice was more likely to be retained compared to *Cpox*$^{+/W373X}$ RBCs. During the IVET however a reduction in RBC number was observed during the second cycle, which could be due to spleen-resident macrophages or spleen independent clearance of RBCs. In order to establish the role of spleen-resident macrophages, splenectomized mice could be compared to normal mice to test this postulate.

Although the HCP condition is extremely rare, a blood sample from one symptomatic HCP patient was obtained [418]. The blood was infected with *P. falciparum* and, compared to the control, a significantly lower parasitemia in cycle two was noted. Porphyria attacks are triggered by the build-up of porphyrin precursors in the case of HCP these are porphobilinogen PBG and coproporphyrinogen III [414] and could theoretically lead to the resistance observed in the CPOX rodent study. This is unlikely given the results from a study, where red cells from X-linked dominant protoporphyria (XLDPP) patients, caused by a gain-of function mutation in the first heme enzyme, were infected with *P. falciparum*, and no difference in growth was detected [309]. This is interesting, as XLDPP is characterized by a build-up of porphyrin intermediates due to increased ALAS activity but normal FC activity. These experiments have been performed *in vitro*, and exclude the influence of porphyrin intermediates. However, these results might not be fully comparable to *in vivo* rodent studies undertaken in this thesis, and do not exclude the possibility that a build-up contributed to the increased survival of *Cpox*$^{+/W373X}$ mice. Furthermore, it cannot be discounted that during erythropoiesis and development reduced availability of CPOX lead to a physiological defect in the mice, influencing the host response to malaria.

A previous study has shown that rodent and human parasites are affected, when grown in blood with heme enzyme deficiency [309]. Two additional types of enzymes and the porphyrias they cause are added hereby to the list of porphyrias that influence parasite growth during the blood stage. Porphyrias often display reduced penetrance, and are rare in the population [351]. Amongst the porphyrias, variegate porphyria (caused by reduced PPOX activity) is reported to be more prevalent in South Africa, in the white population [248]. Outside of Africa, AIP, followed by HCP, are amongst the more prevalent porphyria types indicating that host heme enzymes have been under limited genetic pressure by *Plasmodium*. Novel identification of human polymorphisms that do not display a phenotype is difficult, and porphyrias are often clinically silent, so the prevalence of porphyrias could be underrated [419]. While porphyrias potentially could be underdiagnosed, due to asymptomatic carriers and insufficient access to medical care in malaria endemic countries, it could be more prevalent due to pressure exerted onto the host genome. For AIP, there have been a few reports on AIP in people of Black African descent and novel SNPs leading to AIP have been identified which are not found in Caucasians [420]. While the study subject size was small, AIP could be underdiagnosed and common in sub-Saharan Africa and remains to be elucidated in the future.

For further future studies on host heme enzymes a few tools are available to manipulate human RBCs *in vitro* by using cell culture techniques [391]. These could be used to address questions concerning invasion, growth and maturation in RBCs and could be useful in future investigations. CRISPR/CAS made it possible to translate findings into the *in vivo* background; however, this is only possible if the target is identified [421]. Although the parasite heme pathway during the blood stage is no longer a drug target anymore, as many of the genes are non-essential, this target could be shifted to the mosquito and liver stage, where these enzymes appear refractory to gene deletion and critical for development.

3.7 Conclusion and outlook

This PhD has provided new insights into parasite biology and host-parasite interactions. The number of confirmed PVM proteins was significantly increased by establishing a proximity-labeling approach to *in vitro* cultured *P. berghei* parasites. Understanding the composition of the PVM may yield future targets for therapeutic intervention aimed at preventing PVM rupture, therefore preventing parasite spreading. Antimalarials targeting intracellular parasite proteins must cross the PVM, and should not be discharged by the parasite. A better understanding of the transport mechanisms across the PVM could result in better treatment

strategies. By interfering with the PVM transport mechanism the parasite could be starved or accumulation of waste products could be induced, ultimately killing the parasite.

A novel ENU-generated transgenic mouse displayed mild protection against *Plasmodium* infection, which was found to be caused by a disruption in the *Pbdg* gene, an enzyme in the host heme pathway, and therefore has revealed further insight into the role of host heme pathway enzymes during the *Plasmodium* blood stage. Interestingly, mutations in *PBGD* cause AIP in humans, and like other porphyrias we found that *Plasmodium* growth was impaired in erythrocytes from AIP patients. The experiments undertaken in this thesis suggest that the parasite has a reliance upon host PBDG, and therefore this might represent a potential therapeutic target to "starve" the parasite of heme. A mouse strain deficient in CPOX displayed increased survival however but no lower parasitemia, which is usually characteristic of host heme enzyme deficient infected mice. It was therefore concluded that the resistance of $Cpox^{+/W373X}$ mice is not due to limited amounts of CPOX but to a bystanding effect of the *Cpox* mutation. Blood from one HCP patient with natural low levels of CPOX was infected and a maturation defect and/or invasion defect of *P. falciparum* was observed. This was in accordance to previously tested porphyric blood samples from patients with deficiencies in FC, UROS and PBGD. Collectively, both projects of this thesis have added to the deeper understanding of *Plasmodium*, and provide future opportunities for therapeutic intervention to halt malarial infection.

References

1. 2017, W.H.O., World Malaria Report 2017. ISBN: 978-92-4-156552-3.
2. Lu, F., et al., Emergence of Indigenous Artemisinin-Resistant *Plasmodium falciparum* in Africa. N Engl J Med, 2017. **376**(10): p. 991-3.
3. 2016, W.H.O., World malaria report 2016. ISBN: 978 92 4 151171 1, 2016.
4. Kamareddine, L., The biological control of the malaria vector. Toxins (Basel), 2012. **4**(9): p. 748-67.
5. Ramirez, J.L., L.S. Garver, and G. Dimopoulos, Challenges and approaches for mosquito targeted malaria control. Curr Mol Med, 2009. **9**(2): p. 116-30.
6. Guerra, C.A., et al., The limits and intensity of *Plasmodium falciparum* transmission: implications for malaria control and elimination worldwide. PLoS Med, 2008. **5**(2): p. e38.
7. Autino, B., et al., Epidemiology of malaria in endemic areas. Mediterr J Hematol Infect Dis, 2012. **4**(1): p. e2012060.
8. Waxman, M., et al., Characteristics and survival of patients with Ebola virus infection, malaria, or both in Sierra Leone: a retrospective cohort study. Lancet Infect Dis, 2017. **17**(6): p. 654-660.
9. Walker, P.G., et al., Malaria morbidity and mortality in Ebola-affected countries caused by decreased health-care capacity, and the potential effect of mitigation strategies: a modelling analysis. Lancet Infect Dis, 2015. **15**(7): p. 825-32.
10. Beck-Johnson, L.M., et al., The effect of temperature on Anopheles mosquito population dynamics and the potential for malaria transmission. PLoS One, 2013. **8**(11): p. e79276.
11. Onyango, E.A., et al., An integrated risk and vulnerability assessment framework for climate change and malaria transmission in East Africa. Malar J, 2016. **15**(1): p. 551.
12. Paaijmans, K.P., A.F. Read, and M.B. Thomas, Understanding the link between malaria risk and climate. Proc Natl Acad Sci U S A, 2009. **106**(33): p. 13844-9.
13. Patz, J.A., et al., Climate change: Regional warming and malaria resurgence. Nature, 2002. **420**(6916): p. 627-8; discussion 628.
14. Ramasamy, R., Zoonotic malaria - global overview and research and policy needs. Front Public Health, 2014. **2**: p. 123.
15. Idro, R., et al., Cerebral malaria: mechanisms of brain injury and strategies for improved neurocognitive outcome. Pediatr Res, 2010. **68**(4): p. 267-74.
16. Uneke, C.J., Impact of placental *Plasmodium falciparum* malaria on pregnancy and perinatal outcome in sub-Saharan Africa: part III: placental malaria, maternal health, and public health. Yale J Biol Med, 2008. **81**(1): p. 1-7.
17. Baird, J.K., et al., Diagnosis and Treatment of *Plasmodium vivax* Malaria. Am J Trop Med Hyg, 2016. **95**(6 Suppl): p. 35-51.
18. Campo, B., et al., Killing the hypnozoite--drug discovery approaches to prevent relapse in *Plasmodium vivax*. Pathog Glob Health, 2015. **109**(3): p. 107-22.
19. Chu, C.S. and N.J. White, Management of relapsing *Plasmodium vivax* malaria. Expert Rev Anti Infect Ther, 2016. **14**(10): p. 885-900.
20. de Koning-Ward, T.F., P.R. Gilson, and B.S. Crabb, Advances in molecular genetic systems in malaria. Nat Rev Microbiol, 2015. **13**(6): p. 373-87.
21. Lee, M.C. and D.A. Fidock, CRISPR-mediated genome editing of *Plasmodium falciparum* malaria parasites. Genome Med, 2014. **6**(8): p. 63.
22. Bushell, E., et al., Functional Profiling of a *Plasmodium* Genome Reveals an Abundance of Essential Genes. Cell, 2017. **170**(2): p. 260-272 e8.
23. Gomes, A.R., et al., A genome-scale vector resource enables high-throughput reverse genetic screening in a malaria parasite. Cell Host Microbe, 2015. **17**(3): p. 404-13.
24. Schwach, F., et al., PlasmoGEM, a database supporting a community resource for large-scale experimental genetics in malaria parasites. Nucleic Acids Res, 2015. **43**(Database issue): p. D1176-82.
25. Campbell, M.C. and S.A. Tishkoff, African genetic diversity: implications for human demographic history, modern human origins, and complex disease mapping. Annu Rev Genomics Hum Genet, 2008. **9**: p. 403-33.
26. Hedrick, P.W., Resistance to malaria in humans: the impact of strong, recent selection. Malar J, 2012. **11**: p. 349.
27. Longley, R., et al., Host resistance to malaria: using mouse models to explore the host response. Mamm Genome, 2011. **22**(1-2): p. 32-42.
28. Kwiatkowski, D.P., How malaria has affected the human genome and what human genetics can teach us about malaria. Am J Hum Genet, 2005. **77**(2): p. 171-92.
29. Allison, A.C., Protection afforded by sickle-cell trait against subtertian malareal infection. Br Med J, 1954. **1**(4857): p. 290-4.

30. Grosse, S.D., et al., Sickle cell disease in Africa: a neglected cause of early childhood mortality. Am J Prev Med, 2011. **41**(6 Suppl 4): p. S398-405.
31. Elguero, E., et al., Malaria continues to select for sickle cell trait in Central Africa. Proc Natl Acad Sci U S A, 2015. **112**(22): p. 7051-4.
32. Horuk, R., The Duffy Antigen Receptor for Chemokines DARC/ACKR1. Front Immunol, 2015. **6**: p. 279.
33. Mercereau-Puijalon, O. and D. Menard, *Plasmodium vivax* and the Duffy antigen: a paradigm revisited. Transfus Clin Biol, 2010. **17**(3): p. 176-83.
34. Stevenson, M.M., J.J. Lyanga, and E. Skamene, Murine malaria: genetic control of resistance to *Plasmodium chabaudi*. Infect Immun, 1982. **38**(1): p. 80-8.
35. Fortin, A., M.M. Stevenson, and P. Gros, Complex genetic control of susceptibility to malaria in mice. Genes Immun, 2002. **3**(4): p. 177-86.
36. Neill, A.L. and N.H. Hunt, Pathology of fatal and resolving *Plasmodium berghei* cerebral malaria in mice. Parasitology, 1992. **105 (Pt 2)**: p. 165-75.
37. Mackey, L.J., et al., Immunopathological aspects of *Plasmodium berghei* infection in five strains of mice. II. Immunopathology of cerebral and other tissue lesions during the infection. Clin Exp Immunol, 1980. **42**(3): p. 412-20.
38. Lin, E., et al., Mapping of the *Plasmodium chabaudi* resistance locus char2. Infect Immun, 2006. **74**(10): p. 5814-9.
39. Laroque, A., et al., The mouse Char10 locus regulates severity of pyruvate kinase deficiency and susceptibility to malaria. PLoS One, 2017. **12**(5): p. e0177818.
40. Cox, F.E., History of the discovery of the malaria parasites and their vectors. Parasit Vectors, 2010. **3**(1): p. 5.
41. Cui, L. and X.Z. Su, Discovery, mechanisms of action and combination therapy of artemisinin. Expert Rev Anti Infect Ther, 2009. **7**(8): p. 999-1013.
42. Bhattacharjee, S., et al., Endoplasmic reticulum PI(3)P lipid binding targets malaria proteins to the host cell. Cell, 2012. **148**(1-2): p. 201-12.
43. Woodrow, C.J. and N.J. White, The clinical impact of artemisinin resistance in Southeast Asia and the potential for future spread. FEMS Microbiol Rev, 2017. **41**(1): p. 34-48.
44. Ariey, F., et al., A molecular marker of artemisinin-resistant *Plasmodium falciparum* malaria. Nature, 2014. **505**(7481): p. 50-5.
45. Boussaroque, A., et al., Emergence of Mutations in the K13 Propeller Gene of *Plasmodium falciparum* Isolates from Dakar, Senegal, in 2013-2014. Antimicrob Agents Chemother, 2015. **60**(1): p. 624-7.
46. Mbengue, A., et al., A molecular mechanism of artemisinin resistance in *Plasmodium falciparum* malaria. Nature, 2015. **520**(7549): p. 683-7.
47. Miotto, O., et al., Genetic architecture of artemisinin-resistant *Plasmodium falciparum*. Nat Genet, 2015. **47**(3): p. 226-34.
48. White, N.J., Can new treatment developments combat resistance in malaria? Expert Opin Pharmacother, 2016. **17**(10): p. 1303-7.
49. Achan, J., et al., Quinine, an old anti-malarial drug in a modern world: role in the treatment of malaria. Malar J, 2011. **10**: p. 144.
50. Sidhu, A.B., D. Verdier-Pinard, and D.A. Fidock, Chloroquine resistance in *Plasmodium falciparum* malaria parasites conferred by pfcrt mutations. Science, 2002. **298**(5591): p. 210-3.
51. Coatney, G.R., Pitfalls in a discovery: the chronicle of chloroquine. Am J Trop Med Hyg, 1963. **12**: p. 121-8.
52. Verdier, F., et al., Chloroquine uptake by *Plasmodium falciparum*-infected human erythrocytes during in vitro culture and its relationship to chloroquine resistance. Antimicrob Agents Chemother, 1985. **27**(4): p. 561-4.
53. White, N.J., Antimalarial drug resistance. J Clin Invest, 2004. **113**(8): p. 1084-92.
54. Setthaudom, C., et al., Role of *Plasmodium falciparum* chloroquine resistance transporter and multidrug resistance 1 genes on in vitro chloroquine resistance in isolates of *Plasmodium falciparum* from Thailand. Am J Trop Med Hyg, 2011. **85**(4): p. 606-11.
55. Juge, N., et al., *Plasmodium falciparum* chloroquine resistance transporter is a H+-coupled polyspecific nutrient and drug exporter. Proc Natl Acad Sci U S A, 2015. **112**(11): p. 3356-61.
56. Gomez-Saladin, E., et al., *Plasmodium falciparum* mdr1 mutations and in vivo chloroquine resistance in Indonesia. Am J Trop Med Hyg, 1999. **61**(2): p. 240-4.
57. Foote, S.J., et al., Several alleles of the multidrug-resistance gene are closely linked to chloroquine resistance in *Plasmodium falciparum*. Nature, 1990. **345**(6272): p. 255-8.
58. Barnes, D.A., et al., Selection for high-level chloroquine resistance results in deamplification of the pfmdr1 gene and increased sensitivity to mefloquine in *Plasmodium falciparum*. EMBO J, 1992. **11**(8): p. 3067-75.

59. Reiling, S.J. and P. Rohrbach, Monitoring PfMDR1 transport in *Plasmodium falciparum.* Malar J, 2015. **14**: p. 270.
60. Schlitzer, M., Antimalarial drugs - what is in use and what is in the pipeline. Arch Pharm (Weinheim), 2008. **341**(3): p. 149-63.
61. Pradel, G. and M. Schlitzer, Antibiotics in malaria therapy and their effect on the parasite apicoplast. Curr Mol Med, 2010. **10**(3): p. 335-49.
62. Gregson, A. and C.V. Plowe, Mechanisms of resistance of malaria parasites to antifolates. Pharmacol Rev, 2005. **57**(1): p. 117-45.
63. Antony, H.A. and S.C. Parija, Antimalarial drug resistance: An overview. Trop Parasitol, 2016. **6**(1): p. 30-41.
64. Fidock, D.A., et al., Mutations in the P. falciparum digestive vacuole transmembrane protein PfCRT and evidence for their role in chloroquine resistance. Mol Cell, 2000. **6**(4): p. 861-71.
65. Mu, J., et al., Multiple transporters associated with malaria parasite responses to chloroquine and quinine. Mol Microbiol, 2003. **49**(4): p. 977-89.
66. Schwartz, L., et al., A review of malaria vaccine clinical projects based on the WHO rainbow table. Malar J, 2012. **11**: p. 11.
67. Rts, S.C.T.P., Efficacy and safety of RTS,S/AS01 malaria vaccine with or without a booster dose in infants and children in Africa: final results of a phase 3, individually randomised, controlled trial. Lancet, 2015. **386**(9988): p. 31-45.
68. Rts, S.C.T.P., Efficacy and safety of the RTS,S/AS01 malaria vaccine during 18 months after vaccination: a phase 3 randomized, controlled trial in children and young infants at 11 African sites. PLoS Med, 2014. **11**(7): p. e1001685.
69. Olotu, A., et al., Seven-Year Efficacy of RTS,S/AS01 Malaria Vaccine among Young African Children. N Engl J Med, 2016. **374**(26): p. 2519-29.
70. Moorthy, V.S. and J.M. Okwo-Bele, Final results from a pivotal phase 3 malaria vaccine trial. Lancet, 2015. **386**(9988): p. 5-7.
71. Gosling, R. and L. von Seidlein, The Future of the RTS,S/AS01 Malaria Vaccine: An Alternative Development Plan. PLoS Med, 2016. **13**(4): p. e1001994.
72. Hoffman, S.L., et al., The March Toward Malaria Vaccines. Am J Prev Med, 2015. **49**(6 Suppl 4): p. S319-33.
73. Sissoko, M.S., et al., Safety and efficacy of PfSPZ Vaccine against *Plasmodium falciparum* via direct venous inoculation in healthy malaria-exposed adults in Mali: a randomised, double-blind phase 1 trial. Lancet Infect Dis, 2017. **17**(5): p. 498-509.
74. Bennett, J.W., et al., Phase 1/2a Trial of *Plasmodium vivax* Malaria Vaccine Candidate VMP001/AS01B in Malaria-Naive Adults: Safety, Immunogenicity, and Efficacy. PLoS Negl Trop Dis, 2016. **10**(2): p. e0004423.
75. Sirima, S.B., et al., A phase 2b randomized, controlled trial of the efficacy of the GMZ2 malaria vaccine in African children. Vaccine, 2016. **34**(38): p. 4536-4542.
76. Mahmoudi, S. and H. Keshavarz, Efficacy of phase 3 trial of RTS, S/AS01 malaria vaccine: The need for an alternative development plan. Hum Vaccin Immunother, 2017. **13**(9): p. 2098-2101.
77. Scherf, A., J.J. Lopez-Rubio, and L. Riviere, Antigenic variation in *Plasmodium falciparum.* Annu Rev Microbiol, 2008. **62**: p. 445-70.
78. Deitsch, K.W. and R. Dzikowski, Variant Gene Expression and Antigenic Variation by Malaria Parasites. Annu Rev Microbiol, 2017. **71**: p. 625-641.
79. Crompton, P.D., S.K. Pierce, and L.H. Miller, Advances and challenges in malaria vaccine development. J Clin Invest, 2010. **120**(12): p. 4168-78.
80. Hay, S.I., et al., The global distribution and population at risk of malaria: past, present, and future. Lancet Infect Dis, 2004. **4**(6): p. 327-36.
81. Hemingway, J., L. Field, and J. Vontas, An overview of insecticide resistance. Science, 2002. **298**(5591): p. 96-7.
82. Matuschewski, K., Vaccines against malaria-still a long way to go. FEBS J, 2017. **284**(16): p. 2560-2568.
83. McCallum, F.J., et al., Differing rates of antibody acquisition to merozoite antigens in malaria: implications for immunity and surveillance. J Leukoc Biol, 2017. **101**(4): p. 913-925.
84. Bediako, Y., et al., The effect of declining exposure on T cell-mediated immunity to *Plasmodium falciparum* - an epidemiological "natural experiment". BMC Med, 2016. **14**(1): p. 143.
85. Offeddu, V., et al., High Sporozoite Antibody Titers in Conjunction with Microscopically Detectable Blood Infection Display Signatures of Protection from Clinical Malaria. Front Immunol, 2017. **8**: p. 488.
86. Rono, J., et al., Multiple clinical episodes of *Plasmodium falciparum* malaria in a low transmission intensity setting: exposure versus immunity. BMC Med, 2015. **13**: p. 114.

87. Scott, J.A., et al., Relation between *falciparum* malaria and bacteraemia in Kenyan children: a population-based, case-control study and a longitudinal study. Lancet, 2011. **378**(9799): p. 1316-23.
88. Shretta, R., et al., Tracking development assistance and government health expenditures for 35 malaria-eliminating countries: 1990-2017. Malar J, 2017. **16**(1): p. 251.
89. Cohen, J.M., et al., Malaria resurgence: a systematic review and assessment of its causes. Malar J, 2012. **11**: p. 122.
90. Gallup, J.L. and J.D. Sachs, The economic burden of malaria. Am J Trop Med Hyg, 2001. **64**(1-2 Suppl): p. 85-96.
91. Shretta, R., A.L. Avancena, and A. Hatefi, The economics of malaria control and elimination: a systematic review. Malar J, 2016. **15**(1): p. 593.
92. Ferguson, H.M., et al., Ecology: a prerequisite for malaria elimination and eradication. PLoS Med, 2010. **7**(8): p. e1000303.
93. Tanner, M., et al., Malaria eradication and elimination: views on how to translate a vision into reality. BMC Med, 2015. **13**: p. 167.
94. Sinden, R.E., The cell biology of malaria infection of mosquito: advances and opportunities. Cell Microbiol, 2015. **17**(4): p. 451-66.
95. Cowman, A.F., et al., Malaria: Biology and Disease. Cell, 2016. **167**(3): p. 610-624.
96. Frischknecht, F., et al., Imaging movement of malaria parasites during transmission by Anopheles mosquitoes. Cell Microbiol, 2004. **6**(7): p. 687-94.
97. Amino, R., et al., Quantitative imaging of *Plasmodium* sporozoites in the mammalian host. C R Biol, 2006. **329**(11): p. 858-62.
98. Gueirard, P., et al., Development of the malaria parasite in the skin of the mammalian host. Proc Natl Acad Sci U S A, 2010. **107**(43): p. 18640-5.
99. Coppi, A., et al., Heparan sulfate proteoglycans provide a signal to *Plasmodium* sporozoites to stop migrating and productively invade host cells. Cell Host Microbe, 2007. **2**(5): p. 316-27.
100. Ishino, T., et al., Cell-passage activity is required for the malarial parasite to cross the liver sinusoidal cell layer. PLoS Biol, 2004. **2**(1): p. E4.
101. Frevert, U. and U. Krzych, *Plasmodium* cellular effector mechanisms and the hepatic microenvironment. Front Microbiol, 2015. **6**: p. 482.
102. Protzer, U., M.K. Maini, and P.A. Knolle, Living in the liver: hepatic infections. Nat Rev Immunol, 2012. **12**(3): p. 201-13.
103. Graewe, S., et al., Hostile takeover by *Plasmodium*: reorganization of parasite and host cell membranes during liver stage egress. PLoS Pathog, 2011. **7**(9): p. e1002224.
104. Sturm, A., et al., Manipulation of host hepatocytes by the malaria parasite for delivery into liver sinusoids. Science, 2006. **313**(5791): p. 1287-90.
105. Cowman, A.F., et al., The Molecular Basis of Erythrocyte Invasion by Malaria Parasites. Cell Host Microbe, 2017. **22**(2): p. 232-245.
106. Boddey, J.A. and A.F. Cowman, *Plasmodium* nesting: remaking the erythrocyte from the inside out. Annu Rev Microbiol, 2013. **67**: p. 243-69.
107. Olivier, M., et al., Malarial pigment hemozoin and the innate inflammatory response. Front Immunol, 2014. **5**: p. 25.
108. Haldar, K., et al., Malaria: mechanisms of erythrocytic infection and pathological correlates of severe disease. Annu Rev Pathol, 2007. **2**: p. 217-49.
109. Winzeler, E.A., Malaria research in the post-genomic era. Nature, 2008. **455**(7214): p. 751-6.
110. Prado, M., et al., Long-term live imaging reveals cytosolic immune responses of host hepatocytes against *Plasmodium* infection and parasite escape mechanisms. Autophagy, 2015. **11**(9): p. 1561-79.
111. Blackman, M.J., Malarial proteases and host cell egress: an 'emerging' cascade. Cell Microbiol, 2008. **10**(10): p. 1925-34.
112. Dowse, T.J., et al., Roles of proteases during invasion and egress by *Plasmodium* and *Toxoplasma*. Subcell Biochem, 2008. **47**: p. 121-39.
113. Pino, P., et al., A multistage antimalarial targets the plasmepsins IX and X essential for invasion and egress. Science, 2017. **358**(6362): p. 522-528.
114. Nasamu, A.S., et al., Plasmepsins IX and X are essential and druggable mediators of malaria parasite egress and invasion. Science, 2017. **358**(6362): p. 518-522.
115. Gilson, P.R. and B.S. Crabb, Morphology and kinetics of the three distinct phases of red blood cell invasion by *Plasmodium falciparum* merozoites. Int J Parasitol, 2009. **39**(1): p. 91-6.
116. Harvey, K.L., P.R. Gilson, and B.S. Crabb, A model for the progression of receptor-ligand interactions during erythrocyte invasion by *Plasmodium falciparum*. Int J Parasitol, 2012. **42**(6): p. 567-73.
117. Riglar, D.T., et al., Super-resolution dissection of coordinated events during malaria parasite invasion of the human erythrocyte. Cell Host Microbe, 2011. **9**(1): p. 9-20.

118. Crosnier, C., et al., Basigin is a receptor essential for erythrocyte invasion by *Plasmodium falciparum.* Nature, 2011. **480**(7378): p. 534-7.
119. Besteiro, S., J.F. Dubremetz, and M. Lebrun, The moving junction of apicomplexan parasites: a key structure for invasion. Cell Microbiol, 2011. **13**(6): p. 797-805.
120. Counihan, N.A., et al., *Plasmodium* rhoptry proteins: why order is important. Trends Parasitol, 2013. **29**(5): p. 228-36.
121. Srinivasan, P., et al., Binding of *Plasmodium* merozoite proteins RON2 and AMA1 triggers commitment to invasion. Proc Natl Acad Sci U S A, 2011. **108**(32): p. 13275-80.
122. Hale, V.L., et al., Parasitophorous vacuole poration precedes its rupture and rapid host erythrocyte cytoskeleton collapse in *Plasmodium falciparum* egress. Proc Natl Acad Sci U S A, 2017. **114**(13): p. 3439-3444.
123. Sturm, A., et al., Alteration of the parasite plasma membrane and the parasitophorous vacuole membrane during exo-erythrocytic development of malaria parasites. Protist, 2009. **160**(1): p. 51-63.
124. Burda, P.C., et al., A *Plasmodium* phospholipase is involved in disruption of the liver stage parasitophorous vacuole membrane. PLoS Pathog, 2015. **11**(3): p. e1004760.
125. Sologub, L., et al., Malaria proteases mediate inside-out egress of gametocytes from red blood cells following parasite transmission to the mosquito. Cell Microbiol, 2011. **13**(6): p. 897-912.
126. Bano, N., et al., Cellular interactions of *Plasmodium* liver stage with its host mammalian cell. Int J Parasitol, 2007. **37**(12): p. 1329-41.
127. Arisue, N., et al., Clues to evolution of the SERA multigene family in 18 *Plasmodium* species. PLoS One, 2011. **6**(3): p. e17775.
128. McCoubrie, J.E., et al., Evidence for a common role for the serine-type *Plasmodium falciparum* serine repeat antigen proteases: implications for vaccine and drug design. Infect Immun, 2007. **75**(12): p. 5565-74.
129. Arisue, N., et al., Phylogeny and evolution of the SERA multigene family in the genus *Plasmodium.* J Mol Evol, 2007. **65**(1): p. 82-91.
130. Putrianti, E.D., et al., The *Plasmodium* serine-type SERA proteases display distinct expression patterns and non-essential in vivo roles during life cycle progression of the malaria parasite. Cell Microbiol, 2010. **12**(6): p. 725-39.
131. Arastu-Kapur, S., et al., Identification of proteases that regulate erythrocyte rupture by the malaria parasite *Plasmodium falciparum.* Nat Chem Biol, 2008. **4**(3): p. 203-13.
132. Collins, C.R., et al., The *Plasmodium falciparum* pseudoprotease SERA5 regulates the kinetics and efficiency of malaria parasite egress from host erythrocytes. PLoS Pathog, 2017. **13**(7): p. e1006453.
133. Miller, S.K., et al., A subset of *Plasmodium falciparum* SERA genes are expressed and appear to play an important role in the erythrocytic cycle. J Biol Chem, 2002. **277**(49): p. 47524-32.
134. Ruecker, A., et al., Proteolytic activation of the essential parasitophorous vacuole cysteine protease SERA6 accompanies malaria parasite egress from its host erythrocyte. J Biol Chem, 2012. **287**(45): p. 37949-63.
135. Schmidt-Christensen, A., et al., Expression and processing of *Plasmodium berghei* SERA3 during liver stages. Cell Microbiol, 2008. **10**(8): p. 1723-34.
136. Tawk, L., et al., A key role for *Plasmodium* subtilisin-like SUB1 protease in egress of malaria parasites from host hepatocytes. J Biol Chem, 2013. **288**(46): p. 33336-46.
137. Withers-Martinez, C., et al., *Plasmodium* subtilisin-like protease 1 (SUB1): insights into the active-site structure, specificity and function of a pan-malaria drug target. Int J Parasitol, 2012. **42**(6): p. 597-612.
138. Suarez, C., et al., The malarial serine protease SUB1 plays an essential role in parasite liver stage development. PLoS Pathog, 2013. **9**(12): p. e1003811.
139. Falae, A., et al., Role of *Plasmodium berghei* cGMP-dependent protein kinase in late liver stage development. J Biol Chem, 2010. **285**(5): p. 3282-8.
140. Bowyer, P.W., et al., Global profiling of proteolysis during rupture of *Plasmodium falciparum* from the host erythrocyte. Mol Cell Proteomics, 2011. **10**(5): p. M110 001636.
141. Tanaka, T.Q., et al., *Plasmodium* dipeptidyl aminopeptidases as malaria transmission-blocking drug targets. Antimicrob Agents Chemother, 2013. **57**(10): p. 4645-52.
142. Yeoh, S., et al., Subcellular discharge of a serine protease mediates release of invasive malaria parasites from host erythrocytes. Cell, 2007. **131**(6): p. 1072-83.
143. Ishino, T., et al., LISP1 is important for the egress of *Plasmodium berghei* parasites from liver cells. Cell Microbiol, 2009. **11**(9): p. 1329-39.
144. Baer, K., et al., Release of hepatic *Plasmodium yoelii* merozoites into the pulmonary microvasculature. PLoS Pathog, 2007. **3**(11): p. e171.
145. Glushakova, S., et al., New stages in the program of malaria parasite egress imaged in normal and sickle erythrocytes. Curr Biol, 2010. **20**(12): p. 1117-21.

146. Alaganan, A., P. Singh, and C.E. Chitnis, Molecular mechanisms that mediate invasion and egress of malaria parasites from red blood cells. Curr Opin Hematol, 2017. **24**(3): p. 208-214.
147. Salmon, B.L., A. Oksman, and D.E. Goldberg, Malaria parasite exit from the host erythrocyte: a two-step process requiring extraerythrocytic proteolysis. Proc Natl Acad Sci U S A, 2001. **98**(1): p. 271-6.
148. Wickham, M.E., J.G. Culvenor, and A.F. Cowman, Selective inhibition of a two-step egress of malaria parasites from the host erythrocyte. J Biol Chem, 2003. **278**(39): p. 37658-63.
149. Chandramohanadas, R., et al., Biophysics of malarial parasite exit from infected erythrocytes. PLoS One, 2011. **6**(6): p. e20869.
150. Chandramohanadas, R., et al., Apicomplexan parasites co-opt host calpains to facilitate their escape from infected cells. Science, 2009. **324**(5928): p. 794-7.
151. Rohrbach, P., et al., Quantitative calcium measurements in subcellular compartments of *Plasmodium falciparum*-infected erythrocytes. J Biol Chem, 2005. **280**(30): p. 27960-9.
152. Garg, S., et al., Calcium-dependent permeabilization of erythrocytes by a perforin-like protein during egress of malaria parasites. Nat Commun, 2013. **4**: p. 1736.
153. Wirth, C.C. and G. Pradel, Molecular mechanisms of host cell egress by malaria parasites. Int J Med Microbiol, 2012. **302**(4-5): p. 172-8.
154. Dvorin, J.D., et al., A plant-like kinase in *Plasmodium falciparum* regulates parasite egress from erythrocytes. Science, 2010. **328**(5980): p. 910-2.
155. Alam, M.M., et al., Phosphoproteomics reveals malaria parasite Protein Kinase G as a signalling hub regulating egress and invasion. Nat Commun, 2015. **6**: p. 7285.
156. Stallmach, R., et al., *Plasmodium falciparum* SERA5 plays a non-enzymatic role in the malarial asexual blood-stage lifecycle. Mol Microbiol, 2015. **96**(2): p. 368-87.
157. Aoki, S., et al., Serine repeat antigen (SERA5) is predominantly expressed among the SERA multigene family of *Plasmodium falciparum*, and the acquired antibody titers correlate with serum inhibition of the parasite growth. J Biol Chem, 2002. **277**(49): p. 47533-40.
158. Lilburn, T.G., et al., Protease-associated cellular networks in malaria parasite *Plasmodium falciparum*. BMC Genomics, 2011. **12 Suppl 5**: p. S9.
159. Combe, A., et al., Clonal conditional mutagenesis in malaria parasites. Cell Host Microbe, 2009. **5**(4): p. 386-96.
160. Alam, A., Serine Proteases of Malaria Parasite *Plasmodium falciparum*: Potential as Antimalarial Drug Targets. Interdiscip Perspect Infect Dis, 2014. **2014**: p. 453186.
161. Koussis, K., et al., A multifunctional serine protease primes the malaria parasite for red blood cell invasion. EMBO J, 2009. **28**(6): p. 725-35.
162. Das, S., et al., Processing of *Plasmodium falciparum* Merozoite Surface Protein MSP1 Activates a Spectrin-Binding Function Enabling Parasite Egress from RBCs. Cell Host Microbe, 2015. **18**(4): p. 433-44.
163. Dua, M., et al., Recombinant falcipain-2 cleaves erythrocyte membrane ankyrin and protein 4.1. Mol Biochem Parasitol, 2001. **116**(1): p. 95-9.
164. Dhawan, S., et al., Ankyrin peptide blocks falcipain-2-mediated malaria parasite release from red blood cells. J Biol Chem, 2003. **278**(32): p. 30180-6.
165. Deligianni, E., et al., A perforin-like protein mediates disruption of the erythrocyte membrane during egress of *Plasmodium berghei* male gametocytes. Cell Microbiol, 2013. **15**(8): p. 1438-55.
166. de Koning-Ward, T.F., et al., The role of osmiophilic bodies and Pfg377 expression in female gametocyte emergence and mosquito infectivity in the human malaria parasite *Plasmodium falciparum*. Mol Microbiol, 2008. **67**(2): p. 278-90.
167. Ponzi, M., et al., Egress of *Plasmodium berghei* gametes from their host erythrocyte is mediated by the MDV-1/PEG3 protein. Cell Microbiol, 2009. **11**(8): p. 1272-88.
168. Talman, A.M., et al., PbGEST mediates malaria transmission to both mosquito and vertebrate host. Mol Microbiol, 2011. **82**(2): p. 462-74.
169. Kehrer, J., F. Frischknecht, and G.R. Mair, Proteomic Analysis of the *Plasmodium berghei* Gametocyte Egressome and Vesicular bioID of Osmiophilic Body Proteins Identifies Merozoite TRAP-like Protein (MTRAP) as an Essential Factor for Parasite Transmission. Mol Cell Proteomics, 2016. **15**(9): p. 2852-62.
170. Bargieri, D.Y., et al., *Plasmodium* Merozoite TRAP Family Protein Is Essential for Vacuole Membrane Disruption and Gamete Egress from Erythrocytes. Cell Host Microbe, 2016. **20**(5): p. 618-630.
171. McRobert, L., et al., Gametogenesis in malaria parasites is mediated by the cGMP-dependent protein kinase. PLoS Biol, 2008. **6**(6): p. e139.
172. Rupp, I., et al., Effect of protease inhibitors on exflagellation in *Plasmodium falciparum*. Mol Biochem Parasitol, 2008. **158**(2): p. 208-12.
173. Torres, J.A., et al., *Plasmodium berghei*: effect of protease inhibitors during gametogenesis and early zygote development. Exp Parasitol, 2005. **111**(4): p. 255-9.

174. Kuehn, A. and G. Pradel, The coming-out of malaria gametocytes. J Biomed Biotechnol, 2010. **2010**: p. 976827.
175. Percy, A.K., et al., Phospholipid biosynthesis in the membranes of immature and mature red blood cells. Biochemistry, 1973. **12**(13): p. 2456-61.
176. Desai, S.A. and R.L. Rosenberg, Pore size of the malaria parasite's nutrient channel. Proc Natl Acad Sci U S A, 1997. **94**(5): p. 2045-9.
177. Spielmann, T., et al., Molecular make-up of the *Plasmodium* parasitophorous vacuolar membrane. Int J Med Microbiol, 2012. **302**(4-5): p. 179-86.
178. Desai, S.A., Why do malaria parasites increase host erythrocyte permeability? Trends Parasitol, 2014. **30**(3): p. 151-9.
179. Nguitragool, W., et al., Malaria parasite clag3 genes determine channel-mediated nutrient uptake by infected red blood cells. Cell, 2011. **145**(5): p. 665-77.
180. Deschermeier, C., et al., Mitochondrial lipoic acid scavenging is essential for *Plasmodium berghei* liver stage development. Cell Microbiol, 2012. **14**(3): p. 416-30.
181. Falkard, B., et al., A key role for lipoic acid synthesis during *Plasmodium* liver stage development. Cell Microbiol, 2013. **15**(9): p. 1585-604.
182. Lopes da Silva, M., et al., The host endocytic pathway is essential for *Plasmodium berghei* late liver stage development. Traffic, 2012. **13**(10): p. 1351-63.
183. Grutzke, J., et al., The spatiotemporal dynamics and membranous features of the *Plasmodium* liver stage tubovesicular network. Traffic, 2014. **15**(4): p. 362-82.
184. Thieleke-Matos, C., et al., Host PI(3,5)P2 activity is required for *Plasmodium berghei* growth during liver stage infection. Traffic, 2014. **15**(10): p. 1066-82.
185. Gehde, N., et al., Protein unfolding is an essential requirement for transport across the parasitophorous vacuolar membrane of *Plasmodium falciparum.* Mol Microbiol, 2009. **71**(3): p. 613-28.
186. Alleva, L.M. and K. Kirk, Calcium regulation in the intraerythrocytic malaria parasite *Plasmodium falciparum.* Mol Biochem Parasitol, 2001. **117**(2): p. 121-8.
187. Garcia, C.R., Calcium homeostasis and signaling in the blood-stage malaria parasite. Parasitol Today, 1999. **15**(12): p. 488-91.
188. Gazarini, M.L., et al., Calcium signaling in a low calcium environment: how the intracellular malaria parasite solves the problem. J Cell Biol, 2003. **161**(1): p. 103-10.
189. Agarwal, S., et al., Ca(2+) -mediated exocytosis of subtilisin-like protease 1: a key step in egress of *Plasmodium falciparum* merozoites. Cell Microbiol, 2013. **15**(6): p. 910-21.
190. Spielmann, T. and T.W. Gilberger, Critical Steps in Protein Export of *Plasmodium falciparum* Blood Stages. Trends Parasitol, 2015. **31**(10): p. 514-25.
191. Matthews, K., et al., The *Plasmodium* translocon of exported proteins (PTEX) component thioredoxin-2 is important for maintaining normal blood-stage growth. Mol Microbiol, 2013. **89**(6): p. 1167-86.
192. Matz, J.M., K. Matuschewski, and T.W. Kooij, Two putative protein export regulators promote *Plasmodium* blood stage development in vivo. Mol Biochem Parasitol, 2013. **191**(1): p. 44-52.
193. Bullen, H.E., et al., Biosynthesis, localization, and macromolecular arrangement of the *Plasmodium falciparum* translocon of exported proteins (PTEX). J Biol Chem, 2012. **287**(11): p. 7871-84.
194. Elsworth, B., et al., Proteomic analysis reveals novel proteins associated with the *Plasmodium* protein exporter PTEX and a loss of complex stability upon truncation of the core PTEX component, PTEX150. Cell Microbiol, 2016. **18**(11): p. 1551-1569.
195. de Koning-Ward, T.F., et al., *Plasmodium* species: master renovators of their host cells. Nat Rev Microbiol, 2016. **14**(8): p. 494-507.
196. Singh, A.P., et al., *Plasmodium* circumsporozoite protein promotes the development of the liver stages of the parasite. Cell, 2007. **131**(3): p. 492-504.
197. Orito, Y., et al., Liver-specific protein 2: a *Plasmodium* protein exported to the hepatocyte cytoplasm and required for merozoite formation. Mol Microbiol, 2013. **87**(1): p. 66-79.
198. Kalanon, M., et al., The *Plasmodium* translocon of exported proteins component EXP2 is critical for establishing a patent malaria infection in mice. Cell Microbiol, 2016. **18**(3): p. 399-412.
199. Vaughan, A.M., et al., Complete *Plasmodium falciparum* liver-stage development in liver-chimeric mice. J Clin Invest, 2012. **122**(10): p. 3618-28.
200. Matz, J.M., et al., The *Plasmodium berghei* translocon of exported proteins reveals spatiotemporal dynamics of tubular extensions. Sci Rep, 2015. **5**: p. 12532.
201. Ingmundson, A., et al., Feeling at home from arrival to departure: protein export and host cell remodelling during *Plasmodium* liver stage and gametocyte maturation. Cell Microbiol, 2014. **16**(3): p. 324-33.
202. Maier, A.G., et al., Exported proteins required for virulence and rigidity of *Plasmodium falciparum*-infected human erythrocytes. Cell, 2008. **134**(1): p. 48-61.

203. Przyborski, J.M., B. Nyboer, and M. Lanzer, Ticket to ride: export of proteins to the *Plasmodium falciparum*-infected erythrocyte. Mol Microbiol, 2016. **101**(1): p. 1-11.
204. Mundwiler-Pachlatko, E. and H.P. Beck, Maurer's clefts, the enigma of *Plasmodium falciparum.* Proc Natl Acad Sci U S A, 2013. **110**(50): p. 19987-94.
205. De Niz, M., et al., The machinery underlying malaria parasite virulence is conserved between rodent and human malaria parasites. Nat Commun, 2016. **7**: p. 11659.
206. Brancucci, N.M.B., et al., Lysophosphatidylcholine Regulates Sexual Stage Differentiation in the Human Malaria Parasite *Plasmodium falciparum.* Cell, 2017. **171**(7): p. 1532-1544 e15.
207. Ward, G.E., L.H. Miller, and J.A. Dvorak, The origin of parasitophorous vacuole membrane lipids in malaria-infected erythrocytes. J Cell Sci, 1993. **106 (Pt 1)**: p. 237-48.
208. Gaur, D., C.E. Chitnis, and V.S. Chauhan, Advances in malaria research. Wiley-IUBMB series on biochemistry and molecular biology. 2017, Hoboken, New Jersey: John Wiley & Sons, Inc. p.
209. Mordue, D.G., et al., Invasion by *Toxoplasma gondii* establishes a moving junction that selectively excludes host cell plasma membrane proteins on the basis of their membrane anchoring. J Exp Med, 1999. **190**(12): p. 1783-92.
210. Beckers, C.J., et al., The *Toxoplasma gondii* rhoptry protein ROP 2 is inserted into the parasitophorous vacuole membrane, surrounding the intracellular parasite, and is exposed to the host cell cytoplasm. J Cell Biol, 1994. **127**(4): p. 947-61.
211. Ghosh, S., et al., The *Plasmodium* rhoptry associated protein complex is important for parasitophorous vacuole membrane structure and intraerythrocytic parasite growth. Cell Microbiol, 2017. **19**(8).
212. Hiller, N.L., et al., Identification of a stomatin orthologue in vacuoles induced in human erythrocytes by malaria parasites. A role for microbial raft proteins in apicomplexan vacuole biogenesis. J Biol Chem, 2003. **278**(48): p. 48413-21.
213. Counihan, N.A., et al., *Plasmodium falciparum* parasites deploy RhopH2 into the host erythrocyte to obtain nutrients, grow and replicate. Elife, 2017. **6**.
214. Ling, I.T., et al., The *Plasmodium falciparum* clag9 gene encodes a rhoptry protein that is transferred to the host erythrocyte upon invasion. Mol Microbiol, 2004. **52**(1): p. 107-18.
215. Spielmann, T., D.J. Fergusen, and H.P. Beck, etramps, a new *Plasmodium falciparum* gene family coding for developmentally regulated and highly charged membrane proteins located at the parasite-host cell interface. Mol Biol Cell, 2003. **14**(4): p. 1529-44.
216. Mueller, A.K., et al., *Plasmodium* liver stage developmental arrest by depletion of a protein at the parasite-host interface. Proc Natl Acad Sci U S A, 2005. **102**(8): p. 3022-7.
217. Matuschewski, K., et al., Infectivity-associated changes in the transcriptional repertoire of the malaria parasite sporozoite stage. J Biol Chem, 2002. **277**(44): p. 41948-53.
218. Mikolajczak, S.A., et al., L-FABP is a critical host factor for successful malaria liver stage development. Int J Parasitol, 2007. **37**(5): p. 483-9.
219. Mackellar, D.C., et al., *Plasmodium falciparum* PF10_0164 (ETRAMP10.3) is an essential parasitophorous vacuole and exported protein in blood stages. Eukaryot Cell, 2010. **9**(5): p. 784-94.
220. Mueller, A.K., et al., Genetically modified *Plasmodium* parasites as a protective experimental malaria vaccine. Nature, 2005. **433**(7022): p. 164-7.
221. Doolan, D.L., et al., Identification and characterization of the protective hepatocyte erythrocyte protein 17 kDa gene of *Plasmodium yoelii*, homolog of *Plasmodium falciparum* exported protein 1. J Biol Chem, 1996. **271**(30): p. 17861-8.
222. Simmons, D., et al., A malaria protein exported into a new compartment within the host erythrocyte. EMBO J, 1987. **6**(2): p. 485-91.
223. Sa, E.C.C., et al., *Plasmodium berghei* EXP-1 interacts with host Apolipoprotein H during *Plasmodium* liver-stage development. Proc Natl Acad Sci U S A, 2017. **114**(7): p. E1138-E1147.
224. Ingmundson, A., et al., The exported *Plasmodium berghei* protein IBIS1 delineates membranous structures in infected red blood cells. Mol Microbiol, 2012. **83**(6): p. 1229-43.
225. Silvie, O., K. Goetz, and K. Matuschewski, A sporozoite asparagine-rich protein controls initiation of *Plasmodium* liver stage development. PLoS Pathog, 2008. **4**(6): p. e1000086.
226. Tribensky, A., et al., Trafficking of PfExp1 to the parasitophorous vacuolar membrane of *Plasmodium falciparum* is independent of protein folding and the PTEX translocon. Cell Microbiol, 2017. **19**(5).
227. Siau, A., et al., Proteome mapping of *Plasmodium*: identification of the P. yoelii remodellome. Sci Rep, 2016. **6**: p. 31055.
228. Schulz, I., Permeabilizing cells: some methods and applications for the study of intracellular processes. Methods Enzymol, 1990. **192**: p. 280-300.
229. Baumeister, S., et al., Novel insights into red blood cell physiology using parasites as tools. Eur J Cell Biol, 2015. **94**(7-9): p. 332-9.
230. Stevenson, M.M. and E.M. Riley, Innate immunity to malaria. Nat Rev Immunol, 2004. **4**(3): p. 169-80.

231. Wacker, R., et al., LC3-association with the parasitophorous vacuole membrane of *Plasmodium berghei* liver stages follows a noncanonical autophagy pathway. Cell Microbiol, 2017.
232. Liehl, P. and M.M. Mota, Innate recognition of malarial parasites by mammalian hosts. Int J Parasitol, 2012. **42**(6): p. 557-66.
233. Liehl, P., et al., Host-cell sensors for *Plasmodium* activate innate immunity against liver-stage infection. Nat Med, 2014. **20**(1): p. 47-53.
234. Agop-Nersesian, C., et al., Shedding of host autophagic proteins from the parasitophorous vacuolar membrane of *Plasmodium berghei*. Sci Rep, 2017. **7**(1): p. 2191.
235. Renia, L. and Y.S. Goh, Malaria Parasites: The Great Escape. Front Immunol, 2016. **7**: p. 463.
236. Malleret, B., et al., *Plasmodium vivax*: restricted tropism and rapid remodeling of CD71-positive reticulocytes. Blood, 2015. **125**(8): p. 1314-24.
237. Jakub Gruszczyk, U.K., Li-Jin Chan, Sébastien Menant, Benoit Malleret, Nicholas T. Y. Lim, Christoph Q. Schmidt, Yee-Foong Mok, Kai-Min Lin, Richard D. Pearson, Gabriel Rangel, Brian J. Smith, Melissa J. Call, Michael P. Weekes, Michael D. W. Griffin, James M. Murphy, Jonathan Abraham, Kanlaya Sriprawat, Maria J. Menezes, Marcelo U. Ferreira, Bruce Russell, Laurent Renia, Manoj T. Duraisingh, Wai-Hong Tham, Transferrin receptor 1 is a reticulocyte-specific receptor for *Plasmodium vivax*. Science, 2018. **359**(6371): p. 48-55.
238. Sigala, P.A. and D.E. Goldberg, The peculiarities and paradoxes of *Plasmodium* heme metabolism. Annu Rev Microbiol, 2014. **68**: p. 259-78.
239. Weed, R.I., C.F. Reed, and G. Berg, Is hemoglobin an essential structural component of human erythrocyte membranes? J Clin Invest, 1963. **42**: p. 581-8.
240. Hamasaki, N., The role of band 3 protein in oxygen delivery by red blood cells. Indian J Clin Biochem, 1999. **14**(1): p. 49-58.
241. Chung, J., C. Chen, and B.H. Paw, Heme metabolism and erythropoiesis. Curr Opin Hematol, 2012. **19**(3): p. 156-62.
242. Dailey, H.A., et al., Ferrochelatase at the millennium: structures, mechanisms and [2Fe-2S] clusters. Cell Mol Life Sci, 2000. **57**(13-14): p. 1909-26.
243. Dailey, H.A. and P.N. Meissner, Erythroid heme biosynthesis and its disorders. Cold Spring Harb Perspect Med, 2013. **3**(4): p. a011676.
244. Sassa, S., Modern diagnosis and management of the porphyrias. Br J Haematol, 2006. **135**(3): p. 281-92.
245. Matkovic, L.B., et al., How porphyrinogenic drugs modeling acute porphyria impair the hormonal status that regulates glucose metabolism. Their relevance in the onset of this disease. Toxicology, 2011. **290**(1): p. 22-30.
246. Bressler, J.P. and G.W. Goldstein, Mechanisms of lead neurotoxicity. Biochem Pharmacol, 1991. **41**(4): p. 479-84.
247. Handschin, C., et al., Nutritional regulation of hepatic heme biosynthesis and porphyria through PGC-1alpha. Cell, 2005. **122**(4): p. 505-15.
248. James, M.F. and R.J. Hift, Porphyrias. Br J Anaesth, 2000. **85**(1): p. 143-53.
249. Anderson, G.J. and G. McLaren, Iron physiology and pathophysiology in humans. Nutrition and health. 2009, New York: Humana. xxii, 704 p.
250. Munakata, H., et al., Role of the heme regulatory motif in the heme-mediated inhibition of mitochondrial import of 5-aminolevulinate synthase. J Biochem, 2004. **136**(2): p. 233-8.
251. Seager, M.J., et al., X-linked dominant protoporphyria: a new porphyria. Clin Exp Dermatol, 2014. **39**(1): p. 35-7.
252. Helliwell, J.R., et al., Time-resolved and static-ensemble structural chemistry of hydroxymethylbilane synthase. Faraday Discuss, 2003. **122**: p. 131-44; discussion 171-90.
253. Puy, H., L. Gouya, and J.C. Deybach, Porphyrias. Lancet, 2010. **375**(9718): p. 924-37.
254. Pischik, E. and R. Kauppinen, An update of clinical management of acute intermittent porphyria. Appl Clin Genet, 2015. **8**: p. 201-14.
255. Sassa, S., Gene-environmental interactions: Lessons from porphyria. Environ Health Prev Med, 2003. **7**(6): p. 254-63.
256. Ahmed, R. and F.J. Leeper, A new synthesis of porphobilinogen analogues, inhibitors of hydroxymethylbilane synthase. Org Biomol Chem, 2003. **1**(1): p. 21-3.
257. Freesemann, A.G., et al., Immunological, enzymatic and biochemical studies of uroporphyrinogen III-synthase deficiency in 20 patients with congenital erythropoietic porphyria. Eur J Biochem, 1998. **257**(1): p. 149-53.
258. Layer, G., et al., Structure and function of enzymes in heme biosynthesis. Protein Sci, 2010. **19**(6): p. 1137-61.
259. Bissell, D.M., B. Wang, and J. Lai, Hereditary Coproporphyria, in GeneReviews(R), R.A. Pagon, et al., Editors. 1993: Seattle (WA).

260. Taketani, S., T. Furukawa, and K. Furuyama, Expression of coproporphyrinogen oxidase and synthesis of hemoglobin in human erythroleukemia K562 cells. Eur J Biochem, 2001. **268**(6): p. 1705-11.
261. Elder, G., et al., The incidence of inherited porphyrias in Europe. J Inherit Metab Dis, 2013. **36**(5): p. 849-57.
262. Lamoril, J., et al., Neonatal hemolytic anemia due to inherited harderoporphyria: clinical characteristics and molecular basis. Blood, 1998. **91**(4): p. 1453-7.
263. Blake, D., et al., Fecal coproporphyrin isomers in hereditary coproporphyria. Clin Chem, 1992. **38**(1): p. 96-100.
264. Rossi, E., P.V. Attwood, and P. Garcia-Webb, Inhibition of human lymphocyte coproporphyrinogen oxidase activity by metals, bilirubin and haemin. Biochim Biophys Acta, 1992. **1135**(3): p. 262-8.
265. Ferreira, G.C., et al., Structure and function of ferrochelatase. J Bioenerg Biomembr, 1995. **27**(2): p. 221-9.
266. Gouya, L., et al., The penetrance of dominant erythropoietic protoporphyria is modulated by expression of wildtype FECH. Nat Genet, 2002. **30**(1): p. 27-8.
267. Padmanaban, G. and P.N. Rangarajan, Heme metabolism of *Plasmodium* is a major antimalarial target. Biochem Biophys Res Commun, 2000. **268**(3): p. 665-8.
268. van Dooren, G.G., A.T. Kennedy, and G.I. McFadden, The use and abuse of heme in apicomplexan parasites. Antioxid Redox Signal, 2012. **17**(4): p. 634-56.
269. Liu, J., et al., *Plasmodium falciparum* ensures its amino acid supply with multiple acquisition pathways and redundant proteolytic enzyme systems. Proc Natl Acad Sci U S A, 2006. **103**(23): p. 8840-5.
270. Ke, H., et al., The heme biosynthesis pathway is essential for *Plasmodium falciparum* development in mosquito stage but not in blood stages. J Biol Chem, 2014. **289**(50): p. 34827-37.
271. Huy, N.T., et al., Neutralization of toxic heme by *Plasmodium falciparum* histidine-rich protein 2. J Biochem, 2003. **133**(5): p. 693-8.
272. Pagola, S., et al., The structure of malaria pigment beta-haematin. Nature, 2000. **404**(6775): p. 307-10.
273. Abshire, J.R., et al., Quantification of labile heme in live malaria parasites using a genetically encoded biosensor. Proc Natl Acad Sci U S A, 2017. **114**(11): p. E2068-E2076.
274. Pasini, E.M., et al., In-depth analysis of the membrane and cytosolic proteome of red blood cells. Blood, 2006. **108**(3): p. 791-801.
275. Pasini, E.M., et al., Deep-coverage rhesus red blood cell proteome: a first comparison with the human and mouse red blood cell. Blood Transfus, 2010. **8 Suppl 3**: p. s126-39.
276. Ponka, P., Tissue-specific regulation of iron metabolism and heme synthesis: distinct control mechanisms in erythroid cells. Blood, 1997. **89**(1): p. 1-25.
277. Hamza, I. and H.A. Dailey, One ring to rule them all: trafficking of heme and heme synthesis intermediates in the metazoans. Biochim Biophys Acta, 2012. **1823**(9): p. 1617-32.
278. Besur, S., et al., Clinically important features of porphyrin and heme metabolism and the porphyrias. Metabolites, 2014. **4**(4): p. 977-1006.
279. Fujita, H., Molecular mechanism of heme biosynthesis. Tohoku J Exp Med, 1997. **183**(2): p. 83-99.
280. Correia, M.A., P.R. Sinclair, and F. De Matteis, Cytochrome P450 regulation: the interplay between its heme and apoprotein moieties in synthesis, assembly, repair, and disposal. Drug Metab Rev, 2011. **43**(1): p. 1-26.
281. Seeber, F. and D. Soldati-Favre, Metabolic pathways in the apicoplast of apicomplexa. Int Rev Cell Mol Biol, 2010. **281**: p. 161-228.
282. Nagaraj, V.A., et al., Unique properties of *Plasmodium falciparum* porphobilinogen deaminase. J Biol Chem, 2008. **283**(1): p. 437-44.
283. Surolia, N. and G. Padmanaban, de novo biosynthesis of heme offers a new chemotherapeutic target in the human malarial parasite. Biochem Biophys Res Commun, 1992. **187**(2): p. 744-50.
284. Rathnapala, U.L., C.D. Goodman, and G.I. McFadden, A novel genetic technique in *Plasmodium berghei* allows liver stage analysis of genes required for mosquito stage development and demonstrates that de novo heme synthesis is essential for liver stage development in the malaria parasite. PLoS Pathog, 2017. **13**(6): p. e1006396.
285. Nagaraj, V.A., et al., Malaria parasite-synthesized heme is essential in the mosquito and liver stages and complements host heme in the blood stages of infection. PLoS Pathog, 2013. **9**(8): p. e1003522.
286. Sigala, P.A., et al., Deconvoluting heme biosynthesis to target blood-stage malaria parasites. Elife, 2015. **4**.
287. Rizopoulos, Z., K. Matuschewski, and J.M. Haussig, Distinct Prominent Roles for Enzymes of *Plasmodium berghei* Heme Biosynthesis in Sporozoite and Liver Stage Maturation. Infect Immun, 2016. **84**(11): p. 3252-3262.
288. Lim, L. and G.I. McFadden, The evolution, metabolism and functions of the apicoplast. Philos Trans R Soc Lond B Biol Sci, 2010. **365**(1541): p. 749-63.

289. Koreny, L., et al., Tetrapyrrole synthesis of photosynthetic chromerids is likely homologous to the unusual pathway of apicomplexan parasites. Plant Cell, 2011. **23**(9): p. 3454-62.
290. Ralph, S.A., et al., Tropical infectious diseases: metabolic maps and functions of the *Plasmodium falciparum* apicoplast. Nat Rev Microbiol, 2004. **2**(3): p. 203-16.
291. Wilson, R.J., Parasite plastids: approaching the endgame. Biol Rev Camb Philos Soc, 2005. **80**(1): p. 129-53.
292. Stanway, R.R., et al., GFP-targeting allows visualization of the apicoplast throughout the life cycle of live malaria parasites. Biol Cell, 2009. **101**(7): p. 415-30, 5 p following 430.
293. Graewe, S., et al., Chronicle of a death foretold: *Plasmodium* liver stage parasites decide on the fate of the host cell. FEMS Microbiol Rev, 2012. **36**(1): p. 111-30.
294. Yeh, E. and J.L. DeRisi, Chemical rescue of malaria parasites lacking an apicoplast defines organelle function in blood-stage *Plasmodium falciparum*. PLoS Biol, 2011. **9**(8): p. e1001138.
295. Arisue, N., et al., The *Plasmodium* apicoplast genome: conserved structure and close relationship of P. ovale to rodent malaria parasites. Mol Biol Evol, 2012. **29**(9): p. 2095-9.
296. Heiny, S.R., et al., Protein Traffic to the *Plasmodium falciparum* apicoplast: evidence for a sorting branch point at the Golgi. Traffic, 2014. **15**(12): p. 1290-304.
297. Goldberg, D.E. and P.A. Sigala, *Plasmodium* heme biosynthesis: To be or not to be essential? PLoS Pathog, 2017. **13**(9): p. e1006511.
298. Dailey, H.A., et al., Noncanonical coproporphyrin-dependent bacterial heme biosynthesis pathway that does not use protoporphyrin. Proc Natl Acad Sci U S A, 2015. **112**(7): p. 2210-5.
299. Soltys, B.J. and R.S. Gupta, Mitochondrial proteins at unexpected cellular locations: export of proteins from mitochondria from an evolutionary perspective. Int Rev Cytol, 2000. **194**: p. 133-96.
300. Bonday, Z.Q., et al., Heme biosynthesis by the malarial parasite. Import of delta-aminolevulinate dehydrase from the host red cell. J Biol Chem, 1997. **272**(35): p. 21839-46.
301. Varadharajan, S., et al., Localization of ferrochelatase in *Plasmodium falciparum*. Biochem J, 2004. **384**(Pt 2): p. 429-36.
302. Dhanasekaran, S., et al., Delta-aminolevulinic acid dehydratase from *Plasmodium falciparum*: indigenous versus imported. J Biol Chem, 2004. **279**(8): p. 6934-42.
303. Koncarevic, S., et al., The malarial parasite *Plasmodium falciparum* imports the human protein peroxiredoxin 2 for peroxide detoxification. Proc Natl Acad Sci U S A, 2009. **106**(32): p. 13323-8.
304. Foth, B.J., et al., Quantitative time-course profiling of parasite and host cell proteins in the human malaria parasite *Plasmodium falciparum*. Mol Cell Proteomics, 2011. **10**(8): p. M110 006411.
305. Bonday, Z.Q., et al., Import of host delta-aminolevulinate dehydratase into the malarial parasite: identification of a new drug target. Nat Med, 2000. **6**(8): p. 898-903.
306. Bryk, A.H. and J.R. Wisniewski, Quantitative Analysis of Human Red Blood Cell Proteome. J Proteome Res, 2017. **16**(8): p. 2752-2761.
307. Alvarez-Llamas, G., et al., A novel methodology for the analysis of membrane and cytosolic sub-proteomes of erythrocytes by 2-DE. Electrophoresis, 2009. **30**(23): p. 4095-108.
308. Zhang, Q., et al., Proteomic profiling of nonenzymatically glycated proteins in human plasma and erythrocyte membranes. J Proteome Res, 2008. **7**(5): p. 2025-32.
309. Smith, C.M., et al., Red cells from ferrochelatase-deficient erythropoietic protoporphyria patients are resistant to growth of malarial parasites. Blood, 2015. **125**(3): p. 534-41.
310. Padmanaban, G., V.A. Nagaraj, and P.N. Rangarajan, An alternative model for heme biosynthesis in the malarial parasite. Trends Biochem Sci, 2007. **32**(10): p. 443-9.
311. Nagaraj, V.A., et al., Characterization of coproporphyrinogen III oxidase in *Plasmodium falciparum* cytosol. Parasitol Int, 2010. **59**(2): p. 121-7.
312. O'Brien, C., et al., Recent clinical and molecular insights into emerging artemisinin resistance in *Plasmodium falciparum*. Curr Opin Infect Dis, 2011. **24**(6): p. 570-7.
313. Plowe, C.V., Malaria: Resistance nailed. Nature, 2014. **505**(7481): p. 30-1.
314. Seder, R.A., et al., Protection against malaria by intravenous immunization with a nonreplicating sporozoite vaccine. Science, 2013. **341**(6152): p. 1359-65.
315. Marsh, K., Africa in transition: the case of malaria. Int Health, 2016. **8**(3): p. 155-6.
316. Steketee, R.W. and B.L. Nahlen, The Future of Measuring Impact against Malaria: From Saving Lives to Eliminating Transmission. Am J Trop Med Hyg, 2017. **97**(3_Suppl): p. 3-5.
317. Sherling, E.S. and C. van Ooij, Host cell remodeling by pathogens: the exomembrane system in *Plasmodium*-infected erythrocytes. FEMS Microbiol Rev, 2016. **40**(5): p. 701-21.
318. Roux, K.J., et al., A promiscuous biotin ligase fusion protein identifies proximal and interacting proteins in mammalian cells. J Cell Biol, 2012. **196**(6): p. 801-10.
319. Chen, A.L., et al., Novel components of the *Toxoplasma* inner membrane complex revealed by BioID. MBio, 2015. **6**(1): p. e02357-14.

320. Nadipuram, S.M., et al., In Vivo Biotinylation of the *Toxoplasma* Parasitophorous Vacuole Reveals Novel Dense Granule Proteins Important for Parasite Growth and Pathogenesis. MBio, 2016. **7**(4).
321. Gaji, R.Y., et al., Phosphorylation of a Myosin Motor by TgCDPK3 Facilitates Rapid Initiation of Motility during *Toxoplasma gondii* egress. PLoS Pathog, 2015. **11**(11): p. e1005268.
322. Khosh-Naucke, M., et al., Identification of novel parasitophorous vacuole proteins in P. falciparum parasites using BioID. Int J Med Microbiol, 2017.
323. Varnaite, R. and S.A. MacNeill, Meet the neighbors: Mapping local protein interactomes by proximity-dependent labeling with BioID. Proteomics, 2016. **16**(19): p. 2503-2518.
324. Kim, D.I., et al., An improved smaller biotin ligase for BioID proximity labeling. Mol Biol Cell, 2016. **27**(8): p. 1188-96.
325. Wang, K., et al., Identification of Novel O-Linked Glycosylated *Toxoplasma* Proteins by Vicia villosa Lectin Chromatography. PLoS One, 2016. **11**(3): p. e0150561.
326. Karpievitch, Y.V., A.R. Dabney, and R.D. Smith, Normalization and missing value imputation for label-free LC-MS analysis. BMC Bioinformatics, 2012. **13 Suppl 16**: p. S5.
327. Ansorge, I., et al., Permeabilization of the erythrocyte membrane with streptolysin O allows access to the vacuolar membrane of *Plasmodium falciparum* and a molecular analysis of membrane topology. Mol Biochem Parasitol, 1997. **84**(2): p. 259-61.
328. Gunther, K., et al., An exported protein of *Plasmodium falciparum* is synthesized as an integral membrane protein. Mol Biochem Parasitol, 1991. **46**(1): p. 149-57.
329. Rhee, H.W., et al., Proteomic mapping of mitochondria in living cells via spatially restricted enzymatic tagging. Science, 2013. **339**(6125): p. 1328-1331.
330. Kim, D.I., et al., BioSITe: A Method for Direct Detection and Quantitation of Site-Specific Biotinylation. J Proteome Res, 2017.
331. Lam, S.S., et al., Directed evolution of APEX2 for electron microscopy and proximity labeling. Nat Methods, 2015. **12**(1): p. 51-4.
332. Udeshi, N.D., et al., Antibodies to biotin enable large-scale detection of biotinylation sites on proteins. Nat Methods, 2017. **14**(12): p. 1167-1170.
333. Voss, S. and A. Skerra, Mutagenesis of a flexible loop in streptavidin leads to higher affinity for the Strep-tag II peptide and improved performance in recombinant protein purification. Protein Eng, 1997. **10**(8): p. 975-82.
334. Cheah, J.S. and S. Yamada, A simple elution strategy for biotinylated proteins bound to streptavidin conjugated beads using excess biotin and heat. Biochem Biophys Res Commun, 2017. **493**(4): p. 1522-1527.
335. De Munter, S., et al., Split-BioID: a proximity biotinylation assay for dimerization-dependent protein interactions. FEBS Lett, 2017. **591**(2): p. 415-424.
336. Schopp, I.M., et al., Split-BioID a conditional proteomics approach to monitor the composition of spatiotemporally defined protein complexes. Nat Commun, 2017. **8**: p. 15690.
337. Branon, T.C.B., Justin A; Sanchez, Ariana D; Udeshi, Namrata D; Svinkina, Tanya; Carr, Steven A ; Feldman, Jessica L ; Perrimon, Norbert; Ting, Alice Y Directed evolution of TurboID for efficient proximity labeling in living cells and organisms. bioRxiv preprint, 2017.
338. Rees, J.S., et al., Protein Neighbors and Proximity Proteomics. Mol Cell Proteomics, 2015. **14**(11): p. 2848-56.
339. Ong, S.E., et al., Stable isotope labeling by amino acids in cell culture, SILAC, as a simple and accurate approach to expression proteomics. Mol Cell Proteomics, 2002. **1**(5): p. 376-86.
340. Mann, M., Functional and quantitative proteomics using SILAC. Nat Rev Mol Cell Biol, 2006. **7**(12): p. 952-8.
341. Nirmalan, N., P.F. Sims, and J.E. Hyde, Quantitative proteomics of the human malaria parasite *Plasmodium falciparum* and its application to studies of development and inhibition. Mol Microbiol, 2004. **52**(4): p. 1187-99.
342. Prieto, J.H., et al., Large-scale differential proteome analysis in *Plasmodium falciparum* under drug treatment. PLoS One, 2008. **3**(12): p. e4098.
343. Cobbold, S.A., et al., Proteome-wide analysis reveals widespread lysine acetylation of major protein complexes in the malaria parasite. Sci Rep, 2016. **6**: p. 19722.
344. Nebl, T., et al., Quantitative in vivo analyses reveal calcium-dependent phosphorylation sites and identifies a novel component of the *Toxoplasma* invasion motor complex. PLoS Pathog, 2011. **7**(9): p. e1002222.
345. Opitz, N., et al., Capturing the Asc1p/Receptor for Activated C Kinase 1 (RACK1) Microenvironment at the Head Region of the 40S Ribosome with Quantitative BioID in Yeast. Mol Cell Proteomics, 2017. **16**(12): p. 2199-2218.
346. Ma, Y., et al., HILAQ: A Novel Strategy for Newly Synthesized Protein Quantification. J Proteome Res, 2017. **16**(6): p. 2213-2220.

347. Batinovic, S., et al., An exported protein-interacting complex involved in the trafficking of virulence determinants in *Plasmodium*-infected erythrocytes. Nat Commun, 2017. **8**: p. 16044.
348. Fougere, A., et al., Variant Exported Blood-Stage Proteins Encoded by *Plasmodium* Multigene Families Are Expressed in Liver Stages Where They Are Exported into the Parasitophorous Vacuole. PLoS Pathog, 2016. **12**(11): p. e1005917.
349. Fonager, J., et al., Reduced CD36-dependent tissue sequestration of *Plasmodium*-infected erythrocytes is detrimental to malaria parasite growth in vivo. J Exp Med, 2012. **209**(1): p. 93-107.
350. Zhang, M., et al., UIS2: A Unique Phosphatase Required for the Development of *Plasmodium* Liver Stages. PLoS Pathog, 2016. **12**(1): p. e1005370.
351. Ludin, P., et al., In silico prediction of antimalarial drug target candidates. Int J Parasitol Drugs Drug Resist, 2012. **2**: p. 191-9.
352. Cowman, A.F., D. Berry, and J. Baum, The cellular and molecular basis for malaria parasite invasion of the human red blood cell. J Cell Biol, 2012. **198**(6): p. 961-71.
353. Eksi, S. and K.C. Williamson, Protein targeting to the parasitophorous vacuole membrane of *Plasmodium falciparum*. Eukaryot Cell, 2011. **10**(6): p. 744-52.
354. Culvenor, J.G. and P.E. Crewther, S-antigen localization in the erythrocytic stages of *Plasmodium falciparum.* J Protozool, 1990. **37**(1): p. 59-65.
355. Bickle, Q. and R.L. Coppel, A fourth family of the *Plasmodium falciparum* S-antigen. Mol Biochem Parasitol, 1992. **56**(1): p. 141-50.
356. Anders, R.F., G.V. Brown, and A. Edwards, Characterization of an S antigen synthesized by several isolates of *Plasmodium falciparum.* Proc Natl Acad Sci U S A, 1983. **80**(21): p. 6652-6.
357. Carlton, J.M., et al., Genome sequence and comparative analysis of the model rodent malaria parasite *Plasmodium yoelii yoelii*. Nature, 2002. **419**(6906): p. 512-9.
358. DeBarry, J.D. and J.C. Kissinger, Jumbled genomes: missing Apicomplexan synteny. Mol Biol Evol, 2011. **28**(10): p. 2855-71.
359. Tachibana, S., et al., *Plasmodium cynomolgi* genome sequences provide insight into *Plasmodium vivax* and the monkey malaria clade. Nat Genet, 2012. **44**(9): p. 1051-5.
360. Kooij, T.W., et al., A *Plasmodium* whole-genome synteny map: indels and synteny breakpoints as foci for species-specific genes. PLoS Pathog, 2005. **1**(4): p. e44.
361. Frech, C. and N. Chen, Genome comparison of human and non-human malaria parasites reveals species subset-specific genes potentially linked to human disease. PLoS Comput Biol, 2011. **7**(12): p. e1002320.
362. Pearce, J.A., et al., Characterisation of two novel proteins from the asexual stage of *Plasmodium falciparum*, H101 and H103. Mol Biochem Parasitol, 2005. **139**(2): p. 141-51.
363. Singh, S., et al., A conserved multi-gene family induces cross-reactive antibodies effective in defense against *Plasmodium falciparum.* PLoS One, 2009. **4**(4): p. e5410.
364. Gondeau, C., et al., The C-terminal domain of *Plasmodium falciparum* merozoite surface protein 3 self-assembles into alpha-helical coiled coil tetramer. Mol Biochem Parasitol, 2009. **165**(2): p. 153-61.
365. Rodriguez, L.E., et al., Identifying *Plasmodium falciparum* merozoite surface antigen 3 (MSP3) protein peptides that bind specifically to erythrocytes and inhibit merozoite invasion. Protein Sci, 2005. **14**(7): p. 1778-86.
366. Carlton, J.M., Gene synteny across *Plasmodium* spp: could 'operon-like' structures exist? Parasitol Today, 1999. **15**(5): p. 178-9.
367. Bozdech, Z., et al., The transcriptome of the intraerythrocytic developmental cycle of *Plasmodium falciparum.* PLoS Biol, 2003. **1**(1): p. E5.
368. Otto, T.D., et al., A comprehensive evaluation of rodent malaria parasite genomes and gene expression. BMC Biol, 2014. **12**: p. 86.
369. de Souza, J.B., et al., Cerebral malaria: why experimental murine models are required to understand the pathogenesis of disease. Parasitology, 2010. **137**(5): p. 755-72.
370. Finn, R.D., et al., HMMER web server: 2015 update. Nucleic Acids Res, 2015. **43**(W1): p. W30-8.
371. Carlton, J.M., et al., Comparative genomics of the neglected human malaria parasite *Plasmodium vivax*. Nature, 2008. **455**(7214): p. 757-63.
372. Rice, B.L., et al., The origin and diversification of the merozoite surface protein 3 (msp3) multi-gene family in *Plasmodium vivax* and related parasites. Mol Phylogenet Evol, 2014. **78**: p. 172-84.
373. Richards, J.S., et al., Identification and prioritization of merozoite antigens as targets of protective human immunity to *Plasmodium falciparum* malaria for vaccine and biomarker development. J Immunol, 2013. **191**(2): p. 795-809.
374. Sakamoto, H., et al., Antibodies against a *Plasmodium falciparum* antigen PfMSPDBL1 inhibit merozoite invasion into human erythrocytes. Vaccine, 2012. **30**(11): p. 1972-80.

375. Chiu, C.Y., et al., Antibodies to the *Plasmodium falciparum* Proteins MSPDBL1 and MSPDBL2 Opsonize Merozoites, Inhibit Parasite Growth, and Predict Protection From Clinical Malaria. J Infect Dis, 2015. **212**(3): p. 406-15.
376. Van Tyne, D., et al., Modulation of PF10_0355 (MSPDBL2) alters *Plasmodium falciparum* response to antimalarial drugs. Antimicrob Agents Chemother, 2013. **57**(7): p. 2937-41.
377. Beeson, J.G., et al., Merozoite surface proteins in red blood cell invasion, immunity and vaccines against malaria. FEMS Microbiol Rev, 2016. **40**(3): p. 343-72.
378. Koch, M. and J. Baum, The mechanics of malaria parasite invasion of the human erythrocyte - towards a reassessment of the host cell contribution. Cell Microbiol, 2016. **18**(3): p. 319-29.
379. Kadekoppala, M. and A.A. Holder, Merozoite surface proteins of the malaria parasite: the MSP1 complex and the MSP7 family. Int J Parasitol, 2010. **40**(10): p. 1155-61.
380. Lin, C.S., et al., The merozoite surface protein 1 complex is a platform for binding to human erythrocytes by *Plasmodium falciparum*. J Biol Chem, 2014. **289**(37): p. 25655-69.
381. Lin, C.S., et al., Multiple *Plasmodium falciparum* Merozoite Surface Protein 1 Complexes Mediate Merozoite Binding to Human Erythrocytes. J Biol Chem, 2016. **291**(14): p. 7703-15.
382. Hodder, A.N., et al., Insights into Duffy binding-like domains through the crystal structure and function of the merozoite surface protein MSPDBL2 from *Plasmodium falciparum*. J Biol Chem, 2012. **287**(39): p. 32922-39.
383. Drew, D.R., P.R. Sanders, and B.S. Crabb, *Plasmodium falciparum* merozoite surface protein 8 is a ring-stage membrane protein that localizes to the parasitophorous vacuole of infected erythrocytes. Infect Immun, 2005. **73**(7): p. 3912-22.
384. Hillier, C.J., et al., Process development and analysis of liver-stage antigen 1, a preerythrocyte-stage protein-based vaccine for *Plasmodium falciparum*. Infect Immun, 2005. **73**(4): p. 2109-15.
385. Lelliott, P.M., et al., The influence of host genetics on erythrocytes and malaria infection: is there therapeutic potential? Malar J, 2015. **14**: p. 289.
386. Lell, B., et al., The role of red blood cell polymorphisms in resistance and susceptibility to malaria. Clin Infect Dis, 1999. **28**(4): p. 794-9.
387. Barnwell, J.W., M.E. Nichols, and P. Rubinstein, In vitro evaluation of the role of the Duffy blood group in erythrocyte invasion by *Plasmodium vivax*. J Exp Med, 1989. **169**(5): p. 1795-802.
388. Verra, F., V.D. Mangano, and D. Modiano, Genetics of susceptibility to *Plasmodium falciparum*: from classical malaria resistance genes towards genome-wide association studies. Parasite Immunol, 2009. **31**(5): p. 234-53.
389. Jallow, M., et al., Genome-wide and fine-resolution association analysis of malaria in West Africa. Nat Genet, 2009. **41**(6): p. 657-65.
390. Reed, F.A. and S.A. Tishkoff, African human diversity, origins and migrations. Curr Opin Genet Dev, 2006. **16**(6): p. 597-605.
391. Bei, A.K. and M.T. Duraisingh, Functional analysis of erythrocyte determinants of *Plasmodium* infection. Int J Parasitol, 2012. **42**(6): p. 575-82.
392. Richer, E., et al., Chemical mutagenesis: a new strategy against the global threat of infectious diseases. Mamm Genome, 2008. **19**(5): p. 309-17.
393. Barbaric, I., et al., Spectrum of ENU-induced mutations in phenotype-driven and gene-driven screens in the mouse. Environ Mol Mutagen, 2007. **48**(2): p. 124-42.
394. Brown, S.D. and R.E. Hardisty, Mutagenesis strategies for identifying novel loci associated with disease phenotypes. Semin Cell Dev Biol, 2003. **14**(1): p. 19-24.
395. Bauer, D.C., et al., Genome-wide analysis of chemically induced mutations in mouse in phenotype-driven screens. BMC Genomics, 2015. **16**: p. 866.
396. Brown, F.C., et al., ENU mutagenesis identifies the first mouse mutants reproducing human beta-thalassemia at the genomic level. Blood Cells Mol Dis, 2013. **50**(2): p. 86-92.
397. Greth, A., et al., A novel ENU-mutation in ankyrin-1 disrupts malaria parasite maturation in red blood cells of mice. PLoS One, 2012. **7**(6): p. e38999.
398. Hortle, E., et al., Adenosine monophosphate deaminase 3 activation shortens erythrocyte half-life and provides malaria resistance in mice. Blood, 2016. **128**(9): p. 1290-301.
399. Huang, H.M., et al., Ankyrin-1 Gene Exhibits Allelic Heterogeneity in Conferring Protection Against Malaria. G3 (Bethesda), 2017. **7**(9): p. 3133-3144.
400. Huang, H.M., et al., A novel ENU-induced ankyrin-1 mutation impairs parasite invasion and increases erythrocyte clearance during malaria infection in mice. Sci Rep, 2016. **6**: p. 37197.
401. Lelliott, P.M., et al., Erythrocytic Iron Deficiency Enhances Susceptibility to *Plasmodium chabaudi* Infection in Mice Carrying a Missense Mutation in Transferrin Receptor 1. Infect Immun, 2015. **83**(11): p. 4322-34.
402. Brown, F.C., et al., Activation of the erythroid K-Cl cotransporter Kcc1 enhances sickle cell disease pathology in a humanized mouse model. Blood, 2015. **126**(26): p. 2863-70.

403. Brown, F.C., et al., Loss of Dynamin 2 GTPase function results in microcytic anaemia. Br J Haematol, 2017. **178**(4): p. 616-628.
404. Solis, C., et al., Acute intermittent porphyria: studies of the severe homozygous dominant disease provides insights into the neurologic attacks in acute porphyrias. Arch Neurol, 2004. **61**(11): p. 1764-70.
405. Strand, L.J., et al., Heme biosynthesis in intermittent acute prophyria: decreased hepatic conversion of porphobilinogen to porphyrins and increased delta aminolevulinic acid synthetase activity. Proc Natl Acad Sci U S A, 1970. **67**(3): p. 1315-20.
406. Hessels, J., et al., Homozygous acute intermittent porphyria in a 7-year-old boy with massive excretions of porphyrins and porphyrin precursors. J Inherit Metab Dis, 2004. **27**(1): p. 19-27.
407. Cassera, M.B., et al., Purine and pyrimidine pathways as targets in *Plasmodium falciparum.* Curr Top Med Chem, 2011. **11**(16): p. 2103-15.
408. Huthmacher, C., et al., Antimalarial drug targets in *Plasmodium falciparum* predicted by stage-specific metabolic network analysis. BMC Syst Biol, 2010. **4**: p. 120.
409. Avitia-Dominguez, C., et al., Targeting *Plasmodium* Metabolism to Improve Antimalarial Drug Design. Curr Protein Pept Sci, 2016. **17**(3): p. 260-74.
410. Lazarus, M.D., T.G. Schneider, and T.F. Taraschi, A new model for hemoglobin ingestion and transport by the human malaria parasite *Plasmodium falciparum.* J Cell Sci, 2008. **121**(11): p. 1937-49.
411. Sanderson, T. and J.C. Rayner, PhenoPlasm: a database of disruption phenotypes for malaria parasite genes. Wellcome Open Res, 2017. **2**: p. 45.
412. Foth, B.J., et al., Dissecting apicoplast targeting in the malaria parasite *Plasmodium falciparum*. Science, 2003. **299**(5607): p. 705-8.
413. Taylor-Robinson, A.W. and R.S. Phillips, Predominance of infected reticulocytes in the peripheral blood of CD4+ T-cell-depleted mice chronically infected with *Plasmodium chabaudi chabaudi*. Parasitol Res, 1994. **80**(7): p. 614-9.
414. Conway, A.J., et al., A mouse model of hereditary coproporphyria identified in an ENU mutagenesis screen. Dis Model Mech, 2017. **10**(8): p. 1005-1013.
415. Lew, V.L., T. Tiffert, and H. Ginsburg, Excess hemoglobin digestion and the osmotic stability of *Plasmodium falciparum*-infected red blood cells. Blood, 2003. **101**(10): p. 4189-94.
416. Fogel, B.J., C.E. Shields, and A.E. Von Doenhoff, Jr., The osmotic fragility of erythrocytes in experimental malaria. Am J Trop Med Hyg, 1966. **15**(3): p. 269-75.
417. Herricks, T., et al., Estimating physical splenic filtration of *Plasmodium falciparum*-infected red blood cells in malaria patients. Cell Microbiol, 2012. **14**(12): p. 1880-91.
418. Siegesmund, M., et al., The acute hepatic porphyrias: current status and future challenges. Best Pract Res Clin Gastroenterol, 2010. **24**(5): p. 593-605.
419. Zumla, A., et al., Host-directed therapies for infectious diseases: current status, recent progress, and future prospects. Lancet Infect Dis, 2016. **16**(4): p. e47-63.
420. Robreau-Fraolini, A.M., et al., Porphobilinogen deaminase gene in African and Afro-Caribbean ethnic groups: mutations causing acute intermittent porphyria and specific intragenic polymorphisms. Hum Genet, 2000. **107**(2): p. 150-9.
421. Lelliott, P.M.H., Hong & W. Dixon, Matthew & Namvar, Arman & J. Blanch, Adam & Rajagopal, Vijay & Tilley, Leann & Coban, Cevayir & J. McMorran, Brendan & J. Foote, Simon & Burgio, Gaetan, Erythrocyte β spectrin can be genetically targeted to protect mice from malaria. Blood Advances, 2017. **1**(26): p. 2624-2636.

Acknowledgements

I would like to thank my supervisors and mentors, Gaetan Burgio, Volker Heussler, Simon Foote, Brendan McMorran, Roger Chung, Pascal Mäser and Charaf Benerafa. I would like to thank them all for their continuous support and the possibility to work with them which was a great honor. Gaetan, I thank you for the excellent supervision throughout this thesis and all the effort you put into the continuation of this thesis in Switzerland. Thanks for showing me that science can be full of fun and for all the critical discussions. Volker I thank you dearly for your support and accepting me into your laboratory to continue my thesis. I am grateful for your mentorship and all the helpful suggestions and comments on my work.

I would like to thank past and present members of the Foote lab, Ceri Flowers, Pat Lelliott, Nazneen Adenwalla, Ning Huang, Bernadette Pedersen, Shelley Lampkin and Emmaline Brown. Special tanks to Tony Jerkovic for providing his expertise with the UHPLC. I'd also like to thank especially Andy Greth and Hong Ming Huang for all the fun times we had in the lab. Elinor Hortle for your positive attitude to everything, our candy adventures and all other memories we've shared.

I am also thankful to have worked with past and present members of the Heussler lab: Reto Caldelari, Jacqueline Schmuckli, Cihan Elci, Magali Roques, Anthony Zakher and Gesine Kaiser. Thanks to fellow PhD students Mariana de Niz, Rahel Wacker and Livia Niklaus and to Rebecca Limenitakis for answering so many of my questions and the helpful discussions. Thanks to Ruth Rehmann for being the mouse and mosquito master. I would also like to thank Francis Brühlmann, for his help in last few weeks of lab work, it was always fun to work with you. Last but no least Paul-Christian Burda for the bigger picture and all the exciting discussions about PVM biology. I am sure you'll be part of solving the puzzle in the future.

My thanks goes to Tania de Koning-Ward, who welcomed me to her laboratory at Deakin and gave me the first introduction into *Plasmodium* manipulation, to her involvement in the PBGD project and for her kind and warm welcome into her laboratory.

I would also like to thank Damaris Bausch-Fluck who helped me when I was lost in mass spectrometry data. Highly appreciated to extend our friendship into the professional world. It's great to have some nerdy friends.

I thank Denis C Bauer from the CSIRO. Her bioinformatics expertise has helped to identify the causative mutation in the *Pbgd*^{MRI58155} strain. I wish to thank Steve Jane, David Curtis, Fiona Brown and Ashlee Conway at the Monash University in Melbourne for providing the *Cpox*$^{+/W373X}$ strain. Thanks to Kerry Woods and Sandra Huber for sharing the BioID plasmid and experimental advice in planning the BioID.

This work would not have been possible without the funding of the Macquarie University towards my scholarship. I would like to thank the Graduate School of Bern for travel funding towards the visit of the BioMalPar conference in Heidelberg. It was a great opportunity to meet many leaders in the malaria field and discuss the results of the BioID screen.

I further wish to thank all the people that were involved in organizing of the Cotutelle between the Macquarie University and the University of Bern, but special thanks to Marlene Wolf and Roger Chung.

I would like to thank my Australian, Swiss and German “village”; the friends who helped me achieving this by lending my all their moral support, reading through parts of the thesis, bringing me food and entertaining Milla and Annabelle.

Most of all I thank my mother, grandmother, sister and Karin for always being there; my parents-in-law for their continuous support; and of course, my gorgeous husband also, and again, for letting me write this thesis on your/our big table :o)

Appendices

Table S1: Full list of PVM proteins. An extensive literature search revealed 41 proteins that locate to the PVM.

***P. berghei* identifier**	**Protein name**	**Location in *P. berghei* (Pb) or *P. falciparum* (Pf)**	**Ref**	***P. falciparum* identifier**
PBANKA_1008500	translocon component PTEX150 (PTEX150)	Pb: PVM	[1]	PF3D7_1436300
PBANKA_1328000	serine/threonine protein phosphatase, putative (UIS2)	Pb: PVM, Candidate	[2]	PF3D7_1464600
PBANKA_0931200	heat shock protein 101 (HSP101)	Pb: PVM	[1]	PF3D7_1116800
PBANKA_0830200	high molecular weight rhoptry protein 2, putative (RhopH2)	Pf: After invasion delivered to PVM	[3]	PF3D7_0929400
PBANKA_0305100	serine repeat antigen 1 (SERA1)	Pb: PV and PVM (C-terminus) during late liver stage	[4]	0
PBANKA_0305000	serine repeat antigen 2 (SERA2)	Pb: PV and PVM (middle part of SERA2) during late liver stage	[4]	0
-	serine repeat antigen 6 (SERA6)	Pf: PV and PVM (middle part of SERA2) during blood stage	[5]	PF3D7_0207500
PBANKA_0416000	high molecular weight rhoptry protein 3, putative (RhopH3)	Pf: parasite apical end	[6]	PF3D7_0905400
PBANKA_1365500	exported protein IBIS1 (IBIS1)	Pb: exported during blood stage, PVM during liver stage but distinct from UIS4	[7]	0
PBANKA_0519300	conserved *Plasmodium* protein, unknown function	Pb: PVM and cytoplasm; nice IFA	[8]	0
PBANKA_0517000	early transcribed membrane protein (ETRAMP10.2)	Pf: PVM, Etramp10.2 and Exp1 do not colocalize	[9]	0
PBANKA_0519200	CCAT-binding transcription factor-like protein	Py: beyond PVM, Candidate	[10]	0
PBANKA_0926700	circumsporozoite-related antigen (EXP1)	Pf: PVM, Bait	[11]	PF3D7_1121600
PBANKA_0941300	translocon component PTEX88 (PTEX88)	Pb: PVM	[1]	PF3D7_1105600

***P. berghei* identifier**	**Protein name**	**Location in *P. berghei* (Pb) or *P. falciparum* (Pf)**	**Ref**	***P. falciparum* identifier**
PBANKA_1358000	thioredoxin 2 (TRX2)	Pb: PVM	[1]	PF3D7_1345100
PBANKA_0201600	early transcribed membrane protein (ETRAMP)	Py: PVM both blood stage and liver stage	[12]	Absent in PF but PY02667
PBANKA_1032100	rhoptry-associated protein 1, putative (RAP1)	Pf: PV, associated with PVM & rhoptry, after secretion from rhoptries, RAP1 is injected into PV and peripherally associates with PVM, where it remains for the duration of ring stages.	[13]	PF3D7_1410400
PBANKA_1302900	copper transporter, putative	Pf: Erythrocyte plasma membrane, PVM, PPM, PEXEL negative membrane protein	[14]	#NV
PBANKA_1334300	exported protein 2 (EXP2)	Pf: PVM	[1]	PF3D7_1471100
-	early transcribed membrane protein 2 (ETRAMP2)	Pf: PVM	[9]	PF3D7_0202500
-	early transcribed membrane protein 4 (ETRAMP4)	Pf: PVM	[9]	PF3D7_0423700
-	early transcribed membrane protein 5 (ETRAMP5)	Pf: PVM	[15]	PF3D7_0532100
	early transcribed membrane protein 10.1 (ETRAMP10)	Pf: PVM	[9]	PF3D7_1001500
	early transcribed membrane protein 10.2 (ETRAMP10.2)	Pf: PVM	[9]	PF3D7_1033200
=UIS4 [16]	early transcribed membrane protein 10.3 (ETRAMP10.3)	Pf: PVM	[16]	PF3D7_1016900
PBANKA_0524800 SEP1	early transcribed membrane protein 11.1 (ETRAMP11.1/ SEP1)	Pf: PVM	[17, 18]	PF3D7_1102700
PBANKA_0501200	early transcribed membrane protein, (UIS4)	Pb: PVM	[16, 19]	
PBANKA_0524200	early transcribed membrane protein, (SEP2)	Pb: PVM, exported in to RRBC cytoplasm	[18]	
PBANKA_050110	early transcribed membrane protein, (SEP3)	Pb: PVM, exported in to RRBC cytoplasm	[18]	

***P. berghei* identifier**	**Protein name**	**Location in *P. berghei* (Pb) or *P. falciparum* (Pf)**	**Ref**	***P. falciparum* identifier**
	hypothetical protein	Py: PVM both blood stage and liver stage	[12]	*PY03652*
PBANKA_0807100	stomatin-like protein protein coding	Pf: PVM	[3]	PF3D7_0318100
	sexual stage-specific protein precursor (Pfs16)	Pf: PVM in gametocytes	[20]	PF3D7_0406200
PBANKA_1400800	early transcribed membrane protein (UIS3)	Pb: PVM in liver	[21]	PF3D7_1302200 ETRAMP13
PBANKA_1128100	Phospholipase (PL)	Pb: PVM in liver	[22]	PF3D7_0629300
PBANKA_1024600	liver specific protein 1 (Lisp1)	Pb: PVM in liver	[23]	PF3D7_1418100
PBANKA_1006300	Perforin-like protein 1 (PPLP1)	Pf: localizes to PVM in blood stage parasites during egress (and microneme prior to egress)	[24]	PF3D7_0408700
PBANKA_1432200	male development gene 1 (Pfpeg3/mdv1)	Pf: PVM in gametocytes (and osmiophilic bodies prior to egress)	[25]	PF3D7_1216500
PBANKA_1030600	p1/s1 nuclease	Py: PVM (IFA and SLO and saponin lysis, EXP2-like pattern)	[10]	PF3D7_1411900 PF3D7_1412000
-	Conserved *Plasmodium* protein, unknown function	Pf: PVM	[2]	PF3D7_1135400
PBANKA_1441700	Conserved *Plasmodium* protein, unknown function	Pf: PVM, also picked up in the BioID in both runs, only in BioID sample, not in wild-type parental strain	[2]	PF3D7_1226900
PBANKA_1032100	rhoptry-associated protein 1 (RAP1)	Pf: PV, associated with PVM after invasion in ring stage, disappears after and reappears in rhoptry bulb	[13]	PF3D7_1410400

References:

1. de Koning-Ward, T.F., et al., A newly discovered protein export machine in malaria parasites. Nature, 2009. **459**(7249): p. 945-9.
2. Khosh-Naucke, M., et al., Identification of novel parasitophorous vacuole proteins in *P. falciparum* parasites using BioID. Int J Med Microbiol, 2017.
3. Hiller, N.L., et al., Identification of a stomatin orthologue in vacuoles induced in human erythrocytes by malaria parasites. A role for microbial raft proteins in apicomplexan vacuole biogenesis. J Biol Chem, 2003. **278**(48): p. 48413-21.
4. Putrianti, E.D., et al., The *Plasmodium* serine-type SERA proteases display distinct expression patterns and non-essential in vivo roles during life cycle progression of the malaria parasite. Cell Microbiol, 2010. **12**(6): p. 725-39.
5. Ruecker, A., et al., Proteolytic activation of the essential parasitophorous vacuole cysteine protease SERA6 accompanies malaria parasite egress from its host erythrocyte. J Biol Chem, 2012. **287**(45): p. 37949-63.
6. Coppel, R.L., et al., A cDNA clone expressing a rhoptry protein of *Plasmodium falciparum*. Mol Biochem Parasitol, 1987. **25**(1): p. 73-81.
7. Ingmundson, A., et al., The exported *Plasmodium berghei* protein IBIS1 delineates membranous structures in infected red blood cells. Mol Microbiol, 2012. **83**(6): p. 1229-43.
8. Fougere, A., et al., Variant Exported Blood-Stage Proteins Encoded by *Plasmodium* Multigene Families Are Expressed in Liver Stages Where They Are Exported into the Parasitophorous Vacuole. PLoS Pathog, 2016. **12**(11): p. e1005917.
9. Spielmann, T., D.J. Fergusen, and H.P. Beck, etramps, a new *Plasmodium falciparum* gene family coding for developmentally regulated and highly charged membrane proteins located at the parasite-host cell interface. Mol Biol Cell, 2003. **14**(4): p. 1529-44.
10. Siau, A., et al., Proteome mapping of *Plasmodium*: identification of the *P. yoelii* remodellome. Sci Rep, 2016. **6**: p. 31055.
11. Simmons, D., et al., A malaria protein exported into a new compartment within the host erythrocyte. EMBO J, 1987. **6**(2): p. 485-91.
12. MacKellar, D.C., et al., A systematic analysis of the early transcribed membrane protein family throughout the life cycle of *Plasmodium yoelii*. Cell Microbiol, 2011. **13**(11): p. 1755-67.
13. Ghosh, S., et al., The *Plasmodium* rhoptry associated protein complex is important for parasitophorous vacuole membrane structure and intraerythrocytic parasite growth. Cell Microbiol, 2017. **19**(8).
14. Choveaux, D.L., J.M. Przyborski, and J.P. Goldring, A *Plasmodium falciparum* copper-binding membrane protein with copper transport motifs. Malar J, 2012. **11**: p. 397.
15. Spielmann, T., et al., A cluster of ring stage-specific genes linked to a locus implicated in cytoadherence in *Plasmodium falciparum* codes for PEXEL-negative and PEXEL-positive proteins exported into the host cell. Mol Biol Cell, 2006. **17**(8): p. 3613-24.
16. Mueller, A.K., et al., *Plasmodium* liver stage developmental arrest by depletion of a protein at the parasite-host interface. Proc Natl Acad Sci U S A, 2005. **102**(8): p. 3022-7.
17. Birago, C., et al., A gene-family encoding small exported proteins is conserved across *Plasmodium* genus. Mol Biochem Parasitol, 2003. **126**(2): p. 209-18.
18. Curra, C., et al., Erythrocyte remodeling in *Plasmodium berghei* infection: the contribution of SEP family members. Traffic, 2012. **13**(3): p. 388-99.
19. Spielmann, T., et al., Molecular make-up of the Plasmodium parasitophorous vacuolar membrane. Int J Med Microbiol, 2012. **302**(4-5): p. 179-86.
20. Baker, D.A., et al., Subcellular localization of Pfs16, a *Plasmodium falciparum* gametocyte antigen. Parasitology, 1994. **108 (Pt 2)**: p. 129-37.
21. Mikolajczak, S.A., et al., L-FABP is a critical host factor for successful malaria liver stage development. Int J Parasitol, 2007. **37**(5): p. 483-9.
22. Burda, P.C., et al., A *Plasmodium* phospholipase is involved in disruption of the liver stage parasitophorous vacuole membrane. PLoS Pathog, 2015. **11**(3): p. e1004760.
23. Ishino, T., et al., LISP1 is important for the egress of *Plasmodium berghei* parasites from liver cells. Cell Microbiol, 2009. **11**(9): p. 1329-39.
24. Garg, S., et al., Calcium-dependent permeabilization of erythrocytes by a perforin-like protein during egress of malaria parasites. Nat Commun, 2013. **4**: p. 1736.
25. Lanfrancotti, A., et al., *Plasmodium falciparum*: mRNA co-expression and protein co-localisation of two gene products upregulated in early gametocytes. Exp Parasitol, 2007. **116**(4): p. 497-503.

Gene family	*P. vivax*	*P. knowlesi*	*P. falciparum*	*P. y. yoelii*
MSP1	1: PVX_099980	1: PKH_072850	1: PF11_0344	1: PY05748
MSP2	0	0	1: PFB0300c	0
MSP3	11: MSP3.1 (γ*): PVX_097670 MSP3.2: PVX_097675 MSP3.3 (β*): PVX_097680 MSP3.4: PVX_097685 MSP3.5: PVX_097690 MSP3.6: PVX_097695 MSP3.7: PVX_097700 MSP3.8: PVX_097705 MSP3.9: PVX_097710 MSP3.10 (α*): PVX_097720 MSP3.11: PVX_097725	2: PKH_103020 PKH_145630	1: PF10_0345**	0
MSP4	1: PVX_003755	1: PKH_041300	1: PFB0310c	1: PY05967
MSP5	1: PVX_003770	1: PKH_041310	1: PFB0305c	0
MSP6	0	0	1: PF10_0346**	0
MSP7	11: PVX_082700 PVX_082695 PVX_082690 PVX_082685 PVX_082680 PVX_082675 PVX_082670 PVX_082665 PVX_082655 PVX_082650 PVX_082645	4: PKH_121820 PKH_121830 PKH_121840 PKH_121860	6: PF13_0197 PF13_0196 MAL13P1.175 (fragment) MAL13P1.174 PF13_0193 MAL13P1.173	3: PY02149 PY02148 PY02147
MSP8	1: PVX_097625	1: PKH_103110	1: PFE0120c	1: PY06415
MSP9	1: PVX_124060	1: PKH_144540	1: PFL1385c	1: PY02883
MSP10	1: PVX_114145	1: PKH_112880	1: PFF0995c	1: PY04226
MAP1	1: PVX_099975	1: PKH_072840	0	0

Supplementary Table 2: MSP gene families in *Plasmodium* species. The number of loci is indicated for each family,
Supplementary Table 2: MSP gene families in *Plasmodium* species. The number of loci is indicated for each family,
followed by the gene identifier. * Three gene members identified from previous studies 77 have been reclassified. ** Two *P. falciparum* MSP3 and MSP6 genes, in addition to four contiguous *P. falciparum* genes (PF10_0347, PF10_0348, PF10_0352 and PF10_0355) in a locus on chromosome 10, share structural features and motifs linking them as a family that are also related to the *P. vivax* MSP3 family. Taken from: [68] Carlton, J.M., et al., *Comparative genomics of the neglected human malaria parasite Plasmodium vivax.* Nature, 2008. 455(7214): p. 757-63.

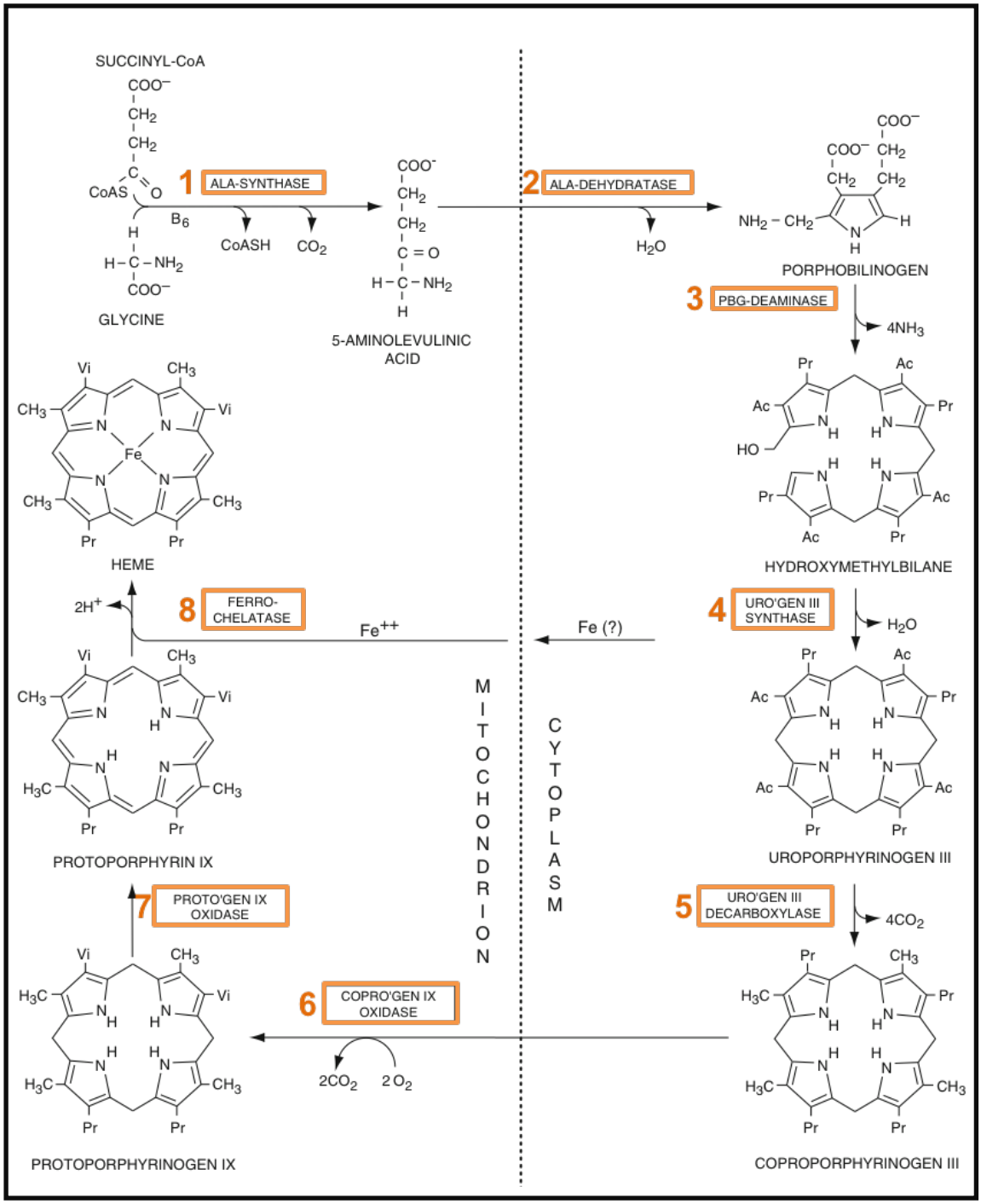

Supplementary Figure 1: The heme pathway, its substrates and products. Heme synthesis is catalyzed by eight subsequent enzymes from the initial substrates succinyl coenzyme A and L-glycine. Adapted from: [249]. Anderson, G.J. and G. McLaren, Iron physiology and pathophysiology in humans. Nutrition and health. 2009, New York: Humana. xxii, 704 p.

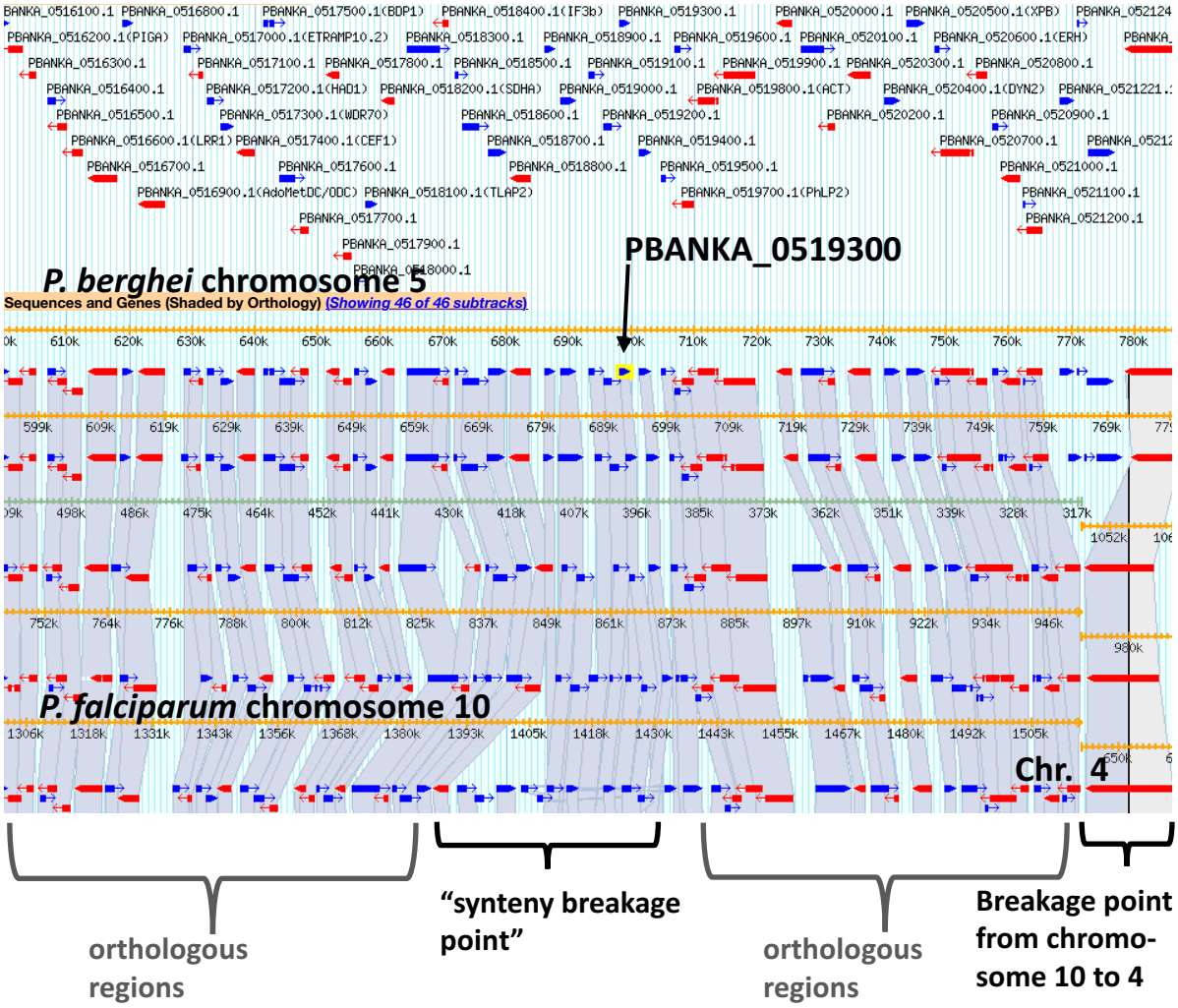

Supplementary Figure 2: Overview of homologous regions between *P. berghei* and *P. falciparum*. Comparing different regions of synteny between *P. berghei* and *P. falciparum* of chromosome 5 and 10 respectively. Prepared using the genome browser at PlasmoDB (http://plasmodb.org), showing 200kbp. A synteny breakage point between these two chromosomes at PBANKA_0519100-400 and at PF3D7_1035200-6600 is indicated. A second synteny breakage point following PBANKA_0521300, which is syntenic to *P. falciparum* chromosome 4 PF3D7_0420000, is specified.

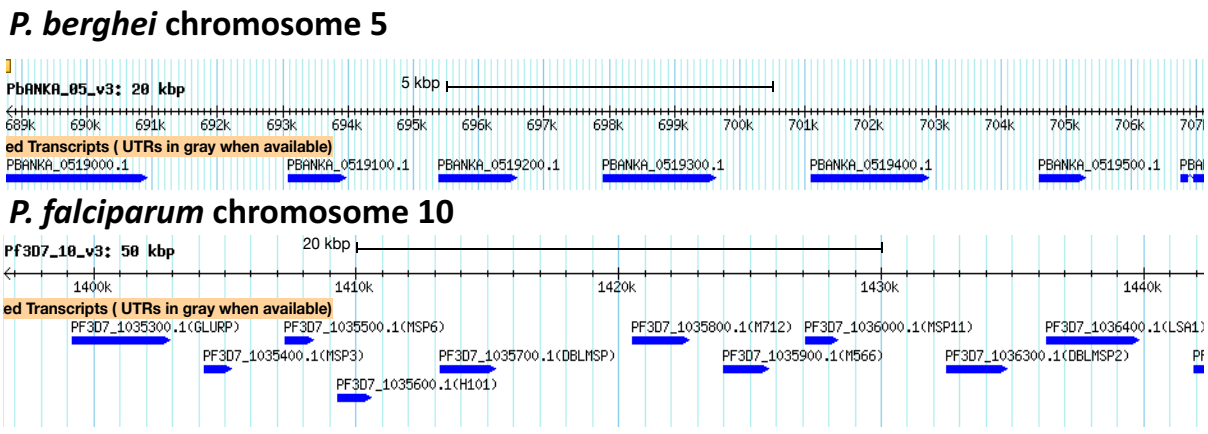

Supplementary Figure 3: Overview of synteny breakage point of syntenic *P. berghei* chromosomes 5 and *P. falciparum* 10. Compared to *P. berghei*, there are twice the numbers of genes found on the *P. falciparum* synteny breakage point. Prepared using the genome browser at PlasmoDB, showing 20kbp.

Supplementary Figure 4: *P. berghei* synteny break and *P. berghei* blood stage mRNA expression data. Graphs adapted from PlasmoDB (http://plasmodb.org). Proteins at the "synteny break" are highly expressed during the late blood stage, compared to preceding and subsequent genes.

PBANKA_0519100

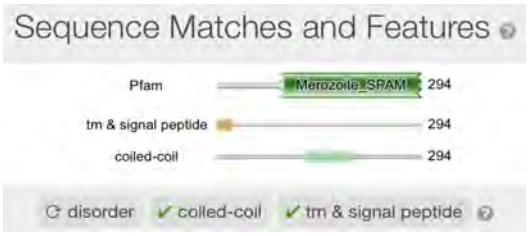

Iteration 1

PCYB_103900 merozoite surface protein 3
E-value: 0.00027
PCOAH_00031440 merozoite surface protein 3 E-value: 0.00072

Iteration 2

PKNH_1457400 merozoite surface protein 3 E-value: 2.5e-28
PVX_097690 merozoite surface protein 3
E-value: 7.0e-25
PF3D7_1035600 merozoite surface protein H101 E-value: 6.2e-06
PF3D7_1035500 merozoite surface protein 6 E-value: 3.3e-05

PBANKA_0519200

Iteration 1

Rodent malaria parasites only above threshhold

Iteration 2

Rodent malaria parasites only above the threshhold
Search converged – no more subsequent iterations possible

PBANKA_0519300

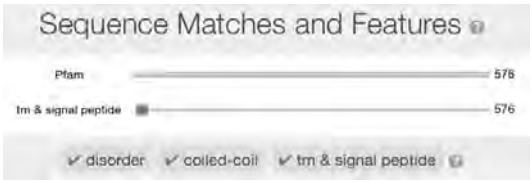

Iteration 1

Rodent malaria parasites only above threshhold

Iteration 2

Rodent malaria parasites only above the threshhold
Search converged – no more subsequent iterations possible

PBANKA_0519400

Iteration 1

Rodent malaria parasites only above threshhold

Iteration 2

PF3D7_1035400 merozoite surface protein 3 E-value: 4.9e-05

Supplementary Figure 5: Jackhmmer search strategy and results. A jackhmmer iterative search using hidden Markov Models on *P. berghei* proteins PBANKA_0519100-400 arrived at human *Plasmodium* species proteins. Minimal threshold value: <0.001

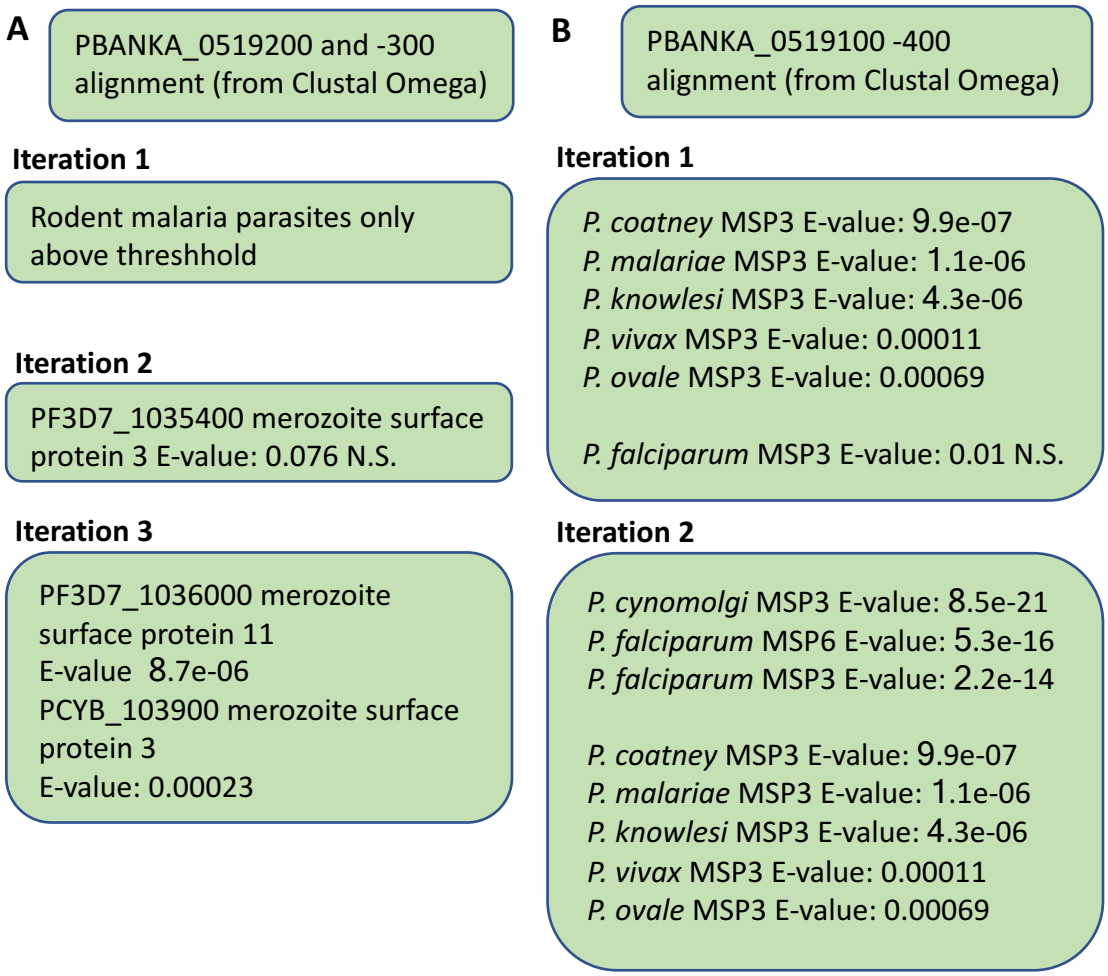

Supplementary Figure 6: Jackhmmer search of aligned. A jackhmmer search initiated with alignments of different *P. berghei* proteins arrived at human malaria species. (A) PBANKA_0519200 and -300 were aligned and subjected to a jackhmmer search, resulting in human *Plasmodium* species after the third iteration. (B) Alignment of PBANKA_0519100 -400 used in a jackhmmer search arrived at non-human and human *Plasmodium* species. Minimal threshold value: <0.001

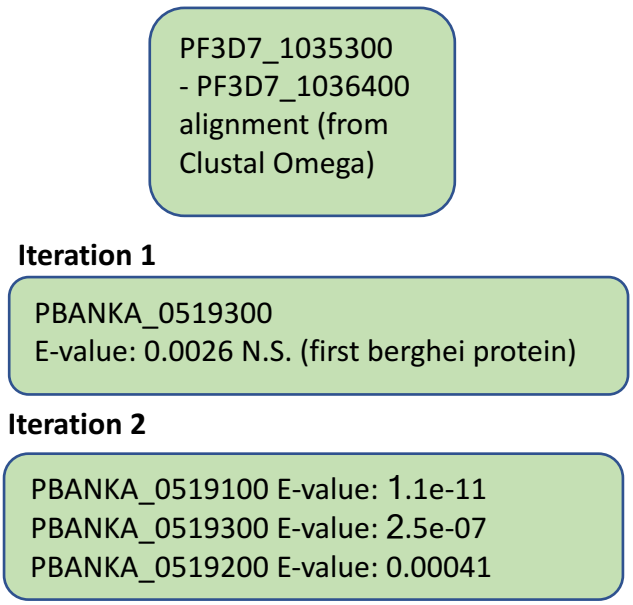

Supplementary Figure 7: Jackhmmer search using a Clustal Omega alignment of all 10 P. *falciparum* synteny break proteins. A protein sequence alignment was prepared using Clustal Omega for all 10 *P. falciparum* synteny breakage points proteins. Alignment was subjected to an iterative jackhmmer search followed by filtering for *P. berghei* proteins. The first iterative search step generated no significant protein results for *P. berghei* but the second iteration identified 3 out of 4 proteins present at the *P. berghei* synteny break. Minimal threshold value: <0.001

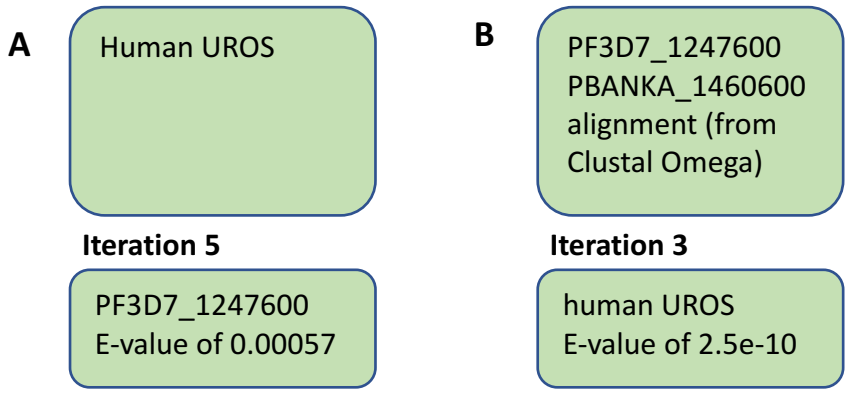

Supplementary Figure 8: Jackhmmer search using human UROS proteins sequence. (A) Human UROS protein sequence was used to initiate a jackhmmer search. After five iterative searches, the first *Plasmodium* protein, PF3D7_1247600 was identified. (B) A protein sequence alignment was prepared using Clustal Omega for PF3D7_1247600 and PBANKA_1460600 (which is the ortholog of PF3D7_1247600) and used in the jackhmmer tool. This was then followed by filtering for human proteins, resulting in the identification of one human protein, UROS.
Minimal threshhold value: <0.001

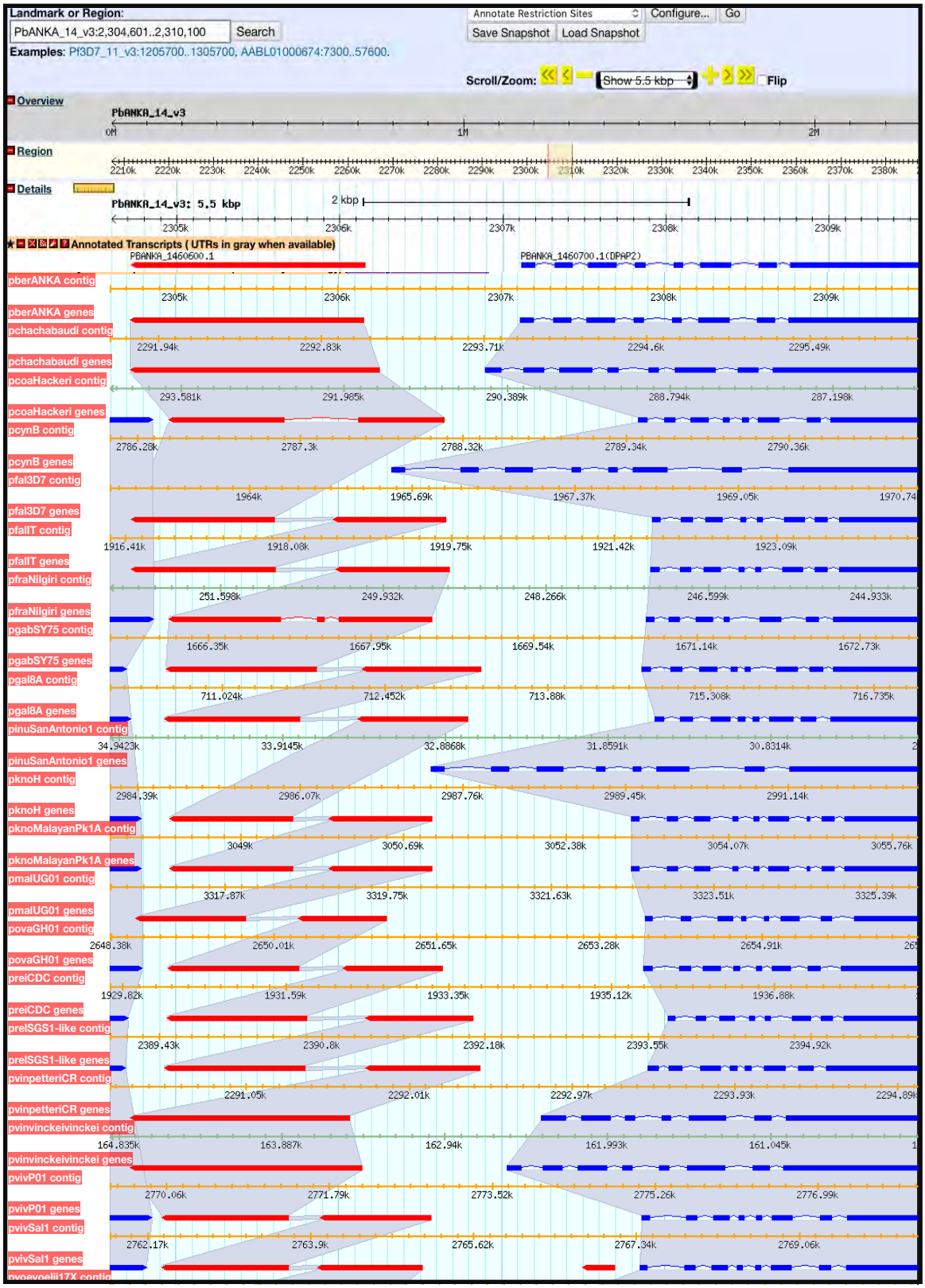

Supplementary Figure 9: Overview of conserved regions between *P. berghei* and *P. falciparum*. Through a JACKHMMER search, PF3D7_1247600 was identified to be a UROS candidate. PF3D7_1247600 is highly conserved throughout *Plasmodium* species.

Curriculum Vitae

Name	Cilly Bernardette Schnider (born Heinz)
Date of birth	6th of April 1986 in Bonn
Nationality	German
Institute address	AG Heussler Institute of Cell Biology University of Bern CH-3012 Bern cilly.schnider@izb.unibe.ch
Private address	Oberwiesenstrasse 78 CH-8050 Zurich +41 79 621 01 19

Education

March 2018	Institute of Cell Biology, University of Bern, Bern, Switzerland and Faculty of Medicine and Health Sciences, Macquarie University, Sydney, Australia **PhD in Cell Biology** of Prof Volker Heussler, Dr Gaetan Burgio and Prof Roger Chung. Research on "Parasite-host interactions during the blood and liver stage of rodent malaria parasites"
October 2010	University of Zurich, Switzerland, **MSc in Molecular and Cellular Biology**.
August 2008	Bonn-Rhein-Sieg University of Applied Sciences, Germany, **BSc in Applied Biology**, Double degree in collaboration with London South Bank University
July 2008	London South Bank University, UK, **BSc in Bioscience**; 1st class Honors degree
June 2005	Municipal Grammar School, Rheinbach, Germany **Biology and Arts**,

Academic work experience

October 2012 – June 2013	Faculty of Medicine and Health Sciences, Macquarie University, Sydney **Research Assistant** of Dr Gaetan Burgio and Prof Simon Foote
November 2010 – November 2011	Institute of Pharmacology and Toxicology, Animal hospital, Zurich **PhD student** of Prof Hanspeter Naegeli; Research on DNA repair "Modulation of NER factors during cell cycle progression"
July 2009 – July 2010	Institute of Paediatric Cancer Research, Children's hospital Zurich **Master student** of Prof Beat Schaefer; Research on "Characterisation of PAX3/FKHR interactome", the oncogenic transcription factor of a childhood sarcoma
December 2008 – December 2010	Institute for veterinary Bacteriology, Animal hospital, Zurich **Research assistant** of Prof Max Wittenbrink; Characterisation of *Lawsonia intracellularis*
September 2007 – July 2008	London South Bank University, United Kingdom **Bachelor student** of Dr Michael Byford; Research on autotaxin, an enzyme generating cancer promoting molecules. Awarded "best final year project"
October 2006 – July 2007	Bonn-Rhein-Sieg University of Applied Sciences, Rheinbach, Germany, **student assistant** of Prof Annette Menke; Department of international relationships

Teaching experience

September 2016 – March 2018	Co-Supervision of Master thesis by Francis Brühlmann, Institute of Cell Biology, University of Bern
November 2016	Supervision of Cell Biology II practical, BSc students, University of Bern
September 2016 – October 2016	Supervision and designing of practical course, BSc students; cloning and bioinformatics part, Institute of Cell Biology, University of Bern
April 2016 – June 2014	Co-Supervision of Murielle Golomingi and Francis Brühlmann as part of the Bachelor thesis at the University of Bern
January 2014 – March 2014	Supervision of James Carey, stipend of Summer Vacation Research Scholarship (full-time), Macquarie University

Awards, presentations and others

May 2017	Poster presentation at the 13th BioMalPar "Identification of novel PVM proteins using BioID" in Heidelberg, Germany
November 2016	Oral presentation at the Swiss Society of Tropical Medicine and Parasitology student meeting. "Identification of novel PVM proteins using BioID"
September 2014	Oral presentation at the Parasitology retreat in Kioloa hosted by the Australian National University, Canberra. "Characterizing the role of haem pathway enzymes during malaria infection"
July 2014	Poster presentation at the 50th Conference of the Australian Society of Parasitology "Identification of novel malaria drug targets using chemical mutagenesis in mice" in Canberra, Australia
October 2010	Oral presentation at European student's conference, Charité Berlin, of Master thesis "Characterization of interactome of PAX3/FKHR"
May 2010	Master thesis presentation at the seminar "Applied Oncology", Zurich University Hospital
March 2009	Award for best final year project, London South Bank University, UK
October 2008	Oral presentation at European student's conference, Charité Berlin, presenting Bachelor thesis results
June 2008	Double degree Scholarship from awarded be the German Academic Exchange Service

Additional skills and qualifications

- **Languages** – German: mother tongue, English: Excellent (Toefl 2008), Spanish/French: low
- Competent **technical skills** in Microsoft Office, Visual Basics, HTML, Cloning manager, Scaffold, ImageJ, Adobe Photoshop and EndNote. Windows and Mac user
- Introductory course in laboratory animal science (LTK module 1)

List of Publications

Schnider CB, Bausch-Fluck D, Brühlmann F, Heussler VT, Burda PC. BioID reveals novel proteins of the *Plasmodium* parasitophorous vacuole membrane. mSphere (2018) *Accepted Manuscript*

Schnider CB, Jensen L, Yang H, Conway AJ, Brown FC, Di Pierro E, Graziadei G, Jane SM, Curtis DJ, Foote SJ, McMorran BJ and Burgio G. Coproporphyrinogen oxidase confers resistance to the blood stage infection of *Plasmodium* species. (2018) *Prepared Manuscript*

Schnider CB, Yang H, Starrs L, Ehmann A, Rahimi F, Di Pierro E, Graziadei G, Bauer DC, Foote SJ, Burgio G and McMorran BJ. *Plasmodium* requires host porphobilinogen deaminase for intraerythrocytic growth. (2018) *Prepared Manuscript*

Heinz CB, Wachtel M, Schaefer BW. Characterisation of the interactome of PAX3/FKHR. Eur J Med Res 15(Supplement I): I-XXII, 1-240(2010) ISSN 0949-2321

Heinz CB, Byford M. Inhibitors of autotaxin in hen egg white. Eur J Med Res 13(Supplement I): I-XX, 1-180 (2008) ISSN 0949-2321